Oyster Creek Probabilistic Risk Assessment (Level 2)

June 1992

Volume 1 of 1

Main Report

Appendix A	Containment Pressure Capacity
Appendix B	Volume for Debris Trapping in Vent Pipe
Appendix C	Procedure to Determine Key Release Categories
Appendix D	Independent Review

OYSTER CREEK

PROBABILISTIC RISK ASSESSMENT

(LEVEL 2)

OYSTER CREEK
PROBABILISTIC RISK ASSESSMENT
(LEVEL 2)
PARTICIPANTS

GPU Nuclear Corporation	PLG, Incorporated
Mansur Alammar - Lead Engineer	Ken Dermer - Lead Engineer
Jack Wetmore	Alfred Torri
Ken Canavan	David Buttermer
Nick Trikouros	David Johnson
Eugene Mozias	

TABLE OF CONTENTS

TABLE OF CONTENTS (Continued)

TABLE OF CONTENTS (Continued)

1. EXECUTIVE SUMMARY

1.1 BACKGROUND AND OBJECTIVES

This report documents the analysis that was performed by GPU Nuclear Corporation to address the "back-end" (or containment performance) requirements of U.S. Nuclear Regulatory Commission (NRC) Generic Letter No. 88-20 (Reference 1-1). This analysis follows the guidance provided in Appendix 1 to the Generic Letter and uses a containment event tree (CET) as the framework for quantifying the frequency of releases into the environment. This report follows the format suggested in NUREG-1335 (Reference 1-2).

The analysis of Oyster Creek containment performance was performed by an integrated team of engineers and probabilistic risk assessment (PRA) specialists from GPU and PLG.

Independent reviews of the study were conducted by an in-house group and an independent consultant. See Appendix D for the comments from these reviews.

1.2 PLANT DESCRIPTION

The Oyster Creek Nuclear Generating Station is a single unit, General Electric boiling water reactor (BWR-2) of 650-MWe capacity housed in a Mark I containment. Important system design features are summarized in Table 1-1 of the Level 1 report (Reference 1-3) and in Section 3 of this report.

Figure 1-1 shows a general arrangement of the Oyster Creek reactor building. Figures 1-2 through 1-7 show the floor plans at various elevations. Of particular note are the torus corner rooms shown in Figure 1-2. The bypass scenarios identified for Oyster Creek exhaust to these torus corner rooms. In addition, the dominant failure mode identified for the Oyster Creek Mark I containment results from failure of the drywell liner at a location in which the sand, which previously was adjacent to the liner, has been removed. There are five open drain pipes, each approximately 4 inches in diameter, that communicate from this region to the torus room. This previously sand-filled region also communicates to the torus room around each of the 10 torus vent lines. Any significant pressurization of the torus rooms will also pressurize the torus corner rooms. The torus rooms provide a significant pathway to the refueling floor located at Elevation 119'3" (see Figure 1-7). Leaks or failures at the drywell head flange will also exhaust the drywell atmosphere to the refueling floor. Figures 1-8 and 1-9 show two additional views of the reactor building arrangement.

1.3 METHODOLOGY

The analysis of Oyster Creek containment performance was accomplished in the context of extending the Level 1 study to Level 2, as defined in NUREG/CR-2300 (Reference 1-4). Thus, the terms "back-end analysis," "containment performance analysis," and "Level 2 analysis" are used interchangeably in this report.

The Level 2 "examination process" is discussed in Section 2. All of the severe accident safety issues identified in the Generic Letter were addressed, and a CET and a set of release categories

were developed to facilitate Level 2 quantification. CET development is discussed in Section 7. The definition of release categories is contained in Section 11.

The CET was quantified for seven key plant damage states (KPDS). The concept of PDSs is discussed in Section 5, and the identification of KPDSs is discussed in Section 8. Representative sequences were selected for each KPDS. The selection process for these sequences is also discussed in Section 8. MAAP3.0B, Rev. 7.03 (see Section 4) was used to establish severe accident event timing and containment loads for each of the representative sequences.

A general discussion of the plant models and methodology for severe accident analysis is provided in Section 4. Details of the MAAP analysis for the KPDS representative sequences are provided in Section 9.

Finally, a state-of-the-art containment strength analysis was performed to characterize containment failure modes probabilistically. This strength analysis is summarized in Section 6.

1.4 SUMMARY OF MAJOR LEVEL 2 FINDINGS

The purpose of this section is to present the results of the Oyster Creek Level 2 analysis in terms of the frequencies of the various types of fission product releases into the environment; i.e., release category frequencies. These results are based on the integration of the Level 1 ("front-end" or "plant") model in which the responses of the plant systems and operators are addressed, and the Level 2 (or "back-end") model whose containment event tree defines the outcome of the core damage scenarios in terms of the timing and magnitude of the release of radioactive material.

To facilitate the proper treatment of intersystem dependencies that result in interactions between the systems involved in preventing core damage and the systems needed to ensure long-term containment integrity, the Level 1 portion of the accident sequence model includes all of the reactor protection, core cooling, active containment, and plant support systems. All pertinent information on the status of the drywell spray, suppression pool cooling, torus vent capability, isolation systems, and containment bypass conditions is transmitted to the Level 2 model via the definition of plant damage states. In this process, the plant damage states serve as the "initiating event" for the containment event tree and the interface between the Level 1 and Level 2 models. As a result of this system treatment, the containment event tree can focus on phenomenological issues such as the integrity of the containment and the conditions that impact source terms in the development and quantification of accident scenarios.

In principle, there is a "continuum" of possible releases (i.e., a specific source term for each plant damage state and pathway through the containment event tree) that could result from a core event. A reasonable treatment of this continuum is afforded by the use of a representative set of discrete "release categories" that span the spectrum from relatively large, early releases to releases that are much smaller in magnitude and that occur over a long period of time. A total of 125 release category end states have been defined for the Oyster Creek CET. The primary reason that this number is so large is to account for plant damage states involving containment and suppression pool bypass. A detailed definition of the Oyster Creek release categories is given in Section 11. The discriminators used to define these release categories are listed below:

- Reactor Coolant System (RCS) Pressure at Time of Vessel Breach (high or low)
- Drywell Sprays Available (yes or no)
- Core Damage Arrested In-Vessel (yes or no)
- Time of Containment Failure (early versus late)
- Size of Containment Failure (large versus small)
- Containment Bypassed (yes or no)
- Suppression Pool Scrubbing prior to Containment Failure (yes or no)
- Reactor Building Mitigation (yes or no)

After quantification of the CET for each KPDS, 28 of the defined release categories were determined to have frequencies greater than 1×10^{-10} per reactor-year. To facilitate the interpretation of these results, these 28 release categories can be placed into 6 general release category groups defined in Table 1-1. Also provided in this table is the percentage of the mean core damage frequency analyzed in Level 2, which is assigned to each general release group.

The term "bypass" refers to the condition when a release path from the reactor coolant system bypasses the drywell and torus and releases directly into the reactor building. Several of the KPDSs involve releases into the torus rooms located in the reactor building, resulting from failures in the reactor water cleanup (RWCU) or scram discharge volume lines.

Experience with published Level 3 PRAs in which offsite consequences are reported (References 1-5 through 1-7) has shown that early fatality risk, however small, is dominated by general release category group IA and 1B events since the scenarios in these groups are the only ones that could result in potentially life-threatening doses in the same time frame as needed to implement protective actions such as sheltering or evacuation. Based on the results developed for this study, the frequency of large, early releases (including early containment failures and bypasses) for Oyster Creek is predicted to be 7.34×10^{-7} per reactor year (see Table 12-1) or once in 1.3 million years. The frequency of large, early containment failure for internal events reported in NUREG/CR-4551 for Peach Bottom (Reference 1-8, Figure 2.5-4) is approximately 2.6×10^{-6} per reactor-year. Furthermore, the conditional probability of large, early containment failure reported for Peach Bottom in this same reference appears to be approximately 0.56 (frequency-weighted average—internal events) compared to a conditional value for Oyster Creek (including bypasses), which is approximately 0.23 (7.34×10^{-7}/Total CDF of 3.17×10^{-6}).

Release category groups II and III involve degraded containment performance but generally have not contributed significantly to early health effects risk. The releases associated with groups IV and V should be comparable to unmitigated design basis accidents.

Table 1-2 lists those individual sequences with frequencies greater than 1×10^{-10} per reactor-year that contribute to release group IA (large, early containment failures). The importance of CET split fractions to the frequency of release group IA is shown in Table 1-3. Table 1-4 lists the individual sequences contributing to release group IB (bypasses).

It should be noted that the probabilities assigned to the CET, such as those listed in Table 1-3, represent a quantification of uncertainty about the outcome of a severe accident. This is inherently a subjective quantification and reflects the current state of knowledge of the reactor safety research and PRA community about the physical processes of core damage events. There are good reasons to believe, and, in fact, many experts believe, that some of the containment

failure mechanisms currently postulated, such as reactor vessel steam explosions and direct heating from a high pressure melt ejection, are physically impossible. Thus, the CET probabilities for such events should be interpreted as a statement of confidence about the outcome of an event rather than the outcome of a random process. So, when we assign a split fraction value of 0.22 to containment failure, it means that we are (1-0.22) x 100 = 78% confident that a containment failure would not occur, given a defined load. Conversely, it means that we assign a 22% chance that a containment failure would occur.

Detailed Level 2 (back-end) results for Oyster Creek are provided in Section 12.

1.5 COMPARISON WITH NUREG-1150 PEACH BOTTOM RESULTS

Since Peach Bottom also has a Mark I containment and the Level 2 analysis is well documented in NUREG-1150, the Oyster Creek results are compared to Peach Bottom.

Table 1-5 compares the fraction of core damage frequency (CDF) assigned to the various release groups for Oyster Creek with those calculated for Peach Bottom (NUREG-1150). As indicated, the Oyster Creek fraction of early containment failures is substantially less than that for Peach Bottom due primarily to the curb in the Oyster Creek drywell that tends to mitigate the impact of molten corium attack on the drywell shell. For Peach Bottom, "the principal cause of early drywell failure is drywell shell melt-through" (drywell failures account for approximately 94% of early containment failures), whereas, as indicated in Table 1-3, liner melt-through contributes only approximately 17% of early containment failures for Oyster Creek.

The drywell concrete floor forms a curb at the liner which is 6 inches high and 1 foot wide. This curb will form a 'basin' which can hold hot liquid (molten fuel) and delay its contact with the steel liner, thus preserving containment integrity for a longer period of time. Assuming a total core UO_2 and Zircaloy volume of approximately 620 ft^3, a pedestal sump volume of 126 ft^3 and a drywell floor area (outside pedestal) of approximately 1000 ft^2, the whole core can be contained in the pedestal/drywell region with the 6" high curb. In other plants with no curb, the molten fuel (corium) will attack the liner as soon as it comes out of the pedestal and spreads on the drywell floor. In such scenarios, it is anticipated that 50% of the core will slump outside the vessel, and the spreading and containment of corium on the drywell floor at Oyster Creek may help the corium to freeze and delay containment breach.

The impact of the curb on the result is a 50% reduction in the probability of liner melt through for the high pressure station blackout scenario (NIFW) which is the worst case, as shown in Table 10-10.

The NUREG-1150 results for Peach Bottom did not specifically address bypasses. It is not clear as to whether such events were ignored in the Peach Bottom analysis or whether they were imbedded in early containment failures. Even if the Oyster Creek results for early containment failures and bypasses are combined, the sum total of the Oyster Creek fraction is only approximately 0.23 compared to 0.56 for Peach Bottom.

It should also be noted that the current Level 2 model for Oyster Creek does not account for recovery of electrical power following core damage. If this recovery action, and others, were to

be included in the Oyster Creek analysis, a substantial fraction of the severe accident scenarios binned to late containment failure would be rebinned to the no-containment failure bin.

1.6 REFERENCES

1-1. U.S. Nuclear Regulatory Commission, Generic Letter No. 88-20, December 1988.

1-2. U.S. Nuclear Regulatory Commission, "Individual Plant Examination: Submittal Guidance," final report, NUREG-1335, August 1989.

1-3. GPU Nuclear Corporation and PLG, Inc., "Oyster Creek Probabilistic Risk Assessment (Level 1)," Vols. 1 through 6, November 1991.

1-4. American Nuclear Society and Institute of Electrical and Electronics Engineers, "PRA Procedures Guide; A Guide to the Performance of Probabilistic Risk Assessments for Nuclear Power Plants," prepared for U.S. Nuclear Regulatory Commission, NUREG/CR-2300, Vols. 1 and 2, January 1983.

1-5. U.S. Nuclear Regulatory Commission, "Severe Accident Risks: An Assessment of Five U.S. Nuclear Power Plants," NUREG-1150, June 1989.

1-6. Pickard, Lowe and Garrick, Inc. "Midland Probabilistic Risk Assessment," prepared for Consumers Power Company, May 1984.

1-7. Pickard, Lowe and Garrick, Inc., "Seabrook Station Probabilistic Safety Assessment," prepared for Public Service Company of New Hampshire and Yankee Atomic Electric Company, PLG-0300, December 1983.

1-8. Sandia National Laboratories, "Evaluation of Severe Accident Risks: Peach Bottom, Unit 2," prepared for U.S. Nuclear Regulatory Commission, NUREG/CR-4551, SAND86-1309, Volume 4, Revision 1, Part 1, December 1990.

1-9. GPU Nuclear, "Oyster Creek Nuclear Station Print Book", Reactor Building General Arrangement Drawings, page numbers 202 through 210, December 1991.

Table 1-1. Definition and Results for General Release Category Groups		
General Release Category Group	Description	Percentage of CDF Analyzed*
IA	Large, Early Containment Failures	15.8
IB	Bypasses**	7.3
II	Small, Early Containment Failures	0.06
III	Late Containment Failures	26.4
IV	Long-Term, Contained Releases (containment intact following vessel breach)	0.00
V	Breach Prevented	50.4

* Group frequency divided by CDF analyzed (see Table 12-1).
** Includes contributions from PDS NJHW (1.54×10^{-6} per year).

Table 1-2. Individual Sequences with Frequencies Greater Than 1E-10 per Reactor-Year Contributing to Release Category Group IA				
Index	**Initiator**	**Frequency**	**Failed Split Fraction***	**End State****
6	NIFW	1.60E-07	/VBN*I2N*L2N*HBF*BEF	NLEGSB
3	MKCU	1.24E-07	/VB3*I1M*L1M*S1F*HBF*BEF	NLEGUB
18	NIFW	5.10E-08	/VBN*ESN*LM2*HBF*BEF	NHEGSB
21	NIFW	4.64E-08	/VBN*ESN*I2N*L2N*HBF*BEF	NHEGSB
5	MKCU	3.44E-08	/VB3*ESM*I1M*L1M*S1F*HBF*BEF	NHEGUB
4	NIFW	3.17E-08	/VBN*LM1*HBF*BEF	NLEGSB
10	NIFW	1.78E-08	/VBN*ET1*I2N*L2N*HBF*BEF	NLEGSB
13	NIFW	9.64E-09	/VBN*S12*I2M*L2M*HBF*BEF	NLEGUB
1	MKCU	8.38E-09	/VB3*I1M*S1F*I2F*L2D*HBF*BEF	NLEGUB
8	OIAU	4.97E-09	/VB1*ESP*S13*I2Q*L2Q*HBF*BEF	WLEGUB
8	NIFW	3.52E-09	/VBN*ET1*LM1*HBF*BEF	NLEGSB
24	NIFW	2.80E-09	/VBN*ESN*S12*I2M*L2M*HBF*BEF	NHEGUB
4	MKCU	2.59E-09	/VB3*ESM*I1M*S1F*I2F*L2D*HBF*BEF	NHEGUB
14	NIFW	2.14E-09	/VBN*S12*ET1*I2X*L2X*HBF*BEF	NLEGUB
2	MKCU	9.31E-10	/VB3*I1M*S1F*ET1*I2F*L2D*HBF*BEF	NLEGUB
23	NIFW	8.55E-10	/VBN*ESN*S12*LM2*HBF*BEF	NHEGUB
12	NIFW	5.30E-10	/VBN*S12*LM1*HBF*BEF	NLEGUB
6	OIAU	4.87E-10	/VB1*ESP*LM3*HBF*BEF	WLEGSB
20	NIFW	1.43E-10	/VBN*ESN*I2N*LM2*HBF*BEF	NHEGSB

* See Table 7-1 for definition of CET top events; Table 10-2 for split fraction values.
** See Figure 11-1 for end state definition.

Table 1-3. Split Fraction Importance Ranking for Release Category Group IA			
Split Fraction Name	Description	Split Fraction Value	Percent Contribution to Group IA Frequency
I2N*L2N	Large, Early Containment Failure; KPDS NIFW at/after Vessel Breach	0.22	44.7
I1M	Early Containment Failure Prior to Vessel Breach; KPDS MKCU	1.0	33.9
L1M	Large, Early Containment Failure Prior to Vessel Breach; KPDS MKCU	0.93	31.5
LM2	Liner Melt-Through; High RCS Pressure at Vessel Breach	0.305	10.4
LM1	Liner Melt-Through; Low RCS Pressure at Vessel Breach	0.055	7.1
* See Table 12-4			

Table 1-4. Individual Sequences with Frequencies Greater Than 1E-10 per Reactor-Year Contributing to Release Category Group IB				
Index	**Initiator**	**Frequency**	**Failed Split Fraction***	**End State****
1	OJAU	1.16E-07	/VBO*ESP	NLVSY
1	MJAU	5.26E-08	/VB4*ESP*I1B*L1B*S1F*HBF*BEF	HEGUBY
4	OJAU	3.72E-08	/VBO*ESP*S34	NLVUY
1	NJHW	1.54E-08	/VB2*ESP*I1B*L1B*S1F*HBF*BEF	HEGUBY
8	OJAU	5.85E-09	/VBO*ESP*S14*S3F	NLVUY
3	OJAU	1.95E-09	/VBO*ESP*DV2*I3J*L3J*HBF*BEF	LDGSBY
7	OJAU	7.98E-10	/VBO*ESP*LM3*HBF*BEF	LEGSBY
2	OJAU	7.86E-10	/VBO*ESP*DV2*I3J*HBF*BEF	LDCSBY
6	OJAU	6.24E-10	/VBO*ESP*S34*DV2*I3J*L3J*HBF*BEF	LDGUBY
5	OJAU	2.51E-10	/VBO*ESP*S34*DV2*I3J*HBF*BEF	LDCUBY

* See Table 7-1 for definition of CET top events; Table 10-2 for split fraction values.
** See Figure 11-1 for end state definitions.

Table 1-5. Comparison of Oyster Creek Level 2 Results with Peach Bottom (NUREG-1150)		
Group	Fraction of CDF Assigned to Various Release Category Groups	
	Peach Bottom*	Oyster Creek
Early Containment Failure	0.56	0.158
Bypasses	None Reported	0.07
Late Containment Failure	0.16	0.265
No Containment Failure	0.18	0.0
No Vessel Breach or Core Damage	0.1	0.504
Total	1.0	1.0
* Frequency weighted average values from Figure 4.4, NUREG-1150.		

Figure 1-1

Withheld Per 10 CFR 2.390

Official Use Only - Security Related Information

Figure 1-2

Withheld Per 10 CFR 2.390

Official Use Only - Security Related Information

Figure 1-3

Withheld Per 10 CFR 2.390

Official Use Only - Security Related Information

Figure 1-4

Withheld Per 10 CFR 2.390

Official Use Only - Security Related Information

Figure 1-5

Withheld Per 10 CFR 2.390

Official Use Only - Security Related Information

Figure 1-6

Withheld Per 10 CFR 2.390

Official Use Only - Security Related Information

Figure 1-7

Withheld Per 10 CFR 2.390

Official Use Only - Security Related Information

Figure 1-8

Withheld Per 10 CFR 2.390

Official Use Only - Security Related Information

Figure 1-9

Withheld Per 10 CFR 2.390

Official Use Only - Security Related Information

2. EXAMINATION PROCESS

2.1 INTRODUCTION

The back-end (or core and containment response) analysis addresses the physical progression of accident sequences with core damage from the onset of this damage through the release of radionuclides into the environment.

In this document, the terms "back-end," "containment response," "containment performance," and "Level 2 PRA" are used interchangeably. This arises from the fact that a Level 2 PRA was performed in this study to meet the individual plant examination (IPE) requirements for the containment performance analysis of Oyster Creek Plant. The overall relationship between the Level 1 and Level 2 portions of the accident sequence model is shown in Figure 2-1.

2.2 GENERAL METHODOLOGY

The approach to conduct the back-end analysis for the Oyster Creek IPE was designed to make use of the results of published safety research and development programs and of core and containment response analyses that were performed for published PRAs, particularly the core and containment response analyses that were performed for the Peach Bottom PRA (References 2-1 and 2-2). As both the Peach Bottom and Oyster Creek reactor plants have boiling water reactors (Mark I type) and there is some similarity in design details, the Peach Bottom core and containment response analysis was reviewed for use for Oyster Creek. However, it was concluded that Peach Bottom analysis could not be used for Oyster Creek primarily due to the differences in the emergency core cooling system (ECCS) between the two plants and the isolation condenser feature provided for Oyster Creek. Accordingly, extensive plant-specific MAAP analyses were performed for Oyster Creek. In addition, a plant-specific state-of-the-art containment capacity analysis was also performed to characterize the timing and mode of failure of the Oyster Creek containment.

The probabilistic aspects of the back-end analysis are quantified with a CET that can interface with the front-end (or plant) analysis by appropriately defining a set of plant damage states (PDS) or by linking the CET directly with the plant (Level 1) model event trees. PDSs are typically the endpoints of the sequences in the Level 1 portion of the event trees and the initiating events for the Level 2 or containment event trees. However, the PDSs defined for Level 1 reporting need not be as detailed as those used for back-end analysis.

The scope of the back-end analysis includes:

1. The definition of the PDS parameters (e.g., RCS pressure or status of containment integrity) applicable to Oyster Creek (Section 5). Various combinations of these parameters are referred to as plant damage states. The thermal-hydraulic response of sequences assigned to a given PDS is expected to be very similar.

2. The selection of KPDSs and accident sequence(s) to represent these KPDSs (Section 8).

3. The determination of containment failure modes (Section 6).

4. The determination of the core and containment response for each important PDS (Section 9).

5. The development (Section 7) and quantification (Section 10) of the Oyster Creek CET.

6. The definition of radionuclide release categories (Section 11) as a function of the degree of core damage, and the mode and timing of containment failure.

7. The quantification of the frequency of each release category and a description of the important sequences contributing to each release category (Section 12).

8. The identification of sequences that satisfy the NUREG-1335 (Reference 2-3) screening criteria (Section 12).

9. The identification of hardware or procedural changes that would influence the Level 2 results.

The end product of back-end analysis is a characterization (in terms of fission product source terms) of the impact of each severe accident sequence on the mode, timing, and magnitude of radionuclides released from the plant. This characterization is accomplished through a range of deterministic engineering analyses of the physical processes that determine core melt progression, containment response, containment failure mode (if any), and the transport and release of radionuclides. These analyses determine such physical parameters as the containment pressure and temperature as a function of time, the pressure at which the containment will fail, containment failure mode (including direct thermal attack of the drywell liner by debris), the rate at which the molten debris penetrates into the concrete basemat, and the rate and quantity of hydrogen produced and released into the containment. The probabilistic quantification for the containment event tree is a statement of the analyst's confidence about the outcome of a severe accident. A unique CET quantification can be defined for individual sequences or for each group of severe accident sequences having the same plant damage state. Different split fractions for the containment event tree nodes characterize the different plant damage states.

The end products of the back-end analysis include a set of release categories, which defines the radionuclide releases into the environment, and a quantification of the frequency of each release category. The release categories constitute the endpoints of this Level 2 PRA, and the associated source terms provide a measure of the potential consequences of severe accidents.

An important product of the back-end analysis is the identification of individual accident sequences whose frequencies exceed the screening frequency prescribed in NUREG-1335 (Reference 2-3). This product may be the most important of all because it is the key to the development of insights into plant safety characteristics.

2.3 REFERENCES

2-1. Sandia National Laboratories, "Evaluation of Severe Accident Risks: Peach Bottom, Unit 2,", NUREG/CR-4551, SAND86-1309, Volume 4, Revision 1, Part 1, December 1990.

2-2. U.S. Nuclear Regulatory Commission, "Severe Accident Risks: An Assessment of Five U.S. Nuclear Power Plants," NUREG-1150, June 1989.

2-3. U.S. Nuclear Regulatory Commission, "Individual Plant Examination: Submittal Guidance," final report, NUREG-1335, August 1989.

Figure 2-1. Overview of Risk Model Development

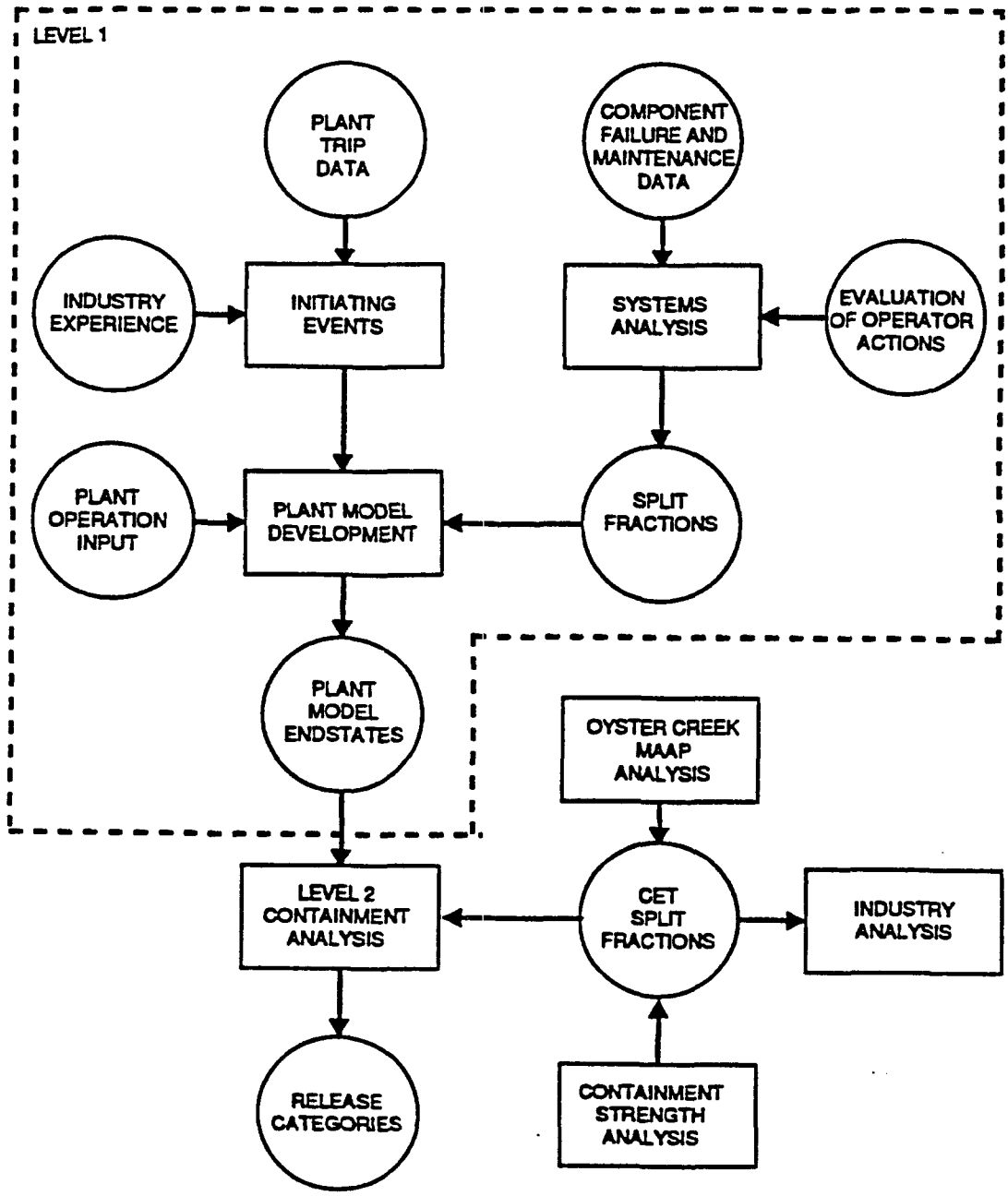

3. PLANT DATA AND PLANT DESCRIPTION

3.1 COMPARISON OF OYSTER CREEK AND PEACH BOTTOM

The Oyster Creek and Peach Bottom plants both contain General Electric BWRs housed in Mark I containments. Given this general characterization of similarity and the significant severe accident database that has been generated for Peach Bottom, (analyzed in NUREG-1150) it is clearly appropriate to compare Oyster Creek and Peach Bottom features in some detail; first, to attempt to make use of published Peach Bottom results, if appropriate, and second, to review any differences in the results for each plant to determine whether they are traceable to differences in plant features reflected in the analyses.

Although the containment configuration and major dimensions are very similar, there are significant differences in the NSSS (e.g., reactor power level, Peach Bottom has jet pumps for reactor coolant circulation, whereas Oyster Creek does not) as well as the systems that would be called on to mitigate a severe accident. In particular, for events in which the RCS is isolated, Peach Bottom has both high and low pressure injection systems and a core spray injection system. Oyster Creek does not have these injection systems; instead, it relies on isolation condensers and a core spray system.

As noted in Section 2, these design differences result in substantial differences in plant response compared to Peach Bottom, and accordingly, extensive plant-specific analyses were performed for Oyster Creek.

Table 3-1 provides a limited comparison of RCS and containment design features for the two plants.

The Oyster Creek isolation condenser system is described in detail in Appendix F.1 of the Level 1 PRA report (Reference 3-2). The isolation condenser system is a standby, high pressure system that can remove decay heat from the reactor vessel following a reactor trip by rejection to the atmosphere. The system is operable and ready for service at all times during power operation of the reactor. Operation of the system can be initiated and makeup can be provided to the secondary side of the condensers even if AC power is unavailable. Operation of either one of the two isolation condensers is adequate to remove decay heat following successful reactor trip.

Heat is transferred to the isolation condenser by natural circulation. Reactor steam flows to the isolation condenser where it is condensed, and the condensate drains back to the reactor vessel. The valves in the steam inlet lines to the isolation condensers are normally open so that the tube bundles are at reactor pressure even during standby conditions. Only the DC motor-operated condensate return isolation valves are normally closed. Makeup to the shell side of the isolation condenser, which is vented to the atmosphere following plant trip, is provided by the condensate transfer system, or the fire protection system if the former is not available.

3.2 CONTAINMENT WALK-THROUGH

The containment walk-through was carried out by the utility team and videotaped for later viewing and study by the whole team. This walk-through was done during the 1991 outage when the core was defueled and the control rod drive tubes were under going maintenance, thus creating

excellent access to the pedestal region. The walk-through objective was to get an overall view of the drywell region, layout of equipment, and any tortuous paths from the undervessel region to the concrete/liner curb.

The inspection of the pedestal region showed a 6 inch-deep, approximately 1 to 2 foot-wide "recess" or trench around the perimeter of the inside region. Also, the CRD/instrument penetrations to the pedestal were in the upper region close to the vessel, which would not interfere with the corium outflow from the pedestal. The pedestal opening to the drywell was measured during the walk-through and found to be 3 feet wide and 6 feet high. The concrete curb at the drywell wall liner was also measured and found to be 6-inches high. The drywell/torus vent pipes were carefully inspected, and this information was used in the liner melt-through split fraction calculation. The locations of the five recirculation pumps/ piping were carefully inspected because these pumps are hung from the top with enough clearing from the floor such that they do not obstruct the spread of the corium outside the pedestal. Still photographs were taken of the pedestal sump on other occasions when easy access was available, showing the pump/piping/cabling layout to see any leakage paths for corium through the piping and cable conduits.

Still photographs were also available for the torus corner rooms showing the ECCS/radwaste pumps and possible tortuous paths for gaseous effluents if the drywell liner were to fail at the sandbed region, which is in that vicinity. The videotaping of the walk-through was narrated with all measurements spoken out, and this was found to be extremely valuable to the whole team.

3.3 CONTAINMENT SYSTEMS ANALYSIS

All of the active containment and reactor building systems (e.g., drywell sprays, SGTS, etc.) that are important in Level 2 analysis are included in the front-end event trees described in Level 1 analysis. These systems are included in the front-end trees to ensure proper treatment of system dependencies between the front-end safety systems that are needed for preventing core damage, the containment systems, and support systems that tie together both types. For example, electric power, instrument air, component cooling water, and safeguards actuation systems mutually support both the core damage prevention and the containment safeguards systems. Considering these systems in the Level 1 event trees simplifies the implementation of dependencies.

Another reason for putting the active containment systems in the Level 1 model is that the resulting CETs are left to examine primarily phenomenological issues. This is important because the probabilities assigned to the CET have a meaning that is entirely different from the probabilities assigned to random variables, such as whether a system will work in the plant event trees.

Finally, it should be noted that, even though the containment systems are included in the Level 1 model, information on the status of these systems is passed into the Level 2 model in the definitions of the plant damage states or directly if the containment event tree is linked to the frontline trees as was performed in this study. This is explained more fully in Section 5.

3.4 REFERENCES

3-1. U.S. Nuclear Regulatory Commission, "Severe Accident Risks: An Assessment of Five U.S. Nuclear Power Plants," NUREG-1150, June 1989.

3-2. GPU Nuclear Corporation and PLG, Inc., "Oyster Creek Probabilistic Risk Assessment (Level 1)," Vols. 1 through 6, November 1991.

Table 3-1 (Page 1 of 2). Basic RCS and Containment Comparison Table		
Plant Name **Type of Reactor** **Type of Containment**	**Peach Bottom** **BWR/4** **Mark I**	**Oyster Creek** **BWR/2** **Mark I**
Reactor Core		
Thermal Power (MWt)	3,293	1,930
Number of Fuel Assemblies	764	560
Number of Control Rods	185	137
Reactor Vessel		
Inside Diameter (inches)	251	213
Inside Height (feet)	72.92	64
Design Pressure (psig)	1,250	1,250
Number of Safety Valves	2	9
Lowest Safety Valve Setpoint (psig)	1,230	1,224
Safety Valve Capacity (klb/hr)	925	654
Number of Relief Valves	11	5
Lowest Relief Valve Setpoint (psig)	1,105	1,070
Relief Valves Capacity (klb/hr)	889	558
Reactor Coolant Recirculation		
Number of Loops	2	5
Number of Pumps	2	5
Inlet Pressure (psig)	1,148	1,025
Outlet Pressure (psig)	1,326	1,065
Number of Jet Pumps	20	0
Flow Rate per Pump (gpm)	45,200	32,000
RHR System		
Number of Loops	2	3
Number of Pumps	4	3
Flow Rate per Pump (gpm at psid)	10,000 at 20	3,000 at 20
Number of Heat Exchangers	4	3
Maximum Capacity of Heat Exchanger (Btu/hr) per Two Heat Exchanger Set	70,000,000	11,000,000 per Heat Exchanger
RHR Service Water System		
Number of Pumps	3	2
Flow Rate per Pump (gpm at psid)	14,000	6,000

Table 3-1 (Page 2 of 2). Basic RCS and Containment Comparison Table		
Plant Name **Type of Reactor** **Type of Containment**	**Peach Bottom** **BWR/4** **Mark I**	**Oyster Creek** **BWR/2** **Mark I**
Core Isolation Cooling System		
Type	RCIC	None
Capacity (gpm at psid)	616 at 1,120	
Emergency Injection Systems		
Number of HPI Pumps	1	
Flow Rate per Pump (gpm at psid)	5,000 at 1,120	
Number of LPI Pumps	4	0
Flow Rate per LPI Pump (gpm at psid)	10,000 at 20	
Number of Core Spray Pumps	4	2
Flow Rate per Core Spray Pump (gpm at psid)	3,125 at 122	3,400 at 110
Containment		
Drywell Material and Construction	Steel	Steel
Drywell Free Volume (ft^2)	175,800	180,000
Drywell Design Temperature (°F)	281	281
Wetwell Material and Construction	Steel with Steel Liner	Steel
Wetwell Minimum Free Volume (ft^3)	127,000	121,300
Wetwell Minimum Water Volume (ft^3)	123,000	82,000
Wetwell Design Temperature (°F)	281	150
Design Pressure (psig)	56	35
Vent Configuration	Diagonal large-diameter pipes ending in ram's head distribution manifold and vertical piping venting below the water level of the pool.	Diagonal large-diameter pipes ending in ram's head distribution manifold and vertical piping venting below the water level of the pool.

4. PLANT MODELS AND METHODS FOR PHYSICAL PROCESSES

4.1 INTRODUCTION

In this section, the overall methodology used for the analysis of the severe accident scenarios will be presented, and the various models that impact the course of the accident will be discussed. . .

It was decided to use the MAAP code as the basis of the methodology rather than using comparative analysis with similar plants because of the specific features of Oyster Creek (isolation condensers, nonjet pumps plant, etc.) that were not part of the BWRs analyzed in NUREG-1150. An Oyster Creek-specific parameter file for MAAP was built, with special adaptation to BWR-2 features, which will be discussed in this section.

The impact of MAAP phenomenological models will be discussed first, followed by Oyster Creek-specific features, and, lastly, by a discussion of important physical process inputs. MAAP3.0B, Rev. 7.03, was used in this analysis.

4.2 IMPACT OF MAAP PHENOMENOLOGICAL MODELS

It is not intended here to explain the various MAAP models, as these are well documented in Reference 4-1 but, rather, to discuss the various model options available in the code and the rationale used to choose the specific options in the code for the analyses of the different scenarios. The same chosen options were used throughout.

4.2.1 Core Flow Blockage

The no-blockage option was used throughout. The choice was based on maximizing hydrogen production in order to maximize containment pressure and to arrive at a conservative containment failure pressure. This is based on the fact that more steam zirconium reaction results in more energy generated and more hydrogen, which, combined, would result in higher containment pressure.

4.2.2 Lower Head Failure

The MAAP lower head failure criterion is based on penetrations temperature reaching the melting point when using the mechanistic corium freeze model. When the freeze mode is not used, a hardwired, few-minute delay in vessel failure is used after core slumps into the lower head. The mechanistic freeze model option was chosen. In both of these models, lower head will fail even though it is full of water, which is quite conservative compared to TMI Unit 2 experience. It is recognized that when the core slumps into the lower head (part of it) and if the lower head is full of water (as it usually is), steam will be generated because of the corium decay heat. This steam will rise through the remainder of the core, reacting with it and producing more hydrogen and energy.

A sensitivity analysis was carried out to investigate hydrogen generation if the lower head failure criterion is adjusted to delay lower head failure until it goes dry. In this study, the local nodal blockage option was used in which the zirconium steam reaction is turned off at the core node

undergoing melting, which is a more realistic assumption than the no-blockage where this reaction is not turned off at all. The results of the study showed that the hydrogen generated in this case is approximately the same as that generated when using the no-blockage option and the freeze model with MAAP lower head failure criterion. It was therefore decided to use these two options combined to produce a conservative response.

4.2.3 In-Vessel Recovery

MAAP was not used to investigate in-vessel recovery under damaged core conditions. It was felt that the behavior of the different thermal-hydraulic and conduction models is not well understood under degraded core geometry. In addition, the code was not used for Level 1 success criteria where RETRAN/RELAP5 results were mainly used where needed.

4.3 OYSTER CREEK MAAP MODEL DISCUSSION

4.3.1 Nodal Arrangement

The MAAP nodalization is hardwired, and it was designed for jet pump plants. The Oyster Creek external recirculation loops were represented by a single jet pump with an equivalent area and effectiveness. The MAAP nodalization prohibits breaks in the recirculation loop's node, and such breaks in jet pump plants are made in the downcomer vessel wall, resulting in inventory loss mainly from the downcomer region. For Oyster Creek external loops, a break in a recirculation pump causes inventory loss from the downcomer and lower plenum at the same time through the two sides of the break.

The approach used to represent scenarios with such breaks properly and conservatively was to put the break into the lower plenum region with a break area equivalent to a double-ended break.

4.3.2 Isolation Condenser Model

The MAAP isolation condenser model is a table look-up of heat removal rate versus reactor vessel pressure. Based on GPU experience, such a representation is not adequate because isolation condenser heat removal rate is also a function of vessel level. Based on RELAP5 (MOD2) analysis of isolation condenser effectiveness as a function of pressure and level, a conservative table was chosen for use in MAAP. Conservatism here means minimum heat removal rate.

4.3.3 Other Oyster Creek-Specific Features

The other specific features used were the ATWS level versus power table where a RELAP5 (MOD2) plant-specific table was used. A pump coastdown table for ATWS analysis was also used. This was based on actual plant startup test data for power behavior during recirculation pump trip and transfer to natural circulation.

4.3.4 Summary of Cases Analyzed

A total of seven key plant damage states were finally arrived at and may be grouped as follows:

1. Three station blackout cases: high pressure SBO, low pressure SBO, and an SBO with a bypass LOCA.

2. Two bypass LOCAs (one of them also has a TW sequence).

3. ATWS.

4. DBA LOCA with no ECCS.

4.3.5 Reactor Building Model

No reactor building model was used in the MAAP analyses, and reactor building effectiveness was assumed to be zero (not effective). This is because the containment failure mode analysis showed that the dominant failure mode is a catastrophic one, and the probability of a leak before break is very small. Therefore, when the containment fails, the reactor building will be pressurized, thus failing the blow-out panels and opening a path to the environment, rendering the reactor building ineffective.

4.3.6 Major Assumptions

No major assumptions were made with regard to MAAP models other than those stated above. All code parameters representing physical processes used in the parameter file were those recommended by EPRI.

4.4 IMPORTANT PHYSICAL PROCESS INPUT

The important boundary conditions used that influence physical process behavior are discussed in the following subsections.

4.4.1 Containment Failure/Leak Area

The failure area was based on an actual release path area, which consists of drainage pipes from drywell liner/concrete gap at sand region to torus room. The area used for this region was 1 ft^2. The containment failure mode analyses (Section 6) showed that drywell head lift-off is not the dominant failure mode. Thus, no drywell flange leakage analysis was made.

4.4.2 Isolation Condenser

The isolation condenser model had to be turned off by the user when it becomes ineffective. The criteria used were when vessel pressure was less than 100 psi or when hydrogen mass in vessel was greater than 10 lbm. The pressure limit was based on in-house RELAP5 experience, while the hydrogen limit (in high pressure scenarios) was based on judgment assuming that such noncondensibles will migrate to the isolation condenser steam pipe where they get trapped, rendering it ineffective.

4.4.3 ATWS Power

During the ATWS scenario, it was assumed that when level drops to 40% core height, the core becomes subcritical, and decay heat is used.

4.5 REFERENCES

4-1. *MAAP 3.0B Computer Code Manual,* EPRI NP-7071-CCML.

5. BINS AND PLANT DAMAGE STATES

5.1 SELECTION OF PLANT DAMAGE STATE PARAMETERS

To define the plant damage states for the Oyster Creek PRA, a CET was developed (see Section 7), and the information from the Level 1 model that was needed to evaluate the split fraction values for the CET top events was identified for inclusion in the PDS coding. The relevant phenomenological issues addressed in the Peach Bottom Unit 2 severe accident risk evaluation (as described in NUREG/CR-4551) were considered in the development of the Oyster Creek CET.

The CET considers the influence of physical and chemical processes on challenging the pressure boundary integrity of the containment and, should containment failure or bypass occur, on affecting the release of fission products into the environment. The considerations include those that influence the in-vessel core melt progression, the potential for in-vessel recovery, the characterization of dynamic pressure and thermal loads occurring during or shortly after vessel breach, the characterization of long-term loads, the timing and mode of containment failure, and, should containment failure or bypass occur, the potential mitigating effects of the reactor building, the reactor building fire sprays, and the SGTS on the release of fission products into the environment. To capture these conditions, the pertinent plant damage state information falls into three general categories:

- The physical conditions in the reactor coolant system (RCS) and the primary containment at the time of vessel breach.
- The integrity of the primary containment and the status of its associated active systems.
- The integrity of the secondary containment (i.e., the reactor building) and the status of its associated active systems.

5.2 PLANT DAMAGE STATE DEFINITION

The physical conditions of the reactor coolant system and the primary and secondary containment that define the plant damage state are described below. It should be pointed out that the Level 1 analysis, in principle, ends at the onset of significant core damage; i.e., the top of the active fuel is uncovered, and vessel water level is continuing to drop. The Level 2 analysis will address recovery actions that will limit core damage and prevent vessel breach. The term "at the time of vessel breach" implies that in-vessel recovery has not been successful.

The physical conditions in the RCS and the primary containment are as follows:

- **Pressure inside the Reactor Pressure Vessel at the Time of Vessel Breach.** This is an important parameter because high pressure can more forcefully eject molten debris through penetrations in the vessel bottom head, and the blowdown jet can more forcefully remove debris from the reactor pedestal region. High pressure can also result in more vigorous zirconium oxidation as the in-vessel

steam passes through the debris during blowdown (although this may not be a large effect since it takes place over a short time). A pressure of approximately 300 psia has been identified as the breakpoint below which high pressure effects are no longer a concern.

In many scenarios, the distinction between vessel pressure at the onset of core damage and the pressure prior to vessel breach is unnecessary, especially when only the general descriptions "high" and "low" are used. However, because of the potential importance of high pressure melt ejection, it is necessary to track in the Level 2 analysis the possibility of reducing vessel pressure due to the possibility of EMRVs or safety valves sticking open due to frequent cycling. Thus, for high pressure cases, the Level 2 analysis assumes that the vessel pressure coming out of the Level 1 analysis is that at the onset of core damage.

- **Presence of Water on the Drywell Floor.** The accumulation of a substantial amount of water on the drywell floor and in the in-pedestal sumps is important to containment response because the interaction with hot core debris when vessel breach occurs can have the following effects:

  - Providing a mechanism to quench initially the molten debris and to prevent (or reduce the likelihood of) direct thermal attack of the drywell shell, or the concrete drywell floor by core debris.

  - Fragmenting and dispersing the core debris from the pedestal region into other containment volumes including the torus.

  - Causing the containment pressure to increase by formation of steam and heatup of the containment atmosphere.

  - May enhance the release of some fission products from the fuel caused by the oxidation of fine particulates.

  Water will be present on the drywell floor for most LOCA initiators and, for non-LOCA initiators, by containment spray actuation prior to vessel breach (discharging through the drywell spray spargers). Safety valve discharge is assumed to provide insufficient inventory of condensed steam to significantly affect the above factors.

The primary containment conditions that are considered in the plant damage state matrix are as follows:

- **Containment Pressure Boundary Integrity Status.** Containment pressure boundary integrity at the onset of core damage not only includes addressing concerns related to containment isolation failures and potential containment bypasses but also considers the possibility of early or late containment failures occurring prior to core damage. Containment isolation signals are generated by high drywell pressure or low-low reactor water level. A potential cause for early containment failure could be an unmitigated ATWS event with the vessel isolated. Late containment failures can occur in isolation events

with no isolation condenser cooling, core cooling with decay heat being transferred to the suppression pool, but no suppression pool cooling or venting.

- **Availability of Water To Cool the Core Debris.** Water can be provided to cool core debris (which has melted through the vessel lower head and is located on the drywell floor or sumps) by either the containment spray system injecting through the drywell spray spargers or water being injected into the vessel and (after vessel breach and depressurization) flowing through the failed portion of the lower vessel head onto the drywell floor. If water is available for debris bed cooling, a distinction is made about whether that water is provided by drywell spray because enhanced fission product washout may be important to the evaluation of source terms in the Level 2 analysis; drywell spray will also reduce the likelihood of drywell liner melt-through, especially if it is initiated prior to vessel breach.

- **Suppression Pool Cooling.** If water is available for debris bed cooling, the decay heat and chemical energy generated in the core debris will be transferred to the suppression pool in the form of steam and/or water passing through the vent system. In such a case, the availability of suppression pool cooling (through use of the containment spray system and their associated heat exchangers) is an important plant damage state parameter.

- **Containment Venting.** In core damage scenarios that do not have water available for debris bed cooling or suppression pool cooling, drywell temperature and pressure will increase, and the emergency response team has the ability to actuate the containment vent system to prevent containment failure. The human actions to implement this venting (often referred to as "dirty venting") will be addressed in the Level 2 analysis, but the availability of any power supplies required to open the vent valves must be determined from the Level 1 analysis.

The secondary containment conditions that are considered in the plant damage state matrix are as follows:

- **Reactor Building Isolation and Integrity.** For core damage scenarios that may eventually result in primary containment failure, the reactor building can be effective in reducing the offsite consequences if it is properly isolated and intact. Reactor building isolation signals are generated from high drywell pressure, low-low reactor water level, or high reactor building ventilation radiation. Thus, the Level 1 analysis must evaluate reactor building isolation as a plant damage state parameter. The reactor building is designed for a +0.25-psi internal pressure; pressures greater than this are relieved by blowout panels located above the refueling floor.

- **Standby Gas Treatment System (SGTS).** The SGTS is designed to maintain a slightly negative pressure in a properly isolated reactor building by a filter/fan system taking suction from the building and exhausting up the plant stack. The SGTS is initiated on high drywell pressure or high reactor building ventilation radiation signals. The availability of SGTS is evaluated in the Level 1 model and is a plant damage state parameter. If the reactor building is not isolated, the SGTS is judged to be ineffective, and its status is not questioned.

- **Availability of Fire Water System in Reactor Building.** The availability of fire water for alternate water supplies for core damage prevention is currently addressed in the Level 1 model. In core damage scenarios that result in containment failure, fire water spray in certain areas of the reactor building may provide a means of source term mitigation. Thus, the availability of fire water in the reactor building lines (not the initiation of spray, which will be addressed in the Level 2 analysis) is a plant damage state parameter regardless of the status of reactor building isolation or SGTS operability.

It should be noted here that the above plant damage state descriptions may, in some cases, seem to be overprescriptive and, in other cases, underprescriptive. One example might be the case wherein the containment is isolated, drywell sprays are operable, and suppression pool cooling is available. One could ask why we need to know the status of the reactor building, SGTS, and fire sprays in such a scenario when (on the surface, at least) you would not expect containment failure because all containment safeguards are available. However, the containment event tree will address the possibility of containment failure due to the dynamic loads occurring at vessel breach; e.g., direct containment heating or drywell liner melt-through. If containment failure does occur, these reactor building systems may provide mitigation function.

Another example may be why reactor building fire spray status is tracked. The effectiveness of fire sprays on source term mitigation will be dependent on the predicted location of containment failure (or release location for containment bypass events) and the expected release path through the reactor building; e.g., the blowout panels. If the release path does not pass through a sprayed zone (or if the release is not expected to actuate spray), then sprays may be unimportant.

An example of where the plant damage state parameters are underprescriptive may be unique to a plant with isolation condensers. Consider a core damage scenario wherein the vessel is isolated, the isolation condensers actuate (i.e., the condensate return line valve opens) but the shell sides dry out, vessel pressure remains high, and there is no high pressure makeup. In such a scenario, core uncovery would eventually occur. Temperature levels in the upper portion of the reactor vessel at the "onset of core damage" (when the Level 1 analysis transfers to Level 2) would not be excessive. However, as core uncovery continues and severe core damage progresses, very high temperatures can develop in the vessel, and high pressures will persist until vessel breach occurs. In such a scenario, the Level 2 analysis must evaluate the likelihood of isolation condenser tube failure (due to sustained high temperatures and pressures) and whether they can be isolated on both the steam and condensate side either automatically or manually; isolation condenser tube failures can lead to containment and reactor building bypass. This concern was evaluated for Oyster Creek, and it was determined that thermally-induced bypass via the isolation condenser and its steam piping is extremely unlikely (see Section 7.2.2, Top Event 3).

5.3 COMPREHENSIVE PDS MATRIX FOR OYSTER CREEK

Based on the preceding considerations, a four-character plant damage state coding system has been developed for the Oyster Creek PRA. The plant damage state matrix is presented in Figure 5-1.

The first character of the code is a letter from M to P, which signifies:

1. The pressure in the RPV at that time of vessel breach. (M and N denote high pressure, and O and P denote low pressure.)

2. Whether water is on the drywell floor at the time of vessel failure. (M and O have abundant water on the drywell floor, whereas N and P have an essentially dry drywell floor.)

The second character of the code is one of four letters relating to the status of the containment at the onset of core damage:

- **I.** Containment is isolated and intact at the time of vessel breach.

- **J.** Containment is bypassed.

- **K.** Containment is not isolated or fails prior to core damage within a few hours of event initiation.

- **L.** Late failure, typically caused by suppression pool cooling failures that cause consequential core damage.

The third character of the code is a letter (A through H), indicating the status of active plant systems affecting primary containment performance. This characterization identifies if debris cooling, suppression pool cooling, and/or torus venting are available.

The fourth character of the code is also a letter (U through Z), indicating the condition of the reactor building and its systems at the onset of core damage.

Plant damage states are assigned to each core damage scenario in the Level 1 quantification using RISKMAN end state binning rules. These binning rules are based on the status of preceding top events (e.g., whether they succeed or fail) and, in some cases, on the initiating event. The total number of possible plant damage states, as noted in Figure 5-1, is quite large. After Level 1 quantification is performed, a process known as "conservative condensation" will be used to combine the frequencies of lower frequency and consequence states with those having higher frequency and consequence. This allows the development of a more manageable number of key plant damage states, as described in Section 8.1. Detailed accident progression analyses will be conducted for the representative sequences in key plant damage states to determine the timing of core degradation and vessel breach; the loads imposed on the containment; and an evaluation of the timing, probability, and mode of containment failure as well as the consequence mitigation provided by the reactor building if containment failure occurs.

Figure 5-1. Oyster Creek Plant Damage State Matrix

			Containment Conditions at Onset of Core Damage																
			Intact (I)								Bypassed (J)		Not Isolated or Failed Early (K)			Failed Late (L)			Containment Status:
	Second PDS Digit		Yes						No		Yes	No	Yes		No	Yes		No	Water to core debris
			Yes			No			No		-	-	Yes	No	-	Yes	No	-	Drywell sprays
Conditions at the time of vessel breach:			Yes	No		Yes	No		N/A		-	-	-	-	-	-	-	-	Suppression pool cooling
Vessel Pressure	Drywell Floor	First PDS Digit	-	Yes	No	-	Yes	No	Yes	No	-	-	-	-	-	-	-	-	Torus vent available
			A	B	C	D	E	F	G	H	A	H	C	F	H	C	F	H	Third PDS Digit
High	Wet	M																	
	Dry	N																	
Low	Wet	O																	
	Dry	P																	

Note: Shaded areas indicate that these PDS combinations are not possible due to physical plant dependencies or phenomenological reasons and are included here for completeness.

Reactor Building Status at Containment Failure						
Reactor Building Isolated	Yes				No	
Standby Gas Treatment Operating	Yes		No		-	
Fire Protection Water Available	Yes	No	Yes	No	Yes	No
Fourth PDS Digit	U	V	W	X	Y	Z

6. CONTAINMENT FAILURE CHARACTERIZATION

A plant-specific containment strength analysis has been performed to determine the probability of failure as a function of internal pressure and temperature for critical failure modes of the containment. The variability in the probability of failure and the sizes of the leak areas were also estimated. Details of the overpressure capacity analysis of the Oyster Creek containment structure can be found in Appendix A. The capacities are reported as probabilistic quantities in terms of median failure pressures and their associated variabilities.

Several potential failure modes were investigated for the containment by estimating the median pressure capacities. The controlling failure modes were identified by ranking them according to their estimated median pressure capacities. For the critical failure modes, the variabilities in the pressure capacities were estimated, which allowed for the probability of failure to be described as a function of pressure. In addition, failure modes were evaluated for high temperature conditions.

The Oyster Creek pressure capacity was evaluated using limit state analysis for the various modes considered. The pressure capacities for the individual failure modes are dependent on several factors, including material properties, modeling assumptions, and postulated failure criteria. A major source of uncertainty is the expected strain resulting in failure.

Since many of the base parameters are random and the methods used to evaluate capacities are subject to some uncertainty, the pressure capacity for any failure mode is also considered to be a random variable. It is assumed that the pressure capacities have a lognormal distribution. With the pressure capacity assumed to be a lognormal random variable and denoting it as P, the probability of failure occurring at a pressure less than a specific value p can be expressed by

$$P_f = \text{Prob}(P \le p) = \Phi\left[\frac{\ln(p/\hat{P})}{\beta_C}\right]$$

where

P_f = the probability that failure occurs at a pressure $P \le p$.

P = the random pressure capacity.

β_C = the logarithmic standard deviation of P.

$\hat{P}$ = the median pressure capacity.

$\Phi(\cdot)$ = the cumulative distribution function for a standard normal random variable.

In the above expression, the pressure capacity for a given failure model is probabilistically described by the following expression:

$$P = P \cdot M \cdot S$$

in which P is the median pressure capacity, M is a lognormally distributed random variable having a unit median and a logarithmic standard deviation β_M representing the uncertainty in modeling, and S is also a lognormally distributed random variable with a unit median value and a logarithmic standard deviation β_S representing the uncertainty in the material properties. The overall uncertainty in the median capacity is obtained by taking the square root of the sum of the squares of β_M and β_S.

The median pressure capacity represents the internal pressure level for which there is a 50% probability of failure (leakage) for a given failure mode. The median values are evaluated from limit state analyses for the different failure modes. The uncertainties, β_M and β_S, are associated with variability due to a lack of knowledge related to differences between the analytical model and the real structure. Modeling uncertainties are associated with the assumptions used to develop analytical models and their ability to represent the failure condition properly. The strength uncertainties are associated with variabilities related to the material resistance. Examples of the sources of such uncertainties include: variability in concrete strength, steel yield strength, stress-strain relationships, and the influence of elevated temperatures on material strength.

The controlling failure modes were investigated for containment metal temperatures ranging from 300°F to 1,200°F. The potential failure modes examined included:

- Membrane failures of the drywell shell.
- Failure of the drywell head flange seal.
- Failure of the vent line from the drywell to the suppression chamber (torus).
- Failure of the suppression chamber shell.
- Failure at penetrations.

In all cases, the failure modes were considered to be the result of a quasi-static pressure loading. The pressure rise times were assumed to be sufficiently long such that the dynamic transient response of the containment structure could be neglected. Also, the material temperatures were assumed to have reached a steady state, particularly after some period of time at accident temperatures.

The capacities of the various failure mechanisms at temperatures of 300°F and 700°F are shown in Tables 6-1 and 6-2.

The failure mode identified as having the lowest median pressure capacity was found to be leakage through the bolted drywell head flange connection, which is a pressure unseating seal. The leak area develops when a gap between the flanges opens due to internal pressure in the drywell, which tends to pull apart the flanges. The flanges are held together by 96 bolts, each with a diameter of 2½ inches. The flange bolts are preloaded. To overcome the net flange compression due to bolt preload and the dead weight of the head shell, a median drywell pressure of approximately 36 psig is required. Increasing the pressure beyond 36 psig would then lead to the opening of a gap between the flanges. However, because of the presence of seal rings between the flanges, a slight separation of the flanges does not necessarily permit leakage. At lift-off pressure, the bolt tensile stress is well below yield.

For a given flange gap, the potential for leakage depends on the ability of the seal rings to maintain a seal. This ability to maintain the seal depends on the magnitude of "rebound" of the seal material as the gap opens, as well as the initial compression of the seal rings. The resiliency of the elastomer is measured in terms of its compression set, which is defined as the fraction of the initial compression that is retained as permanent deformation. After being in service, there will be some permanent set in the seal ring due to exposure to normal operating temperatures. In addition, there will also be some compression set due to increased temperatures resulting from the accident. The impact of the accident compression set is indicated by the difference between the values reported for the "instantaneous" and "70 hours" cases.

The quantification of containment failure discussed in Section 10 is based on the instantaneous values for the head flange failure mode. Since the head flange failure mode is the only failure mode that involves controlled leakage, this assumption tends to result in a greater number of early containment failures. The basis for this assumption lies in the fact that the temperature of the bolts can lag the temperature of the flange by a significant amount. It has been estimated that a 100°F lag in bolt temperature will require an additional 70 psi to separate the flanges. Estimates of the bolt temperature lag during severe accidents indicate that substantial differences in temperature may exist.

The pressure capacities of the remaining failure modes are correlated with each other.[1] Therefore, only the most limiting of these correlated failure modes (i.e., the failure mode associated with failure of the drywell shell adjacent to the region previously filled with sand) needs to be addressed (in addition to the drywell head flange failure mode) in the CET quantification.

---

[1] Except for failure of the sphere, which has a very high median failure pressure, the failure mode associated with the drywell shell adjacent to the region previously filled with sand has the greatest uncertainty (β_C), and the lowest median failure pressure of the failure modes not associated with the head flange. Correlation between two failure modes implies that the uncertainties associated with predicting the failure mode arise from similar considerations; e.g., they both use the same model or they are dependent on the same material strength data. Therefore, if one failure mode has a capacity greater than the expected mean, the other failure mode will also exhibit this tendency.

Table 6-1. Capacities of the Controlling Failure Modes at 300°F (mid-fuel cycle)			
Failure Mode*	**P (psig)**	**β_C**	**95% Confidence (psig)**
Head Flange (instantaneous)	142	0.11	119
Head Flange (70 hours)	121	0.18	90
Shell Sand Bed Region (sand removed)	134	0.22	93
Torus	153	0.22	106
Ventline Bellows	156	0.21	110
Cylinder	175	0.19	128
Cylinder/Sphere Knuckle	180	0.21	127
Ventline	192	0.21	136
Sphere	353	0.25	234
* Large, uncontrolled leak areas result for all failure modes except head flange.			

Table 6-2. Capacities of the Controlling Failure Modes at 700°F (mid-fuel cycle)			
Failure Mode*	**P (psig)**	**β_C**	**95% Confidence (psig)**
Head Flange (instantaneous)	128	0.09	110
Head Flange (70 hours)	36	0.09	31
Shell Sand Bed Region (sand removed)	109	0.22	76
Ventline Bellows	114	0.21	81
Torus	124	0.22	86
Cylinder	143	0.19	105
Cylinder/Sphere Knuckle	145	0.21	103
Ventline	156	0.21	110
Sphere	301	0.26	196
*Large, uncontrolled leak areas result for all failure modes except head flange.			

7. CONTAINMENT EVENT TREE

Given that the onset of core damage has occurred, as evaluated in the Level 1 Oyster Creek PRA, the Level 2 analysis evaluates the progression of the accident sequence from a particular PDS to a specific release category through the use of an Oyster Creek-specific CET. The PDS matrix adopted in the Level 1 analysis is described in Section 5 and is shown in Figure 5-1. The CET addresses in-vessel core degradation, the potential for in-vessel recovery of the damaged core, the phenomena associated with the ex-vessel progression of the accident, containment integrity challenges and the potential for containment failure, and, if containment failure occurs, the timing and type of failure, and the effectiveness of the reactor building and its associated safeguards (e.g., SGTS and reactor building fire spray) on the mitigation of the offsite release. For practical reasons, the CET end states are binned into a limited number of release categories in a manner that is similar to that for the binning of plant event tree end states into plant damage states; Section 11.2 describes the release category assignment process. The CET will be quantified for the representative scenario(s) associated with each key PDS. (The KPDSs are described in Section 8.1.) Although unique CETs are not required for each KPDS, the CET branching probabilities will vary, in most cases, for each.

7.1 CONTAINMENT EVENT TREE LOGIC

NUREG-1150 (and its supporting Level 2 document NUREG/CR-4551, Reference 7-1) identified 145 questions for the Peach Bottom Unit 2 Mark I accident progression event tree (APET). These include questions that relate to the type of initiating event, the status of the RCS, the availability of various safety systems, the status of containment isolation or bypass, status of the suppression pool, direct heating, location and size of the containment breach, the hydrogen discharge and burning, conditions in the reactor building, etc. Some questions are repeated for various accident phases. Many questions in the Peach Bottom APET are implicit in the definition of Oyster Creek plant damage states and therefore were not included in the Oyster Creek CET, as the tree will be quantified for each KPDS (see Section 8.1). As each of the 145 questions in the Peach Bottom APET has two or more outcomes (dependent on the PDS being evaluated and on answers to previous questions), the number of possible paths through the fully developed APET is extremely large. The development and quantification of the Oyster Creek CET have been based on NUREG-1150, the results of the EQE containment pressure capacity analysis (Section 6), and the results of core degradation, containment response, and source term accident progression analyses performed by GPU (see Section 9).

The Oyster Creek Level 2 analysis team has developed a more manageable, moderate-sized CET that captures the important attributes of the more complex Peach Bottom APET. Significant design differences between Oyster Creek and Peach Bottom that would affect the insights identified in Reference 7-1 are noted in Section 3.1.

One of the top events (VB) in the Oyster Creek CET addresses whether core damage progression is arrested in-vessel; this category of evaluation is sometimes referred to as Level "1-and-a-half" as it bridges the time frame from the onset of core damage, on the one hand, and vessel breach, on the other. The response to such a question requires sequence-specific detailed thermal-hydraulic analyses, and often there is significant uncertainty in the outcome. The ability to arrest core damage is strongly influenced by the in-vessel core degradation process, the time interval between the onset of core damage (as defined by the Level 1 analysts), and the

time when either vessel melt-through occurs or the in-vessel core debris is no longer coolable. It may also be influenced by operator actions and the availability of plant hardware. It often requires extraordinary efforts because most recovery actions that would prevent the onset of core damage have been addressed in Level 1 but have failed, thus leading to core damage. For many core damage sequences, the time interval between the beginning of core damage and vessel breach is sufficiently short in comparison with the time of core damage initiation, such that the contribution of these arrested sequences to total core damage frequency may be relatively small.

To ensure a proper characterization of risk, the event headings in a CET must provide adequate characterization of the magnitude, timing, and location of the release of radioactivity into the environment. Thus, the development and definition of CET headings and the definition of fission product release categories must be performed integratedly and chronologically. Of major importance to BWRs are such concerns as drywell liner melt-through, containment bypass, suppression pool bypass, containment spray operation, containment venting, direct heating, containment failure timing and location, size of breach, hydrogen burns in the reactor building, and the ability of the reactor building to retain fission products released into the building from the containment.

The Oyster Creek CET is shown in Figure 7-1. Descriptions of the top events are given in Table 7-1. The tree chronologically models core degradation, vessel failure (if in-vessel recovery does not occur), containment behavior, and, finally, reactor building behavior if containment failure occurs. The two-character top event designators have been selected to be different from those used in the Level 1 event trees to allow a fully integrated Level 1/Level 2 model quantification, if this is chosen in the future.

The first top event in the CET represents the entry state (i.e., the plant damage state) to the tree. The next five top events (VB through S1) address questions that are relevant to the time period starting at the initiation of core damage to the point in time when vessel breach is imminent if in-vessel arrest has not occurred.

Top Events ET to LM question phenomena that can occur in the time period during and shortly after vessel breach, and that address issues related to the potential for short-term, highly transient loading conditions that could cause early containment failure. The potentially rapid loads that could fail containment include phenomena associated with blowdown, direct containment heating effects, ex-vessel fuel coolant interactions, or drywell liner melt-through. These rapid loading functions, as a result of sudden mass and energy releases into the containment atmosphere, are characterized by a pressure "spike," as opposed to the slower, longer-term loading function such as a monotonically increasing pressure level, if debris cooling or torus cooling are unavailable.

Top Events DV through L3 address longer-term containment response and, of course, the possibility that containment failure is prevented altogether by adequate debris bed cooling, and either containment heat removal or venting.

The last two top events (HB and BE) in the Oyster Creek CET question phenomena that could affect the reactor building integrity and their ability to reduce the offsite source term when containment failure occurs.

7.2 DESCRIPTION OF CET TOP EVENTS

The following subsections describe the CET structure and the specific conditions or phenomena that are addressed in the CET top events. Section 10 will describe how the status of these events, as well as the PDS characteristics, is used to define the CET end states into radionuclide release categories.

7.2.1 CET Entry State

Top Event 0 — Key Plant Damage State (IE). The KPDS is the entry event to the CET and represents a "bin" or "group" of accident sequences from the Level 1 analysis,[2] which are expected to behave phenomenologically in a similar manner. The phenomenological behavior of the KPDS is defined by the dominant accident sequence(s) with the highest frequency within that bin. The CET applies to essentially all plant damage states. However, the CET is quantified separately for each KPDS because the top event split fractions are usually dependent on the state of the plant as defined by the KPDS.

For example, only sequences in which reactor coolant pressure is high at the time of vessel breach have the potential for significant energy transfer from the debris to the containment atmosphere, which can lead to "direct containment heating" phenomena. Most of the information related to the availability of relevant active containment and reactor building systems is passed into the tree via the definition of the plant damage state and the contributing dominant sequences. This requires that, in addition to representing the systems and functions important to maintaining core cooling, the plant (i.e., "Level 1") event tree(s) must also address those active systems and functions that are important to containment and reactor building isolation, suppression pool heat removal, the presence of water on the drywell floor at the time of vessel breach, and the availability of continued water sources for debris bed cooling.

Because of the dependence of vessel injection and core and drywell spray systems on the state of the containment (e.g., the suppression pool is a source of water for emergency core cooling pumps), there is a significant coupling between events in the plant event tree(s) and those in the containment event tree. In general, the plant damage state addresses the availability of the systems to perform their function, given that any dependency on containment states is satisfied. Implicit in the plant damage state definition are a number of factors that influence the course of events that occur in the containment following vessel breach and the resulting source term. For example, a water source for quenching and cooling the core debris is important because it affects the potential for core-concrete interactions, affects the potential for liner melt-through, provides a means for removing heat from the drywell atmosphere, and can influence the radiological source term.

7.2.2 Events Prior to Vessel Breach

---

[2] In the Level 1 analysis, core damage is conservatively assumed to occur when the core is uncovered. However, some sequences in which the core is uncovered are recoverable before fuel damage or vessel breach. These sequences are nevertheless included in the Level 2 analysis, and credit is given for in-vessel recovery; i.e., the core is assumed to be damaged, but cooling is restored before vessel breach.

Top Event 1 — Vessel Breach Prevented (VB). This top event is defined as successful prevention of vessel breach following core damage. Success of this top event indicates that the core damage progression is terminated inside the vessel, while failure of this top event results in corium penetrating the vessel. Success of Top Event VB relies on success of water to the core debris following the onset of core damage but before vessel breach in sufficient magnitude to remove decay heat. Either fire protection water delivered when the reactor vessel pressure is low or the control rod drive hydraulic system flow is 120 gpm at high reactor vessel pressure more than 1 hour after successful reactor scram is assumed to provide sufficient water to the core to prevent vessel breach.

Top Event 2 — EMRV(s) or Safety Valve(s) Sticks Open Prior to Vessel Breach in High Pressure Melt Scenarios (ES). Detailed analyses of the in-vessel accident progression for high pressure core damage scenarios indicate that (for the in-vessel quenching model) very high temperature gases pass through the EMRVs or safety valves prior to vessel breach as they cycle open-close during this period. Because of the high temperature of gases flowing through the open EMRVs or safety valves, as well as possible vapors and aerosols, it is possible that an EMRV or safety valve could fail to reseat.

Top Event ES addresses that possibility for high pressure damage states. Success of Top Event ES implies that an EMRV or safety valve sticks open. For low pressure PDSs, the EMRVs and safety valves do not cycle when elevated vessel temperature occurs; Top Event ES is set to guaranteed success for these PDS quantifications.

Top Event 3 — Containment Intact Prior to Vessel Breach (I1). This top event questions whether the containment is intact prior to vessel breach. It addresses pre-existing containment leak paths due to isolation failures, clean venting scenarios that subsequently result in core damage, or the possibility that containment failure can occur prior to core damage (as defined by the plant damage state), or any induced containment failures that could occur prior to vessel breach.

Top Event 4 — Small Leak Area if Containment Fails in Top Event I1 (L1). This event questions the containment leak area if Top Event I1 fails. For small, controlled leak areas, the potential for rapid containment pressurization at the time of vessel breach (as will be addressed later in Top Event I2) could further increase the effective leak area. For example, if Top Event I1 failure is caused by a failure to isolate a relatively small line (i.e., Top Event I1 fails and Top Event L1 succeeds), it is possible that the rapid containment pressurization at the time of vessel breach can cause a large leak to develop in Top Event L2.

Top Event 5 — Suppression Pool Not Bypassed Prior to Vessel Breach (S1). This event questions whether the suppression pool is bypassed prior to vessel breach; success implies that any releases into the drywell will be scrubbed in the torus. Potential failure modes include a stuck-open wetwell-to-drywell vacuum breaker or the possibility of a preexisting opening; e.g., a low torus failure prior to vessel breach, containment isolation failure, or an interfacing system LOCA. There are seven wetwell-to-drywell vacuum breakers, each with an equivalent area of 2.9 ft^2. This event will influence the degree of fission product scrubbing of the in-vessel and ex-vessel release. For non-LOCA events, a stuck-open wetwell-to-drywell vacuum breaker itself will not affect the scrubbing potential for the in-vessel release, unless a tail pipe vacuum breaker also sticks open on the lower setpoint pressure EMRV(s).

7.2.3 Events during or Shortly after Vessel Breach

The following four top events question phenomena occurring during or within about 2 hours after vessel breach:

Top Event 6 — Debris Not Entrained (ET). This top event addresses the uncertainties in the behavior of the debris at the time of vessel breach for a high pressure vessel melt-through. In a Mark I BWR, the suppression pool is expected to be effective in preventing a high pressure transient at the time of vessel breach, even if the debris is entrained by the blowdown gases because these gases would be directed to the suppression pool where the steam would be condensed, the debris particles would be quenched, and the noncondensible gases would be cooled and released into the torus airspace. The resulting containment pressurization would not be much different from that without debris entrainment.

The transport path for the entrained debris from the vessel to the suppression pool is very torturous. It must first pass through the control rod support grid and structures below the vessel inside the pedestal; then it must make a right angle turn out the pedestal door towards the two vent pipe deflector plates opposite the pedestal door. The entrained debris must then flow around the deflector plates into the vent pipes and again make a right angle turn into the vent pipe header and another right angle turn into the vent pipe pipes, which discharge into the torus approximately 4 feet below the water surface.

Because of this torturous flow path, only the smallest particles can be entrained all of the way to the torus. The larger particles either are not entrained at all or are deentrained at flow discontinuities. De-entrainment can occur by gravity at points in the flow path where the velocity drops, such as at the exit from the pedestal, or by inertial forces where the flow direction changes abruptly, such as around the deflector plates at the entrance to the vent pipe.

One point of de-entrainment is the right angle turn in the vent pipe where the flow enters the vent pipe header. If de-entrainment occurs at this point, the debris will collect at the end of the vent pipe, and will fill the pipe to the level of overflow into the vent pipe header. Figure 7-2 indicates the volume of debris that accumulates in the vent pipe as a function of the debris depth, measured upward from the lowest point in the vent pipe. A debris depth of approximately 28 inches could accumulate up to the bottom cusp of the vent pipe header. This would require a debris volume of about 47 cubic feet, which corresponds to about 7.5% of the volume of core solids. According to Figure 7-2, a debris depth of 12 inches only requires that about 1% of the core debris is entrained into a vent pipe. This would constitute about 2% of the debris typically expected to be ejected at the time of vessel breach. A debris accumulation of this depth would be likely to cause a melt-through of the vent pipe, causing a suppression pool bypass.

Top Event ET asks whether a sufficient amount of debris is relocated into one of the vent pipes adjacent to the pedestal opening to cause a melt-through of the vent pipe. Success means that an insufficient amount of debris is relocated and the vent pipe remains intact. Failure means that the vent pipe melt-through occurs due to debris relocation, causing a suppression pool bypass. Therefore, failure of Top Event ET causes a guaranteed failure of Top Event S3.

It should be noted that this top event may be less important in Mark I BWRs without a concrete curb to protect the drywell liner because containment failure caused by drywell liner melt-through

at the time of vessel breach may be relatively more likely. In the Oyster Creek design, the concrete curb protects the liner and renders containment failure due to liner melt-through relatively unlikely, as is discussed under Top Event LM. With a substantial likelihood of continued containment integrity at vessel breach, the question of suppression pool bypass becomes more important.

Top Event 7 — Containment Intact after Vessel Breach (I2). This top event addresses the probability of containment structural failure at the time of vessel breach or shortly thereafter (within 3 hours). Drywell liner melt-through is addressed explicitly in Top Event LM. This failure is dependent on conditions in the containment just prior to the vessel breach and the additional dynamic loading (e.g., a pressure spike and perhaps a temperature spike in the drywell atmosphere but not necessarily a significant temperature increase in the drywell shell) on the containment, resulting from the phenomenon that accompanies vessel breach; e.g., blowdown loads, direct containment heating, or ex-vessel fuel coolant interactions.

Top Event 8 — Small Leak Area if Containment Fails in Top Event I2 (L2). This top event is somewhat similar to Top Event L1, except that it addresses the equivalent containment leak area if failure occurs in Top Event I2 at or shortly after vessel breach. A large leak at Top Event L2 is defined as one that can cause a rapid blowdown into the reactor building, such as to challenge reactor building integrity. For example, a scenario in which Top Event I2 fails and Top Event L2 succeeds implies that the blowdown forces associated with the Top Event I2 failure mode are insufficient (in themselves) to cause consequential failure of the reactor building. Conversely, scenarios with Top Events I2 and L2 failed imply that the containment failure blowdown forces will, in turn, impose rapid dynamic loads on the reactor building. As the reactor building has only a 0.25-psig design pressure, it will be assumed in the event tree structure that the reactor building fails (by either the corrugated metal siding or the blowout panels located above the refueling floor), if Top Event L2 fails.

Top Event 9 — No Significant Release of Fission Products into the Reactor Building due to Drywell Liner Melt-Through (LM). This top event questions whether corium thermal attack can fail the drywell liner and, in turn, result in fission product release. Melt-through of the steel drywell shell (liner) due to contact with high temperature core debris is a key uncertainty relative to BWR/Mark I containment performance and is one of the issues specifically addressed by a panel of experts in the analyses performed for NUREG-1150. The NUREG-1150 concern appears to focus on the potential for drywell liner melt-through outside the pedestal region and the thermal attack of the liner at the elevation of the drywell floor. At Oyster Creek, the drywell liner is protected at the floor area by a 1-foot-thick curb. However, at this location, the sand has been removed. Drain pipes that connect the region that was previously occupied by the sand create a pathway for fission product release into the reactor building, if liner melt-through were to occur.

NUREG-1150 does not appear to address liner melt-through in the pedestal sump. The sump that is located inside the Oyster Creek reactor pedestal is rather deep (4.9 feet) and has a total volume of 126 ft^3 (see GE Drawing No. 4059-4). Debris that flows into the sump is unlikely to be cooled. Based on a total core UO_2 and Zircaloy volume of approximately 620 ft^3, the pedestal sump can accommodate only about 20% of the core.

In this study, Top Event LM evaluates the likelihood of liner melt-through at both locations as well as the likelihood of a significant, subsequent fission product release. It is possible that releases

via drywell liner melt-through will encounter a "tortuous" path before being released into the environment. This is especially true of those where the liner breach is associated with the sump. It is possible that debris will freeze in the cracks emanating from the sump.

The magnitude of the LM split fractions will be affected by the reactor pressure at the time of vessel breach, the presence of a significant amount of water on the drywell floor, and whether sprays or vessel injection systems are operating after the vessel breach. Success of Top Event LM implies no (or an insignificant) liner melt-through release path.

7.2.4 Long-Term Containment Events

Top Event 10 — Suppression Pool Not Bypassed Late (S3). This top event is similar to Top Event S1, except that it addresses longer term suppression pool bypass failure modes that occur after vessel breach; success implies torus scrubbing. The two principal failure modes considered are: (1) the possibility that a wetwell-to- drywell vacuum breaker sticks open even though the containment remains intact, and (2) core debris being swept into the vent system and subsequently melting through at the capped vent line ends where debris could collect.

Top Event 11 — Emergency Crew Vents Containment in Core Damage Scenarios (DV). This event questions whether the emergency response crew intentionally vents the suppression pool air space in a core damage scenario. This is sometimes referred to as "dirty venting." i.e. venting after core damage. Success of Top Event DV implies that adequate venting has occurred and that the vent flow capacity is sufficient to preclude long-term containment failure. The vent system is assumed to have insufficient capacity to accommodate an unmitigated ATWS event.

Top Event 12 — Containment Intact Late (I3). This event questions whether long-term containment integrity is maintained. Success requires that no previous failures have occurred (i.e., Top Events I1 and I2 succeed), that fission product release due to liner melt-through does not occur, and that long-term containment heat removal is available, as denoted by the PDS. Note in the event tree structure that Top Event I3 is not questioned if "dirty venting" (by success of Top Event DV) occurs. If a continued water supply is not providing debris bed cooling, corium thermal attack of the drywell floor and sumps is likely, and the containment failure would likely be in the drywell area at high temperature and moderate pressure. Suppression pool cooling would have limited benefit for these scenarios because of the limited energy transfer from the dry debris to the torus. If debris bed cooling is available (i.e., a continued water supply to the debris and abundant steam energy transfer to the torus) but suppression pool cooling is not available, a very slow containment pressurization would occur, and the failure mode would likely be at high pressure and moderate temperature; i.e., the containment would be at or near saturation conditions. Success of Top Event I3 implies no appreciable release of fission products into the environment.

Top Event 13 — Small Leak Area If Containment Fails in Top Event I3 (L3). This top event is similar to Top Events L1 and L2 but differs in two aspects. First, it applies to the longer term failure mode (well past the time of vessel breach) addressed in Top Event I3, wherein the slow pressure rise can be arrested by controlled leakage. Second, it addresses the rapidity of the containment blowdown loads, which influences the decontamination effectiveness of the reactor building as well as the rate of release of fission products into the environment.

7.2.5 Events Pertaining to Reactor Building Effectiveness

Elevation views of the Oyster Creek reactor building are shown in Figures 1-1, 1-8, and 1-9. The grade elevation is about +23 feet. The bottom floor elevation is -19.5 feet; core and containment spray pumps are located in corner rooms on the bottom floor, and the torus is supported off the floor. Intermediate floors are located at around +23 feet, +51 feet, +75 feet, and +93 feet. The refueling floor is located at +119-foot elevation, and the roof is about +170-foot elevation. The building exterior walls are poured-in-place, reinforced concrete up to the refueling floor (+119-foot elevation), and a steel frame with sealed and insulated steel siding is provided above the refueling floor.

The total reactor building free volume is 1,800,000 ft^3, and the building volumes communicate reasonably well through two stairwells and an equipment hatch. The building is designed for a 0.25-psig internal pressure; pressures above 0.25 psig are relieved by large blowout panels located above the refueling floor. The reactor building is designed and tested at each refueling outage for a maximum in-leakage rate not to exceed 4,000 CFM (or 320 volume percent per day), with a negative pressure of a 0.25 inch of water (approximately .009 psid). During plant operation, the normal ventilation system provides one air change per hour of fresh, filtered air to all areas of the reactor building.

Upon high reactor building radiation or high drywell pressure signals, the normal ventilation inlet and outlet ducts are isolated, and the SGTS is initiated. The SGTS takes suction from the isolated reactor building, maintains a negative building pressure, discharges any building in-leakage through dryers and filters, and exhausts through the plant stack. The fire protection system has sprinklers over relatively small portions of the floor areas on the +75-foot and +119-foot elevations.

For accident scenarios that result in primary containment failure, the reactor building can mitigate the offsite release. For those accident scenarios that have significant torus fission product scrubbing prior to containment failure (significant scrubbing of ex-vessel fission product aerosols will likely require debris bed cooling), a large fraction of the fission products (except noble gases) will remain in the water after containment failure, and any further reduction by the reactor building will be of less importance.

As described earlier, the reactor building is designed for a 0.25-psig internal pressure, and blowout panels located above the refueling floor are designed to relieve pressure in excess of this. If the containment failure mode results in a slow, controlled leak (as contrasted to a large, uncontrolled break) and the SGTS is operating and does not subsequently fail due to a harsh environment or excessive filter plugging, it is possible that reactor building integrity will be maintained and a slow, filtered release through the plant stack will occur. (The plant stack exhausts 345 feet above grade.) In such a scenario, one would have to address the possibility that hydrogen burns in the (uninerted) reactor building could cause building or SGTS failure.

If SGTS is not operating, reactor building failure (through the blowout panels) is considered likely regardless of the containment failure mode (although building exfiltration could keep pressure below 0.25 psig for slow containment leak cases). If SGTS is inoperable and the containment failure mode is a controlled leak with a moderately tortuous path from the containment leak location to the blowout panels, considerable fission product holdup and depletion through

settling and plateout are possible (and washout by reactor building fire sprays is also possible, if spray is actuated and the release path flows through the sprayed area), in addition to the slow and elevated release (the blowout panels are about 100 feet above grade).

If the containment failure mode is a large, uncontrolled break, reactor building failure is likely (if the leakage communicates freely to the refueling floor, the blowout panels will fail; otherwise, lower breaks are possible), and the SGTS will have little or no effect.

From the above discussion, it is apparent that the effectiveness of the reactor building in mitigating offsite releases following core damage scenarios with containment failure can range from a filtered, elevated release through the plant stack with no building exfiltration at the one extreme, to a low, direct ground-level release with no reactor building holdup at the other extreme.

Top Event 14 — No Hydrogen Burn in Reactor Building (HB). Top Event HB questions whether hydrogen released from the containment burns within the reactor building, which is not inerted. Factors that will influence Top Event HB include the amount of hydrogen produced, the composition (nitrogen, air, steam, hydrogen, CO, CO_2, etc.) and the rate of gas release from the failed containment, the possibility of localized burning at the release jet or of hydrogen accumulation, whether the SGTS is operating, whether an active ignition source is available, and the possibility of a delayed nonactive ignition. Any significant hydrogen burn will exceed the 0.25-psig design pressure of the blowout panels.

Top Event 15 — Reactor Building Effective (BE). This top event questions whether the reactor building is isolated (as denoted by the PDS) and, if isolated, if it remains intact after any containment blowdown or hydrogen burn loads. The reactor building (and its associated blowout panels) is designed for a 0.25-psig positive internal pressure. If containment failure results in a large leak or if a significant reactor building hydrogen burn occurs, reactor building failure is assumed to occur, BE success implies an elevated release at the refueling floor elevation and BE failure implies a ground level release. (Note: We will need to characterize at least three conditions here: (1) intact, SGTS filters, stack release, (2) blowout panels relieve at 119-foot elevation (no SGTS but some in-building retention with possible scrubbing from the reactor building fire sprays), or (3) low building failure, ground-level release).

The Oyster Creek containment event tree is shown in Figure 7-1. It has 15 top events (not including the entry state), 29 condensed sequences, and 563 total sequences. Quantification of the CET, including the evaluation of the conditional split fraction values, is discussed in Section 10.

7.3 REFERENCES

7-1. Payne, A. C., et al., "Evaluation of Severe Accident Risks: Peach Bottom Unit 2," Sandia National Laboratories, prepared for U.S. Nuclear Regulatory Commission, NUREG/CR-4551, Volume 4, March 1990.

Table 7-1. Oyster Creek CET Top Event Descriptions	
Top Event Designator	**Top Event Description**
IE	Key Plant Damage State
VB	Vessel Breach Prevented
ES	EMRV(s) or Safety Valve(s) Sticks Open Prior to Vessel Breach in High Pressure Melt Scenarios
I1	Containment Intact Prior to Vessel Breach
L1	Small Leak Area if Containment Fails in Top Event I1
S1	Suppression Pool Not Bypassed Prior to Vessel Breach
ET	Debris Not Entrained
I2	Containment Intact after Vessel Breach
L2	Small Leak Area if Containment Fails in Top Event I2
LM	No Significant Release of Fission Products into the Reactor Building due to Drywell Liner Melt-Through
S3	Suppression Pool Not Bypassed Late
DV	Emergency Crew Vents Containment in Core Damage Scenarios
I3	Containment Intact Late
L3	Small Leak Area if Containment Fails in Top Event I3
HB	No Hydrogen Burn in Reactor Building
BE	Reactor Building Effective

Figure 7-1. Oyster Creek Containment Event Tree

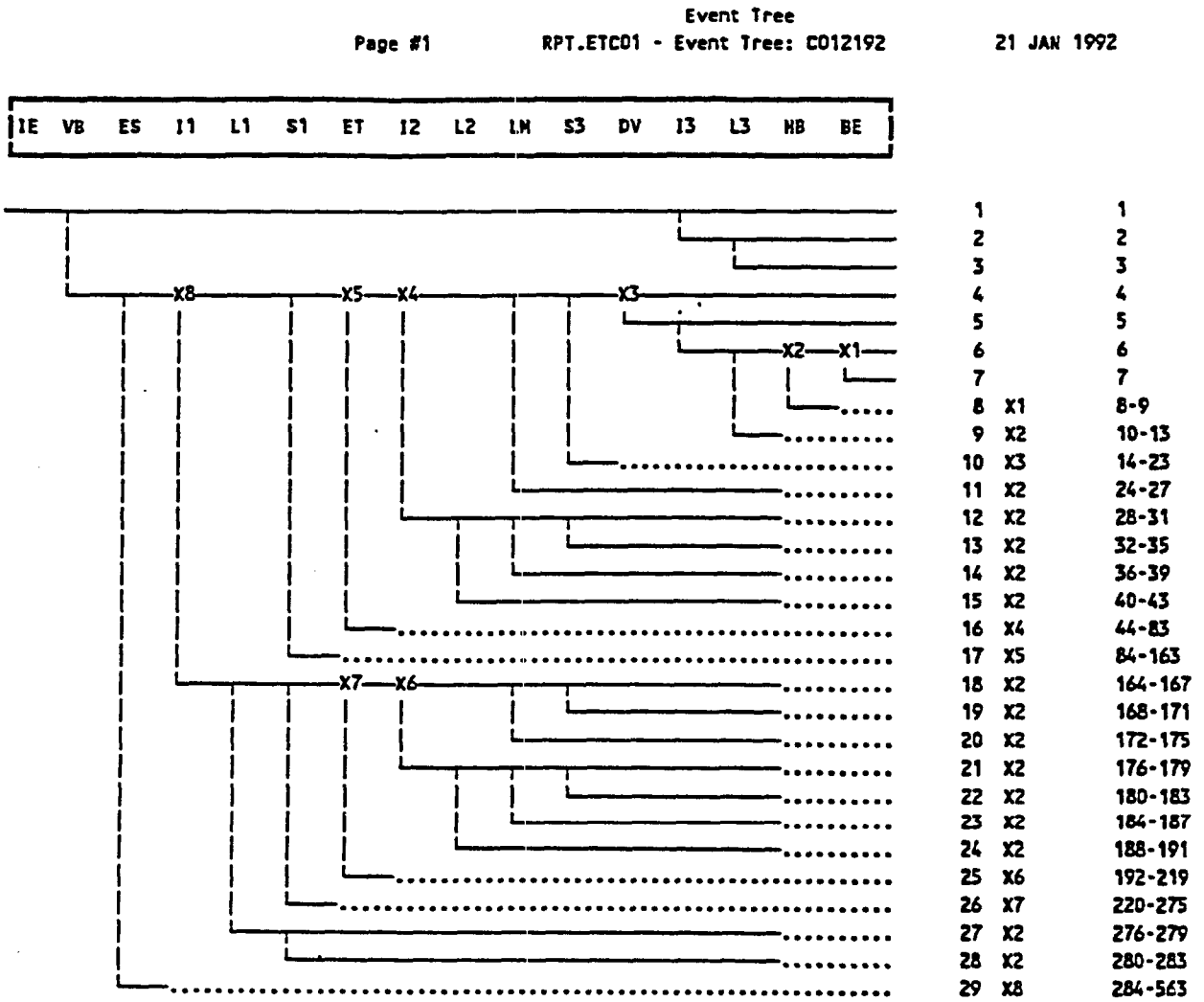

FIGURE 7.2

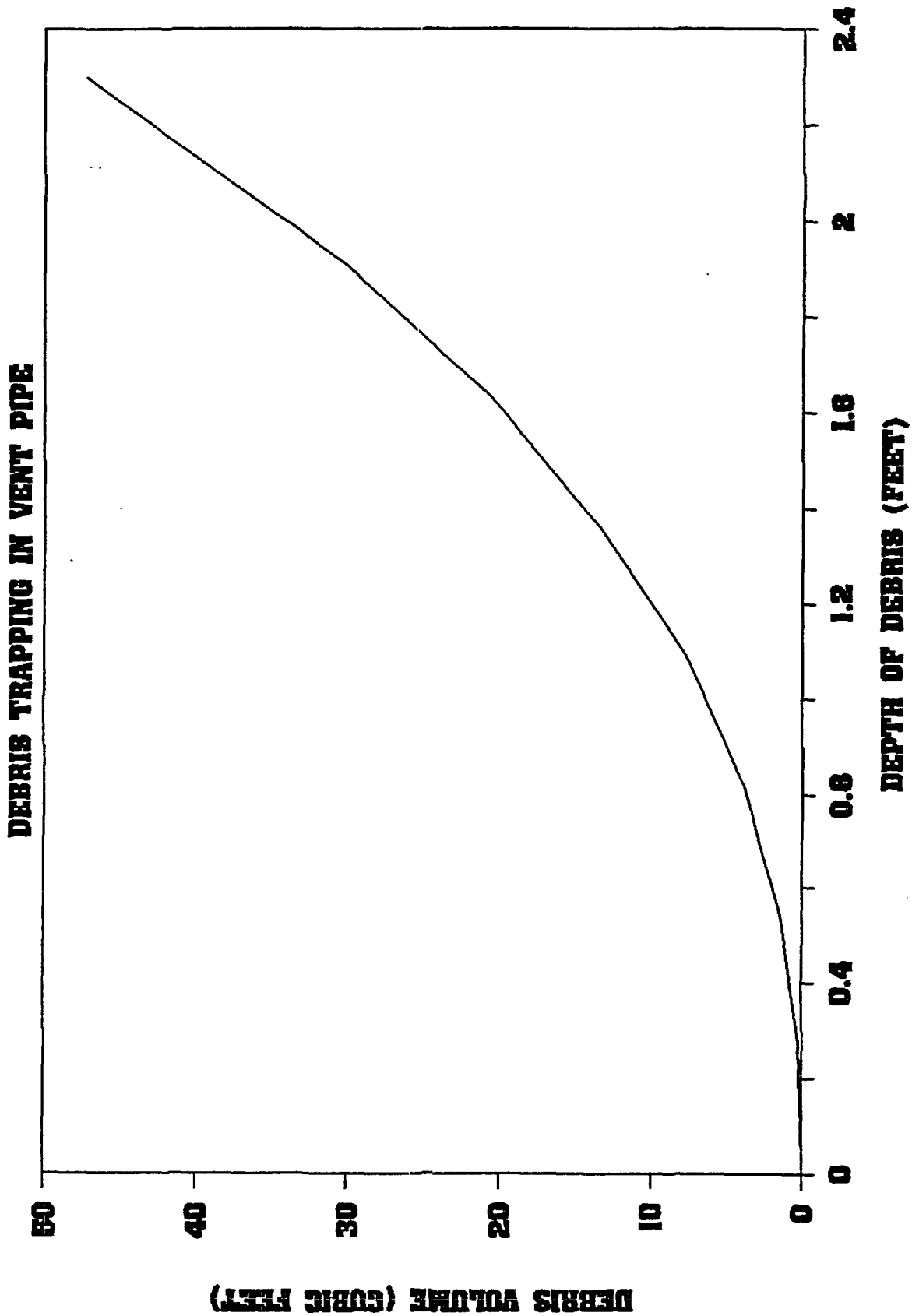
DEBRIS TRAPPING IN VENT PIPE
DEBRIS VOLUME (CUBIC FEET)
0
10
20
30
40
50
DEPTH OF DEBRIS (FEET)
0
0.4
0.8
1.2
1.6
2
2.4

8. KPDSs AND REPRESENTATIVE SEQUENCES

8.1 IDENTIFICATION OF KEY PLANT DAMAGE STATES (KPDS)

The Level 1 model quantification identified 19 PDSs with a frequency of 1×10^{-6} per year or greater [see Table C.4-1 of the Level 1 report (Reference 8-1)]. For Level 2 analysis, these PDSs are condensed into a reduced set of KPDSs. This condensation process is described in this section and is based on a conservative interpretation of the IPE reporting criteria established by the NRC in Appendix 2 of Generic Letter No. 88-20 (Reference 8-2), and it takes advantage of the known frequency and the relative severity or consequence potential for each PDS. Furthermore, in Section 2.2.2.5 of NUREG-1335 (Reference 8-3), it is stated that "all accident sequences (represented now by plant damage states or bins) that meet the screening criteria should be represented by CETs according to standard practice." Thus, the approach used in this study is believed to be in full compliance with the IPE intent.

Because the PDSs represent functional accident sequences, the KPDSs, each of which requires a detailed Level 2 analysis, are selected on the basis of the PDS frequencies in comparison to the IPE reporting criteria. Table C.4-1 of the Level 1 report shows the frequency-ranked list of PDSs.

Table 8-1 lists the IPE criteria for selecting important accident sequences and the conservative interpretation of these criteria for the Level 2 portion of the Oyster Creek IPE. The Oyster Creek IPE sequence selection criteria have been set at a factor of 10 lower than the NRC sequence frequency criteria. The IPE criteria to provide margin for the analysis and review of important sequences and to umbrella the selection criteria numbered 2 and 5 are listed in Table 8-1. In addition, this margin adds a degree of robustness to the Level 2 analysis so that changes or updates in the Level 1 models would be unlikely to require a new Level 2 analysis of any additional KPDSs in the future.

On the basis of the Oyster Creek Level 2 sequence selection criteria listed in Table 8-1, the following seven KPDSs were identified as requiring consideration in the Level 2 analysis:

KPDS	Frequency	Selection Criteria Group	KPDS	Comments
PIFW	1.13×10^{-6}	1	I	Above NRC Cutoff
NIFW	1.06×10^{-6}	1	I	Above NRC Cutoff
OIAU	5.74×10^{-7}	1	II	Margin
MKCU	1.70×10^{-7}	3	II	Margin
OJAU	1.64×10^{-7}	4	I	Above NRC Cutoff
MJAU	5.26×10^{-8}	1	II	Margin
NJHW	1.54×10^{-8}	4	II	Margin

It is noted that the PDSs states represented by the letters B, C, D, E, G, V, X, Y, and Z are not represented because they either are not possible due to system dependencies or assumptions in the Level 1 model or have frequencies below the Oyster Creek sequence selection criteria.

KPDS Group I in the above table contains the three KPDSs whose frequencies are sufficiently high that they exceed the selection criteria for important severe accident sequences in Appendix 2 of NRC Generic Letter No. 88-20. These KPDSs were given the highest priority for analysis in Level 2. The four KPDSs in group II are those KPDSs that are included because of the conservative interpretation of the selection criteria for the Oyster Creek IPE.

The first three KPDSs (PIFW, NIFW, and OIAU) identified in the above table represent scenarios in which the containment is intact at the time of vessel breach. The fourth highest frequency KPDS (MKCU) contains scenarios in which the containment fails prior to core damage. The last three KPDSs (OJAU, MJAU, and NJHW) represent scenarios in which the containment is bypassed at the time of vessel breach.

In the following section, the frequency-ranked list of systemic sequences contributing to each of these seven KPDSs is reviewed, and, for each KPDS, one base case sequence and, in some cases, one or more sensitivity sequences are selected to represent each KPDSs in the Level 2 analysis. The sequences selected for the KPDSs that are indicated to be combination candidates will be compared, and, if the lower consequence potential can be confirmed, the appropriate combination will be made.

Table 8-2 summarizes the PDSs and their frequencies that were analyzed in this study (approximately 85% of the total CDF) as well as those that were not. Of that CDF not analyzed, more than 50% of the frequency involves initially intact containments. It is likely that some of the CDF not analyzed in Level 2 would involve sequences that could be recovered prior to vessel breach. All important KPDSs involving containment bypass have been analyzed in Level 2.

8.2 SELECTION OF REPRESENTATIVE SEQUENCES

8.2.1 Category I Key Plant Damage States

8.2.1.1 Key Plant Damage State PIFW

This KPDS has a frequency of 1.13×10^{-6} per year, which represents approximately 31% of the internal events core damage frequency (CDF). Scenario No. 1 in the dominant scenario list accounts for approximately 68% of the PDS frequency and is clearly the representative sequence for this KPDS. This sequence is initiated by loss of offsite power (LOSP) and involves independent failures of both diesel generators, leading to a loss of all AC power. This power is not recovered prior to core uncovery. In addition, one of the two EMRVs that cycle to control pressure after reactor trip fails to close, causing a sustained loss of vessel inventory. A detailed description of this representative sequence is given in Section C.5.1 of Appendix C to the Level 1 report.

8.2.1.2 Key Plant Damage State NIFW

This KPDS has a frequency of 1.06×10^{-6} per year, which is approximately 29% of the total internal events CDF. The first eight sequences in this KPDS represent approximately 80% of the PDS frequency. Scenario No. 2 (accounting for 24% of the KPDS frequency), initiated by turbine trip, has been selected as the representative sequence for this KPDS. Although each of these eight sequences is caused by different initiators, they all involve independent failures of both divisions of DC power. Loss of DC power results in a station blackout. A detailed description of this accident sequence can be found in Section C.5.2 of Appendix C to the Level 1 report.

8.2.1.3 Key Plant Damage State OJAU

This KPDS has a frequency of 1.64×10^{-7} per year and represents approximately 4% of the CDF. It is also characterized by containment bypass. Scenario No. 8 has been selected to represent this KPDS since it represents approximately 44% of the PDS frequency. Scenario No. 8 is characterized by an accidental overpressurization of the RWCU with relief to both the suppression pool and RBEDT. In effect, this sequence represents a large below-core LOCA with discharge inside and outside containment. The discharge outside the containment is to the southwest corner room of the reactor building via a 1-inch-diameter valve. Scenario No. 22 represents approximately 16% of the PDS frequency and has a different release path and bypass area. Scenario No. 22 involves failure of one of the two scram discharge volumes to isolate. Detailed descriptions of these representative sequences are given in Sections C.5.8 and C.5.22 of Appendix C to the Level 1 report.

8.2.2 Category II Key Plant Damage States

8.2.2.1 Key Plant Damage State OIAU

This KPDS has a frequency of 5.74×10^{-7} per year (approximately 16% of total CDF). Dominant Scenario No. 7, which represents approximately 17% of the PDS frequency, has been selected to represent these KPDSs since the higher-ranking sequences in their KPDSs are expected to be recovered. This sequence is initiated by a large break inside the containment, with subsequent failures of both trains of core spray. Containment spray is operable and provides water to the drywell floor and debris cooling, as well as containment heat removal. A detailed description of this representative sequence for this KPDS is given in Section C.5.7 of Appendix C to the Level 1 report.

8.2.2.2 Key Plant Damage State MKCU

This KPDS has a frequency of 1.70×10^{-7} per year, which amounts to approximately 5% of the total CDF. The dominant sequences in this KPDS are ATWS sequences. Scenario No. 24 (2.23×10^{-8} per year) is initiated by a turbine trip and has independent failures of reactor scram and failure to initiate boron injection. Makeup to the vessel is being supplied by the feedwater system, and reactor heat is being rejected via the turbine bypass and to the isolation condenser. However, these rejection paths are not adequate for dissipation of all of the reactor heat; thus, the EMRVs and SRVs must cycle to control RCS pressure. Although the drywell spray and torus cooling are successful in this sequence, they are overwhelmed by the fraction of reactor power being dissipated by the suppression pool, and the containment pressurizes to failure. Failure of the

containment is assumed to result in the loss of vessel and containment instrumentation, and a severe accident environment in the reactor building, which also fails key equipment. Scenario No. 24 represents approximately 13% of the PDS frequency. A detailed description of this representative sequence is given in Section C.5.23 of Appendix C to the Level 1 report.

8.2.2.3 Key Plant Damage State MJAU

This KPDS has a frequency of only 5.26×10^{-8} per year and, although it represents only approximately 1% of the CDF, it can potentially be very important because it is characterized by containment bypass. The top-ranking sequence for this PDS is Scenario No. 25 from the dominant scenario list and represents approximately 42% of this PDS frequency. Thus, this sequence is clearly the representative sequence for this PDS. This sequence is initiated by loss of feedwater (LOFW), which is followed by independent failures of one of the scram discharge volumes to isolate and emergency depressurization. Failure of the scram discharge volume to isolate results in a LOCA outside containment, with consequent failure of one train of core spray. The control rod drive (CRD) system is assumed to be insufficient to replace vessel inventory, and fuel damage is expected within 30 minutes. Operation of the drywell sprays provides water to the drywell floor prior to vessel breach, and the remaining train of core spray provides vessel injection after the RCS depressurizes following vessel breach. A detailed description of this representative sequence is given in Section C.5.24 of Appendix C to the Level 1 report.

8.2.2.4 Key Plant Damage State NJHW

This KPDS has a frequency of 1.54×10^{-8} per year and is dominated by dominant Scenario No. 52, which represents approximately 58% of the PDS frequency. No other sequence in this PDS has a frequency greater than 1×10^{-8} per year. Scenario No. 52 is initiated by LOSP and results in core damage due to independent failures of both emergency generators and failure to isolate one of two scram discharge volumes. Failure to isolate the scram discharge volume results in a loss of coolant outside the containment at a rate of 400 to 600 gpm. Although the isolation condenser is available, makeup to the vessel is insufficient to prevent core damage. Drywell spray cannot operate, and therefore the drywell floor will not be covered by water at the time of vessel breach. A detailed description of this representative sequence is provided in Section C.5.26 of Appendix C to the Level 1 report.

8.3 REFERENCES

8-1. GPU Nuclear Corporation and PLG, Inc., "Oyster Creek Probabilistic Risk Assessment (Level 1)," Vols. 1 through 6, November 1991.

8-2. U.S. Nuclear Regulatory Commission, Generic Letter No. 88-20, December 1988.

8-3. U.S. Nuclear Regulatory Commission, "Individual Plant Examination: Submittal Guidance," final report, NUREG-1335, August 1989.

Table 8-1. Sequence Selection Criteria and Interpretation for the Oyster Creek IPE		
Sequence Group (Generic Letter No. 88-20, Appendix 2)	IPE Reporting Criterion	
	Generic Letter	Oyster Creek IPE
1. Any functional sequence with core damage frequency greater than or equal to:	$1x10^{-6}$/yr	$1x10^{-7}$/yr
2. Any functional sequence that contributes more than "x" percent to core damage:	5%	1.3%
3. Any functional sequence with containment failure leading to a release > or = to BWR-3 in WASH-1400 at a frequency > or = to:	$1x10^{-6}$/yr	$1x10^{-7}$/yr
4. Any functional sequence leading to containment bypass at a frequency > or equal to:	$1x10^{-7}$/yr	$1x10^{-8}$/yr
5. Any functional sequence judged to be an important contributor to core damage or poor containment performance:	(judgement)	(judgement)

Table 8-2. Core Damage Frequency Analyzed in Level 2									
PDS	Intact (I)		Bypassed (J)		Failed Early (K)		Failed Late (L)		Unaccounted
	Analyzed	Not Analyzed	Analyzed	Not Analyzed	Analyzed	Not Analyzed	Analyzed	Not Analyzed	Not Analyzed
PIFW	1.13-06								
NIFW	1.06-06								
OIAU	5.74-07								
MKCU					1.70-07				
OJAU			1.64-07						
MIAU		1.06-07							
PLHU								6.13-08	
OLHU								6.07-08	
PIHW		5.12-08							
MJAU			5.26-08						
MKHU						4.02-08			
OIHW		2.33-08							
PIFU		2.66-08							
Unacct									2.56-08
OIAW		2.32-08							
NLHW								1.99-08	
NIHW		2.36-08							
NJHW			1.54-08						
NKFW						1.59-08			
NIHX		7.95-09							
PIEU		9.67-09							
NKFU						8.29-09			
Total	2.76-06	2.72-07	2.32-07	0	1.70-07	6.44-08	0	1.47-07	2.56-08
Total PDS Frequency = 3.69-06 Frequency Analyzed = 3.17-06 Fraction Analyzed = 0.859									
Note: Exponential notation is indicated in abbreviated form; i.e., 1.13-06 = 1.13×10^{-06}.									

9. ACCIDENT PROGRESSION ANALYSIS

9.1 INTRODUCTION

In this section, the sequences that were analyzed using the MAAP computer code will be discussed, and important parameters will be presented. The rationale for selecting these sequences for the different KPDSs is discussed in Section 8. The ultimate goal of these analyses is to calculate the source term to the environment, which is a function of the point in time, during the accident, that release into the environment has taken place, the degree of scrubbing that took place before and after release, failure area and location, etc. Answers to such issues can only be obtained satisfactorily by analyzing these sequences and monitoring the key phenomena that influence the accident progression. The different choices made with regard to options available in the MAAP code for the different phenomena (e.g. hydrogen generation, lower head failure, etc.) are discussed in Section 4. The same options were used for all of the sequences analyzed. The actual sequences chosen are discussed in Section 8.2, and, for completeness, they will be listed here, and a discussion of the MAAP analysis will be presented below for each sequence.

The scenarios analyzed are as follows:

1. Low Pressure Station Blackout with Stuck-Open Relief Valve (PIFW)

2. High Pressure Station Blackout (NIFW)

3. Large DBA LOCA with No Core Spray (OIAU)

4. Turbine Trip ATWS with SLC Failure (MKCU)

5. Reactor Water Cleanup (RWCU) System Failure in Pressure Reducing Station (OJAU) - Bypass Sequence

6. Loss of Feedwater with Failure of Scram Discharge Volume (SDV) to isolate (MJAU) - Bypass Sequence

7. Station Blackout with SDV Failure to Isolate (NJHW) - Bypass Sequence

9.2 MAAP ANALYSES

The individual sequences analyzed will be described, and MAAP results will be presented.

9.2.1 Key Plant Damage State PIFW

The sequence chosen in Section 8.2 to represent this KPDS is a station blackout with a stuck-open relief valve (EMRV), scenario 1. The accident progresses with a scram, coupled with a turbine trip, vessel isolation, relief valves cycling with isolation condenser on (these are DC-driven), but one EMRV was assumed to stick open. As the vessel depressurizes, the only inventory source is the fire water system, which can be aligned and turned on but will not deliver

water to the core until low vessel pressure is reached. It was assumed that fire water would not be available to prevent core damage, but that it would prevent vessel breach.

A sensitivity analysis was performed to determine the latest time that fire water could be injected to prevent vessel failure. That was found to be 1 hour into the accident. As discussed in Section 3, MAAP would fail the vessel through the penetrations soon after the core slumps to the lower head (few seconds), regardless of the amount of water available, which is a very conservative behavior when compared to the TMI Unit 2 accident. For this reason, no vessel breach was assumed. It is shown in Section 10.1 that the split fraction for vessel breach is 0.0 for this scenario. This KPDS is therefore recoverable in vessel.

9.2.2 Key Plant Damage State NIFW

The sequence chosen in Section 8.2 to represent this KPDS is scenario 2, which is a station blackout that includes independent failure of all DC power. The accident progresses with a scram, coupled with a turbine trip, vessel isolation, and cycling of safety valves, which would be dumping steam into the drywell. Reactor vessel inventory will be reduced, resulting in core melt and vessel breach. (Isolation condensers and EMRVs are inoperable due to loss of DC power.) Fire water will not inject into the RPV until it depressurizes after vessel breach.

The base case was run with no containment failure, and then was followed by two cases: one with a break area in the drywell of 1 ft^2 at vessel breach, and the other with same break area at drywell mean failure pressure of 137 psia. Venting was not available. The last two cases were repeated with a stuck-open safety valve a few minutes before vessel breach (Section 11.3.3 and 11.3.5). Figures 9-1 through 9-3 show plots of important parameters, while Table 9-1 shows a summary of key events.

9.2.3 Key Plant Damage State OJAU

The sequence chosen in Section 8.2 for this KPDS is scenario 8, which involves failure of the pressure-reducing station of the RWCU system, resulting in pressure relief to the torus (6-inch pipe) and to the reactor building drain tank (1-inch pipe). This scenario basically involved a 0.2 ft^2 LOCA to the torus and a small bypass LOCA (0.8 in^2) to the reactor building at the same time (loss of containment cooling).

The accident progresses with a scram on low level, with feedwater remaining at rated flow for 3 minutes (hotwell capacity), and then switches to 10% flow (CST to hotwell flow). Isolation condenser is available while torus will heat up due to containment spray pump NPSH limits, resulting in loss of containment cooling (TW sequence) and containment pressure buildup due to water hydrostatic pressure. Torus venting was used, but torus level reached vent line elevation, resulting in vent closure and switching to drywell venting. The core will heat up and melt, resulting in vessel breach because part of the feedwater injected into the downcomer is assumed to end up in the RWCU through the recirculation piping. Fire water was injected into the RPV after vessel breach, and RWCU pressure relief terminated because RPV pressure was below the RWCU relief valve setpoint.

After vessel breach, drywell pressure will increase at a higher rate due to the presence of corium, resulting in drywell venting to maintain containment integrity. The source term in this scenario is basically due to drywell venting.

Figures 9-4 through 9-9 show plots of important parameters, while Table 9-1 shows key events.

9.2.4 Key Plant Damage State OIAU

The sequence chosen in Section 8.2 to represent this KPDS is scenario 7, which is characterized by a large break inside containment with failure of core spray. The scenario progresses with feedwater at rated flow for 3 minutes, and then switches to 10% rated flow, which goes into the downcomer and then to the lower plenum, bypassing the core. The unavailability of core spray results in core melt and vessel breach. Containment cooling is available until it is lost due to loss of NPSH because of high torus temperature after vessel breach. Fire water is not used because the core spray failure is assumed in the parallel isolation valves. Results show that late containment failure is the only mode that would be prevented through clean venting through the torus.

Figures 9-10 through 9-13 show containment pressure, temperature, and torus level, while Table 9-1 shows key events.

9.2.5 Key Plant Damage State MKCU

The sequence chosen in Section 8.2 to represent this KPDS is scenario 24, which is characterized by a turbine trip ATWS with failure to inject SLC. The sequence progresses with vessel isolation and recirculation pump trip. The recirculation pump coastdown curve was adjusted to reflect actual core power generation during recirculation pump trip and change to natural circulation. These data were taken from actual pump trip tests done during the plant startup tests. After pumps coast down, the operator is required to reduce power by reducing level and to maintain level at TAF using feedwater with the isolation condenser on. Level is reduced through safety and relief valve cycling, which involves dumping energy into the containment. Drywell sprays are operating within setpoints required by procedure until torus temperature reaches the NPSH limit for containment cooling pumps when the sprays are lost. Containment venting is not sized to remove ATWS power, and the containment pressure starts increasing. At containment failure (T=3.9 hours), all injection to vessel is terminated, which results in vessel water boil-off, core melt, and vessel breach. The ATWS power versus level table used in this analysis was based on Oyster Creek-specific RELAP5 (MOD2) ATWS analysis. The analysis was repeated with a stuck-open EMRV and a stuck-open vacuum breaker (Section 11.3.4). Figures 9-14 through 9-17 show plots of important parameters, while Table 9-1 shows key events.

9.2.6 Key Plant Damage State MJAU

The sequence chosen in Section 8.2 to represent this KPDS is scenario 25, which is initiated by a loss of feedwater, failure of scram discharge volume (SDV) to isolate resulting in a bypass LOCA, failure of ADS, and loss of one core spray train.

The accident progresses with a loss of feedwater, vessel isolation with isolation condenser on. The vessel will depressurize until core spray comes on (one system) with level maintained between low and high level setpoints. Inventory will be lost through the bypass LOCA until torus level drops by 2 feet when procedures require operator to transfer from core spray to fire water. It was assumed that this transfer will take 0.5 hours, and if it takes a few minutes, it was found that core recovery was ensured. The core will be deprived of water for 0.5 hours, which was enough to cause core damage and vessel failure. Figure 9-18 shows containment conditions, while Table 9-1 shows key events.

9.2.7 Key Plant Damage State NJHW

The sequence chosen in Section 8.2 to represent this KPDS is scenario 52, which is initiated by a loss of offsite power, failure of emergency generators, and failure of one scram discharge volume to isolate, resulting in a bypass LOCA. The accident progresses with LOSP, vessel isolation, and loss of inventory with isolation condenser on. The vessel does not depressurize low enough for fire water before core damage start to take effect. The accident therefore results in core damage and vessel breach. Figure 9-19 shows important accident parameters, while Table 9-1 shows key events.

Table 9-1. Key Events Summary			
KPDS	Time of Core Uncovery	Time of Vessel Failure (hours)	Containment Failure Time
NIFW	29.64 minutes	2.404	7.68 hours (137 psia at 500°F)
OJAU	1.067 hours	3.084	12 hours (137 psia at 510°F)
OIAU	52.5 seconds	1.004	20 hours (77 psia at 870°F)
MKCU	3.965 hours	6.512	3.9 hours (breaks at 137 psia)
MJAU	7.771 hours	10.61	None
NJHW	15.65 minutes	1.595	None

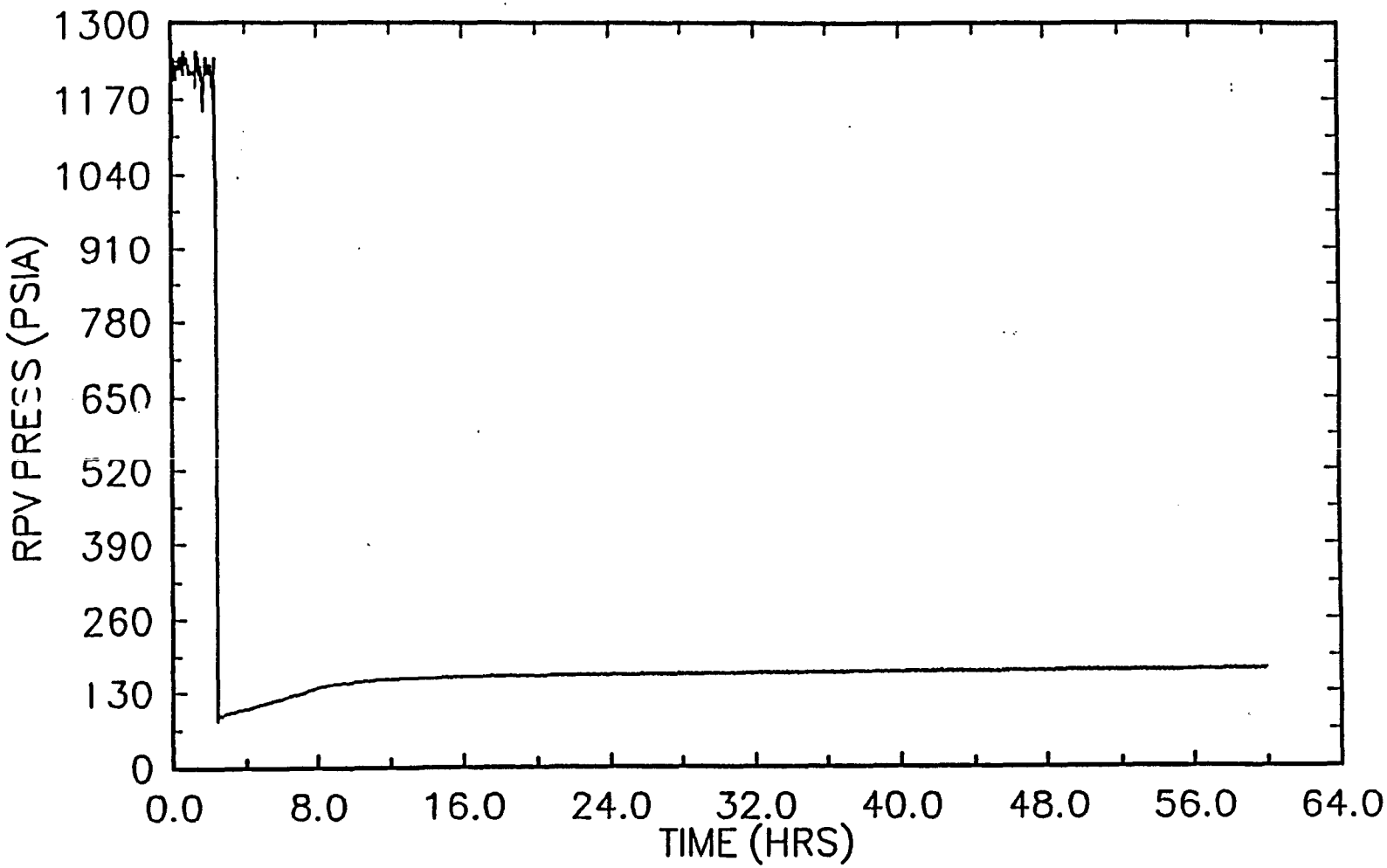

Figure 9-1. NIFW, Vessel Pressure, No Containment Failure (base case)

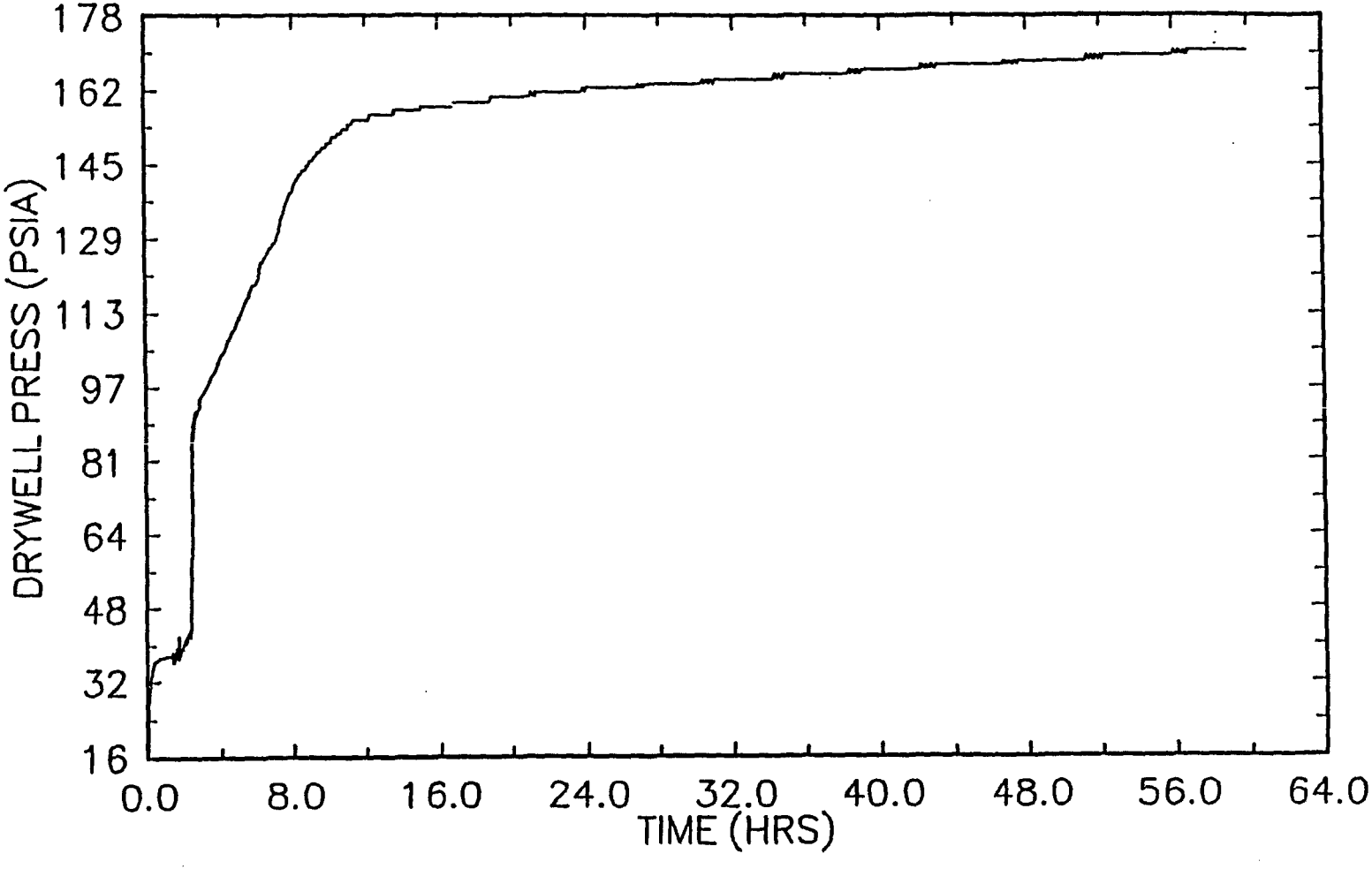

Figure 9-2. NIFW, Drywell Pressure, No Containment Failure (base case)

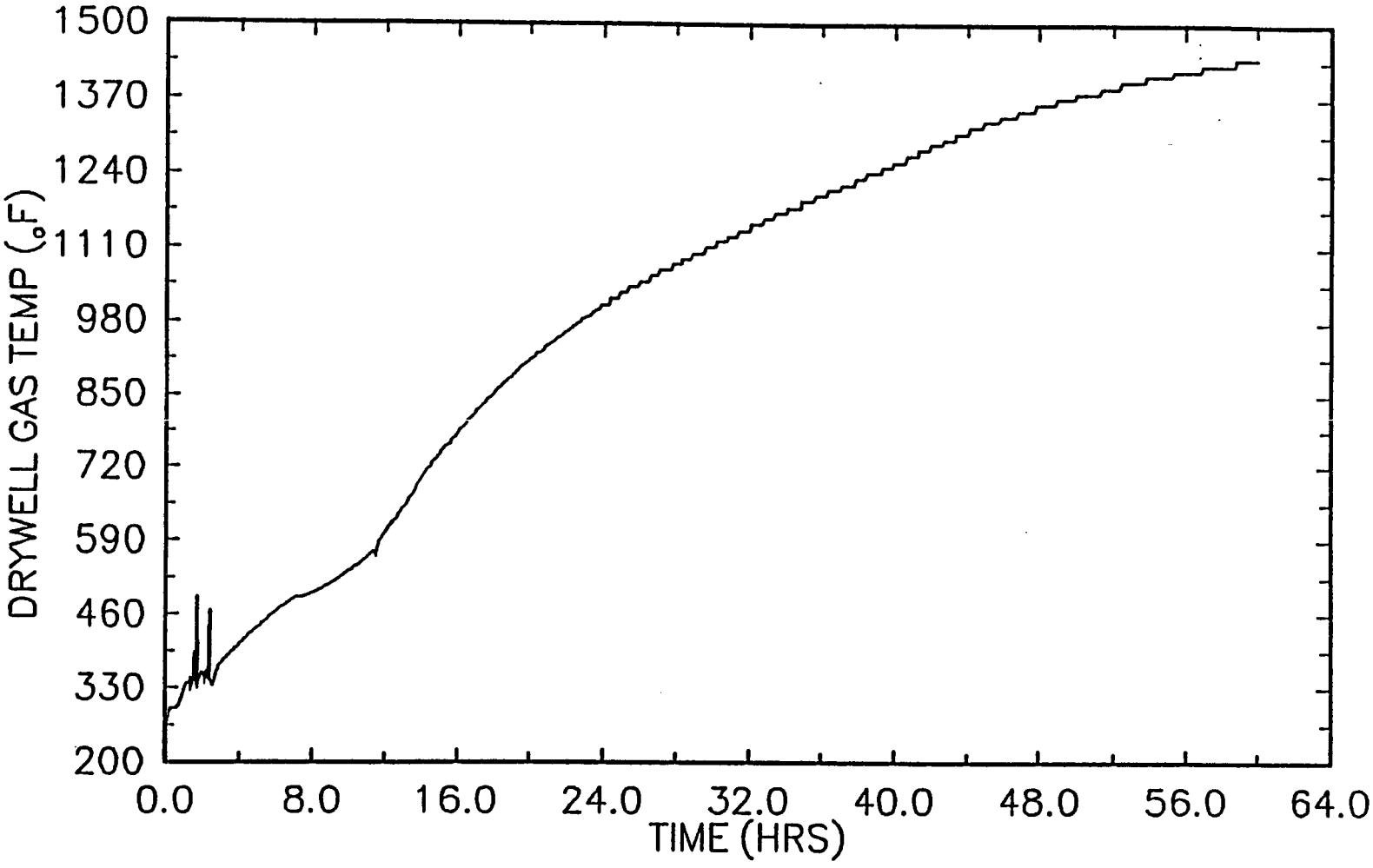

Figure 9-3. NIFW, Drywell Gas Temperature, No Containment Failure (base case)

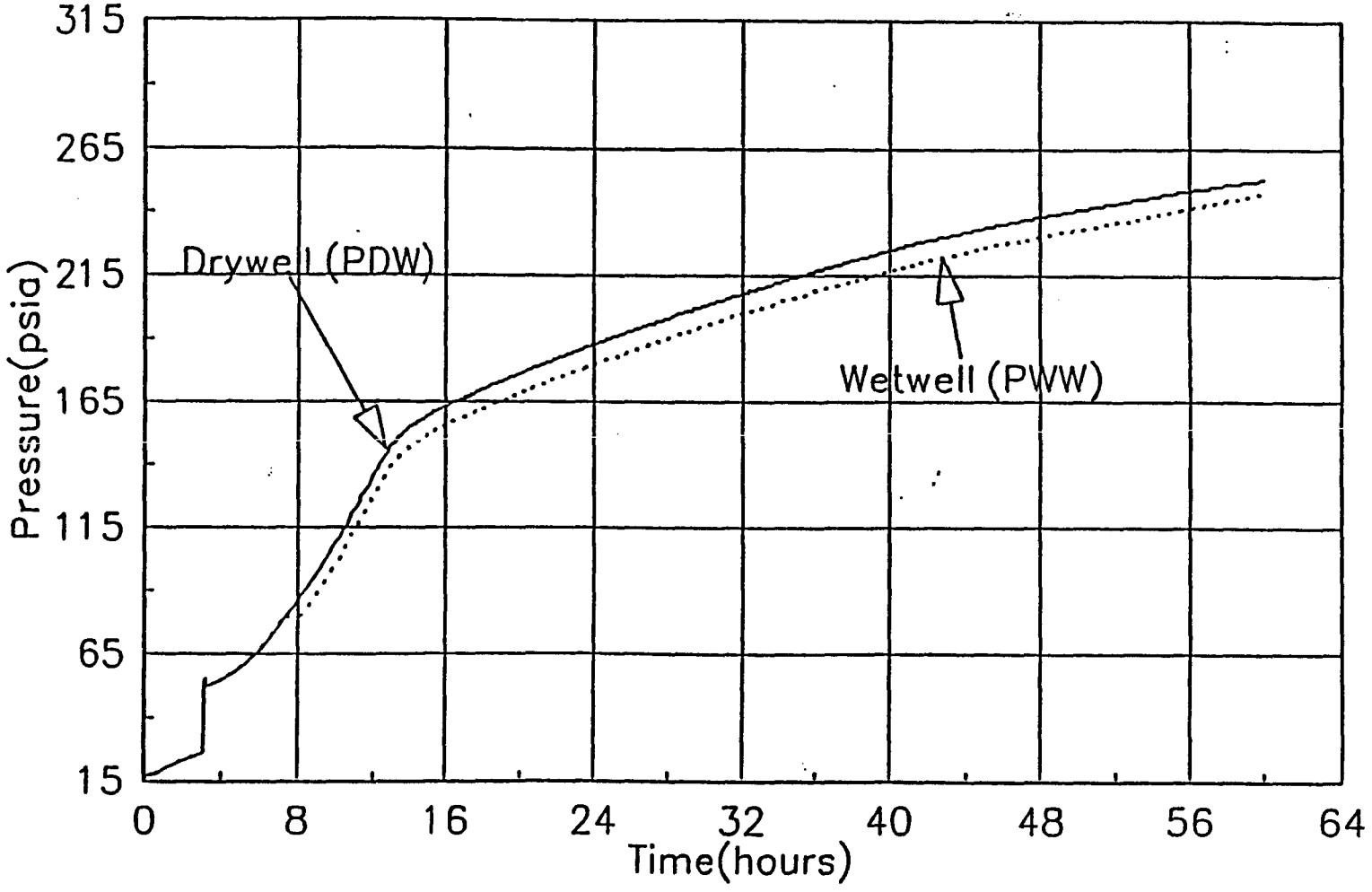

Figure 9-4. OJAU, Drywell and Wetwell Pressure

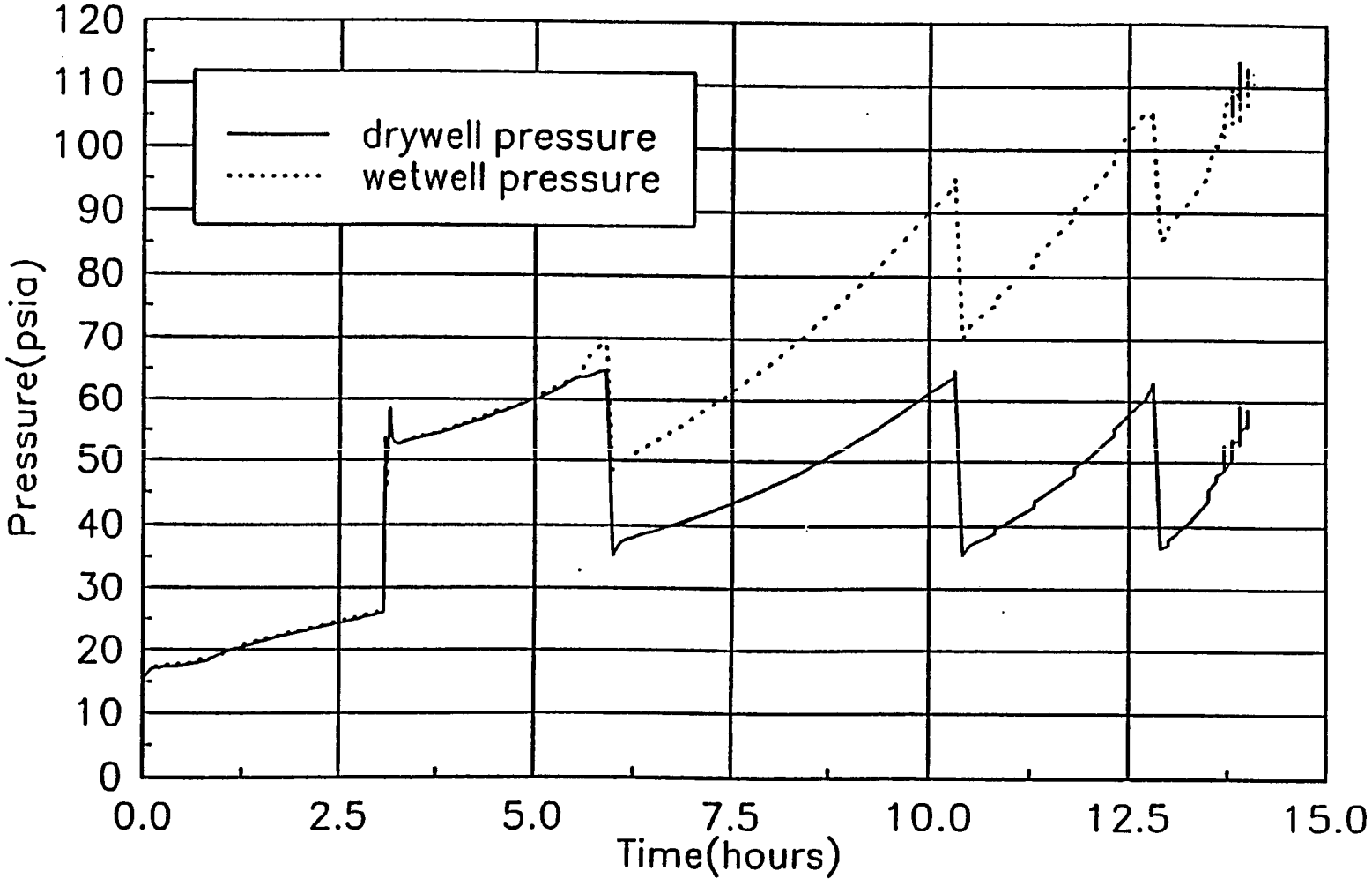

Figure 9-5. OJAU, Drywell and Wetwell Pressure with Drywell Venting

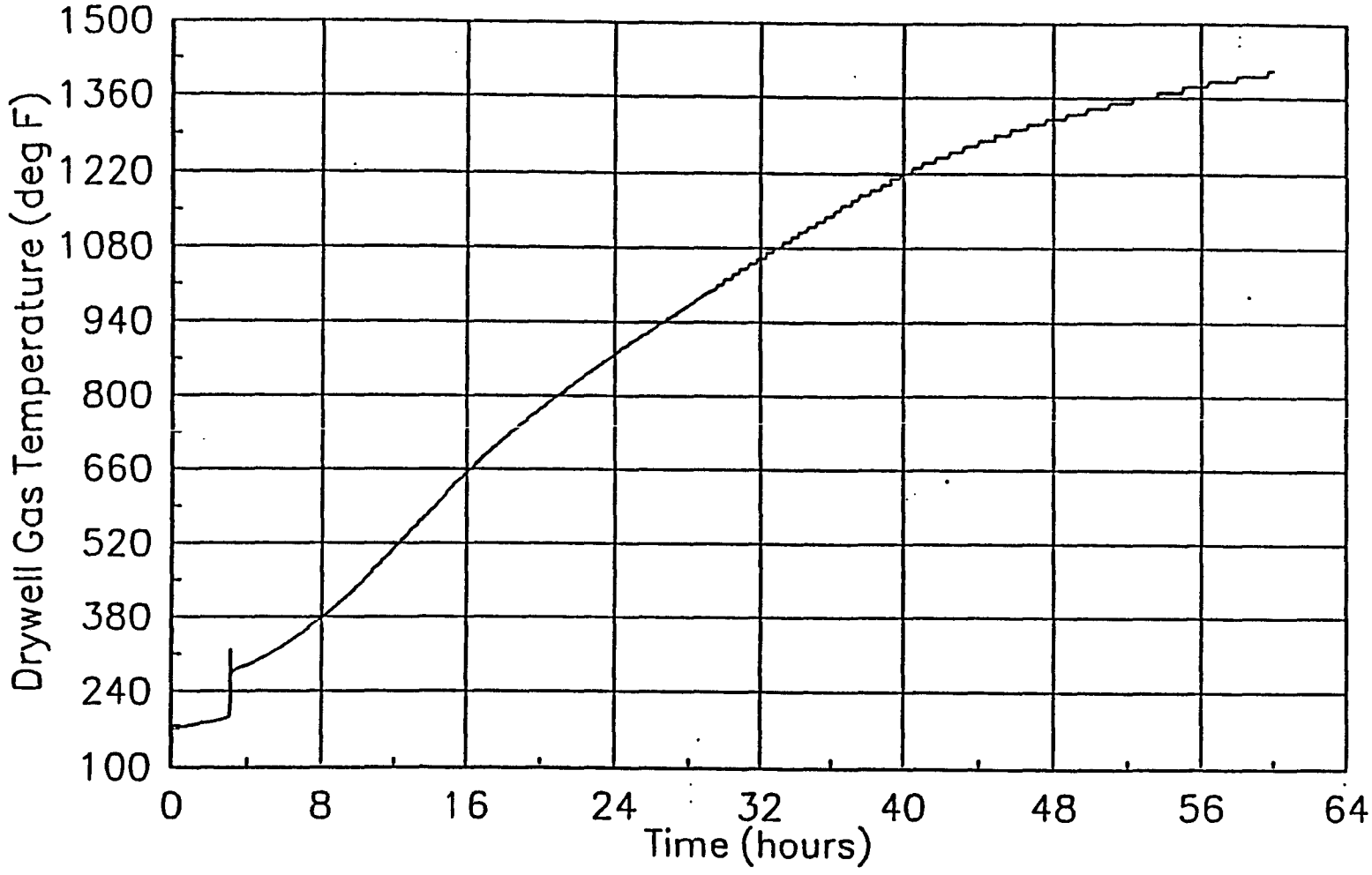

Figure 9-6. OJAU, Drywell Gas Temperature (no venting)

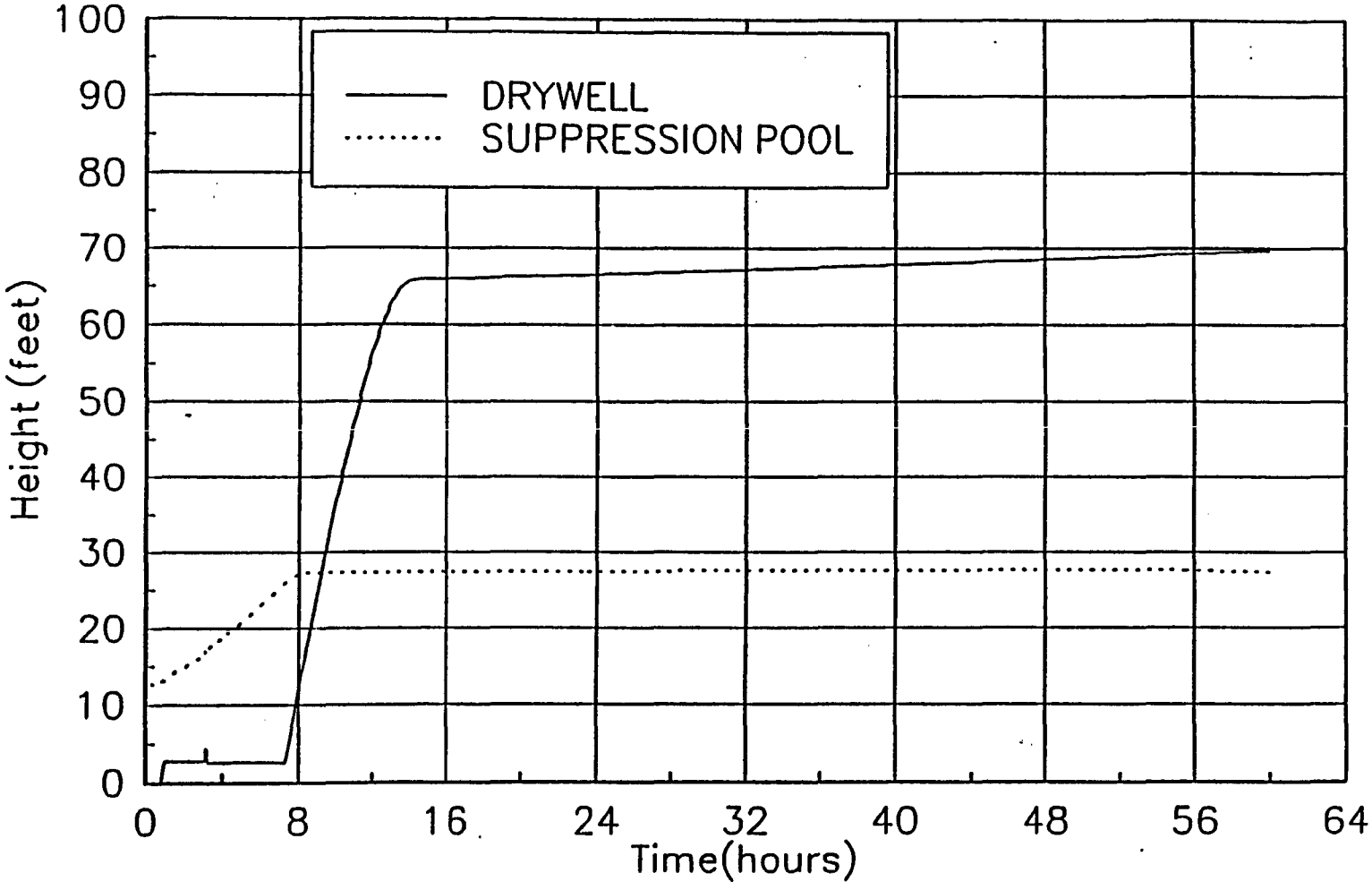

Figure 9-7. OJAU, Drywell/Torus Water Level

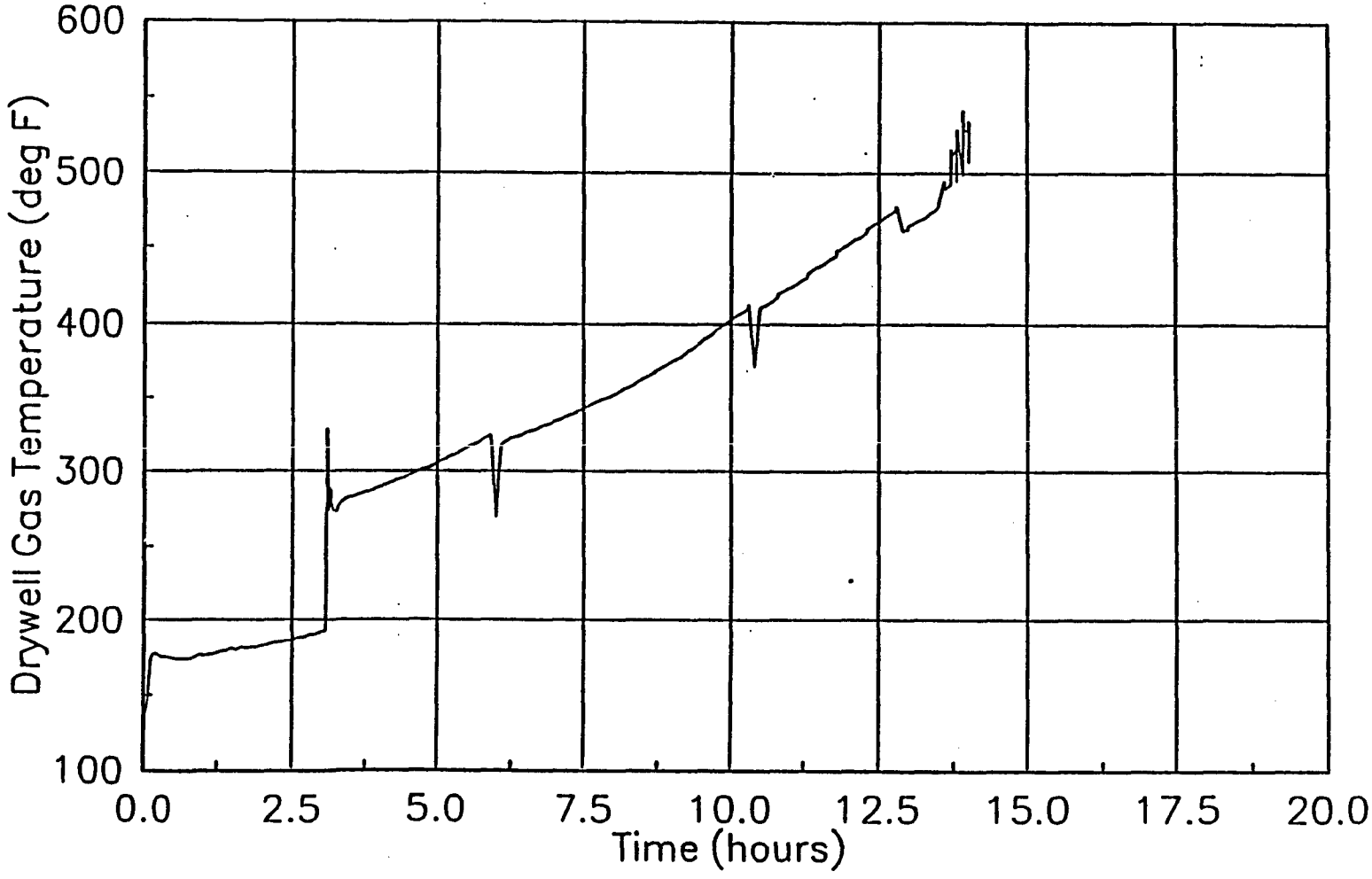

Figure 9-8. OJAU, Drywell Gas Temperature with Venting

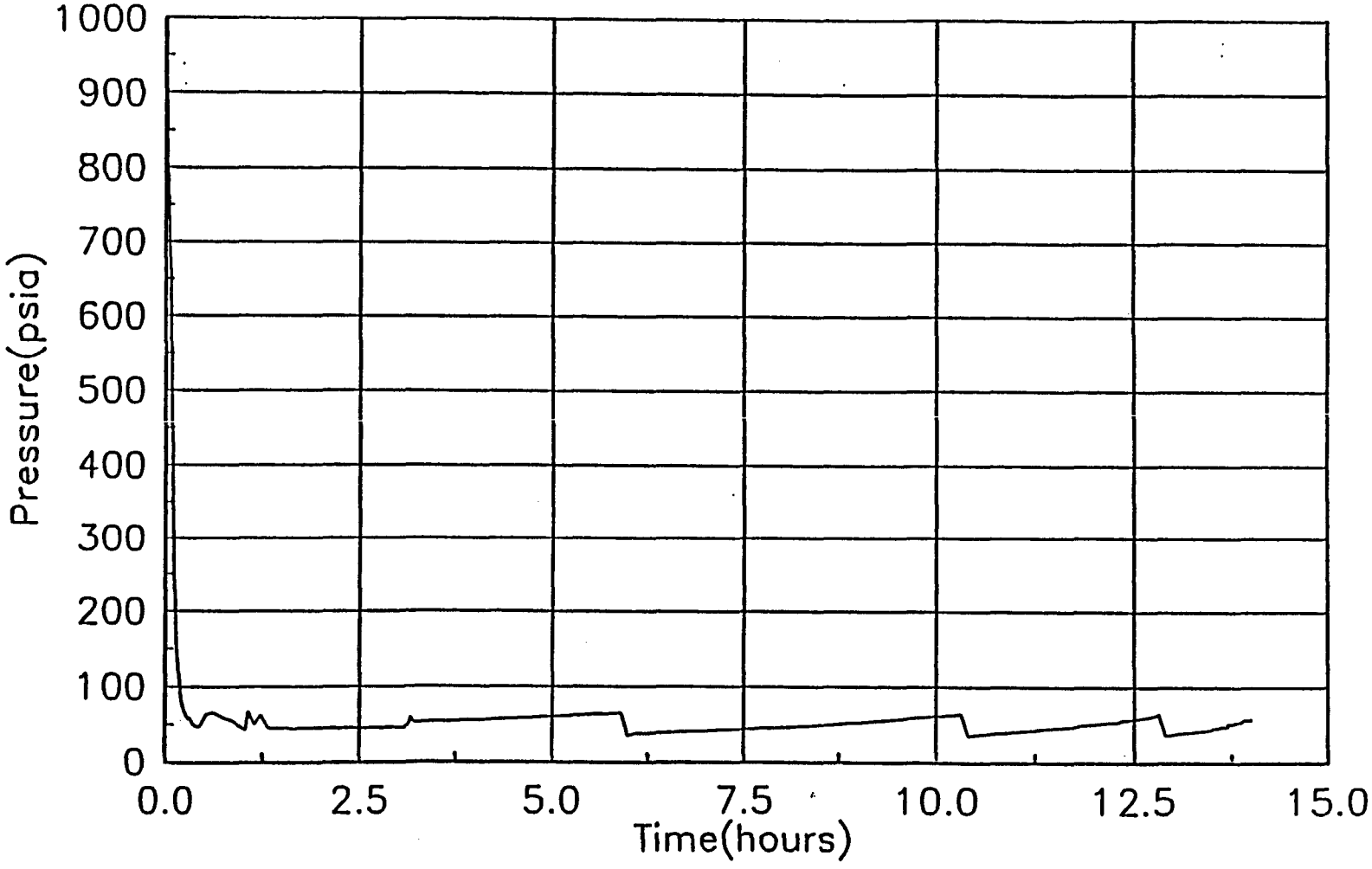

Figure 9-9. OJAU, Vessel Pressure with Drywell Venting

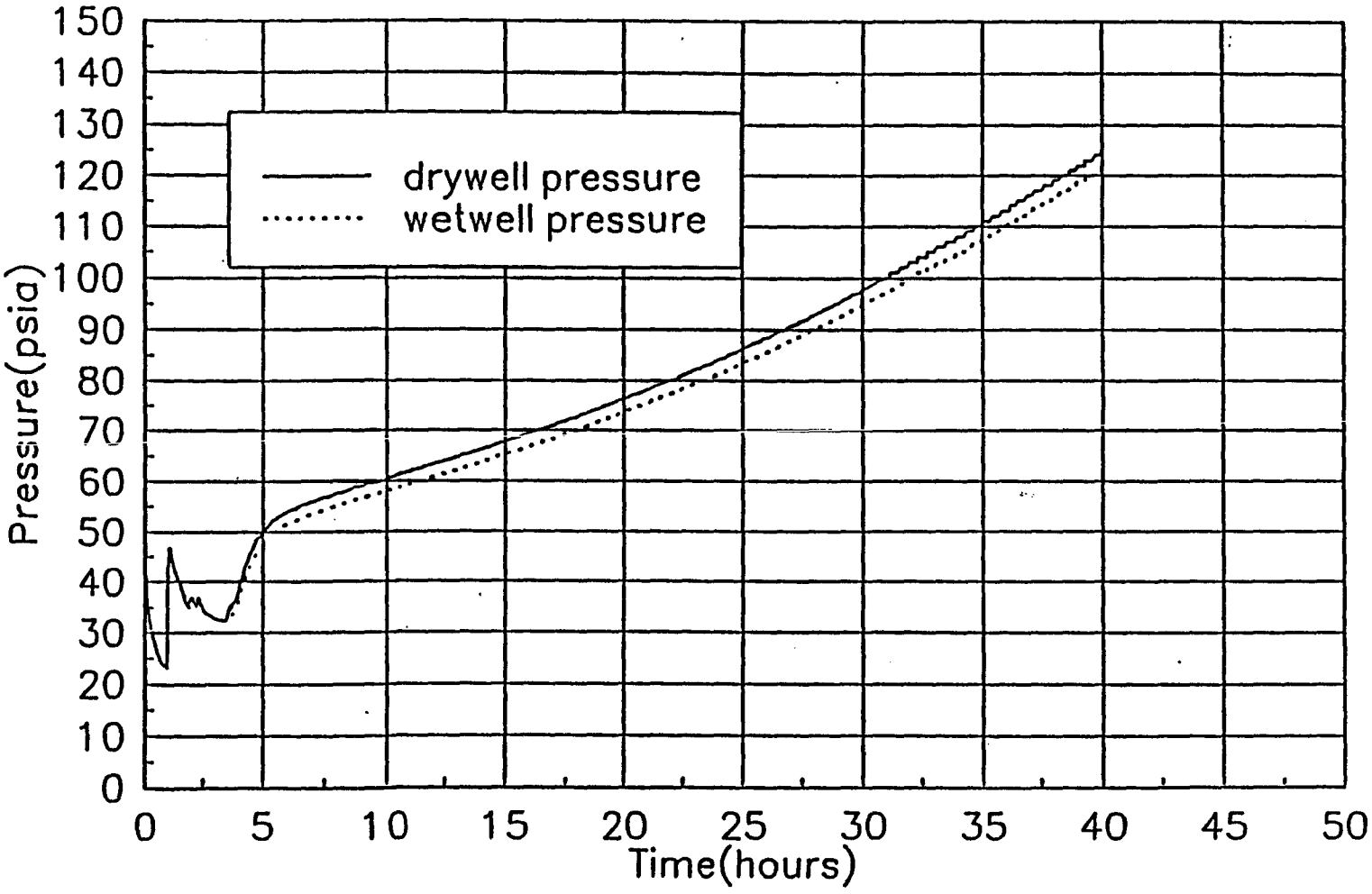

Figure 9-10. OIAU, Drywell/Wetwell Pressure

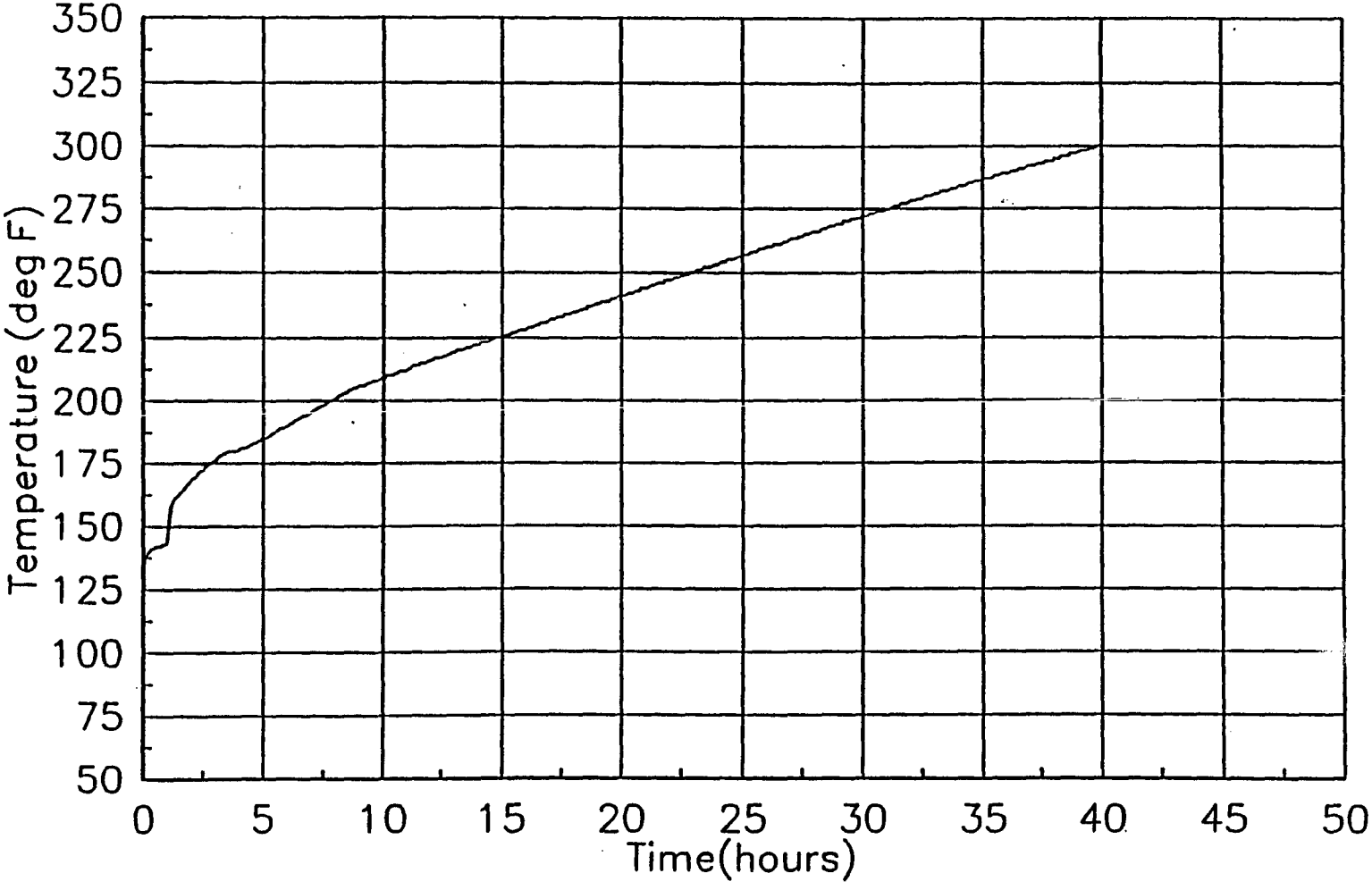

Figure 9-11. OIAU, Torus Water Temperature

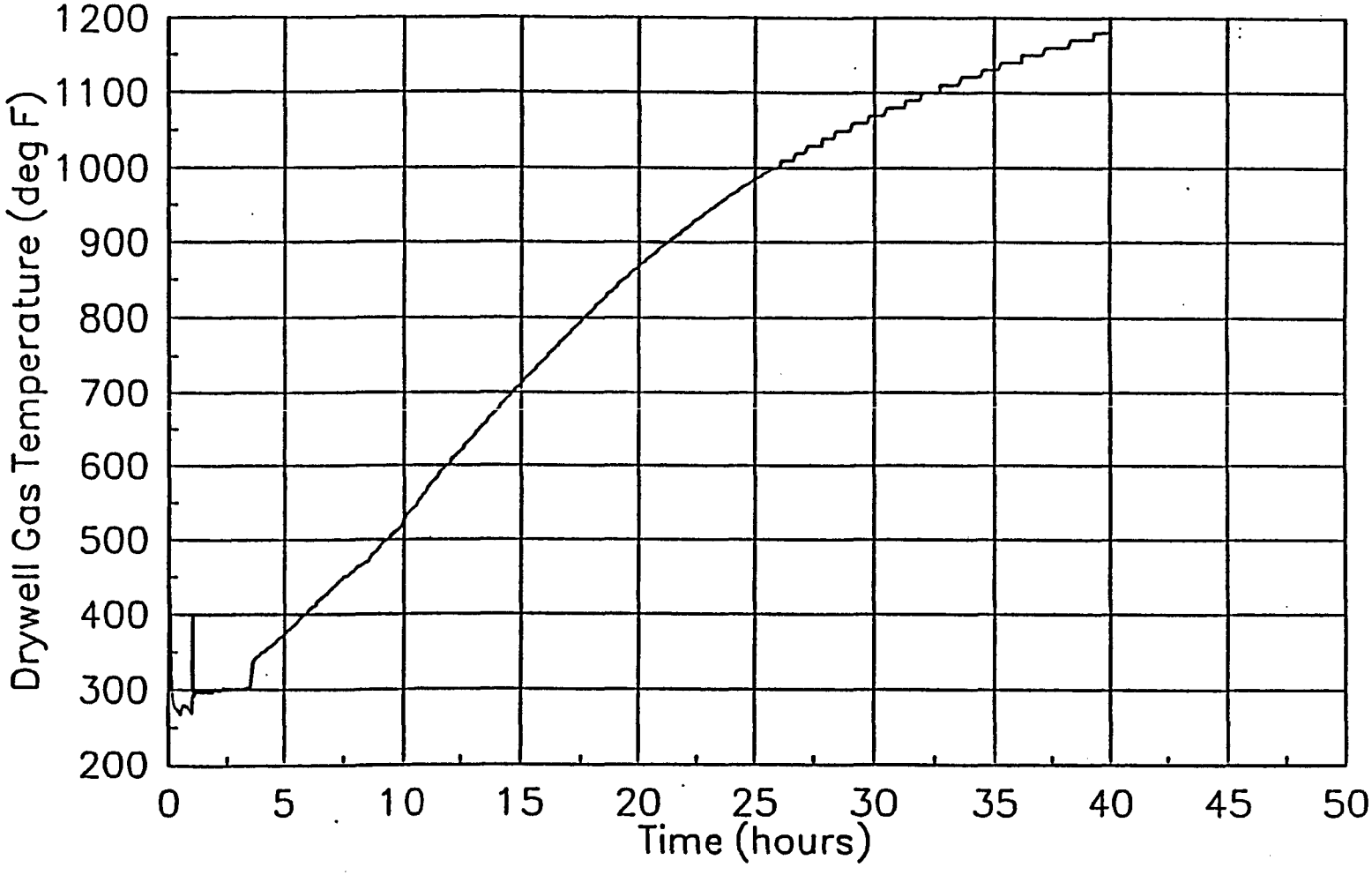

Figure 9-12. OIAU, Drywell Gas Temperature

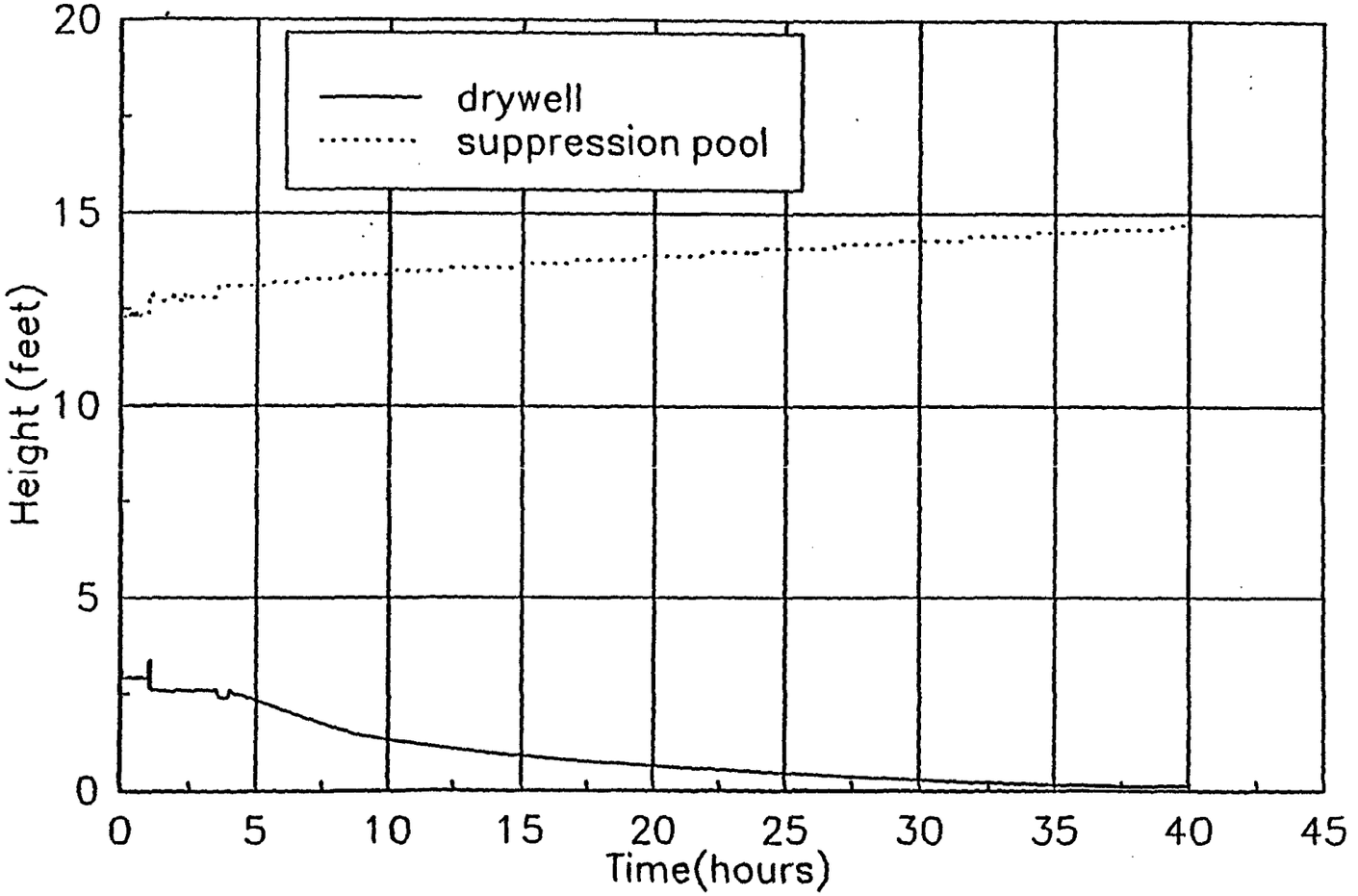

Figure 9-13. OIAU, Drywell/Torus Water Level

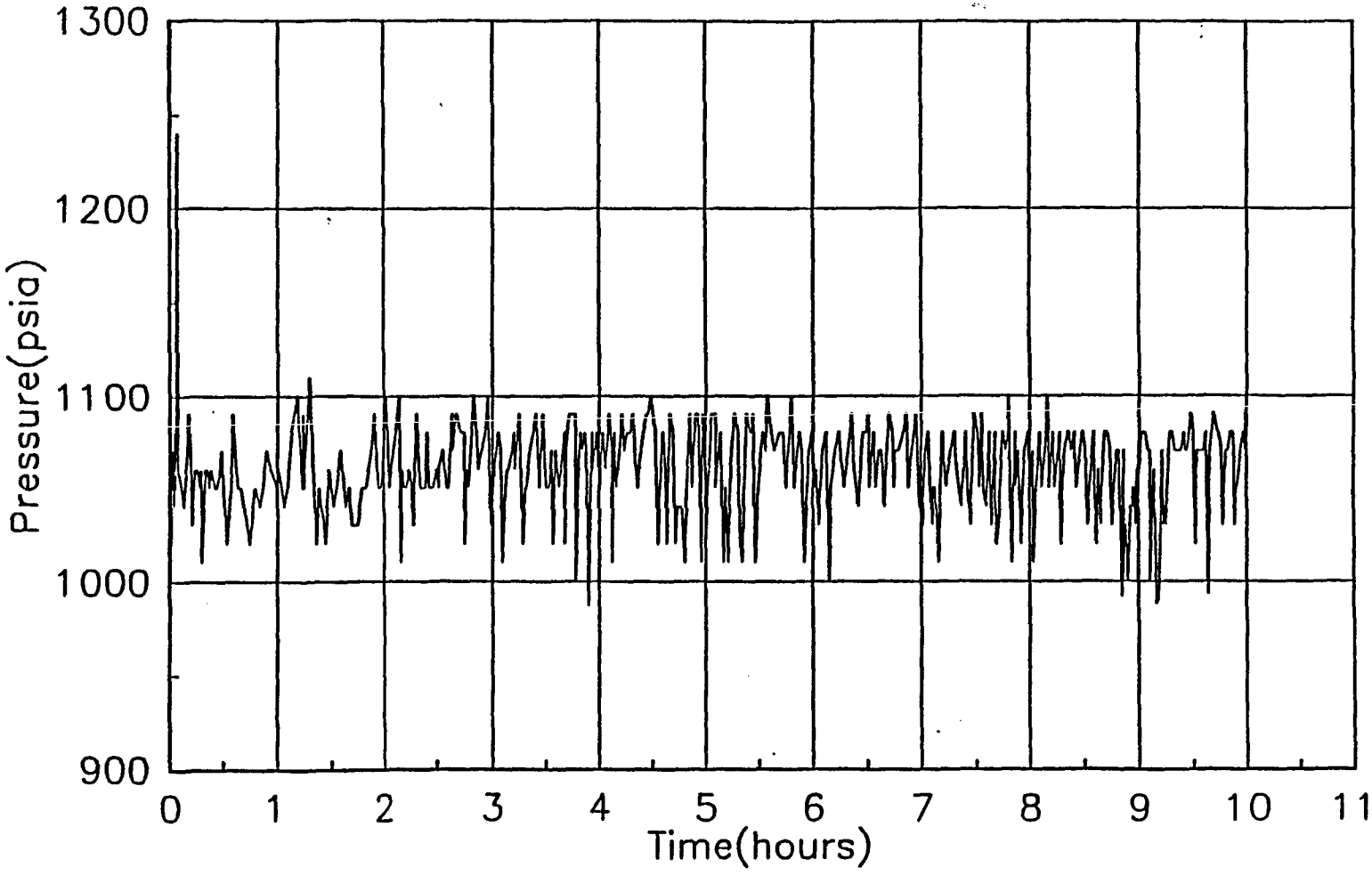

Figure 9-14. MKCU, Vessel Pressure (base case)

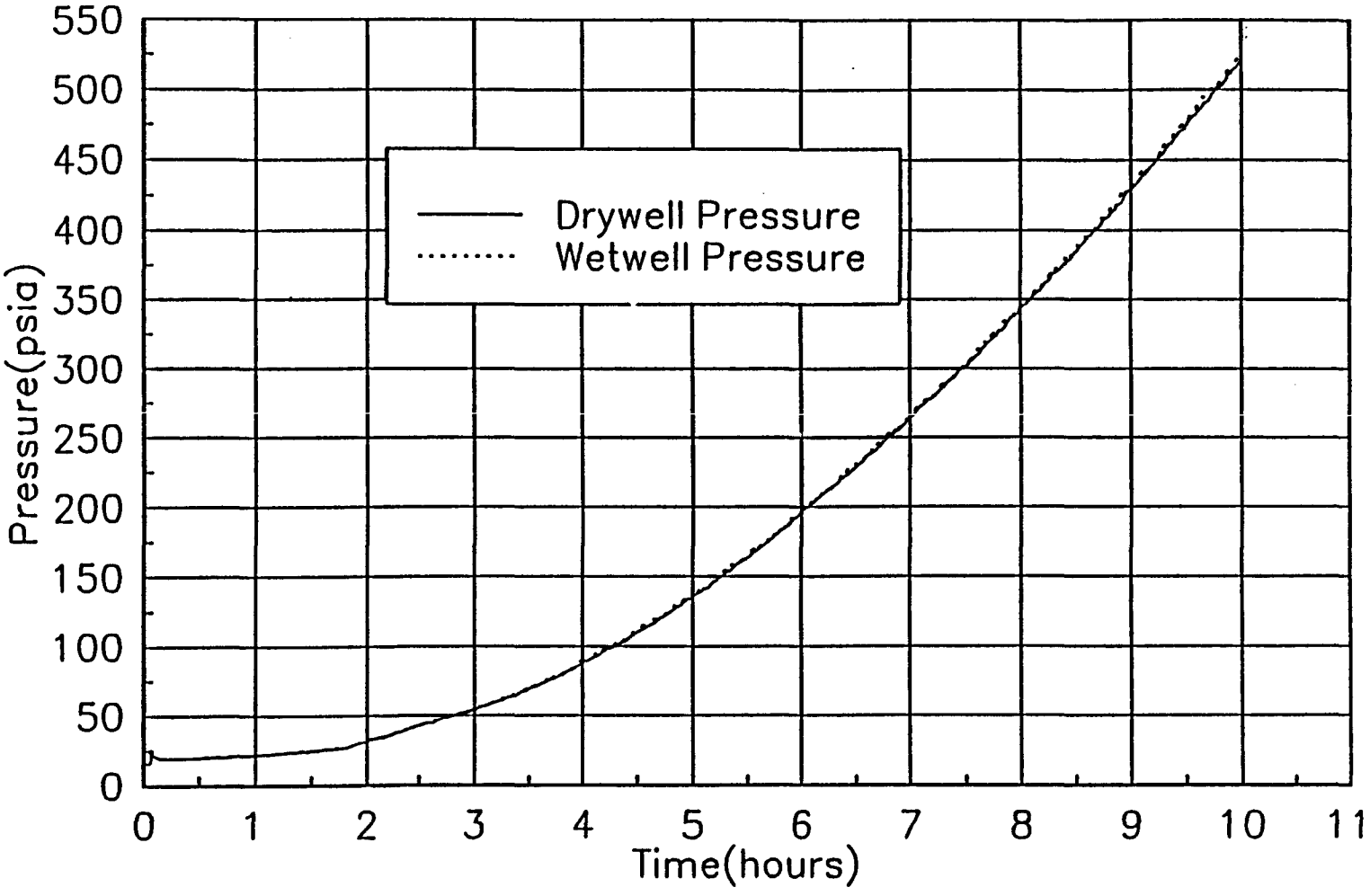

Figure 9-15. MKCU, Drywell/Torus Pressure (base case)

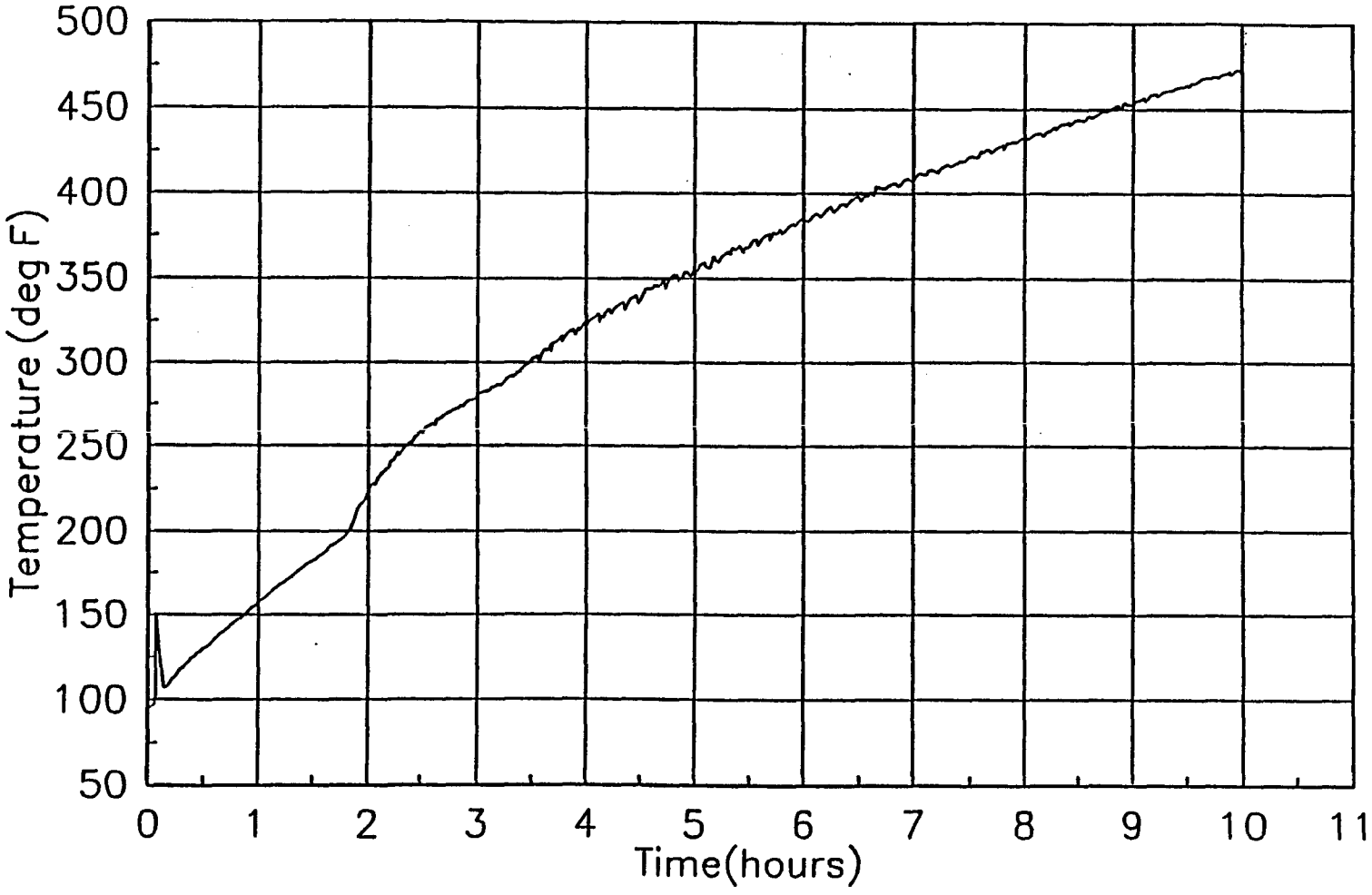

Figure 9-16. MKCU, Torus Gas Temperature (base case)

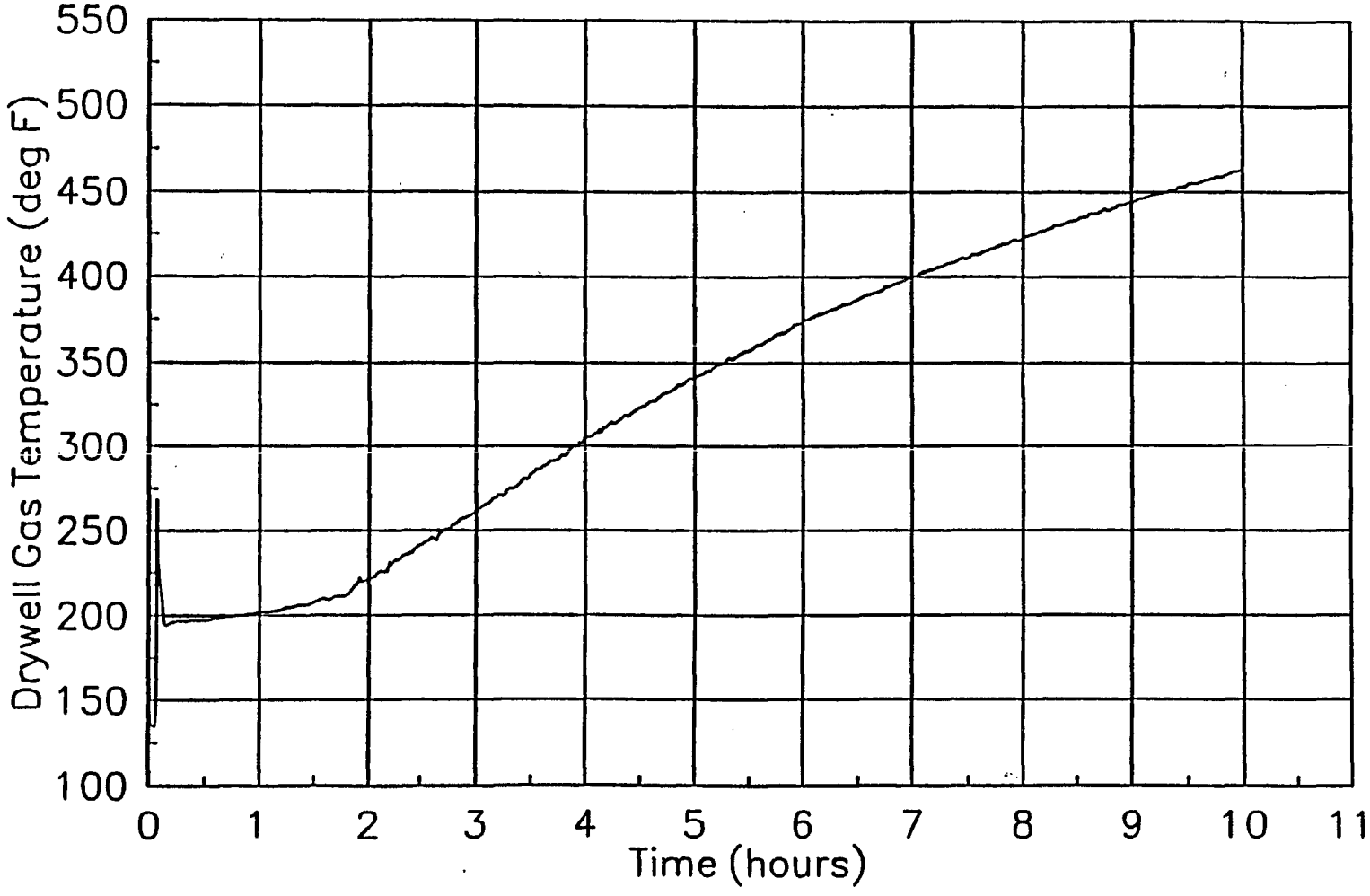

Figure 9-17. MKCU, Drywell Gas Temperature (base case)

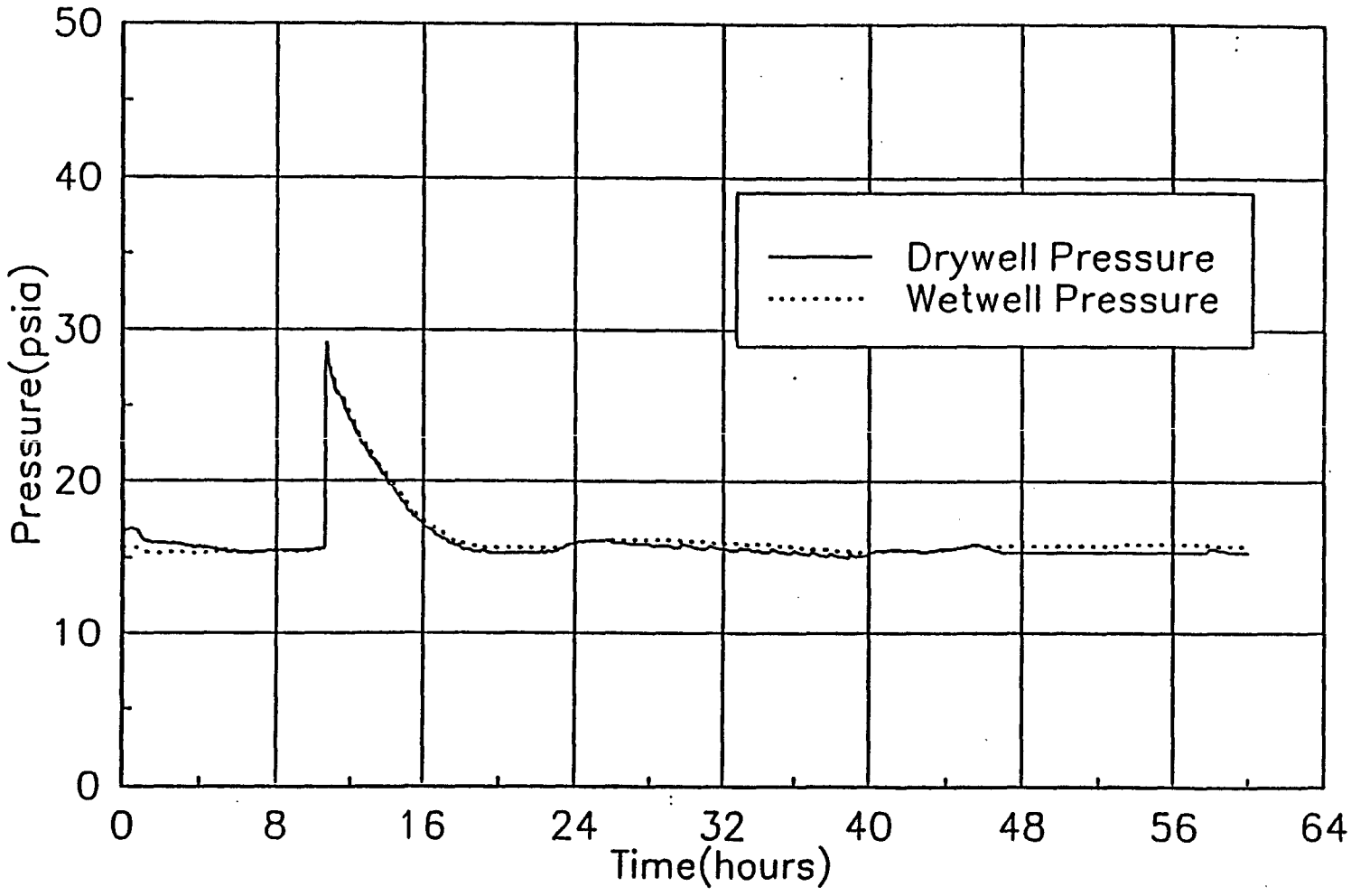

Figure 9-18. MJAU, Drywell/Wetwell Pressure

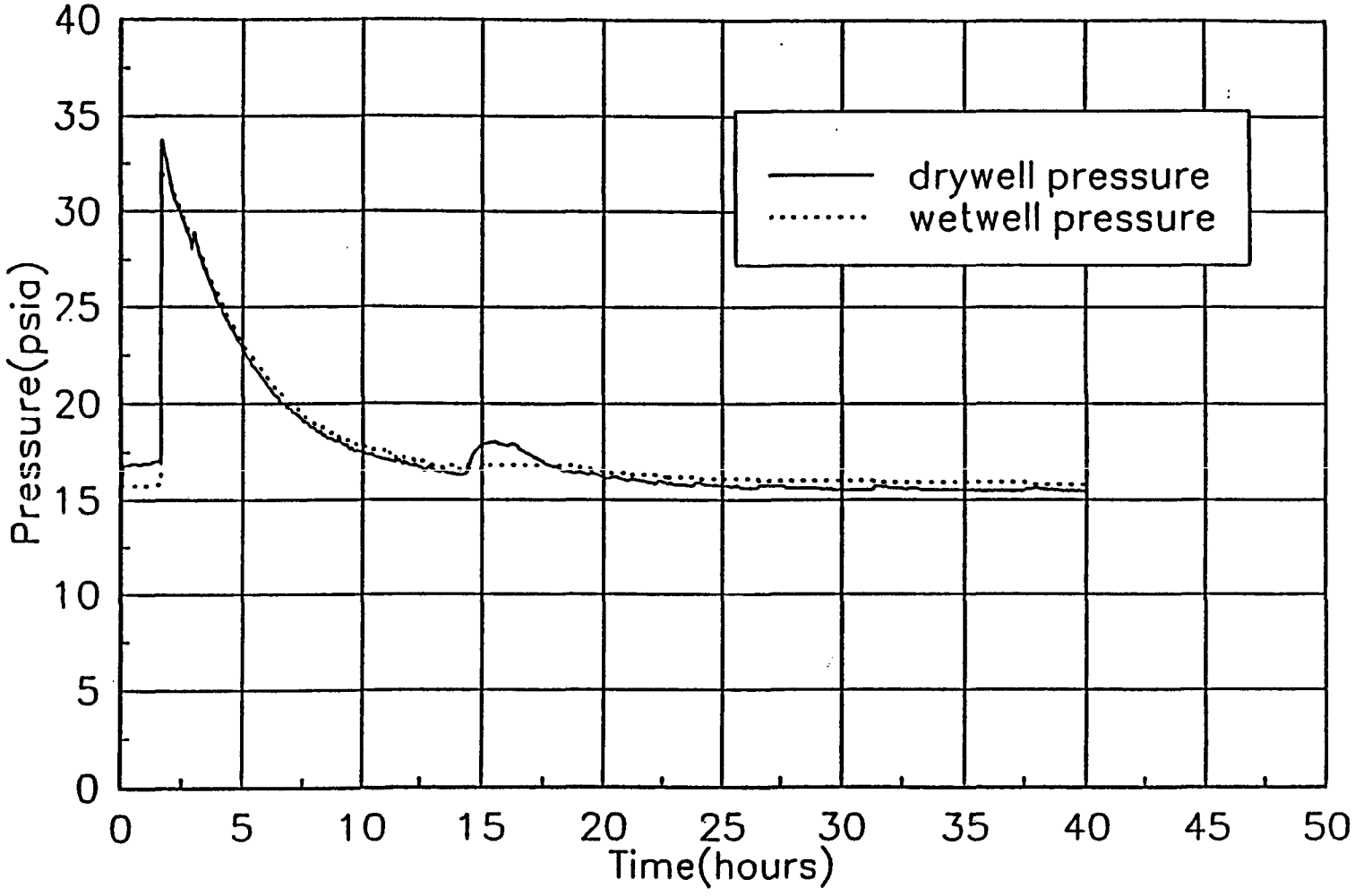

Figure 9-19. NJHW, Drywell/Wetwell Pressure

10. CET QUANTIFICATION

This section documents the bases for the numerical values of the split fractions used to quantify the CET. Since, for a given CET top event, there can be different split fraction values due to dependencies with prior top events and since a common database is used in RISKMAN for the quantification of all KPDSs, numerous unique split fraction designators are required for each top event. Furthermore, logic rules must be written for each unique split fraction. The split fraction logic rules for the Oyster Creek CET are listed in Table 10-1. The values of the conditional split fractions for each of the CET top events are given in Table 10-2.

10.1 Top Event 1 — Vessel Breach Prevented (VB)

As noted in Section 7.2.2, this top event is defined as successful prevention of vessel breach following the onset of core damage. Success of this top event indicates that the core damage progression is terminated inside the vessel while failure of this top event results in corium penetrating the vessel. Success of Top Event VB relies on success of water to the core debris following the onset of core damage but before vessel breach in sufficient magnitude to remove decay heat. Either fire protection water delivered when the reactor vessel pressure is low or the control rod drive hydraulic system flow of 120 gpm at high reactor vessel pressure is assumed to provide sufficient water to the core to prevent vessel breach one hour after successful reactor scram.

Successful CRD injection is a function of the success of Top Event CD in the Level 1 model. This top event (CD) models operator action to open manual bypass valve V-15-30 to provide the required flow. Success of fire protection injection is a function of success of the core spray system at Level 1 split fraction CS5, which is defined as operator injects fire protection through the core spray system. Split fraction CS5 is evaluated in the general transient and loss of feedwater control linked models only, and is applied where electrical power support for the core spray system is failed (EC=F*ED=F), the fire protection system is successful (FP=S), there is no loss of coolant to the reactor building (VS=S), and the reactor vessel pressure is low. This split fraction addresses manual opening of the core spray parallel injection valves and alignment of the fire protection system to the core spray system. Top Events EC, ED, FP, and VS also pertain to Level 1.

The success of fire protection injection through core spray is not addressed in the small and large LOCA linked models. This is due to the uncertainty involved in the ability to access the reactor building in a timely manner to open the core spray parallel inject valves manually during loss of offsite power cases.

Level 1 sequence information is necessary to determine the availability of either CRD or fire protection water for the KPDSs analyzed in the Level 2 analysis. This information is used to determine the appropriate split fraction values that each KPDS should question based on the fraction of the scenarios within each damage state in which the CRD or fire protection water injection has been successful. The details of the process are given in the following steps:

- **Step 1.** Each KPDS was described in detail, and those KPDSs that did not have recovery potential were not examined any further. A table was then developed for the remaining KPDSs in which the sequences contributing greater than 5×10^{-10}

were listed. Information on each sequence, such as frequency, cumulative frequency, and scenario percent, was also displayed.

- **Step 2.** The sequences within those KPDSs, which were not "screened out" in Step 1, were analyzed for their recovery potential. For those sequences that were not bottom breaks and for which CRD was available, vessel breach prevention was considered to be successful. For these sequences, no investigation of the availability of fire protection was necessary.

  For sequences in which CRD was unavailable or failed, the potential for fire protection injection was investigated. Fire protection injection through the core spray system was considered successful if, in the sequence under investigation, the fire protection system was not failed at Level 1 Top Event FP, the core spray system was not failed at Level 1 Top Event CS, and the reactor vessel is at low pressure. If these conditions were satisfied, vessel breach was considered to be successful.

  It should be noted that fire protection injection is failed following the failure of core spray since the parallel injection valves are included in the core spray model. Actually, very little of the core spray split fraction frequency is the result of the failure contribution of the parallel injection valves. Therefore, the above treatment is conservative.

- **Step 3.** For each KPDS for which the prevention of vessel breach was analyzed, the fraction of vessel breach prevention is the total frequency of those scenarios in which vessel breach is prevented divided by the total KPDS frequency.

  The applicable Level 2 Top Event VB split fraction is, then, 1 minus the fraction of each KPDS in which the water injection to the vessel is successful.

Plant damage state PIFW is defined as a low RPV pressure and dry drywell floor (P); containment intact (I); injection through condensate, CRD, or core spray is successful (F); fire protection and reactor building isolation are successful (FP=S*RI=S); and standby gas treatment is failed (W). Scenarios with the PIFW end state are generally characterized by a loss of offsite and onsite power. This results in the unavailability of CRD as an injection source. However, Top Event FP is defined as successful for this plant damage state; successful vessel breach prevention occurs where Top Event CS is not failed and RPV pressure is low.

NIFW is similar to PIFW with the exception that the RPV pressure is high instead of low. Generally, end state NIFW is characterized by either loss of all DC power or a station blackout, followed by failure of the isolation condensers (either initially or as a result of the failure of long-term makeup to the shell side). The loss of all DC power and a station blackout both result in the unavailability of the CRD system as an injection source. Since RPV pressure remains high due to either the loss of all DC power or the eventual depletion of batteries following a station blackout, the fire protection system is ineffective as an RPV injection source. Therefore, no vessel breach prevention of NIFW is considered.

It should be noted that a small percentage of the loss of all DC power scenarios result in a stuck-open safety valve, and the RPV may eventually depressurize to allow fire protection injection through the core spray system. However, this fraction of scenarios is small; therefore, it has been conservatively neglected.

OIAU is defined as low RPV pressure with wet drywell floor (O), containment intact (I), drywell sprays successful (A), and fire protection and standby gas treatment successful (U). Generally, OIAU is characterized by a depressurization event (large LOCA or successful ADS) with failure of core spray injection. When the depressurization event is not the result of a below-the-core break (for example, successful ADS), the CRD system is sufficient to provide inventory for in-vessel mitigation. Where the CRD system is unavailable (Top Event CD failed), the fire protection system is available where both Top Events FP and CS are successful. No assessment of the fractional availability of Top Event FP given Top Event CS failure was addressed.

MKCU is defined as high RPV pressure with wet drywell floor (M), containment failed early (K), containment spray successful (C), and fire protection and standby gas treatment successful (U). Since the Level 1 model assumes that the failure of containment fails all injection sources to the vessel, this damage state (xKxx, containment failed early) indicates that no injection would be available and therefore no analysis of vessel breach prevention for this end state is performed.

OJAU is defined as low RPV pressure with wet drywell floor (O), containment bypassed (J), water to core debris (A), and fire protection and standby gas treatment successful (U). Containment bypass scenarios (xJxx) are generally characterized by losses of coolant outside the containment or the failure of the scram discharge volume to isolate. Since many of the scenarios are the result of losses of coolant from the lower head region of the core and the loss of coolant is usually to the reactor building, no credit is taken for vessel breach prevention with either fire protection or CRD.

MJAU is similar to OJAU, with the exception that the RPV is at high pressure. No credit is taken for vessel breach prevention in containment bypass sequences.

NJHW is defined as high RPV pressure with dry drywell floor (N), containment bypassed (J), no water to core debris (H), fire protection and reactor building isolation is successful, and standby gas treatment is failed (W). No credit is taken for vessel breach prevention for the containment bypass sequences.

As noted above, PIFW and OIAU exhibit significant potential for vessel breach prevention.

Successful fire protection injection requires that the core spray system not be failed at Level 1 split fraction CS5 since the split fraction questions the operator action for the opening of the core spray parallel injection valves and the alignment of the fire protection system for injection. Also required for successful fire protection injection through core spray is successful vessel depressurization. In the case of a loss of offsite power initiating event, the success of ADS in the short term is not sufficient to prevent repressurization on depletion of station batteries. However, since this analysis is to determine whether the core is retained in vessel, a stuck-open safety or EMRV is considered sufficient to allow injection into the vessel before vessel breach. Therefore, a success path fire protection injection is defined as the core spray system not failed and the fire protection system available, and a safety or EMRV valve stuck open.

The percentages of vessel injection and of vessel injection failure (Top Event VB split fraction values) for each KPDS by the process defined above are summarized in the following table:

KPDS	Prevention (percent)	Split Fraction Value	Split Fraction Identification
PIFW	100.00	0.0	VBP
NIFW	0.00	1.0	VBN
OIAU	81.45	0.1855	VB1
MKCU	0.00	1.0	VB3
OJAU	0.00	1.0	VBO
MJAU	0.00	1.0	VB4
NJHW	0.00	1.0	VB2

10.2 Top Event 2—EMRV(s) or Safety Valve(s) Sticks Open Prior to Vessel Breach In High Pressure Melt Scenarios (ES)

The failure rate of Top Event ES is estimated from the number of relief and safety valve opening cycles calculated by MAAP for the sequences representing each KPDS. Table 10-3 lists for each KPDS the time of core uncovery, the time of vessel breach, the expected time of containment failure, and the number of cycles for the drywell to wetwell vacuum breakers, the safety relief valves, and the EMRVs. The number of cycles is given from the time of the initiating event to the time of core uncovery, to the time of vessel breach, to the time of containment failure, and to the time of the end of the MAAP calculation. The number of cycles listed is cumulative from the initiating event. If no containment failure were calculated to occur, the number of vacuum breaker cycles to 24 hours after vessel breach would also be listed. At this time, the fission product aerosol concentration in the drywell atmosphere has been depleted by natural processes to such an extent that a suppression pool bypass at this time would not noticeably affect the source term. In some cases, the number of vacuum breaker cycles had to be extrapolated beyond the end of the MAAP calculation, and this extrapolation rate is also given in Table 10-3.

The possibility of an EMRV or safety valve sticking open before core uncovery was addressed in the Level 1 model. Therefore, the number of open/close cycles after core uncovery was used to calculate the probability that one of the EMRVs or safety valves would fail to close under Top event ES. The following Oyster Creek-specific failure rate was used:

ZTVEMC EMRV Failure To Close 1.22×10^{-2} per demand

Consideration was given to the possibility that the Oyster Creek-specific experience with EMRVs was compiled conservatively in that certain failures may have been counted as one failure only, whereas, in fact, they might have involved several successful test cycles followed by a failure, where the successes were not counted. However, since there was only one event where an EMRV failed to close, and since the Oyster Creek-specific failure rate is a factor of 2 lower than the generic failure rate, this possibility was discounted as having a negligible impact on the plant-

specific failure rate. Furthermore, this is offset by the fact that, for a large number of consecutive cycles, the failure rate might be expected to increase.

In the context of the Level 2 analysis, a low failure rate estimate is conservative since, for sequences without depressurization, a stuck-open EMRV would be desirable because it would depressurize the vessel via the suppression pool. Since the number of valve cycles is large for some cases, the exponential failure rate model, rather than the rare event approximation,was used. The number of EMRV and safety valve cycles, and the split fraction designator and the failure probabilities calculated for all KPDS by this procedure are given in Table 10-4. The calculation is based on the number of valve cycles between core uncovery and vessel breach since a high pressure KPDS ensures that no EMRV has stuck open before core uncovery. Therefore, these failure probabilities are conditional on no failure having occurred before vessel breach. It is noted that the EMRVs only cycle for the high pressure KPDSs NIFW and MKCU, and, that for these two KPDSs, an EMRV is very likely to fail in the open position. No cycling would be expected for low pressure KPDS, and, for the remaining two high pressure KPDSs (MJAU and NJHW), there exists a containment bypass release path from the vessel that prevents EMRV cycling.

Two additional failure mechanisms can be identified that would have the same desirable effect as a stuck-open EMRV: namely, to depressurize the vessel and to transform the sequence from a high pressure sequence to a low pressure sequence. The first of these mechanisms is the failure of an EMRV in the open position due to deposition of aerosols that are purged from the vessel to the suppression pool. This occurs late in the in-vessel portion of the scenario after core degradation has started and significant amounts of aerosols are released from the fuel. The second mechanism is the creep rupture of a steam or steam relief line after exposure to the high temperature gases that flow through these lines when the EMRVs cycle late in the in-vessel accident progression after core degradation has started. This phenomenon is more prevalent in PWRs, but it can potentially occur in BWR high pressure sequences. These two mechanisms for vessel depressurization were not quantified for two reasons: first, the probability of an EMRV failing to close and depressurize the vessel is rather large, and, second, it is conservative to neglect the contribution from these mechanisms because it is desirable to depressurize the vessel before vessel breach. Overall, however, it can be concluded that the Oyster Creek vessel would be very likely to depressurize itself, even if the depressurization system fails to do so.

The above analysis of split fractions for Top Event ES applies to sequences without in-vessel recovery; i.e., Top Event VB=F. The number of EMRV cycles could be different if an injection source were recovered and the debris were retained in-vessel. However, split fraction VB is a guaranteed failure for all high pressure KPDSs (NIFW, MKCU, MJAU, and NJHW), and therefore the need to address Top Event ES for in-vessel recovery sequences does not arise.

10.3 Top Event 3 — Containment Intact Prior to Vessel Breach (I1)

The value of the split fraction for this top event is either 0.0 or 1.0 and is controlled by the PDS. No containment failures are expected or predicted for any of the KPDSs during that period of time beginning with uncovery of the top of the active fuel and vessel breach. Containment challenges that occur at the time of vessel breach are addressed by Top Event I2.

The following KPDSs have values of 0.0 for this split fraction:

- NIFW
- PIFW
- OIAU

The second letter (I) in each of the above KPDs indicates that the containment is intact at the time of vessel breach.

The following KPDSs have values of 1.0 (i.e., the integrity of the containment has been breached prior to vessel breach) for Top Event I1:

- MJAU
- NJHW
- MKCU

The second letter (J) in the first three of the above KPDSs indicates that the containment was bypassed at the inception of core damage. The second letter (K) in the last KPDS indicates that the containment failed prior to core uncovery, and, in fact, containment failure was the direct cause of core damage. KPDS OJAU involves a small containment bypass and was assigned a value of 0.0. CET sequences involving KPDS OJAU were binned with other bypass sequences.

Table 10-5 summarizes the split fractions for Top Event I1.

Pre-existing leaks were not specifically addressed in this study. Because the Oyster Creek containment is continuously monitored for oxygen content to ensure inerting, plant operating staff would be alerted to such leaks and would respond appropriately.

For high pressure core damage scenarios in which the shell side of the isolation condensers "dries out," the Level 2 PRA team examined the possibility of thermally induced creep ruptures of the isolation condenser steam lines or tubes occurring prior to vessel breach, thereby creating containment bypass scenarios. Depending on where the failures were postulated to occur, they could be treated as loss of coolant accidents (LOCA), bypasses to the reactor building, or bypasses directly to the environment, should the isolation condenser tubes fail first.

In core damage scenarios, very high superheated steam, etc., temperatures will develop when the in-vessel core debris dries out. These high temperature gases will rise through the steam driers (which have a significant heat capacity and surface area, and should delay the upper plenum heatup) and collect in the upper portion of the reactor vessel. In these high pressure cases, the electro-magnetic relief valves (EMRV) and/or safety valves will be occasionally cycling, although the gas production rate should be fairly small as most of the decay heat is heating core debris and internals. If the shell side of the isolation condenser dries out, and the steam supply lines are not isolated, significant natural convection flows could develop in the isolation condenser lines (indeed, the isolation condensers are designed for enhanced natural convection), heating the insulated piping and exposed tubes. The isolation condenser piping and tubes are made of 316 stainless steel. As there is about 110 feet of steam piping (or about 130 pipe diameters) before any hot gases would reach the isolation condenser tubes, it would be expected that pipe heat capacity alone (heat losses through the insulated pipe is probably a second order effect) would significantly cool down any gases before they reached the tubes.

Based on evaluations performed for this study, it has been determined that thermal creep failure might be expected in the isolation condenser steam lines and tubes at operating pressure and temperatures greater than approximately 1,300°F. The "exposure" time required for such failures is relatively long compared to the times predicted for vessel breach; however, if materials did achieve such temperatures, there would be some concern. If the material temperatures are less than approximately 1,000°F, thermal creep failures would be very unlikely. Only one important plant damage state, NIFW, is important in this regard. MAAP results for the sequence representing this KPDS indicate peak average gas temperatures in the upper head of the vessel prior to vessel breach of only 1,100°F. Thus, since it is unlikely that the isolation condenser steam lines would be exposed to temperatures that exceed 1,100°F and since that part of the isolation condenser steam line that is nearest to the reactor vessel and therefore attains the highest temperature is located inside the drywell, severe accident-induced containment bypasses through the isolation condenser were not considered in the Oyster Creek CET.

10.4 Top Event 4 — Small Leak Area if Containment Fails in Top Event I1 (L1)

For KPDSs MJAU and NJHW, the bypass to the reactor building is sufficiently large that, except for the moderate pressure spike at vessel breach, the containment does not pressurize appreciably. Therefore, the split fraction for Top Event L1 is assigned a value of 1.0 for these two KPDSs.

For KPDS MKCU, the containment fails prior to vessel breach. Based on the methodology discussed in Section 10.7, it has been determined for KPDS MKCU that the appropriate split fraction for Top Event L1 is 0.93; i.e., large failures are much more likely to occur than small failures.

Because the containment is not predicted to fail early for the remaining KPDSs, no estimates of split fractions for Top Event L1 are required. Table 10-6 summarizes the split fraction designators and values for Top Event L1.

10.5 Top Event 5 — Suppression Pool Not Bypassed Prior to Vessel Breach (S1)

A suppression pool bypass can occur during an accident sequence if one or more of the wetwell to drywell vacuum breakers fails to reclose. The Level 1 model does not address the possibility of a stuck-open vacuum breaker because it is a passive component; i.e., there are no support system dependencies, and it does not influence the frequency of core damage. However, the timing of core damage and the source term associated with the scenario are dependent on the effectiveness of the suppression pool as a heat sink and as a radionuclide scrubbing feature. Therefore, it is addressed as a Level 2 issue. The split fractions for this top event are quantified in a manner that is entirely analogous to the split fractions for Top Event ES. However, since the vacuum breaker cycles prior to core uncovery are not addressed in the Level 1 model, the number of vacuum breaker cycles prior to vessel breach includes all of the cycles from the initiating event to vessel breach. The number of vacuum breaker cycles in each time phase is listed in Table 10-3. The failure rate calculation used following Oyster Creek-specific failure rate for vacuum breakers failing to close:

ZTVCBC	Vacuum Breaker Failure To Close	1.29×10^{-3} per demand

Table 10-7 summarizes for each KPDS the number of cycles prior to vessel breach, the split fraction designator and the corresponding failure fraction. It can be seen that the probability of a suppression pool bypass before vessel breach can be significant for the ATWS sequence (KPDS MKCU) and non-negligible for the remaining KPDSs, except for the two high pressure containment bypass sequences (MJAU and NJHW).

10.6 Top Event 6 — Debris Not Entrained (ET)

Top Event ET addresses the possibility of debris transport into the vent pipe and deposition of a sufficient amount of debris in the vent pipe end cap to melt the vent pipe and cause a suppression pool bypass. This mechanism of debris transport is considered possible for high pressure vessel melt-through scenarios if the debris is fragmented very finely and entrained in the blowdown gas flow into the suppression pool.

This process is not normally addressed in Mark I BWRs. It is addressed here because containment failure due to liner melt-through is less likely in the Oyster Creek design because of the concrete curb, protecting the liner at the drywell floor elevation.

A detailed analysis has not been made to quantify this top event. The approach taken is to define the conditions that are considered necessary to cause vent pipe melt-through. It is assumed that a debris depth of about 12 inches would be required in the vent pipe to melt the end cap. For a much smaller depth, the debris volume becomes very small due to the slanted angle of the vent pipe. Figure 7-2 shows that a 12-inch debris accumulation requires about 6 cubic feet of debris (see Appendix A), which corresponds to about 1% of the debris volume generated from the entire core. Since, at vessel breach, typically about 50% of the core is expected to relocate out of the vessel, and since the entrained flow would be expected to distribute to at least two vent pipes, at least 4% of the debris discharged from the vessel would have to be entrained in particles of a size so small that they can be transported into the vent pipes. If the flow distributes uniformly into all 10 vent pipes, the entrainment fraction would have to be 20%.

It is not likely that a large fraction of the debris would be entrained in the blowdown gas. On the other hand, the possibility of entraining a few percent of the debris cannot be discarded. Therefore, the possibility of vent pipe melt-through is considered to be unlikely but not negligible, and a probability of 10% is assigned to vent pipe melt-through in a high pressure vessel breach scenario; i.e., ET1 = 0.1.

For low pressure vessel breach scenarios, no credible debris transport mechanism into the vent pipes has been identified. Therefore, the probability of vent pipe melt-through is set to zero; i.e., ETS = 0.0.

10.7 Top Event 7 — Containment Intact after Vessel Breach (I2)

This top event addresses containment challenges due to overpressure at the time of vessel breach and within 3 hours of this event. The MAAP simulations of the representative sequences for the KPDSs indicate only minor pressure spikes at the time of vessel breach. These spikes do not threaten containment integrity. However, for many of the KPDSs, containment pressure and temperature increase rapidly following vessel breach. Therefore, the values for the split

fractions for this top event are based on the probability of containment failure at 3 hours following vessel breach.

The probability of containment failure and the associated failure mode are determined using the methodology outlined in Section 3 of PLG-0844.[3] If pressure increases monotonically, the probability of containment failure will eventually attain a value of 1.0. Furthermore, if atmosphere and material temperatures also increase, the materials will lose their strength as well. The MAAP-predicted drywell pressure and temperature histories for the sequence representing KPDS NIFW shown in Figures 10-1 and 10-2 are good examples of such concerns. As indicated in Figure 10-1, drywell pressure increases rapidly during the first 12 hours. Drywell temperatures (see Figure 10-2) also increase monotonically, reaching approximately 1,000°F in 24 hours.

The fundamental questions for such cases are when failure would be predicted and whether the failure mode is characterized as a "leak" or a "large break." The concept of a "leak before break" is introduced if the leak failure mode has a failure pressure that is below the failure pressure corresponding to a break failure mode and that the leak area is sufficient to preclude continued pressurization. In general, leaks will not prevent continued pressurization if the rate of pressure increase is characterized as a pressure spike.

Based on the methodology outlined in PLG-0844 for containment response to slow pressure - temperature transients, the cumulative probability distributions shown in Figure 10-3 for KPDS NIFW were developed for the leak before break and break before leak failure modes. These results are based on the containment failure mode fragility curves discussed in Section 6 of this report and include the effect of increased temperatures. As indicated in Figure 10-1, drywell pressure prior to vessel breach is approximately 27 psig due primarily to drywell temperature increase and the partial pressure of hydrogen. Vessel breach occurs at approximately 2.4 hours, and the pressure increases by approximately 50 psi at vessel breach with no discernible pressure "spike." Pressure increases rapidly from 90 psia shortly after vessel breach to approximately 145 psia at 9 hours. After approximately 11 hours, the rate of pressure rise decreases substantially, and the drywell temperature rise increases substantially, indicating that the water previously on the drywell floor has "boiled off."

Since all structural failure modes, except those associated with the drywell closure flange, are correlated, only the corroded drywell (sand-filled region) and the drywell closure flange failure modes were investigated. The former failure mode is classified as a break, and the latter as a leak. The closure flange incipient leakage pressure at mid-fuel cycle was used, and no seal degradation due to accident temperature was considered. Neglecting seal degradation increases the probability of break before leak. However, if the average temperature of the drywell head closure bolts lags the temperature of the closure flange, the bolts impose an even greater "clamping force" than that used in defining incipient leakage. As a point of reference, a lag in bolt temperature of 100°F relative to the flange results in a 70-psi increase in incipient leakage pressure. Calculations performed by GPU indicate that the bolt temperatures will lag the flange temperature by appreciable amounts, although the precise lag would be difficult to determine

[3] Fleming, K. N., et al., "Methods for Estimating Containment Failure Probability," PLG, Inc., proprietary, PLG-0844, November 1991.

without experimental data. Thus, neglecting seal degradation will not significantly impact the probability of leak before break.

Assuming that Top Event I2 addresses containment failure up to and including a time that is 3 hours after vessel breach (t=5.4 hours), the value of Top Event I2 for KPDS NIFW can be determined directly from the total failure curve in Figure 10-3 at a time of 5.4 hours. This value is 0.22 (split fraction I2N).

A similar analysis has been performed for KPDS PIFW, assuming that debris cooling in the vessel was not accomplished and that vessel breach did, in fact, occur. The value of Top Event I2 split fraction was determined to be 0.041, assuming fire water is delivered to the core through core spray piping operated after vessel breach.

By definition, the containment fails prior to core damage (i.e., I1=1.0) for KPDS MKCU. Therefore, the split fraction for Top Event I2 for KPDS MKCU is guaranteed to also have a value of 1.0. Top Event I2 is asked only if the containment failure prior to vessel breach (Top Event I1) was characterized as a leak (success path of Top Event L2).

Based on the drywell pressure and temperature histories for the sequence representing KPDS OIAU (see Figures 10-4 and 10-5), no containment failure was predicted at vessel breach or within 3 hours of vessel breach (see Figure 10-6). Thus, I2=0.0 for KPDS OIAU.

Key plant damage states MJAU, NJHW, and OJAU are characterized by containment bypass prior to and during core damage. KPDS MJAU is dominated by sequences involving failure to isolate the scram discharge volume (SDV), allowing reactor coolant to escape directly to the RBEDT. The leak area is controlled by a 2 inch diameter pipe. As shown in Figure 10-7, except for a modest pressure spike at vessel breach, there is no subsequent pressurization of the containment. KPDS NJHW also involves failure of the SDV to isolate, and, as indicated in Figure 10-8, there is only a modest pressure spike at vessel breach, and there is no subsequent pressurization of the containment.

KPDS OJAU involves overpressurization of the RWCU with loss of reactor coolant to both the suppression pool via a 6 inch diameter relief valve and to the RBEDT via a 1 inch diameter relief valve. The relief valves are assumed to close after vessel breach. Accordingly, the containment function is re-established after vessel breach, and the drywell and torus repressurize. When the torus water level reaches 26 feet, suppression pools to drywell vacuum breakers are closed. With continued operation of the drywell sprays, water level in the drywell rises rapidly. If existing emergency procedures are followed, venting of the drywell will be initiated when the drywell pressure reaches 50 psig. As shown in Figure 10-9, this pressure is attained at about 6 hours. If emergency procedures are followed, the drywell and wetwell pressure histories will approximate those shown in Figure 10-9. The difference between the drywell and wetwell pressures is caused by the static head of water in the drywell. As indicated in Figure 10-9, the pressure spike at vessel breach (approximately 3 hours) is relatively modest, and by 6 hours (3 hours after vessel breach), the drywell and wetwell pressures are less than that required for drywell venting. As shown in Figure 10-10, no early containment failures would be predicted.

Table 10-8 summarizes the split fraction designators and values for Top Event I2. As indicated, a number of entries were added for cases in which the suppression pool was bypassed prior to vessel breach. The basis for these values is judgmental.

10.8 Top Event 8 — Small Leak Area if Containment Fails in Top Event I2 (L2)

The calculations discussed in Section 10.7 for the probability of containment failure also yield the split between leak and break failure modes. Referring to Figure 10-3, it can be seen that cumulative probability of containment failure at a time 3 hours after vessel breach is due primarily to the break failure mode. The value of Top Event L2 is equal to the cumulative probability of a break divided by the cumulative probability of failure by any mode. As shown in Figure 10-3, nearly all of the containment failure probability at 5.4 hours (3 hours after vessel breach) is due to the break failure mode. A review of the data used for Figure 10-3 indicates that the value of split fractions for Top Event L2 is 0.99.

For the unarrested PIFW sequence discussed in Section 10.7, the calculated value of Top Event L2 is approximately 1.0.

For KPDS MKCU, Top Event L2 is addressed only for "leaks" at Top Event L1. It is assumed that the pressure spike at vessel breach results in a break containment failure at this time.

Table 10-9 summarizes the split fraction designators and values for Top Event L2. Similar to Top Event I2, split fractions were provided for cases in which the suppression pool was bypassed prior to vessel breach. In all cases, it was judgmentally assumed that if the containment failed at Top Event I2 because of suppression pool bypass, that failure would be a break rather than a leak. This assumption appears to be consistent with calculated split fraction values for the no suppression pool bypass cases.

10.9 Top Event 9 — No Significant Release of Fission Products into the Reactor Building due to Drywell Liner Melt-Through (LM)

As shown in Figure 10-11, there are two potential pathways leading to a significant release to the reactor building via drywell liner melt-through. One of these pathways involves the accumulation of debris at the intersection of the drywell floor (or on top of the curb) and drywell wall. As shown in Table 10-10, the fundamental basis for the release probabilities for this pathway is NUREG/CR-5423; however, judgmental estimates have been given for credit for the curb in the Oyster Creek drywell. As shown in Table 10-10, the probabilities are dependent on PDS parameters and are therefore KPDS dependent.

The second pathway for release involves the pedestal sump. It is very likely, even if concrete ablation is prevented elsewhere, that the lines in the sump will be breached even if water overlies debris on the pedestal and drywell floor. However, even if the liner is breached, a significant release will be prevented if there are no significant cracks in the concrete or if debris "freezes" in any cracks that do exist. Figure 10-11 provides some subjective estimates for these possibilities.

The split fraction for Top Event LM is the sum of the probabilities of release via the two pathways.

10.10 Top Event 10 — Suppression Pool Not Bypassed Late (S3)

A suppression pool bypass can also occur after vessel breach if one or more of the wetwell-to-drywell-vacuum breakers fails to reclose, which is addressed in this top event. The split fractions for this top event are quantified in a manner that is entirely analogous to the split fractions for Top Event S1, except that the number of vacuum breaker cycles after vessel breach is used from Table 10-3. The failure rate calculation used the same Oyster Creek-specific failure rate for vacuum breakers:

ZTVCBC	Vacuum Breaker Failure To Close	1.29×10^{-3} per demand

Table 10-11 summarizes for each KPDS the number of cycles after vessel breach, the split fraction designator, and the corresponding failure fraction. It is noted that suppression pool bypass after vessel breach is significant for all KPDS.

Top Event S3 is a guaranteed failure (S3F) if Top Event S1 is failed or a preceding containment failure has occurred (Top Event I2 or LM failed) or a containment bypass has occurred (Top Events XS, XD, and XI failed) because these failures are in the drywell or directly from the vessel into the environment, and the leakage path, by definition, does not go through the suppression pool. Top Event S3 is also a guaranteed failure (S3F) if Top Event ET is failed, which means that sufficient debris has been deposited in a vent pipe opposite the pedestal door to cause a vent pipe melt-through above the suppression pool water level. These dependencies are modeled in the split fraction rules for Top Event S3 (see Table 10-1).

10.11 Top Event 11 — Emergency Crew Vents Containment in Core Damage Scenarios (DV)

By definition, torus venting is not available for KPDSs NIFW and PIFW. Thus, the value of the split fraction for Top Event DV for these two KPDSs is set to 1.0; i.e., venting is impossible.

Furthermore, the containment fails prior to core damage for accident sequences contained in KPDS MKCU. Thus, venting is not required for this KPDS, and the corresponding split fraction is set to 1.0.

For KPDSs MJAU and NJHW, the containment is bypassed and containment pressure is maintained at nominal levels after the pressure spike at vessel breach. For these two KPDSs, the split fraction is also set to 1.0.

For KPDS OIAU, the torus vent is available, and it is assumed that venting will be implemented effectively in accordance with existing procedures. Therefore, the split fraction for Top Event DV for KPDS OIAU is assigned a value of 0.017, which is the same value as OV1 in the Level 1 model.

The representative sequence for OJAU involves a procedure-actuated dirty venting via the drywell. For this KPDS, the split fraction for Top Event DV is also assigned a value of 0.023, which is the same value as OV2 in the Level 1 model.

10.12 Top Event 12 — Containment Intact Late (I3)

As noted in Section 10.7, the containment will eventually fail if the containment pressure monotonically increases. At some point in time, it can be argued that containment heat removal is restored or extraordinary measures could be implemented to arrest containment pressurization. However, for the purpose of this submittal, it will be assumed that sequences (and the KPDSs they represent) with monotonically increasing containment pressure will eventually fail. Thus, for KPDS NIFW, the value of Top Event I3 is 1.0.

For the unarrested PIFW sequence discussed in Section 10.7, the containment will eventually overpressure. The probability of containment failure is 0.9992 at 20 hours. Therefore, Top Event I3 is assumed to be 1.0 for this KPDS (if core damage is not arrested).

Based on the MAAP-predicted drywell pressure and temperature histories for KPDS OIAU, the probability of containment failure is approximately 0.12 at 25.0 hours. However, drywell gas temperatures are sufficiently high by about 18 hours that thermal creep becomes a significant concern. Thus, it will be assumed that containment failure is guaranteed in the time period of interest. Therefore, it is assumed that the value of the split fraction for Top Event I3 for KPDS OIAU is 1.0.

For OJAU without venting, the containment will also pressurize to failure, and the value of Top Event I3 is 1.0.

Table 10-12 summarizes the split fraction designators and values for Top Event I3.

10.13 Top Event 13 — Small Leak Area If Containment Fails in Top Event I3 (L3)

As in the calculation of the split fraction for Top Event L2, the magnitude of Top Event L3 is equal to the cumulative probability of containment failure due to break divided by the cumulative probability of all containment failure modes at the time of interest. In this case, however, the time of interest is the assumed "end of accident" time.

As shown in Figure 10-3 for NIFW, the cumulative failure probabilities are approaching asymptotic values at approximately 16 hours after the initiating event. The value of the split fraction for Top Event L3 for NIFW is therefore 0.7.

For the unarrested PIFW case, the value of Top Event L3 has been calculated to be 0.655.

For OJAU without vent, the value of Top Event L3 was determined to be 0.713. The values of all split fractions were increased appreciably if the suppression pool became bypassed during core degradation. The split fraction values for such cases are given in Table 10-2.

Table 10-13 summarizes the split fraction designators and values for Top Event L3.

10.14 Top Event 14 — No Hydrogen Burn in Reactor Building (HB)

Hydrogen is generated from the oxidation of metallic components in the core, which occurs in a steam environment at high temperatures. Hydrogen is released into the containment via the

EMRVs, through a LOCA breach, or at the time of vessel breach. Typically, on the order of a thousand pounds of hydrogen can be generated in this manner. At the time of containment failure, most of this hydrogen is released into the reactor building as a mixture of hydrogen, nitrogen, and steam. If the hydrogen ignites in the reactor building when it mixes with the air, it would cause a sufficient pressure rise to fail at the portion of the reactor building above the operating deck. This would be assumed to render all active fission product mitigation in the reactor building ineffective, although it is possible that the actuation of the reactor building fire sprinkler system could provide some mitigation of fission products. However, the reactor building sprinkler system is limited to certain rooms and there are no sprinklers in the stairways, which constitute the major release pathways through the reactor building.

Two of the major findings of the containment failure analysis are that any containment overpressure failure is very likely to be a gross failure at the drywell floor where the sand fill has been removed behind the liner plate, and that a leak before break failure mode is very unlikely. The quantification of Top Event L2, the leak before break failure probability for containment failure occurring at or within 3 hours of vessel breach, shows that the leak before break probability is 1% or less. Even for late containment failure modes, the expected leak before break probability is only on the order of 10%. Therefore, it is only necessary to consider gross containment failure modes at the drywell floor level.

The only reason to address a hydrogen burn in the reactor building is to treat correctly the reactor building effectiveness in reducing source terms. Reactor building effectiveness is addressed in Top Event BE. For a gross containment failure, the reactor building cannot maintain its effectiveness for active fission product removal as it is defined for Top Event BE. Therefore, the numerical assessment of the hydrogen burn question becomes irrelevant, and the probability of a hydrogen burn has been set to 1.0; i.e., the split fraction HBF = 1.0 is used in all cases.

10.15 Top Event 15 — Reactor Building Effective (BE)

This top event addresses the effectiveness of the reactor building to provide active fission product scrubbing after containment failure. For active fission product scrubbing, it is necessary that the reactor building remain structurally intact, (including the section above the operating deck where the blowout panels are located), and that the SGTS continue to operate and to filter the radionuclide release into the environment. Any gross containment failure mode will cause a pressure increase in the reactor building that is sufficient to fail the blowout panels, and therefore the reactor building effectiveness cannot be maintained. Since, as discussed for Top Event HB, it is only necessary to address gross containment failure modes, it is very unlikely that reactor building effectiveness would be maintained in any sequence involving containment failure. Therefore, a guaranteed failure of Top Event BE has been assumed in all cases; i.e., split fraction BEF = 1.0 is used in all cases.

The guaranteed failure of the reactor building effectiveness only involves the active fission product scrubbing by the SGTS in an intact reactor building maintained at a slightly negative pressure. Even without the active fission product scrubbing, the reactor building will provide some passive mitigation by fission product plateout on surfaces in the building in the release path for the source term. This passive mitigation will be discussed in the source term section.

Table 10-1. Split Fraction Logic for Oyster Creek CET			
Split Fraction	Split Fraction Logic		Comments
	N:=	INIT=PIFW + INIT=NIFW + INIT=MKCU + INIT=OJAU + INIT=MJAU + INIT=NJHW	DRYWELL SPRAYS NOT AVAILABLE OR INEFFECTIVE IF OPERABLE (I.E., CONTAINMENT BYPASSED)
	W:=	INIT=OIAU	DRYWELL SPRAYS AVAILABLE (NO BYPASS)
	Y:=	INIT=OJAU + INIT=MJAU + INIT=NJHW	DRYWELL SPRAYS INEFFECTIVE IF OPERABLE (CONTAINMENT BYPASSED TO REACTOR BUILDING)
	H:=	ES=F*(INIT=NIFW + INIT=MKCU + INIT=MJAU + INIT=NJHW)	RCS PRESSURE HIGH PRIOR TO VESSEL BREACH
	L:=	ES=S + INIT=PIFW + INIT=OIAU + INIT=OJAU	RCS PRESSURE LOW PRIOR TO VESSEL BREACH
	E:=	I1=F + I2=F + LM=F	EARLY CONTAINMENT FAILURE
	D:=	I3=F * -(I1=F + I2=F + LM=F)	LATE CONTAINMENT FAILURE (> 3.0 HRS AFTER VB)
	G:=	L1=F + L2=F + L3=F + LM=F	LARGE CONTAINMENT FAILURE
	U:=	S1=F + S3=F	NO TORUS SCRUBBING
	BP:=	BE=F	REACTOR BUILDING INEFFECTIVE IN REDUCING SOURCE TERM
	V:=	DV=S	CONTAINMENT VENTED AFTER CORE DAMAGE
	I:=	(I1=S+I1=B) * (I2=S+I2=B) * (I3=S+I3=B) * (LM=S+LM=B)	CONTAINMENT INTACT
	R:=	VB=S	CORE DAMAGE ARRESTED PRIOR TO VESSEL BREACH
ESM	INIT=MKCU		
ESP	INIT=PIFW + INIT=OIAU + INIT=OJAU + INIT=MJAU + INIT=NJHW		
ESN	INIT=NIFW		
ESF	1		
I1M	INIT=MKCU		CONTAINMENT FAILED PRIOR TO CORE DAMAGE
I1J	INIT=OJAU		TREATED AS INTACT SINCE BYPASSES CLOSE
I1B	INIT=NJHW + INIT=MJAU		CONTAINMENT BYPASSED DURING CORE DEGRADATION
I1I	INIT=NIFW + INIT=OIAU + INIT=PIFW		
I1D	1		

Table 10-1. Split Fraction Logic for Oyster Creek CET		
Split Fraction	Split Fraction Logic	Comments
L1M	INIT=MKCU	
L1J	INIT=OJAU	
L1I	INIT=NIFW + INIT=OIAU + INIT=PIFW	
L1B	INIT=MJAU + INIT=NJHW	LARGE BYPASS
L1D	1	
S1F	I1=F	
S1S	INIT=MJAU + INIT=NJHW	
S17	INIT=MKCU	
S14	INIT=OJAU	
S13	INIT=OIAU	
S12	INIT=NIFW	
S11	INIT=PIFW	
S1D	1	
VB4	INIT=MJAU	
VB3	INIT=MKCU	
VB2	INIT=NJHW	
VB1	INIT=OIAU	
VBP	INIT=PIFW	
VBN	INIT=NIFW	
VBO	INIT=OJAU	
VBF	1	
ET1	(INIT=NIFW + INIT=MJAU + INIT=NJHW + INIT=MKCU) * VB=F *ES=S	
ETS	1	
I2F	I1=F	
I2X	S1=F * ET=F * (INIT=OIAU + INIT=NIFW)	GUARANTEED FAILURE GIVEN S1=F AND ET = F
I2Q	S1=F * INIT=OIAU	INCREASED PROBABILITY DUE TO S/P BYPASS
I2O	INIT=OIAU	
I2P	INIT=PIFW	
I2M	S1=F * INIT=NIFW	
I2N	INIT=NIFW	

Table 10-1. Split Fraction Logic for Oyster Creek CET		
Split Fraction	Split Fraction Logic	Comments
I2J	INIT=OJAU	
I2D	1	
L2X	S1=F * ET=F * (INIT=OIAU +INIT=NIFW)	GUARANTEED LARGE FAILURE IF S1=F AND ET=F
L2Q	S1=F * INIT=OIAU	INCREASED PROBABILITY OF LARGE FAILURE FOR S/P BYPASS
L2O	INIT=OIAU	
L2P	INIT=PIFW	
L2M	S1=F * INIT=NIFW	INCREASED PROBABILITY OF LARGE FAILURE GIVEN S/P BYPASS
L2N	INIT=NIFW	
L2J	INIT=OJAU	
L2D	1	
LM6	(INIT=NJHW) * ES=S	
LM5	(INIT=NJHW) * ES=F	
LM4	(INIT=MJAU + INIT=MKCU) * ES=F	
LM3	INIT=OJAU + INIT=OIAU + (INIT=MKCU + INIT=MJAU) * ES=S	
LM2	(INIT=NIFW) * ES=F	
LM1	INIT=PIFW + (INIT=NIFW) * ES=S	
LMD	1	
S3F	S1=F + LM=F + I2=F + ET=F	
S31	S1=S * INIT=PIFW	
S32	S1=S * INIT=NIFW	
S33	S1=S * INIT=OIAU	
S34	S1=S * INIT=OJAU	
S35	S1=S * INIT=MJAU	
S36	S1=S * INIT=NJHW	
S31	S1=S * INIT=PIFW	
S3D	1	

Table 10-1. Split Fraction Logic for Oyster Creek CET		
Split Fraction	Split Fraction Logic	Comments
DV6	INIT=MJAU + INIT=NJHW	CONTAINMENT BYPASSED - VENTING NOT REQUIRED
DV5	INIT=MKCU	CONTAINMENT FAILED PRIOR TO CORE DAMAGE - VENTING NOT REQUIRED
DV4	INIT=OIAU	TORUS VENTING PER PROCEDURE
DV3	INIT=NIFW + INIT=PIFW	TORUS VENTING NOT AVAILABLE (PDS PARAMETER)
DV2	INIT=OJAU	"DIRTY VENTING" OF DRYWELL IN ACCORDANCE WITH PROCEDURE
DV1	1	
I3F	I1=F + I2=F	
I3X	VB=F * (S1=F + S3=F) * ET=F * INIT=OIAU	GUARANTEED FAILURE IF (S1=F + S3=F) * ET=F
I3Q	VB=F * (S1=F + S3=F) * INIT=OIAU	INCREASED FAILURE PROBABILITY FOR S/P BYPASS
I3Z	VB=S * INIT=OIAU	
I3Y	VB=S * INIT=PIFW	
I3O	INIT=OIAU	
I3P	INIT=PIFW	
I3N	INIT=NIFW	
I3J	INIT=OJAU	
I3D	1	
L3Z	VB=S * INIT=OIAU	
L3X	VB=F * (S1=F + S3=F) * INIT=OIAU	
L3Y	VB=S * INIT=PIFW	
L3O	INIT=OIAU	
L3P	INIT=PIFW	
L3R	VB=F * (S1=F + S3=F) * INIT=NIFW	INCREASED PROBABILITY OF LARGE CF IF S/P BYPASSED
L3N	INIT=NIFW	
L3J	INIT=OJAU	
L3D	1	
HBF	1	
BEF	1	

Table 10-2. Oyster Creek Master Frequency File			
Split Fraction	Top Event	Value	Description
ESM	ES	2.1760E-01	MKCU - 125 CYCLES
ESP	ES	1.0000E+00	PIFW, OIAU, OJAU, MJAU, NJHW
ESN	ES	2.0730E-01	NIFW - 129 CYCLES
ESF	ES	1.0000E+00	
I1Z	I1	0.0000E+00	VB=S * INIT=OIAU - NO EARLY CF
I1Y	I1	0.0000E+00	VB=S * INIT=PIFW - NO EARLY CF
I1M	I1	1.0000E+00	MKCU - CONTAINMENT FAILS PRIOR TO CORE DAMAGE
I1I	I1	0.0000E+00	NO CF PRIOR TO V/B - NIFW, OIAU, PIFW
I1J	I1	0.0000E+00	OJAU
I1B	I1	1.0000E+00	MJAU, NJHW - CONT BYPASS DURING CORE DEGRAD
I1D	I1	1.0000E+00	DEFAULT FOR INTACT CONTAINMENT PRIOR TO VESSEL BREACH
L1Z	L1	0.0000E+00	VB=S * INIT=OIAU - NO EARLY CF
L1Y	L1	0.0000E+00	VB=S * INIT=PIFW - NO EARLY CF
L1M	L1	9.3000E-01	MKCU - (DRB MEMO - 12/3/91)
L1J	L1	0.0000E+00	
L1B	L1	1.0000E+00	MJAU, NJHW - LARGE BYPASS
L1I	L1	0.0000E+00	NO CF PRIOR TO V/B - NIFW, OIAU, PIFW
L1D	L1	1.0000E+00	DEFAULT FOR INTACT CONTAINMENT
S1Z	S1	0.0000E+00	VB=S * INIT=OIAU - ALL RELEASE THRU SP
S1Y	S1	0.0000E+00	VB=S * INIT=PIFW - ALL RELEASE THRU SP
S17	S1	4.1980E-01	MKCU - 422 CYCLES
S1S	S1	0.0000E+00	MJAU, NJHW
S14	S1	3.6700E-02	OJAU - 29 CYCLES
S13	S1	9.3400E-02	OIAU - 76 CYCLES
S12	S1	2.5500E-02	NIFW - 20 CYCLES
S11	S1	1.0730E-01	PIFW - 88 CYCLES
S1F	S1	1.0000E+00	GUARANTEED FAILURE
S1D	S1	1.0000E+00	DEFAULT
VB4	VB	1.0000E+00	MJAU - GPU LETTER 5430-91-0062, DEC 10, 1991
VB3	VB	1.0000E+00	MKCU - GPU LETTER 5430-91-0062, DEC 10, 1991
VB2	VB	1.0000E+00	NJHW - GPU LETTER 5430-91-0062, DEC 10, 1991

Table 10-2. Oyster Creek Master Frequency File			
Split Fraction	Top Event	Value	Description
VB1	VB	1.8550E-01	OIAU - CANAVAN FAX DATED JAN 21, 1992
VBP	VB	0.0000E+00	PIFW - GPU LETTER 5430-91-0062, DEC 10, 1991
VBN	VB	1.0000E+00	NIFW - GPU LETTER 5430-91-0062, DEC 10, 1991
VBO	VB	1.0000E+00	OJAU - GPU LETTER 5430-91-0062, DEC 10,1991
VBF	VB	1.0000E+00	
ETS	ET	0.0000E+00	LOW PRESSURE MELT EJECTION
ET1	ET	1.0000E-01	HIGH PRESSURE MELT EJECTION
ETF	ET	1.0000E+00	
I2X	I2	1.0000E+00	GUARANTEED FAILURE IF LARGE S/P BYPASS
I2Q	I2	5.0000E-01	INCREASED FAILURE PROBABILITY FOR S/P BYPASS - OIAU
I2M	I2	5.0000E-01	INCREASED FAILURE PROBABILITY FOR S/P BYPASS - NIFW
I2O	I2	0.0000E+00	OIAU (DRB MEMO - 12/23/91)
I2P	I2	4.1000E-02	PIFW (DRB MEMO - 12/23/91)
I2N	I2	2.1900E-01	NIFWW (DRB MEMO - NOV. 8, 1991)
I2J	I2	0.0000E+00	OJAU
I2F	I2	1.0000E+00	GUARANTEED FAILED IF I1=F
I2D	I2	1.0000E+00	
L2X	L2	1.0000E+00	GUARANTEED LARGE FAILURE IF LARGE S/P BYPASS
LQ2	L2	1.0000E+00	
L2M	L2	1.0000E+00	
L2O	L2	0.0000E+00	OIAU (DRB MEMO - 12/23/91, NO EARLY CF)
L2P	L2	1.0000E+00	PIFW (DRB MEMO - 12/23/91)
L2N	L2	9.9000E-01	NIFWW (DRB MEMO - NOV. 8, 1991)
L2J	L2	0.0000E+00	OJAU
L2D	L2	1.0000E+00	
LMD	LM	1.0000E+00	DEFAULT
LM1	LM	5.5000E-02	PR LOW AT VB;NO H2O ON D/W FL;NO SPR;VES INJ
LM2	LM	3.0500E-01	PR HI AT VB;NO H2O ON D/W FL;NO SPR;VES INJ AFT VB
LM3	LM	5.0500E-03	PR LOW AT VB;H2O ON D/W FL;D/W SPR OPER AFTER VB
LM4	LM	5.1000E-03	PR HI AT VB;H2O ON D/W FL;D/W SPR OPER AFTER VB
LM5	LM	5.0500E-01	PR HI AT VB;NO H2O ON D/W FL;NO SPR OR VES INJ

Table 10-2. Oyster Creek Master Frequency File			
Split Fraction	Top Event	Value	Description
LM6	LM	1.0500E-01	PR LOW AT VB;NO H2O ON D/W FL;NO SPR OR VES INJ
S3Z	S3	0.0000E+00	VB=S * INIT=OIAU - ALL RELEASE THRU SP
S3Y	S3	0.0000E+00	VB=S * INIT=PIFW - ALL RELEASE THRU SP
S36	S3	1.3790E-01	NJHW - 115 CYCLES (S1=S)
S35	S3	1.0040E-01	MJAU - 82 CYCLES (S1=S)
S34	S3	2.4220E-01	OJAU - 215 CYCLES (S1=S)
S33	S3	1.0040E-01	OIAU - 82 CYCLES (S1=S)
S32	S3	9.4600E-02	NIFW - 77 CYCLES (S1=S)
S31	S3	3.8830E-01	PIFW - 381 CYCLES (S1=S)
S3F	S3	1.0000E+00	S1=F
S3D	S3	1.0000E+00	
DV1	DV	1.0000E+00	
DV2	DV	2.3000E-02	OJAU - DRYWELL VENT (OV2)
DV3	DV	1.0000E+00	NIFW, PIFW - TORUS VENT NOT AVAILABLE
DV4	DV	1.7000E-03	OIAU - TORUS VENT PER PROCEDURE (OV1 FROM LEVEL 1)
DV5	DV	1.0000E+00	MKCU - CONT FAIL PRIOR TO CORE DAM - NO VENT REQ
DV6	DV	1.0000E+00	MJAU, NJHW - CONT BYPASSED - NO VENT REQ
I3X	I3	1.0000E+00	GUARANTEED FAILURE FOR LARGE S/P BYPASS
I3Q	I3	5.0000E-01	INCREASED PROBABILITY OF CF FOR S/P BYPASS
I3Z	I3	1.3000E-02	VB=S * INIT=OIAU - FAILURE TO VENT
I3Y	I3	1.0000E+00	VB=S * INIT=PIFW - NO CHR UNLESS POWER RECOVERED
I3O	I3	1.0000E+00	OIAU (DRB MEMO - 12/23/91)
I3P	I3	1.0000E+00	PIFW (DRB MEMO - 12/23/91)
I3N	I3	1.0000E+00	NIFWW (DRB MEMO - 11/8/91)
I3F	I3	1.0000E+00	GUARANTEED FAILED IF I1=F OR I2=F OR LM=F
I3J	I3	1.0000E+00	OJAU WITHOUT VENTING
I3D	I3	1.0000E+00	
L3X	L3	1.0000E+00	INCREASED PROBBILITY OF LARGE CF GIVEN LARGE S/P BYPASS
L3Z	L3	0.0000E+00	VB=S * INIT=OIAU - CHR EFFECTIVE FOR RECOVERED SEQUENCES
L3Y	L3	6.5500E-01	VB=S * INIT=PIFW - SAME AS VB=F
L3O	L3	1.0000E+00	OIAU (DRB MEMO - 12/23/91, NO THERMAL CREEP)

Table 10-2. Oyster Creek Master Frequency File			
Split Fraction	Top Event	Value	Description
L3P	L3	6.5500E-01	PIFW (DRB MEMO - 12/23/91)
L3N	L3	7.0000E-01	NIFWW (DRB MEMO - Nov. 8, 1991)
L3R	L3	1.0000E-01	INCREASED PROBABILITY OF LARGE CF GIVEN S/P
L3J	L3	7.1300E-01	OJAU WITH NO VENT (DRB MEMO - JAN. 22, 1992)
L3D	L3	1.0000E+00	
HBF	HB	1.0000E+00	
BEF	BE	1.0000E+00	

Table 10-3 (Page 1 of 3). Number of Safety Valves, Relief Valves, and Vacuum Breaker Cycles

Description	PIFW				NIFW			
Case:								
Time of "Core Uncovery"	20.81 Minutes				29.64 Minutes			
Time of "Vessel Failed"	1.656 Hours				2.404 Hours			
Containment Failure Time	10.0 Hours (142 psia, 440°F)				7.68 Hours (137 psia, 500°F)			
Cycles To:	**20.81 Min.**	**1.656 Hrs.**	**9.816 Hrs.**	**Long-Term Rate**	**29.64 Min.**	**2.404 Hrs.**	**7.68 Hrs.**	**53.52 Hrs.**
"Vacuum Breakers Open"	0	88	469	14 per hour	0	20	97	97
"Safety Valves Open"	0	0	0	0	134	263	266	266
"Relief Valve Open"	5	5	5	0		0	0	0

Description	OIAU				OJAU			
Case:								
Time of "Core Uncovery"	52.5 Seconds				1.067 Hours			
Time of "Vessel Failed"	1.004 Hours				3.084 Hours			
Containment Failure Time	20.0 Hours (72 psia, 870°F)				12.0 Hours (137 psia, 500°F)			
Cycles To:	**52.5 Sec.**	**1.004 Hrs.**	**3.528 Hrs.**	**Long-Term Rate**	**1.067 Hrs.**	**3.084 Hrs.**	**7.322 Hrs.**	**Long-Term Rate**
"Vacuum Breakers Open"	0	76	158	17 per hour	12	29	244	41 per hour
"Safety Valves Open"	0	0	0	0	0	0	0	0
"Relief Valve Open"	4	4	4	0	4	4	4	0

Table 10-3 (Page 2 of 3). Number of Safety Valves, Relief Valves, and Vacuum Breaker Cycles

Description	MJAU				NJHW			
Case:								
Time of "Core Uncovery"	7.771 Hours				15.65 Minutes			
Time of "Vessel Failed"	10.61 Hours				1.595 Hours			
Containment Failure Time	None				None			
Cycles To:	**7.771 Hrs.**	**10.61 Hrs.**	**58.82 Hrs**	**34.61 Hrs.**	**15.65 Min.**	**1.595 Hrs.**	**37.57 Hrs.**	**25.60 Hrs.**
"Vacuum Breakers Open"	0	0	87	82	0	0	117	115
"Safety Valves Open"	0	0	0	0	0	0	0	0
"Relief Valve Open"	0	0	5	0	3	3	3	0

Description	MKCUTTP				MKCUTTPL			
Case:								
Time of "Core Uncovery"	None				1.067 Hours			
Time of "Vessel Failed"	None				3.084 Hours			
Containment Failure Time	Expected at 5.25 Hrs. (147 psia, 345°F)				12.0 Hours (137 psia, 500°F)			
Cycles To:	**4 Hrs.**	**5.25 Hrs.**	**10 Hrs.**		**8.079 Hrs.**	**10.98 Hrs.**	**20 Hrs.**	**Long-Term Rate**
"Vacuum Breakers Open"	336	481	1,192		746	857	967	38 per hour
"Safety Valves Open"	5	5	5		5	5	5	0
"Relief Valve Open"	737	938	1,675		1,316	1,428	1,432	0

Table 10-3 (Page 3 of 3). Number of Safety Valves, Relief Valves, and Vacuum Breaker Cycles

Description	MKCUTTPB			
Case:	CF Break at 3.9 Hours.			
Time of "Core Uncovery"	3.965 Hours			
Time of "Vessel Failed"	6.512 Hours			
Containment Failure Time	3.90 Hours (break)			
Cycles To:	**3.965 Hrs.**	**6.512 Hrs.**	**20 Hrs.**	**Long-Term Rate**
"Vacuum Breakers Open"	279	422	898	45 per hour
"Safety Valves Open"	5	5	5	0
"Relief Valve Open"	712	837	839	0

Valves, and Vacuum Breaker Cycles

Table 10-4. Split Fractions for Top Event ES			
Case/KPDS	Number of Cycles	Split Fraction	
		Designator	Value
PIFW	0	ESP	1.0
NIFW	129	ESN	0.2073
OIAU	0	ESP	1.0
OJAU	0	ESP	1.0
MJAU	0	ESP	1.0
NJHW	0	ESP	1.0
MKCU	125	ESM	0.2176

Table 10-5. Split Fractions for Top Event I1			
KPDS	Conditions	Split Fraction	
		Designator	Value
OIAU	Core Damage Arrested in Vessel	I1Z	0.0
PIFW	Core Damage Arrested in Vessel	I1Y	0.0
MKCU	Containment Failure Prior To Vessel Breach	I1M	1.0
NIFW, OIAU, PIFW	Core Damage Not Arrested	I1I	0.0
OJAU	Small Bypass	I1J	0.0
MJAU, NJHW	Large Bypass	I1B	1.0

Table 10-6. Split Fractions for Top Event L1			
KPDS	Conditions	Split Fraction	
		Designator	Value
OIAU	Core Damage Arrested in Vessel	L1Z	0.0*
PIFW	Core Damage Arrested in Vessel	L1Y	0.0*
MKCU	Containment Failure Prior To Vessel Breach	L1M	0.93
NIFW, OIAU, PIFW	Core Damage Not Arrested	L1I	0.0*
OJAU	Small Bypass	L1J	0.0*
MJAU, NJHW	Large Bypass	L1B	1.0
* Assigned a value of 0.0, but no failure occurs.			

Table 10-7. Split Fractions for Top Event S1			
Case/KPDS	Number of Cycles	Split Fraction	
		Designator	Value
PIFW	88	S11	0.1073
NIFW	20	S12	0.0255
OIAU	76	S13	0.0934
OJAU	29	S14	0.0367
MJAU	0	S1S	0
NJHW	0	S1S	0
MKCU	422	S17	0.4198

Table 10-8. Split Fractions for Top Event I2			
KPDS	Conditions	Split Fraction	
		Designator	Value
NIFW, OIAU	Large Suppression Pool Bypass (SI=F * ET=F)	I2X	1.0
OIAU	Suppression Pool Bypassed (SI=F)	I2Q	0.5
OIAU	No Suppression Pool Bypass	I2O	0.0
PIFW	Core Damage Not Arrested; No Suppression Pool Bypass	I2P	0.041
NIFW	Suppression Pool Bypassed (SI=F)	I2M	0.5
NIFW	No Suppression Pool Bypass	I2N	0.219
OJAU	No Suppression Pool Bypass	I2J	0.0

Table 10-9. Split Fractions for Top Event L2			
KPDS	Conditions	Split Fraction	
		Designator	Value
NIFW, OIAU	Large Suppression Pool Bypass (SI=F * ET=F)	L2X	1.0
OIAU	Suppression Pool Bypassed (SI=F)	L2Q	1.0
OIAU	No Suppression Pool Bypass	L2O	0.0*
PIFW	Core Damage Not Arrested; No Suppression Pool Bypass	L2P	1.0
NIFW	Suppression Pool Bypassed (SI=F)	L2M	1.0
NIFW	No Suppression Pool Bypass	L2N	0.99
OJAU	No Suppression Pool Bypass	L2J	0.0*
* Assigned a value of 0.0, but no failure occurs.			

Table 10-10. Probability of Release from Drywell Liner Melt-Through at Floor							
Parameter Set	RCS Press at VB	Water on DW Floor at VB	Drywell Spray after VB	Vessel Injection after VB	Release Probability	Basis (note)	Applicable KPDSs
1	Low	Yes	Yes	--	$5x10^{-5}$	1	
2	Low	Yes	No	Yes	$5x10^{-5}$	1	
3	Low	No	Yes	--	0.01	2	PIFW
4	Low	No	No	Yes	0.05	8	
5	Low	No	No	No	0.1	4	
6	High	Yes	Yes	--	$1x10^{-4}$	5	
7	High	Yes	No	Yes	$1x10^{-3}$	6	
8	High	No	Yes	--	0.05	7	
9	High	No	No	Yes	0.3	8	NIFW
10	High	No	No	No	0.5	9	

Notes:

1. NUREG/CR-5423 estimates probability of liner melt-through at floor for these conditions to be $< 1x10^{-4}$. Because of curb, Oyster Creek should be even lower.

2. 100 times NUREG/CR-5423 value of $1x10^{-4}$.

3. 500 times NUREG/CR-5423 value of $1x10^{-4}$. Vessel injection not as effective as drywell spray in preventing melt-through.

4. Credit for curb; consistent with other low pressure ejection values.

5. NUREG/CR-5423.

6. 10 times NUREG/CR-5423 value; vessel injection not given some credit for HP ejection as drywell sprays.

7. NUREG/CR-5423 with credit for curb and drywell spray.

8. 0.5 times NUREG/CR-5423 value of 0.6; credit for curb and vessel injection.

9. NUREG/CR-5432 assumes conditional failure probability of 0.6 - 1.0 if no water is present. Due to presence of curb, Oyster Creek should be better.

Table 10-11. Split Fractions for Top Event S3			
Case/KPDS	Number of Cycles	Split Fraction	
		Designator	Value
PIFW	381	S31	0.3883
NIFW	77	S32	0.0946
OIAU	82	S33	0.1004
OJAU	215	S34	0.2422
MJAU	82	S35	0.1004
NJHW	115	S36	0.1379
MKCU	–	S3F	1.0000

Table 10-12. Split Fractions for Top Event I3			
KPDS	Conditions	Split Fraction	
		Designator	Value
OIAU	Large Suppression Pool Bypass	I3X	1.0
OIAU	Suppression Pool Bypassed	I3Q	0.5
OIAU	Core Damage Arrested; No Suppression Pool Bypass	I3Z	0.013
PIFW	Core Damage Arrested; No Containment Heat Removal	I3Y	1.0
OIAU	Vessel Breached; No Suppression Pool Bypass	I3O	0.12
PIFW	Vessel Breached; No Suppression Pool Bypass	I3P	1.0
NIFW	–	I3N	1.0
OJAU	No Venting	I3J	1.0

Table 10-13. Split Fractions for Top Event L3			
KPDS	Conditions	Split Fraction	
		Designator	Value
OIAU	Large Suppression Pool Bypass	L3X	1.0
OIAU	Suppression Pool Bypassed	L3Q	0.0
OIAU	Core Damage Arrested; No Suppression Pool Bypass	L3Z	0.0
PIFW	Core Damage Arrested; No Containment Heat Removal	L3Y	0.655
OIAU	Vessel Breached; No Suppression Pool Bypass	L3O	1.0
PIFW	Vessel Breached; No Suppression Pool Bypass	L3P	0.655
NIFW	Vessel Breached; No Suppression Pool Bypass	L3N	0.7
NIFW	Vessel Breached; Suppression Pool Bypasses	L3R	1.0
OJAU	No Venting	L3J	0.713

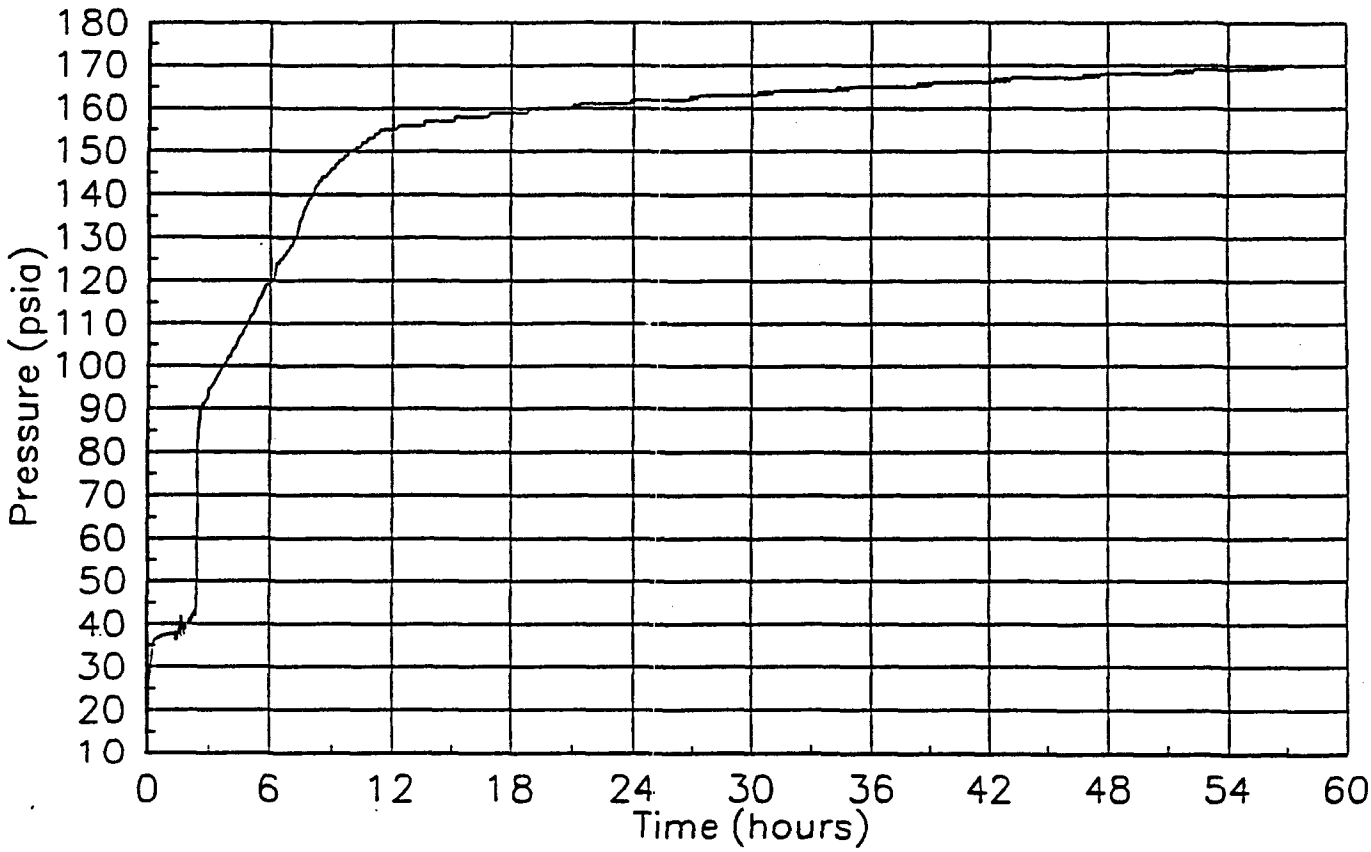

Figure 10-1. Drywell Pressure — NIFW

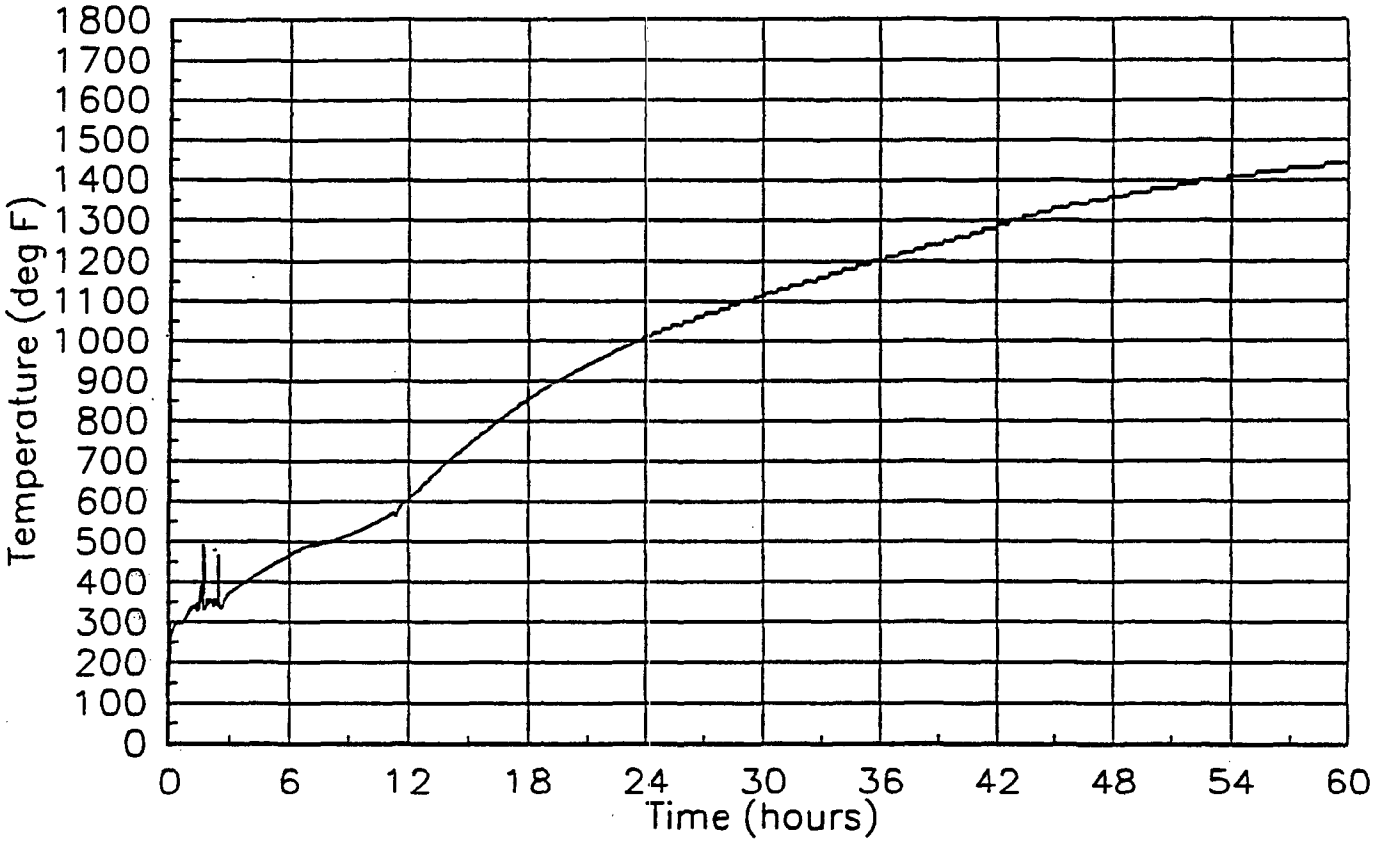

Figure 10-2. Drywell Gas Temperature — NIFW

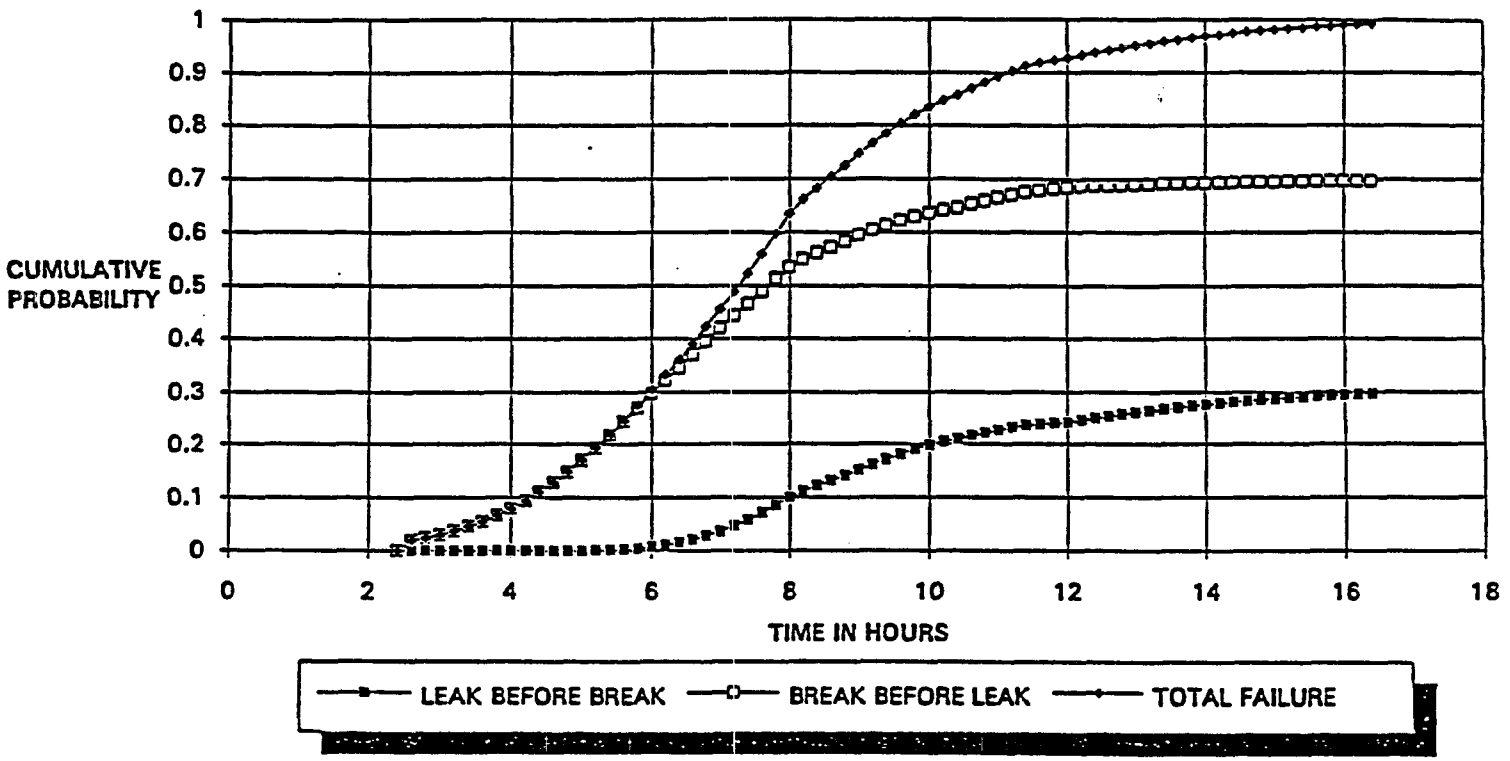

Figure 10-3. Cumulative Containment Failure Probability Distributions for KPDS NIFW

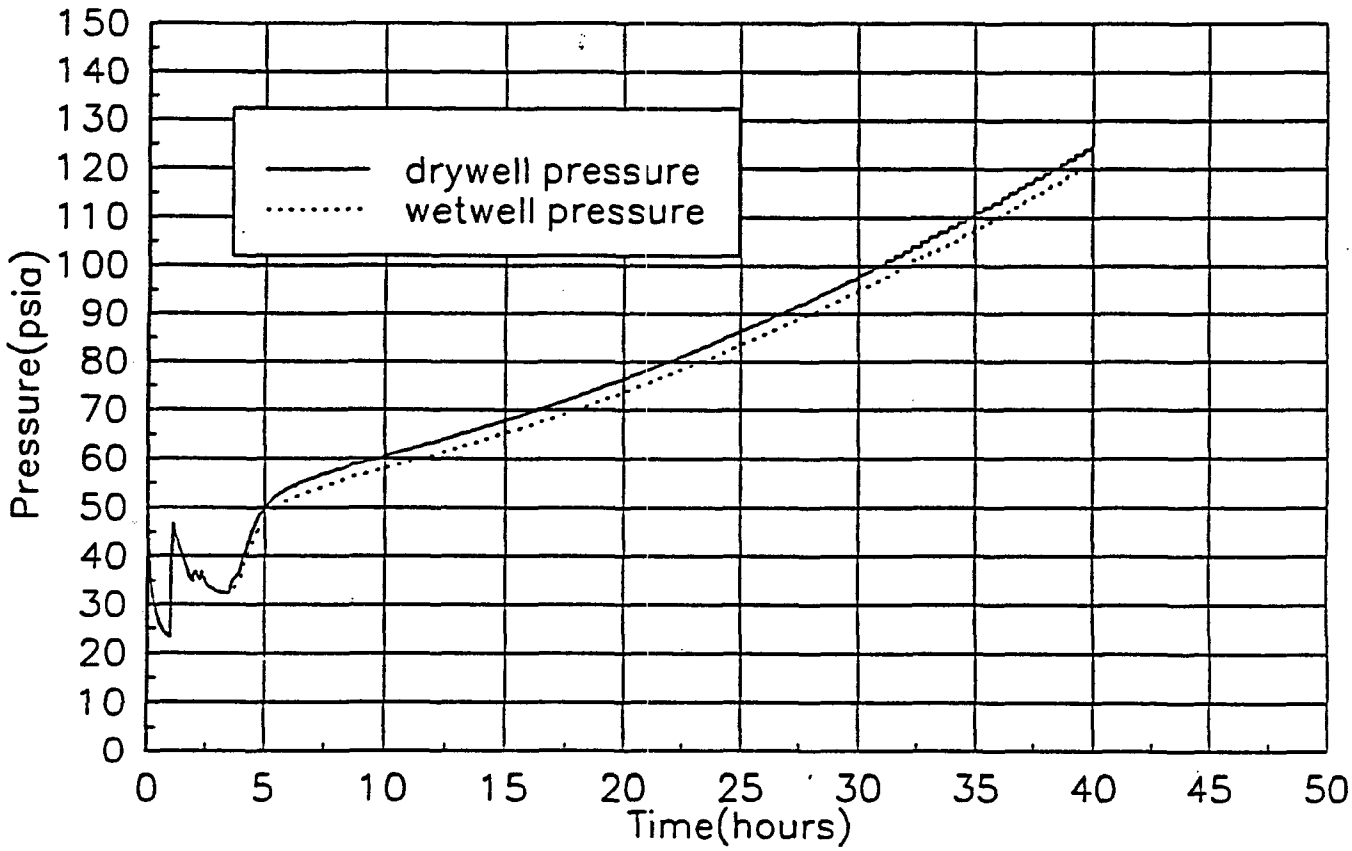

Figure 10-4. Containment Pressure — OIAU

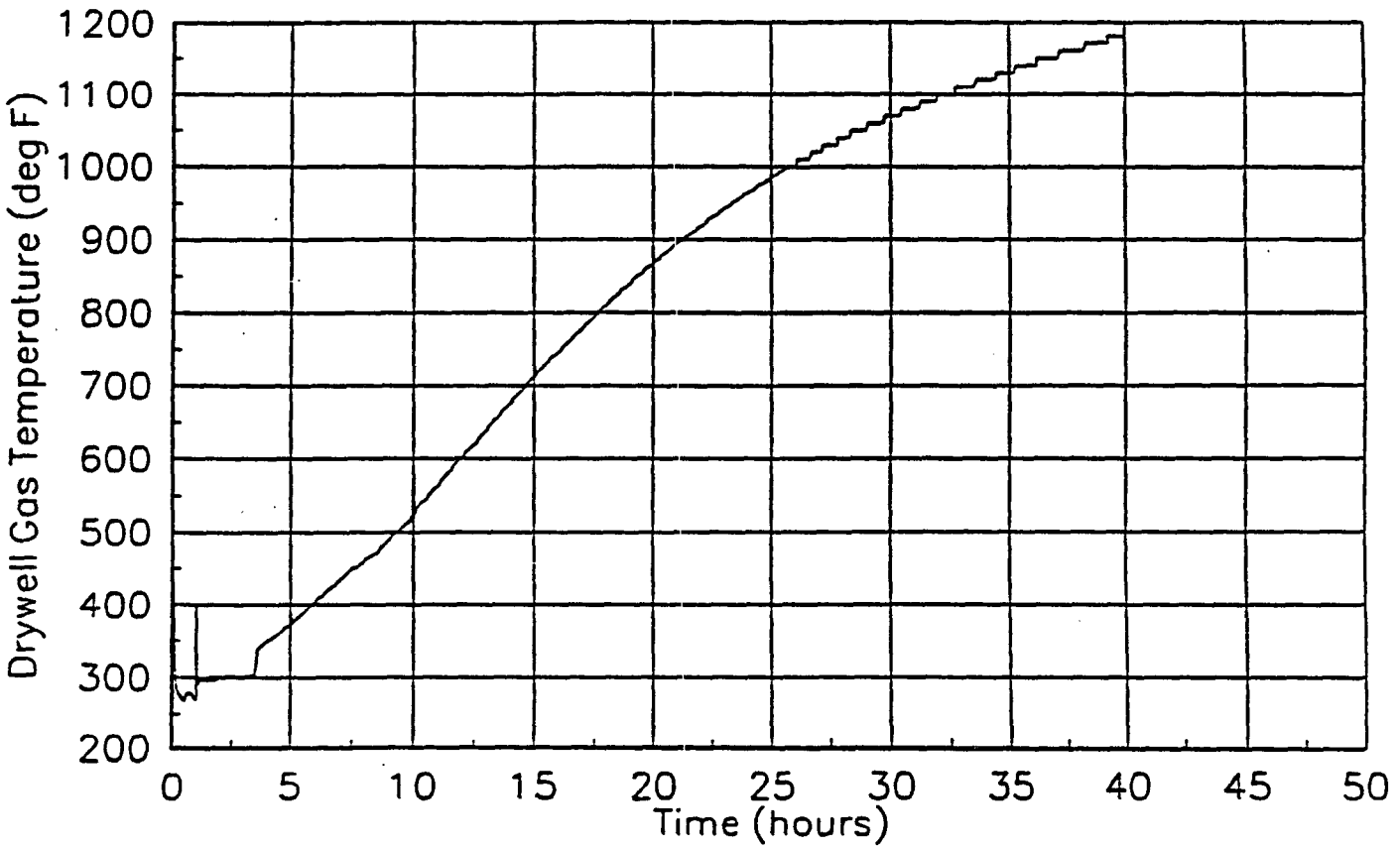

Figure 10-5. Drywell Gas Temperature — OIAU

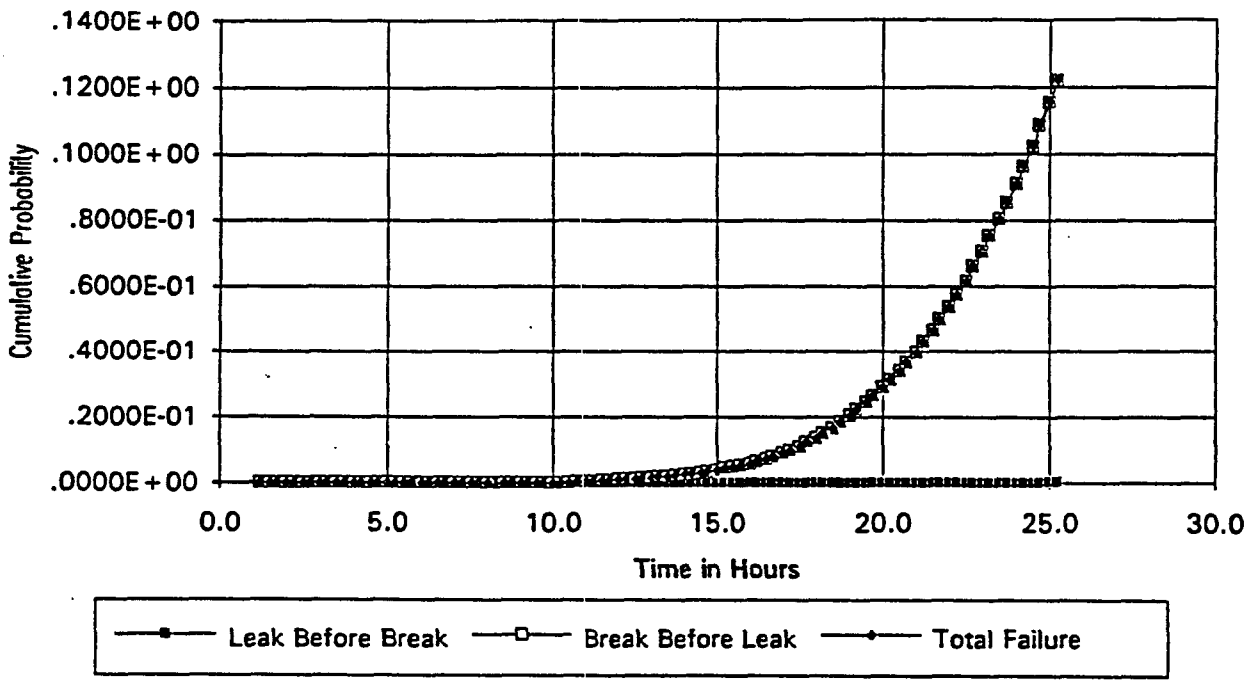

Figure 10-6. Cumulative Failure Probability Distributions for KPDS OIAU

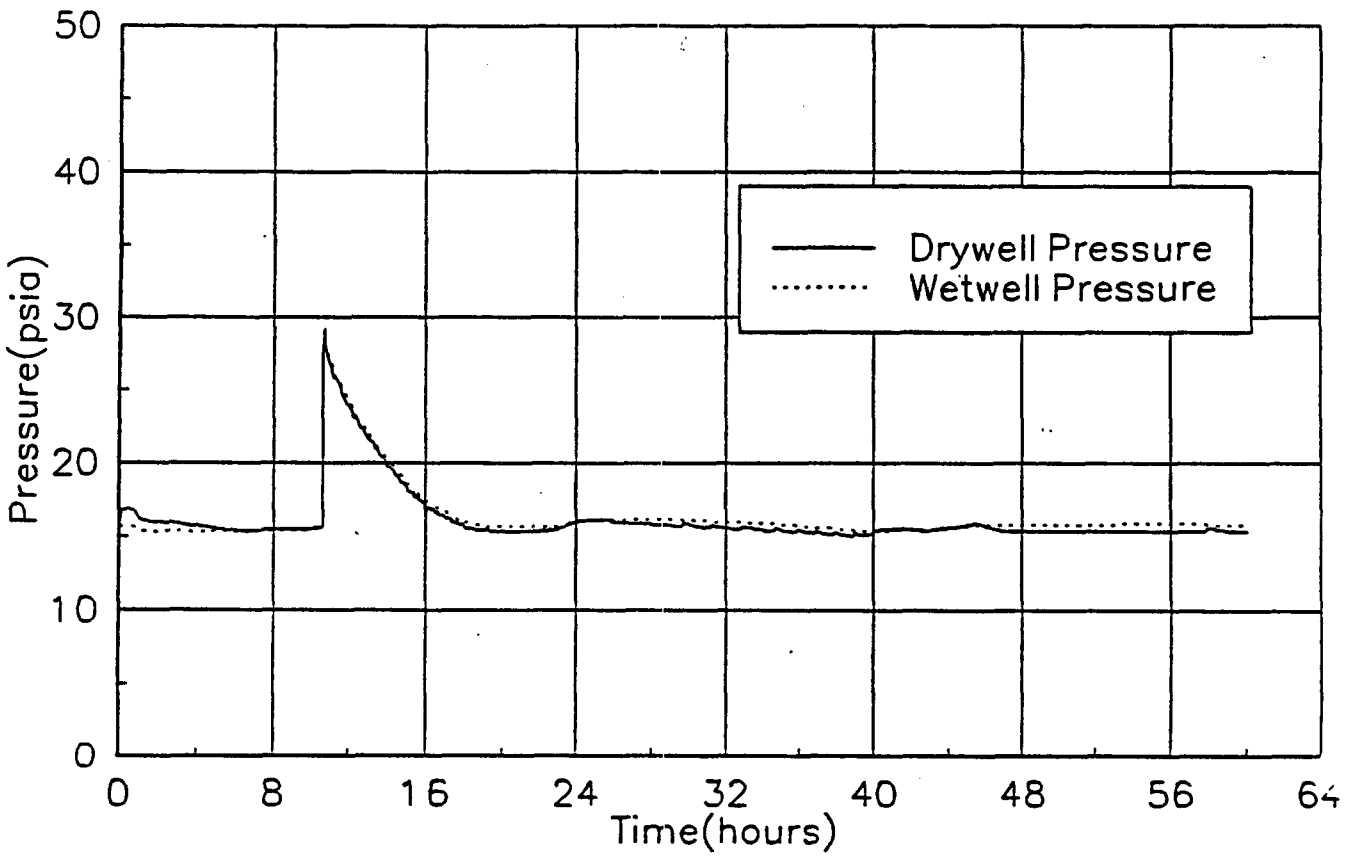

Figure 10-7. Containment Pressure — MJAU

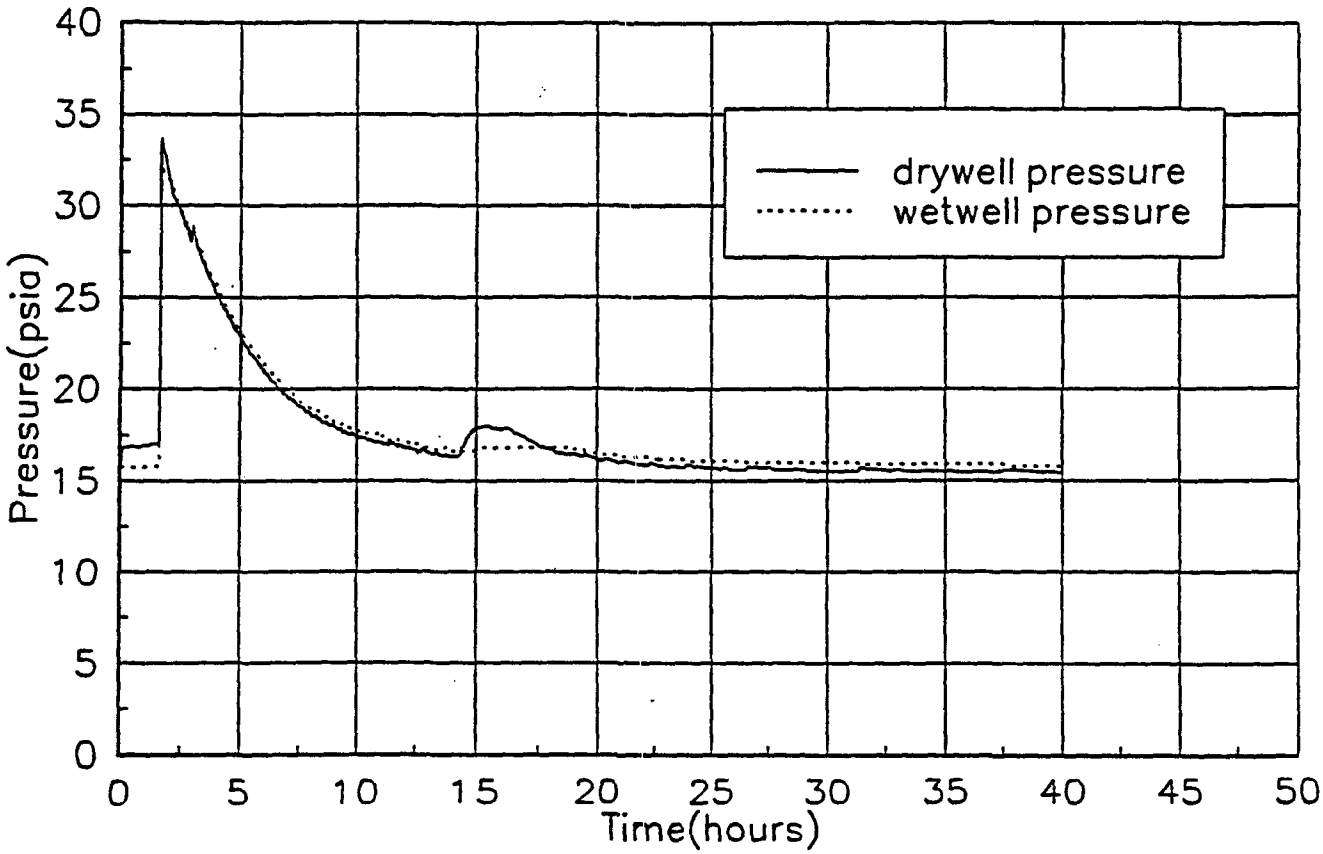

Figure 10-8. Containment Pressure — NJHW

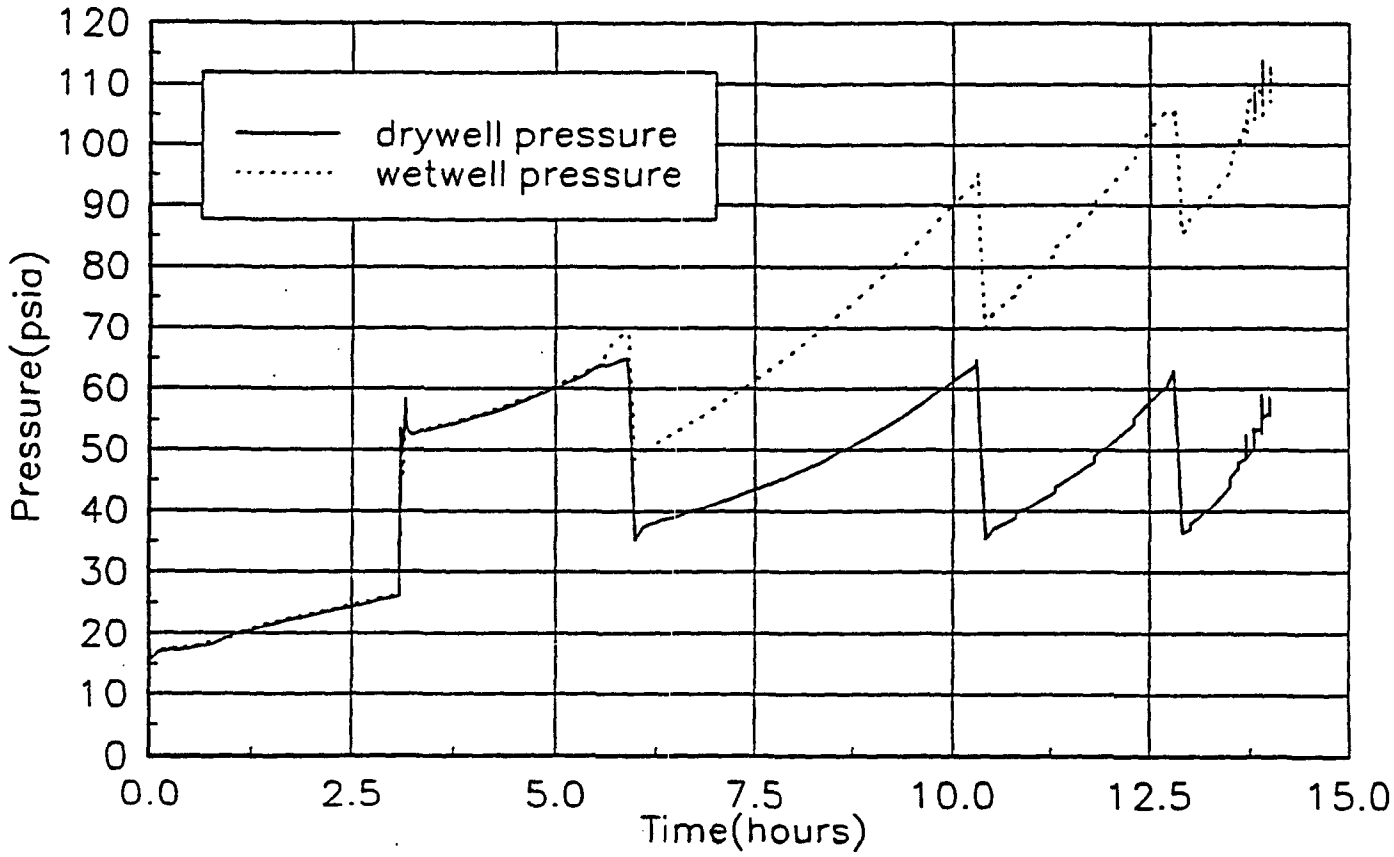

Figure 10-9. Containment Pressure — OJAU

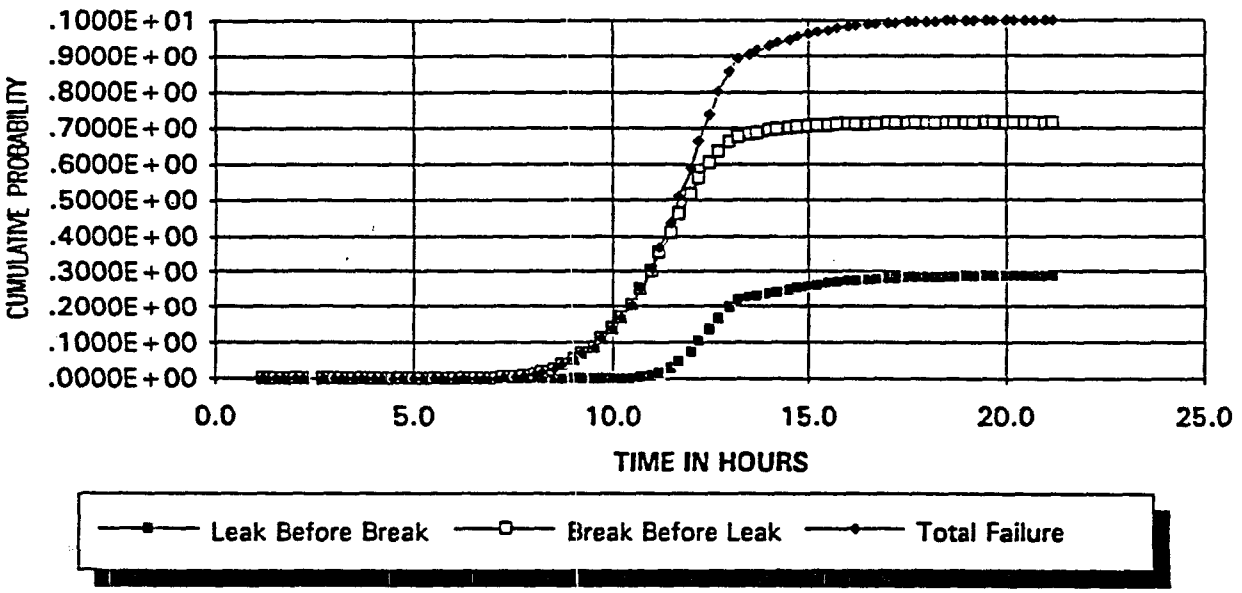

Figure 10-10. Cumulative Failure Probability Distributions for KPDS OJAU

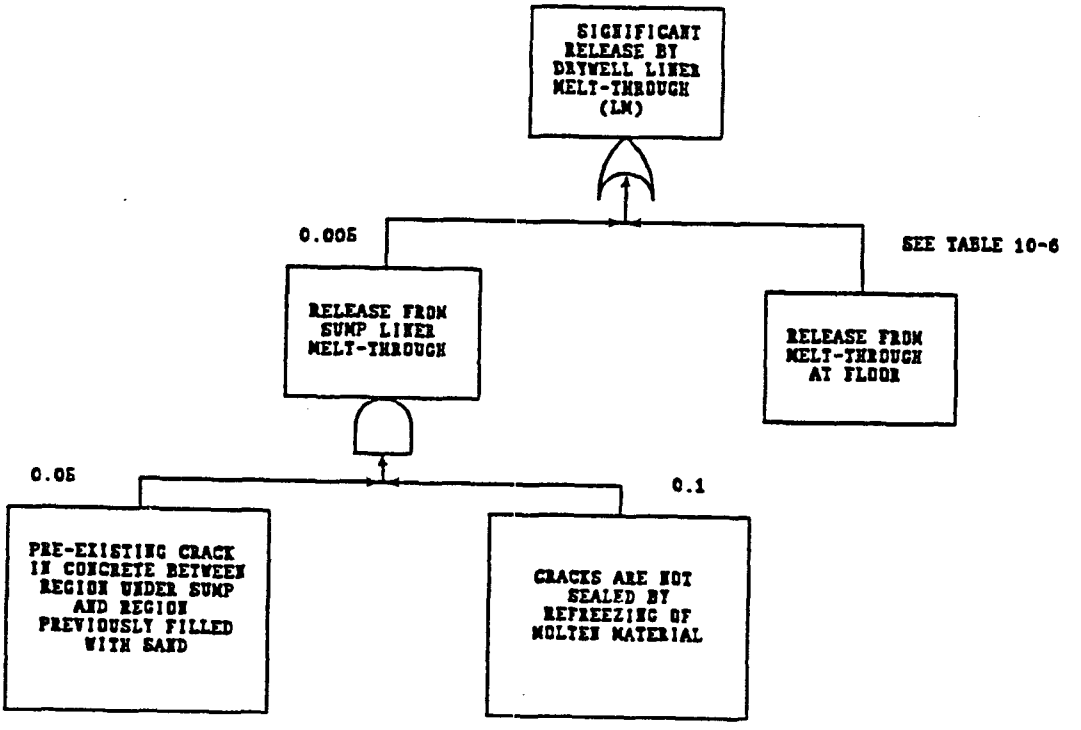

Figure 10-11. Fault Tree Representation for Liner Melt-Through Release

11. RADIONUCLIDE RELEASE CHARACTERISTICS

11.1 RELEASE CATEGORY DEFINITION

The end states of Level 2 quantification are called release categories. A release category is a qualitative description of the CET end state bin, whereas the source term is the corresponding quantitative description of the bin; i.e., release fractions, release timing, etc.

The definition of release categories is greatly facilitated through the use of a source term event tree (STET). The purpose of such a tree is to define the different release categories for which the source term characteristics could be sufficiently different to warrant a separate source term definition. The Oyster Creek STET is shown in Figure 11-1. It is used to develop the CET binning logic for assigning the appropriate release categories for each CET sequence.

The first two STET top events are keyed to PDS groups. The first top event asks whether vessel breach is prevented, and if it is not prevented, whether drywell spray is available. Vessel breach is prevented if vessel injection is established in time to quench and cool the overheated core in the vessel, even though core overheating and some core damage may have occurred. This is what actually happened in the TMI-2 accident. If drywell spray is available according to the PDS, then it is assumed that it is available for the entire accident sequence. Failures of drywell spray function as a result of the drywell accident environment prior to containment failure are not considered because only passive equipment (piping and spray nozzles) are located in the drywell.

The second STET top event, which is also keyed to PDS groups, asks whether the RCS pressure at vessel breach is high or low. This distinction is made for release category differentiation so that the source term effects associated with high pressure vessel melt-through can be addressed.

The third and fourth top events question whether the containment remains intact or whether dirty venting has occurred. If neither of these top events is successful, containment failure will occur, and the remaining top events question the timing of containment failure, the degree of scrubbing by the suppression pool prior to containment failure, and the effectiveness of the reactor building and its engineered safeguards after containment failure. Although the ability of the suppression pool to trap fission products after containment failure would also be an important consideration, the containment failure modes discussed in Section 6 appear to preclude the possibility of post-containment failure scrubbing by the suppression pool.

The time of release distinction is made in relation to the core melt accident progression. An early release occurs if the containment is failed, unisolated, or bypassed at the time when core damage occurs, or where the containment fails due to the conditions of the accident progression before, at, or shortly after the time of vessel breach. Early release modes are characterized by limited opportunities for release mitigation by natural processes, such as aerosol agglomeration and deposition, plateout, and suppression pool scrubbing prior to containment failure.

A late release occurs if the containment is intact at the time of vessel breach, but it fails in the long term, usually several hours after vessel breach, due to a slow pressure buildup in the absence of containment heat removal.

The early failure mode characterization does not necessarily bear a direct relationship to either the time of release, as measured in hours after the initiating event, or the warning time for evacuation of the population surrounding the plant. An early release mode could occur late if the onset of core damage is delayed; for example, scenarios in which vessel makeup fails as a result of containment overpressurization; i.e., the so-called TW sequences. An early release could also have a long warning time if the need for an evacuation is recognized well before core damage begins.

In principle, there could be release paths where the release is scrubbed by the water in the isolation condenser (IC). However, analysis has shown that thermally induced IC tube failures are unlikely even in the absence of water in the IC; therefore, this pathway has not been considered in the definition of release categories.

The release category definition is an identifier with up to seven characters defined as follows:

- **First Character: Drywell Spray Available**

  R = Debris recovered in vessel, no vessel melt-through.

  W = Drywell spray is available for the duration of the accident sequence. Drywell spray initiation occurs when the conditions for automatic or operator initiation are satisfied. All questions related to system availability and actuation are addressed in the Level 1 model and reflected in the PDS assignment. The W-state exists for PDSs where the third letter designator is A, B, or C. The PDS matrix and the definition of the letter designators are shown in Figure 5-1.

  N = No drywell spray or wetwell airspace spray is available. The N-state exists for PDSs where the third letter designator is D, E, F, G, or H.

- **Second Character: RCS Pressure at Vessel Breach**

  L = Low pressure, vessel has been depressurized and has not repressurized at vessel breach. The L-state exists for low pressure PDS (first PDS letter O or P) or for high pressure PDS (first PDS letter M or N) with CET Top Event ES successful.

  H = High pressure, vessel has not been depressurized or it has repressurized at vessel breach. The H-state exists for high pressure PDS (first PDS letter M or N) with CET Top Event ES failed.

- **Third Character: Containment Failure**

  I = Containment remains intact throughout accident sequence. The I-state exists if CET Top Event VB is successful or if none of the Top Events I1, I2, I3, or LM is failed.

  V = Containment has been vented after core damage. The V-state exists if CET Top Event DV is successful.

  F = Containment is failed. The F-state applies for all CET sequences where neither the I-state nor the V-state applies.

- **Fourth Character: Containment Failure Time**

  D = Containment fails late, implying that failure occurs more than 3 hours after vessel breach, resulting in adequate time for fission product settling, plateout, etc. The D-state exists if CET Top Events I1, I2, and LM are successful but Top Event I3 is failed.

  E = Containment fails early, implying that failure occurs before, at, or shortly after vessel breach. The E-state exists if one of the CET Top Events I1, I2, or LM is failed.

- **Fifth Character: Containment Failure Mode**

  C = Controlled (leak) failure, containment source term is released to reactor building over a time period longer than 1 hour. The C-state exists if CET Top Events L1, L2, L3, and LM are either bypassed or successful.

  G = Gross failure (large leak), containment source term is rapidly released to reactor building. The G-state exists if one of the CET Top Events L1, L2, L3, and LM is failed.

- **Sixth Character: Suppression Pool Scrubbing**

  S = Torus scrubs nongaseous fission products out of the vent pipe flow up to the time of containment failure. For vent scenarios, the torus scrubs the entire vent release; i.e., venting is from the wetwell and the suppression pool is not bypassed. The S-state exists if CET Top Events S1 and S3 are both successful.

  U = No torus scrubbing. The U-state exists if either CET Top Event S1 or S3 is failed.

- **Seventh Character: Reactor Building Mitigation**

  M = Release at containment failure is mitigated by the intact reactor building. No fire sprays and no SGTS operation are assumed; i.e., their effects are conservatively neglected. The M-state exists if CET Top Event BE is successful.

  B = Release at containment failure is not mitigated by the reactor building; i.e., the reactor building is effectively bypassed. The B-state exists if CET Top Event BE is failed.

The STET itself has 64 sequences (and end states), meaning that source terms would have to be defined for 64 release categories if each has a significant frequency. However, many of these release categories will have very small frequencies. After the frequency of each release category is known, the 64 release categories can be condensed into key release categories.

The first four sequences address source terms from TMI-2-type sequences where the debris is recovered in-vessel and vessel breach is prevented. Under these conditions, a source term distinction is made according to whether the containment is intact, and whether any fission products from the vessel are scrubbed by the suppression pool before release into the environment. The next 30 release categories represent conditions where the drywell spray operates during the accident sequence, whereas the second set of 30 source terms has no drywell spray scrubbing. In each set,

the first 15 STET sequences represent end states with low RCS pressure at vessel breach, and the second set of 15 sequences represents source terms for high pressure vessel melt-through sequences.

In each of these four groups of 15 release categories, the first sequence has the containment remaining intact with no appreciable release. The second and third sequences have dirty venting; sequence 2 has full scrubbing from the torus, and sequence 3 has no torus scrubbing. The next 12 sequences in each set represent the combinations of containment failure and source term mitigation by the suppression pool and the reactor building.

The discussion of source terms above applies to sequences in which the containment may be failed but not bypassed. For bypass sequences, there is a release, at least initially, from the vessel directly into the reactor building or environment, bypassing the containment. The bypass release may be a large or small leak area, and it may or may not be isolated at some point in time. Since, at Oyster Creek, there are predominant bypass sequences that are small leaks and that are isolated during the accident progression, it is necessary to address all of the questions on the STET in addition to the bypass question. Therefore, for KPDS that involves a containment bypass (OJAU, MJAU, and NJHW), the same source term event tree is used; however, all source term category designators are appended with a "Y" to designate a containment bypass source term. The source term designators without an appended "Y" therefore only apply to the nonbypass KPDS (PIFW, NIFW, OIAU, and MKCU).

11.2 RELEASE CATEGORY ASSIGNMENT

The end state of each STET sequence is defined in the second-to-last column as a designator with up to seven letters. This series of letters simply defines the STET path as given by the branch designators in square brackets. The last column in Figure 11-1 lists the source term category designators. These are identical to the end state designators in the second-to-last column, except that the third letter is suppressed if it is an "F." An "F" means that the containment is failed and that is also known if the next letter is a "D" or an "E," which indicates the time of containment failure. In subsequent discussions, the source terms will be referred to by the source term designator in the last column in Figure 11-1.

With the current RISKMAN software, the STET logic is used to develop CET end state binning rules. Thus, the outcome (e.g., success or failure branch) of each source term event tree top event is keyed to either a PDS group or the status of certain CET top events. The keying to PDS groups or CET top events is defined by the CET binning rules.

The RISKMAN rules for binning CET sequences to release categories are listed in Tables 11-1 and 11-2. The binning process is simplified significantly if "MACRO" rules are defined. These MACROS must be identified in the CET split fraction rules file. The definition of MACROS (related to end state binning) for the Oyster Creek CET is shown in Table 11-1. Table 11-2 represents the RISKMAN binning rules for the CET.

11.3 SOURCE TERMS

11.3.1 Key Release Categories

The CET quantification, which is performed for each KPDS, determines the frequency of all release categories that are defined as the end states of the CET. Table 11-3 lists these frequencies of the Oyster Creek release categories, ordered by decreasing frequency. Each release category is assigned to an enveloping release category (see Appendix B), according to the rules of conservative condensation. This enveloping release category is shown in the third column of Table 11-3.

In a conservative condensation, a low frequency and low consequence release category can be assigned to a higher frequency and higher consequence release category. This ensures that the total frequency of core damage is preserved in the release category frequencies, that the important release categories are retained, and that their frequency is somewhat conservative, but generally by less than about a factor of 2. The development of the condensed set of release categories is shown below, and the frequency multiplier is tabulated in Table 11-4. This condensed set of release categories, which envelopes the total set of release categories, is called the key release categories (KRC).

The six KRCs determined by conservative condensation for the Oyster Creek IPE are shown in Table 11-4. The cumulative frequency of each KRC is listed in the second column. The third column lists the percentage of the KRC frequency that is due to the release category that defines the KRC. It can be seen that, in all cases that have a source term (KRC 2 to 6), this percentage is over 40%, meaning that the combined frequency of all lower consequence release categories, which were conservatively binned into the KRC, represents less than 60% of the KRC frequency. The last column on Table 11-4 gives a summary description of the KRC.

Source terms for all KRCs for which there is a release were estimated by the MAAP code. The sequence definition for the source term calculations consisted of two parts. First, the definition of system failures that lead to a condition of core damage was taken from the dominant sequence representing that KPDS that dominated the contribution to the KRC frequency. Second, the containment response was modeled according to the dominant path through the CET that leads from that KPDS to the KRC in question. This two-part definition of the accident sequences for the source term calculation is illustrated in detail for KRC 2 below.

The MAAP code models the behavior and release of 12 radionuclide groups, which are as follows:

1. Noble Gases
2. Cesium Iodide (CsI) and Rubidium Iodide (RbI)
3. Tellurium Dioxide (TeO_2)
4. Strontium Oxide (SrO)
5. Molybdenum Dioxide (MoO_2)
6. Cesium Hydroxide (CsOH)
7. Barium Oxide (BaO)
8. Lanthanides (La, Pr, Nd, Sm, and Yb)
9. Cerium Oxide (CeO_2)
10. Antimony (Sb)
11. Elemental Tellurium (Te_2)
12. Oxides of Uranium, Neptunium, and Plutonium

The time-dependent release fractions for all the non-zero radionuclide groups are shown graphically for each KRC, and the total release fractions are tabulated in Table 11-5. The dominant sequences

that represent the six KRCs in the source term calculation, the MAAP model for the sequence, and the source term calculated by the MAAP code are summarized in the following.

11.3.2 KRC 1: RDGS

The highest frequency KRC is release category RDGS. This release category represents sequences that are enveloped by the following conditions:

1. The debris is recovered in-vessel, and vessel melt-through is prevented (R).

2. Containment failure occurs late with a large leak area (D, G).

3. The source term is scrubbed by the suppression pool up to the time of containment failure (S).

The actual set of sequences collected in this KRC is actually more narrow. Credit was taken for successful in-vessel recovery only in sequences in which there may have been only a temporary or partial core uncovery, because either CRD flow or fire water injection was available and prevented melt progression and vessel breach. While these cases are included as core damage sequences in the Level 1 model, they are considered benign with respect tot he Level 2 source term development. Therefore, there is no source term of any magnitude for any of the sequences in KRC 1, and no source term is quantified.

11.3.3 KRC 2: NLDGSB

The KRC with the second highest frequency is NLDGSB. This KRC represents sequences that are enveloped by the following conditions:

1. A dry drywell at vessel breach (N).

2. A low RCS pressure at vessel breach (L).

3. The containment fails late with a large leak area (D, G).

4. The suppression pool scrubs the source term up to the time of containment failure (S).

5. There is no source term mitigation by the reactor building after containment failure (B).

The Level 1 portion of the accident sequence definition for the source term calculation is determined by the Level 2 initiating event that dominates the frequency contribution to the release category (NLDGSB). Table 12-6 shows that initiating event NIFW is the only initiating event contributing to NLDGSB. Therefore, the Level 1 sequence that was selected to represent the KPDS NIFW in the Level 2 analysis is chosen as the Level 1 sequence for the source term analysis. This sequence is discussed in detail in Section 8.2.1.2. Section 9.2.2 discusses how this sequence is modeled in the MAAP code. This information is not repeated here.

The Level 2 portion of the sequence definition for the source term calculation is determined by the dominant path through the CET for sequences that proceed from initiating event NIFW to release

category NLDGSB. The first sequence in Table 12-6 is the sequence of interest, and it has the CET top event failure string VBN*DV3*I3N*L3N*HBF*BEF. VBN means that the sequence is not recovered in-vessel. DV3 means that dirty venting is not successful. I3N*L3N means that the containment fails late and it fails by a gross failure mode. The dominant gross failure mode is a drywell failure at the thinned region of the former sand-backed section, and the most likely failure pressure is 137 psia. HBF*BEF means that, due to the gross containment failure mode, there is no source term mitigation by the reactor building. Caution is required in completing the Level 2 sequence definition because it is also necessary to consider the effect of the successful top events on the source term calculation. In particular, Top Event ES is successful, which means that an EMRV or a safety relief valve sticks open before vessel breach and depressurizes the vessel, resulting in a low pressure vessel melt-through without debris entrainment. Last, both Top Events S1 and S3 are successful, indicating that, until containment failure, there is no suppression pool bypass. This completes the sequence definition for the source term calculation of release category NLDGSB. To summarize therefore, the dominant sequence represented in the MAAP source term calculation is as follows:

1. KPDS NIFWW sequence.

2. One safety valve sticks open after 1.9 hours.

3. No dirty venting.

4. No suppression pool bypass before containment failure.

5. The containment fails in the drywell sand region at a drywell pressure of 137 psia. This represents the median failure pressure according to the containment overpressure failure analysis. The leak area of the five 4-inch-diameter drain lines from the sand region is about 63 square inches. This area was doubled to account for the leak path around the vent pipes. Therefore, the leak area is approximately 1 square foot.

6. No source term mitigation by the reactor building.

The time of 1.9 hours for the safety valve to stick open was chosen approximately 100 seconds before vessel breach, which is sufficient to depressurize the vessel to below 300 psia for a low pressure vessel breach condition. By this time, the large number of valve cycles since core uncovery yields a probability for a valve to stick open well above 0.5.

Containment failure occurs at about 4.9 hours, or 3 hours after vessel breach. This is classified as a late containment failure.

The time-dependent release of radionuclides into the environment calculated by the MAAP code for this sequence is shown in Figure 11-2. The release starts at about 4.9 hours when containment failure occurs, and at, 8.1 hours, over 90% of the total release has occurred. Releases occur for the following radionuclide groups: Noble Gases, CsI, RbI, SrO, MoO_2, and CsOH. No releases are predicted for the remaining radionuclide groups.

The release timing and the total release fractions are listed in Table 11-5. The end time for the release is defined as that time when at least 90% of the release at the time of the MAAP run end time

has occurred. The 90% time is chosen instead of the MAAP end time so that the time from the start to the end of the release is a realistic representation of the release duration. Most of the noble gases and about 10% of the Cesium, Iodine, and Rubidium are released. The distribution of CsI at the end of the MAAP calculation is listed in Table 11-6. It shows that the majority of the CsI is retained in the vessel and in the suppression pool.

11.3.4 KRC 3: NLEGUB

The KRC with the third highest frequency is NLEGUB. This KRC represents sequences that are enveloped by the following conditions:

1. A dry drywell at vessel breach (N).

2. A low RCS pressure at vessel breach (L).

3. The containment fails early with a large leak area (E, G).

4. The suppression pool is bypassed by a stuck-open vacuum breaker (U).

5. There is no source term mitigation by the reactor building after containment failure (B).

The dominant sequence represented in the MAAP source term calculation is determined by a procedure that is entirely analogous to that described for KRC 2. For this release category, it is the MJAU-ATWS sequence. The containment fails before core damage, and the suppression pool does not scrub the source term. The vessel pressure at vessel breach is low, and there is no makeup to the drywell after vessel breach. This sequence is represented in the MAAP source term calculation as follows:

1. KPDS MKCU sequence (ATWS).

2. One EMRV sticks open on the first cycle.

3. One wetwell-to-drywell vacuum breaker sticks open on the first cycle (suppression pool bypass).

4. The containment fails in the drywell sand region at a drywell pressure of 137 psia, with a leak area of 1 square foot.

5. The containment failure causes failure of all safety equipment.

6. No source term mitigation by the reactor building.

The time-dependent release of radionuclides into the environment calculated by the MAAP code for this sequence is shown in Figure 11-3. The release starts at about 6.3 hours, and, at 16.5 hours, over 90% of the total release has occurred. Releases occur for the following radionuclide groups: Noble Gases, CsI, RbI, SrO, MoO_2 and CsOH. No releases are predicted for the remaining radionuclide groups. The release timing and the total release fractions are listed in Table 11-5. Most of the noble gases and about 1% of the Cesium, Iodine, and Rubidium are released. The distribution

of CsI at the end of the MAAP calculation listed in Table 11-6 shows that the majority of the CsI is retained in the vessel and in the suppression pool.

11.3.5 KRC 4: NLEGSB

The KRC with the fourth highest frequency is represented by a sequence identical to the sequence for KRC 2, except that the containment fails shortly after vessel breach (E instead of D). It is a low pressure sequence with a dry drywell. The containment fails at vessel breach, and the suppression pool scrubs the source term up to the time of containment failure. The dominant sequence represented in the MAAP source term calculation is as follows:

1. KPDS NIFWW sequence.

2. One safety valve sticks open after 1.9 hours (see KRC 2).

3. No suppression pool bypass before containment failure.

4. Containment fails at vessel breach in the drywell sand region with a leak area of 1 square foot.

5. No source term mitigation by the reactor building.

The time-dependent release of radionuclides into the environment calculated by the MAAP code for this sequence is shown in Figure 11-4. The release starts at about 1.9 hours, and, at 10.7 hours, over 90% of the total release has occurred. Releases occur for the following radionuclide groups: Noble Gases, CsI, RbI, SrO, MoO_2, and CsOH. No releases are predicted for the remaining radionuclide groups. The release timing and the total release fractions are listed in Table 11-5. Most of the noble gases and about 10% of the Cesium, Iodine, and Rubidium are released. The distribution of CsI at the end of the MAAP calculation is listed in Table 11-6. It shows that the majority of the CsI is retained in the vessel and in the drywell.

11.3.6 KRC 5: NHEGUBY

The KRC with the fifth highest frequency is NHEGUBY. This KRC represents sequences that are enveloped by the following conditions:

1. A dry drywell at vessel breach (N).

2. A high RCS pressure at vessel breach (H).

3. The containment is bypassed early with a large leak area (E, G, Y).

4. The suppression pool is bypassed by a stuck-open vacuum breaker (U).

5. There is no source term mitigation by the reactor building after containment failure (B).

The dominant sequence representing KRC 5 is determined by a procedure entirely analogous to that described for KRC 2. For this release category, it is the containment bypass sequence MJAU.

Therefore, the containment is bypassed by the initiating event, and the suppression pool does not scrub the source term. The vessel pressure at vessel breach is high and there is no makeup to the drywell after vessel breach. The dominant sequence is represented in the MAAP source term calculation as follows:

1. KPDS MJAU sequence.

2. The containment is bypassed according to the sequence representing KPDS MJAU. If the containment pressure should nevertheless reach 137 psia, an overpressure failure occurs in the drywell sand region with a leak area of 1 square foot.

3. No source term mitigation by the reactor building.

The time-dependent release of radionuclides into the environment calculated by the MAAP code for this sequence is shown in Figure 11-5. The release starts at about 10 hours, and, at 40 hours, over 90% of the total release has occurred. Releases occur for the following radionuclide groups: Noble Gases, CsI, RbI, SrO, MoO_2, and CsOH. No releases are predicted for the remaining radionuclide groups. The release timing and the total release fractions are listed in Table 11-5. An almost complete release of the noble gases, Cesium, Iodine, and Rubidium occurs. The distribution of CsI at the end of the MAAP calculation listed in Table 11-6 shows that the remaining CsI is mostly retained in the vessel.

11.3.7 KRC 6: NLVSY

The KRC with the sixth highest frequency is NLVSY. This KRC represents sequences that are enveloped by the following conditions:

1. A dry drywell at vessel breach (N).

2. A low RCS pressure at vessel breach (L).

3. The containment is bypassed early with a small leak area, but dirty venting prevents containment overpressurization (V, Y).

4. The suppression pool is scrubbing the source term (S).

The dominant sequence representing KRC 6 is determined by a procedure entirely analogous to that described for KRC 2. For this release category, it is the containment bypass sequence OJAUV, a large LOCA below the core with a simultaneous 1-inch-diameter bypass into the reactor building. The containment bypass condition is isolated at vessel breach, and dirty venting is successful to prevent containment overpressurization. The vessel pressure at vessel breach is low, and there is no makeup to the drywell after vessel breach. The dominant sequence represented in the MAAP source term calculation is as follows:

1. KPDS OJAUV sequence.

2. The containment is bypassed according to the sequence representing KPDS OJAU.

3. Containment venting occurs from the wetwell at the setpoint pressure, and is switched to the drywell if the switchover level is reached.

4. No source term mitigation by the reactor building.

The time-dependent release of radionuclides into the environment calculated by the MAAP code for this sequence is shown in Figure 11-6. The release starts at about 2.1 hours, and, at 12.9 hours, about 90% of the release calculated to occur by the MAAP run termination at 14 hours has occurred. Releases occur for the following radionuclide groups: Noble Gases, CsI, RbI, SrO, MoO_2, and CsOH. No releases are predicted for the remaining radionuclide groups. The release timing and the total release fractions are listed in Table 11-5. About 30% of the noble gases and 1% of the Cesium, Iodine, and Rubidium is released.

The significant retention of fission products, even the noble gases in the containment is due to the fact that only a limited release occurs at each vent cycle. However, as vent cycling continues beyond the time when the MAAP run was terminated at 14 hours, more of the noble gasses and a small amount of the remaining radionuclides would be released. The distribution of CsI at the end of the MAAP calculation listed in Table 11-6 shows that the remaining CsI is mostly retained in the suppression pool with significant retention occurring also in the vessel and in the drywell.

Table 11-1. Split Fraction Macros Related to End State Binning

Split Fraction Logic	Comments
N:= INIT=PIFW + INIT=NIFW + INIT=HKCU + INIT=OJAU + INIT=HJAU + INIT=NJHW	DRYWELL SPRAYS NOT AVAILABLE OR INEFFECTIVEIF OPERABLE (I.E., CONTAINMENT BYPASSED)
W:= INIT=OIAU	DRYWELL SPRAYS AVAILABLE (NO BYPASS)
Y:= INIT=OJAU + INIT=HJAU + INIT=NJHW	DRYWELL SPRAYS INEFFECTIVE IF OPERABLE (CONTAINMENT BYPASSED TO REACTOR BUILDING)
H:= ES=F*(INIT=NIFW + INIT=HKCU + INIT=HJAU + INIT=NJHW)	RCS PRESSURE HIGH PRIOR TO VESSEL BREACH
L:= ES=S + INIT=PIFW + INIT=OIAU + INIT=OJAU	RCS PRESSURE LOW PRIOR TO VESSEL BREACH
E:= I1=F + I2=F + LM=F	EARLY CONTAINMENT FAILURE
D:= I3=F * -(I1=F + I2=F + LM=F)	LATE CONTAINMENT FAILURE (> 3.0 HRS AFTER VB)
G:= L1=F + L2=F + L3=F + LM=F	LARGE CONTAINMENT FAILURE
U:= S1=F + S3=F	NO TORUS SCRUBBING
BP:= BE=F	REACTOR BUILDING INEFFECTIVE IN REDUCING SOURCE TERM
V:= DV=S	CONTAINMENT VENTED AFTER CORE DAMAGE
I:= (I1=S+I1=B) * (I2=S+I2=B) * (I3=S+I3=B) * (LM=S+LM=B)	CONTAINMENT INTACT
R:= VB=S	CORE DAMAGE ARRESTED PRIOR TO VESSEL BREACH

Table 11-2 (Page 1 of 2). RISKMAN Binning Rules for the Oyster Creek CET

Bin.....	Binning Rules....
RIS	R*I
RDGS	R*D*G
RDCS	R*D
WHEGUBY	W*H*E*G*U*BP*Y
WHEGUB	W*H*E*G*U*BP
WHEGSBY	W*H*E*G*BP*Y
WHEGSB	W*H*E*G*BP
WHECUBY	W*H*E*U*BP*Y
WHECUB	W*H*E*U*BP
WHECUMY	W*H*E*U*Y
WHECUM	W*H*E*U
WHECSBY	W*H*E*BP*Y
WHECSB	W*H*E*BP
WHECSMY	W*H*E*Y
WHECSM	W*H*E
WLEGUBY	W*L*E*G*U*BP*Y
WLEGUB	W*L*E*G*U*BP
WLEGSBY	W*L*E*G*BP*Y
WLEGSB	W*L*E*G*BP
WLECUBY	W*L*E*U*BP*Y
WLECUB	W*L*E*U*BP
WLECUMY	W*L*E*U*Y
WLECUM	W*L*E*U
WLECSBY	W*L*E*BP*Y
WLECSB	W*L*E*BP
WLECSMY	W*L*E*Y
WLECSM	W*L*E

Bin.....	Binning Rules....
WHDGUBY	W*H*D*G*U*BP*Y
WHDGUB	W*H*D*G*U*BP
WLDGUBY	W*L*D*G*U*BP*Y
WLDGUB	W*L*D*G*U*BP
WHDGSBY	W*H*D*G*BP*Y
WHDGSB	W*H*D*G*BP
WLDGSBY	W*L*D*G*BP*Y
WLDGSB	W*L*D*G*BP
WHDCUBY	W*H*D*U*BP*Y
WHDCUB	W*H*D*U*BP
WHDCUMY	W*H*D*U*Y
WHDCUM	W*H*D*U
WLDCUBY	W*L*D*U*BP*Y
WLDCUB	W*L*D*U*BP
WLDCUMY	W*L*D*U*Y
WLDCUM	W*L*D*U
WHDCSBY	W*H*D*BP*Y
WHDCSB	W*H*D*BP
WHDCSMY	W*H*D*Y
WHDCSM	W*H*D
WLDCSBY	W*L*D*BP*Y
WLDCSB	W*L*D*BP
WLDCSMY	W*L*D*Y
WLDCSM	W*L*D
WHVUY	W*H*V*U*Y
WHVU	W*H*V*U

Bin.....	Binning Rules....
WLVUY	W*L*V*U*Y
WLVU	W*L*V*U
WHVSY	W*H*V*Y
WHVS	W*H*V
WLVSY	W*L*V*Y
WLVS	W*L*V
WHIY	W*H*I*Y
WHI	W*H*I
WLIY	W*L*I*Y
WLI	W*L*I
NHEGUBY	H*E*G*U*BP*Y
NHEGUB	H*E*G*U*BP
NHEGSBY	H*E*G*BP*Y
NHEGSB	H*E*G*BP
NHECUBY	H*E*U*BP*Y
NHECUB	H*E*U*BP
NHECUMY	H*E*U*Y
NHECUM	H*E*U
NHECSBY	H*E*BP*Y
NHECSB	H*E*BP
NHECSMY	H*E*Y
NHECSM	H*E
NLEGUBY	L*E*G*U*BP*Y
NLEGUB	L*E*G*U*BP
NLEGSBY	L*E*G*BP*Y
NLEGSB	L*E*G*BP
NLECUBY	L*E*U*BP*Y

Table 11-2 (Page 2 of 2). RISKMAN Binning Rules for the Oyster Creek CET

Bin.....	Binning Rules....
NLECUB	L*E*U*BP
NLECUMY	L*E*U*Y
NLECUM	L*E*U
NLECSBY	L*E*BP*Y
NLECSB	L*E*BP
NLECSMY	L*E*Y
NLECSM	L*E
NHDGUBY	H*D*G*U*BP*Y
NHDGUB	H*D*G*U*BP
NLDGUBY	L*D*G*U*BP*Y
NLDGUB	L*D*G*U*BP
NHDGSBY	H*D*G*BP*Y
NHDGSB	H*D*G*BP
NLDGSBY	L*D*G*BP*Y
NLDGSB	L*D*G*BP
NHDCUBY	H*D*U*BP*Y
NHDCUB	H*D*U*BP
NHDCUMY	H*D*U*Y
NHDCUM	H*D*U
NLDCUBY	L*D*U*BP*Y
NLDCUB	L*D*U*BP
NLDCUMY	L*D*U*Y
NLDCUM	L*D*U
NHDCSBY	H*D*BP*Y
NHDCSB	H*D*BP
NHDCSMY	H*D*Y
NHDCSM	H*D
NLDCSBY	L*D*BP*Y
NLDCSB	L*D*BP
NLDCSMY	L*D*Y
NLDCSM	L*D
NHVUY	H*V*U*Y
NHVU	H*V*U
NLVUY	L*V*U*Y
NLVU	L*V*U
NHVSY	H*V*Y
NHVS	H*V
NLVSY	L*V*Y
NLVS	L*V
NHIY	H*I*Y
NHI	H*I
NLIY	L*I*Y
NLI	L*I
NERROR	1

Table 11-3. Release Category Binning for Oyster Creek		
Release Category	**Frequency**	**Enveloping Release Category**
RDGS	7.40E-07	RDGS
RIS	4.61E-07	RDGS
RDCS	3.96E-07	RDGS
NLDGSB	3.45E-07	NLDGSB
NLEGSB	2.13E-07	NLEGSB
NLDCSB	1.48E-07	NLDGSB
NLEGUB	1.45E-07	NLEGUB
NLDGUB	1.21E-07	NLEGUB
NLVSY	1.16E-07	NLVSY
NHEGSB	9.76E-08	NLDGSB
WLVS	8.63E-08	NLDGSB
NHDGSB	7.37E-08	NLDGSB
NHEGUBY	6.80E-08	NHEGUBY
NLVUY	4.30E-08	NHEGUBY
NHEGUB	4.06E-08	NLEGUB
NHDCSB	3.16E-08	NLDGSB
WLVU	1.46E-08	NLEGUB
NHDGUB	1.29E-08	NLEGUB
WLEGUB	4.97E-09	NLEGUB
NLDGSBY	1.95E-09	NHEGUBY
NLECUB	1.69E-09	NLEGUB
NLEGSBY	7.98E-10	NHEGUBY
NLDCSBY	7.86E-10	NHEGUBY
NLDGUBY	6.24E-10	NHEGUBY
WLEGSB	4.87E-10	NLEGSB
NHECUB	3.26E-10	NLEGUB
NLDCUBY	2.51E-10	NHEGUBY
WILDGSB	1.47E-10	NLDGSB
Total	**3.17E-06**	

Table 11-4. Key Release Categories for Oyster Creek IPE			
Key Release Category	Frequency	Percent of Original CDF	Comments
1 RDGS	1.60-06	46.3	All sequences no vessel breach, no release.
2 NLDGSB	7.82-07	44.1	KPDS NIFW, EMRV sticks open, no venting, late overpressure failure.
3 NLEGUB	3.41-07	2.6	KPDS MKCU, EMRV sticks open, containment fails before core damage, suppression pool bypassed before vessel breach.
4 NLEGSB	2.13-07	99.8	KPDS NIFW, EMRV sticks open, containment fails at vessel breach.
5 NHEGUBY	1.15-07	58.9	KPDS MJAU, containment and suppression pool bypassed.
6 NLVSY	1.16-07	100	KPDS OJAU, venting after core damage.
Total	**3.17-06**		
NOTE: Exponential notation is indicated in abbreviated form; i.e., 1.60-06 = 1.60×10^{-06}.			

Table 11-5. Oyster Creek Release Categories									
Key Release Category	MAAP Case	Release Time (hours)		MAAP End Time (hours)	Radionuclide Release Group				
		Start	End		N.G.	CsI, RbI	SrO	MoO2	CsOH
KRC 2	NIFWB1	4.9	8.1	10	0.7	0.1	2-09	2-08	0.1
KRC 3	MKCUB1	6.3	16.5	20	0.9	7-03	7-05	3-04	7-03
KRC 4	NIFWB2	1.9	10.7	12	0.7	0.1	9-05	9-04	0.1
KRC 5	MJAU	9.8	40.0	60	0.9	0.9	4-04	2-03	0.9
KRC 6	OJAUV	2.1	12.9	14	0.3	0.01	1-06	6-06	0.01
Note: Exponential notation is indicated in abbreviated form; e.g., 2-09 = 2×10^{-09}.									

Table 11-6. Distribution of CsI for Each Release Category						
Key Release Category	MAAP Case	MAAP End Time (hours)	CsI Distribution at End of MAAP Run			
			In-Vessel	Drywell	Wetwell	Released
KRC 2	NIFWB1	10	0.53	9-03	0.38	0.08
KRC 3	MKCUB1	20	0.20	1-03	0.79	7-03
KRC 4	NIFWB2	12	0.49	0.40	1-03	0.11
KRC 5	MJAU	60	0.11	6-03	0.02	0.87
KRC 6	OJAUV	14	0.24	0.23	0.52	0.01
Note: Exponential notation is indicated in abbreviated form; e.g., 9-03 = 9×10^{-03}.						

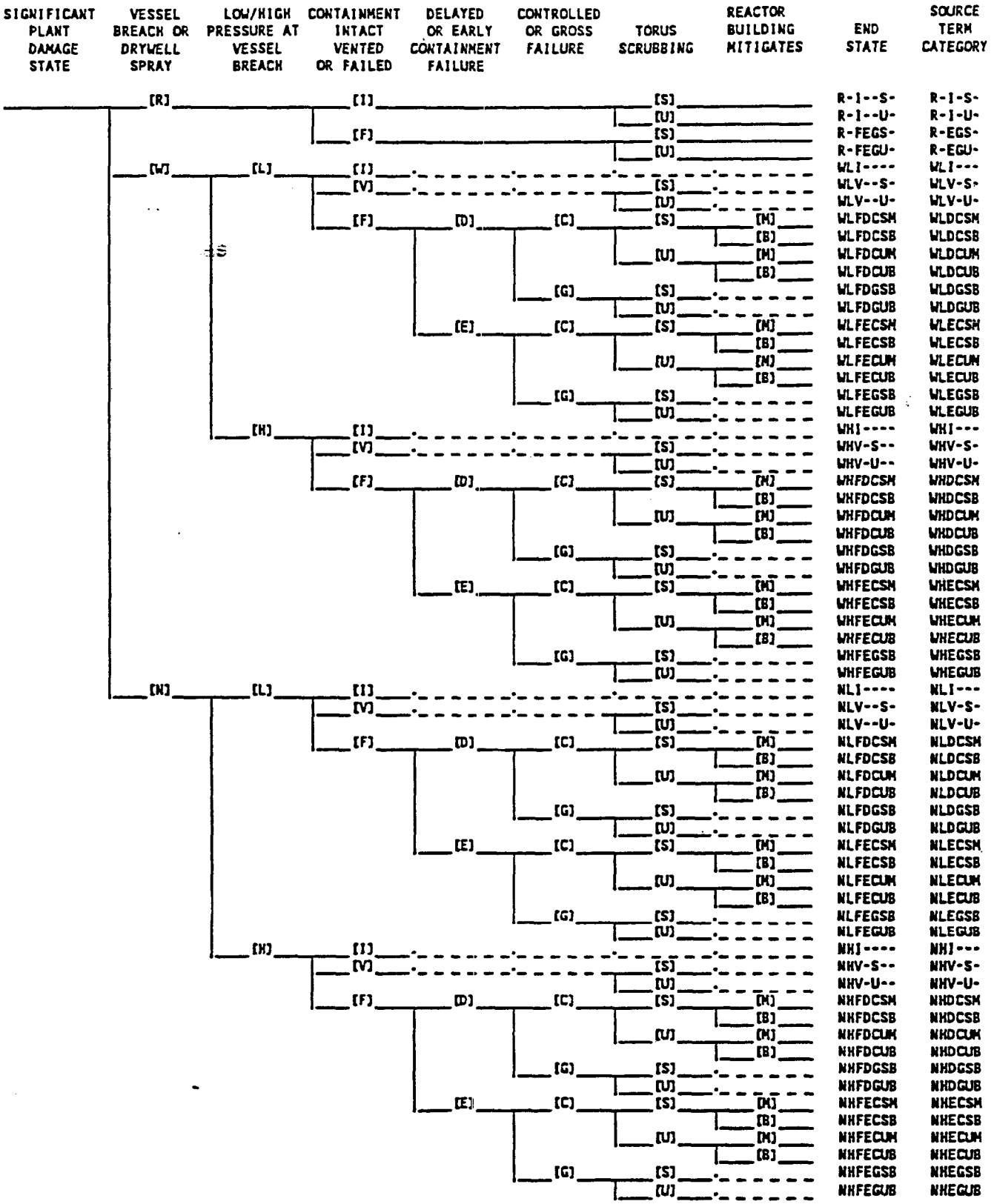

Figure 11-1. Oyster Creek Level 2 Generalized Source Term Event Tree

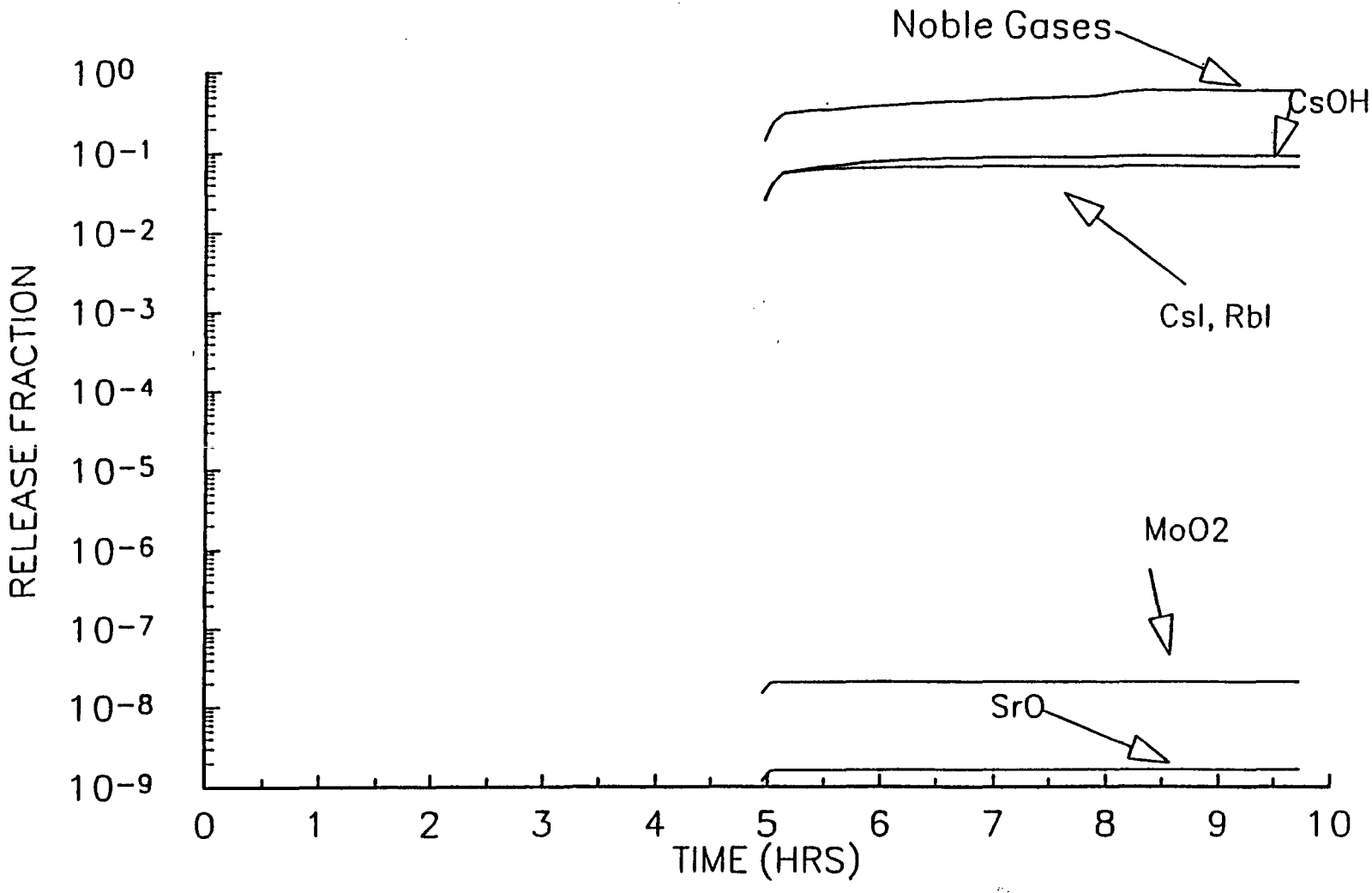

Figure 11-2. Release Category KRC 2

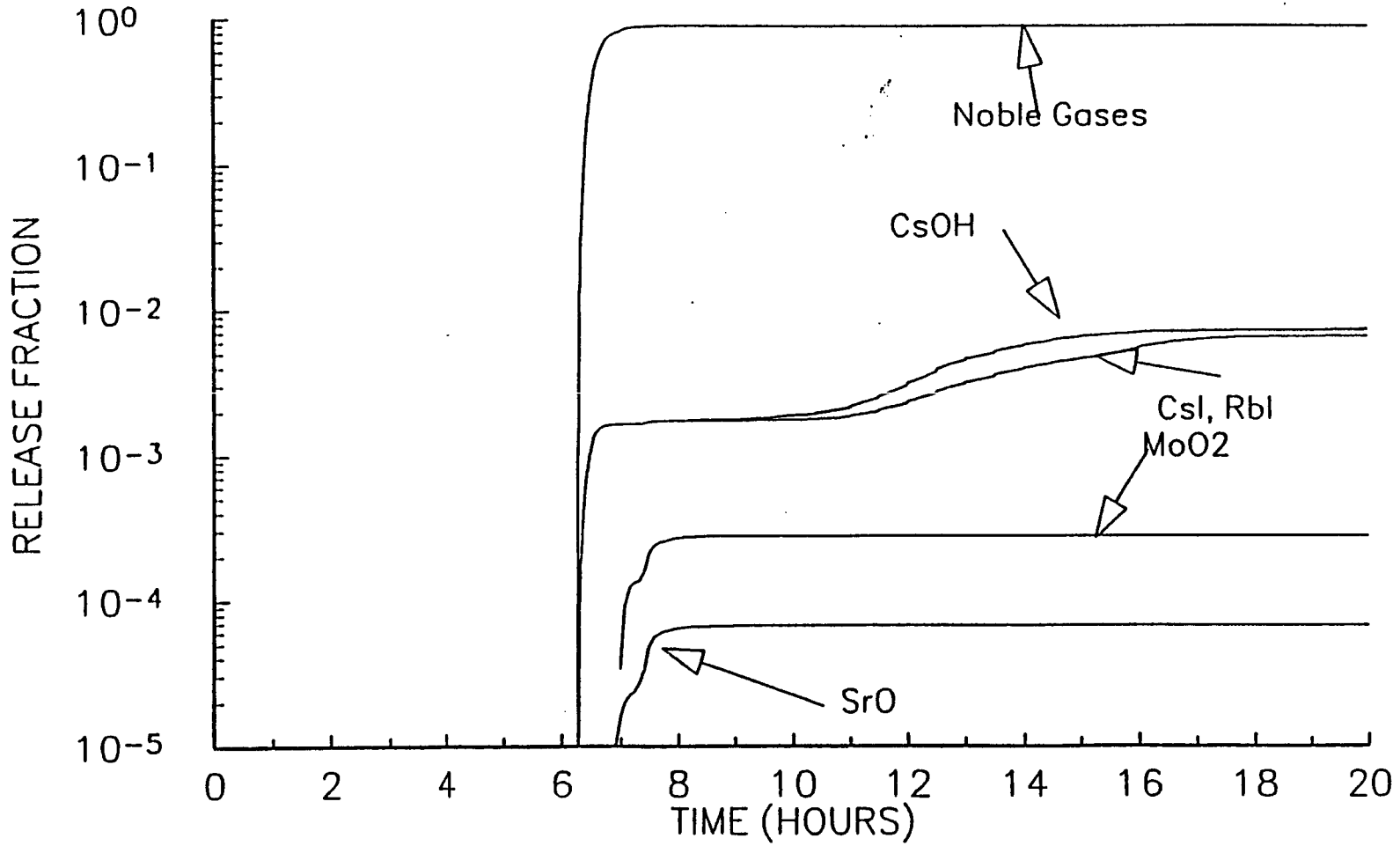

Figure 11-3. Release Category KRC 3

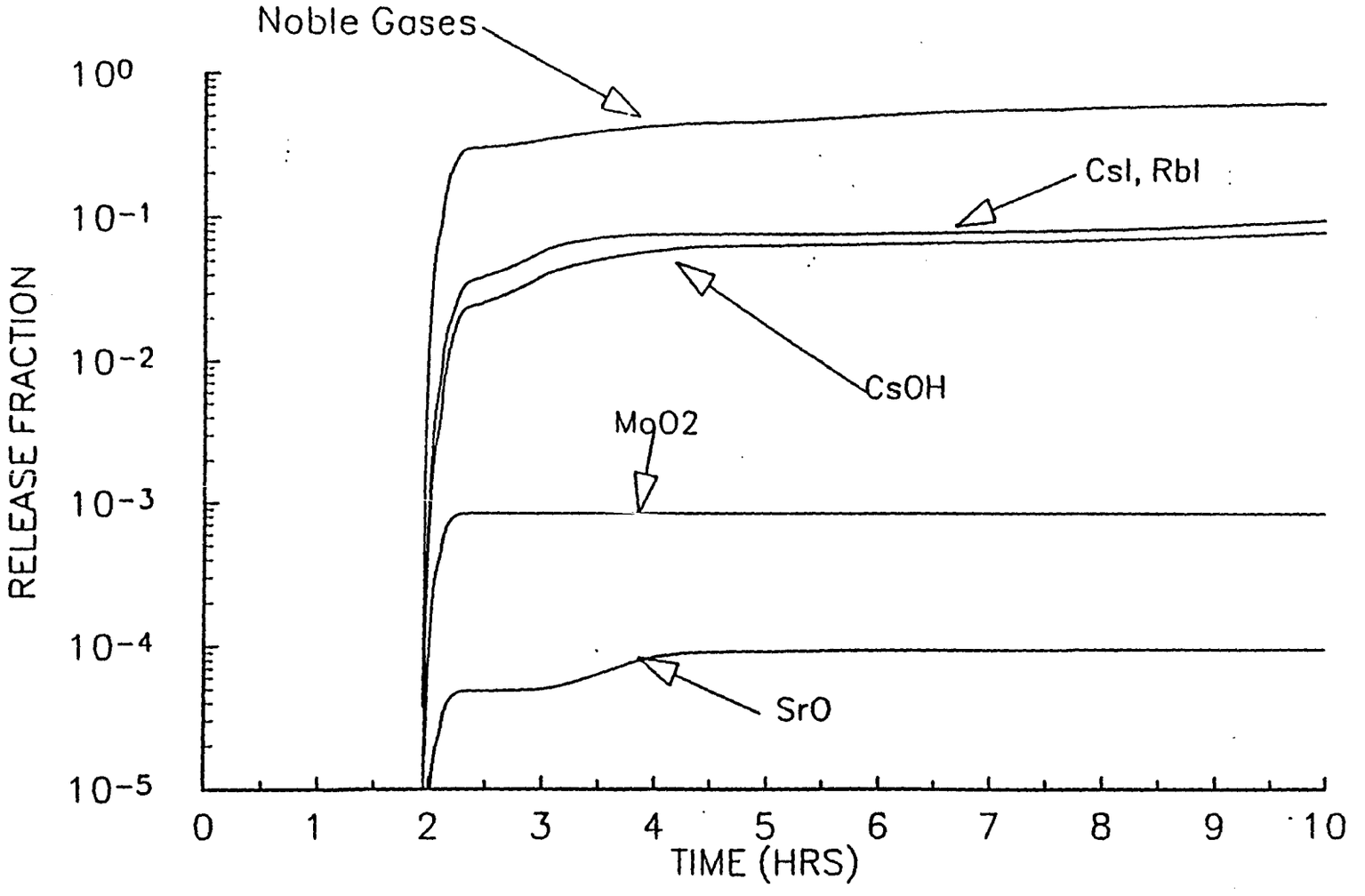

Figure 11-4. Release Category KRC 4

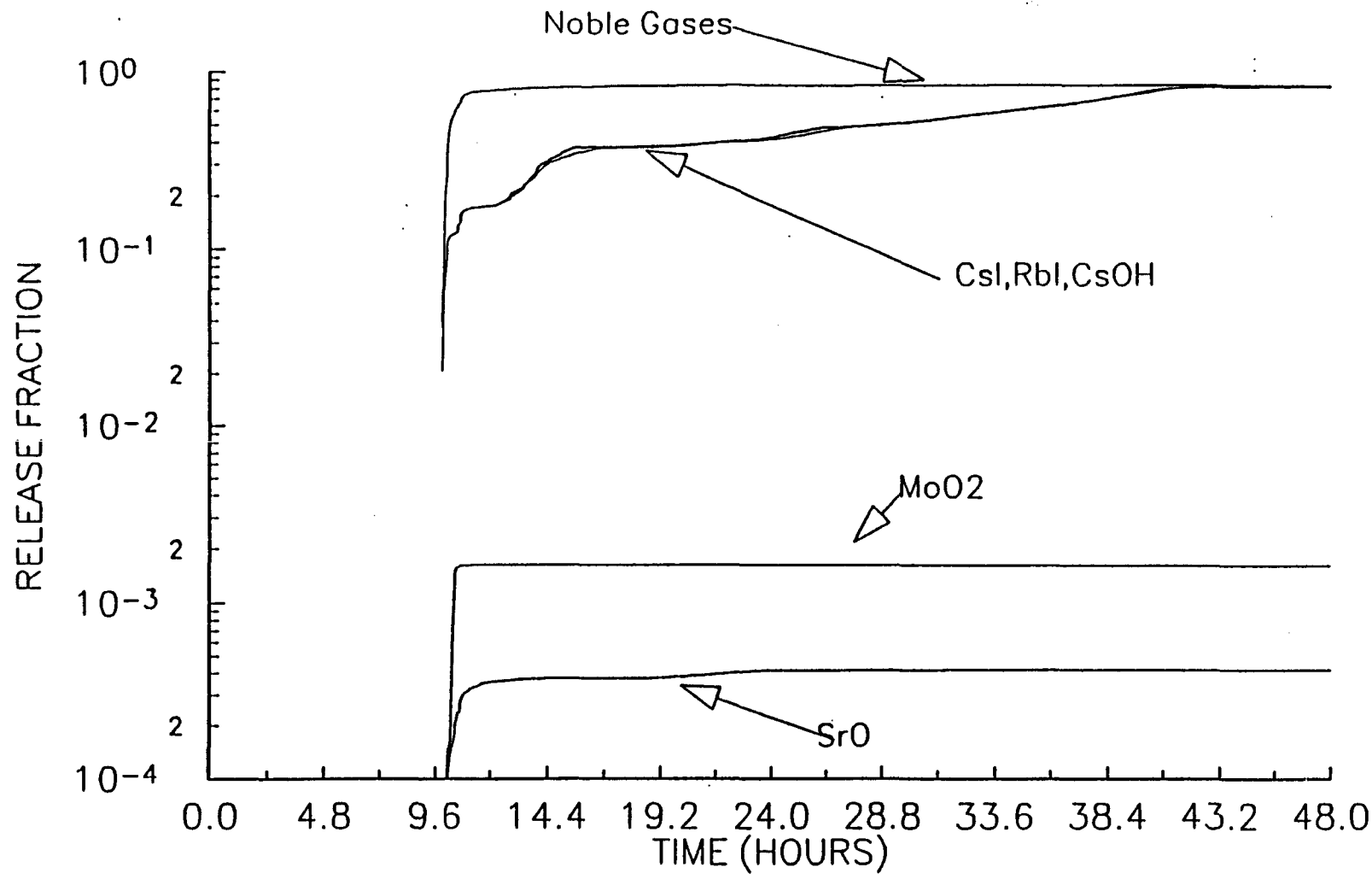

Figure 11-5. Release Category KRC 5

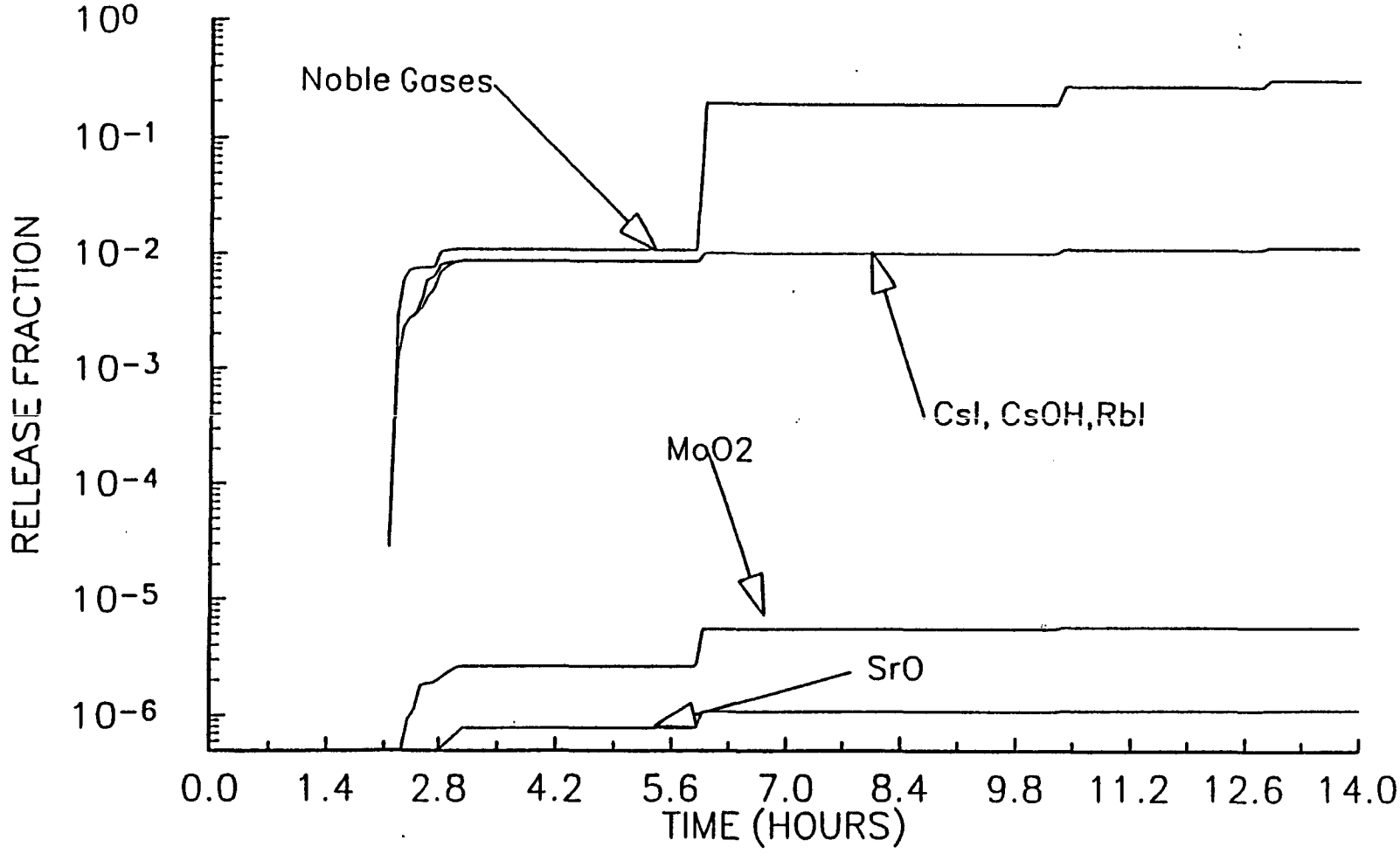

Figure 11-6. Release Category KRC 6

12. BACK-END RESULTS

This section summarizes the results of the Oyster Creek Level 2 examination process. For reporting purposes, the individual release categories have been binned into six major groups. These groups are described below, along with their relative contributions.

General Release Category Group	Description	Percentage of CDF Analyzed*
IA	Large, Early Containment Failures	15.8
IB	Bypasses**	7.3
II	Small, Early Containment Failures	.06
III	Late Containment Failures	26.4
IV	Long-Term, Contained Releases (containment intact following vessel breach)	.00
V	Breach Prevented	50.4

*Group frequency divided by CDF analyzed (see Table 12-1).
**Includes contributions from PDS NJHW (1.54×10^{-8} per year).

Table 12-1 summarizes the assignment of individual release categories into these general release groups. Some of the groups shown in Table 12-1 were combined (e.g., small, late containment failures were combined with large, late containment failures) to form the six groups identified above.

12.1 RELEASE CATEGORY GROUPS IA AND IB (LARGE, EARLY CONTAINMENT FAILURE AND BYPASS)

Table 12-2 lists those individual sequences whose frequency is greater than 1×10^{-10} per reactor-year and that contribute to release category group I.

As shown in Table 12-3, KPDSs NIFW, MKCU, and OIAU are the only contributors to release category group IA.

KPDS NIFW contributes approximately 64% of the release category group IA frequency. Since the frequency of NIFW is 1.13×10^{-6} per reactor-year, nearly 31% of NIFW results in large, early containment failure.

None of the PIFW core damage frequency results in large, early containment failures since significant core damage and vessel breach are prevented in each accident scenario considered for this KPDS.

Only a small fraction of OIAU results in large, early containment failures. Most of the core damage frequency in this KPDS is arrested prior to vessel breach. That portion of the core damage frequency not arrested in-vessel, prior to vessel breach, does not result in early containment failure.

All of the core damage frequency associated with KPDS MKCU was assigned to release category group IA even though a small fraction (.07) of the failures prior to vessel breach (Top Event L1) were classified as leak before break.

The importance evaluation of the split fractions contributing to release category group IA is shown in Table 12-4. Four importance measures are summarized: (1) the percentage contributions with that split fraction failed; (2) the factor increase in the group frequency when the split fraction is arbitrarily assigned a failure frequency of 1.0 (risk achievement worth); (3) the factor decrease in the group frequency when the split fraction is arbitrarily assigned a failure frequency of 0.0 (risk reduction worth); and (4) the rate of change in group frequency with respect to a particular split fraction (derivative).

As can be seen in Table 12-4, the combination of I2N and L2N (the split fractions for KPDS NIFW without suppression pool bypass) is contained in 44% of the release category group IA frequency. The contribution of liner melt-through to large, early containment failures is approximately 17%.[4] Most of the liner melt-through contribution results from high pressure vessel breach; i.e., KPDS NIFW with ES=F.

Table 12-4 indicates that only three split fractions (I2N, LM1, and S12) have a significant potential to increase the frequency of release category group IA. Only two split fractions (I2N and L2N) have a significant potential for decreasing the frequency of release category group IA.

Table 12-5 lists those release category group IB sequences whose frequencies are greater than $1x10^{-10}$ per reactor-year. As indicated in Table 12-6, only the KPDSs involving containment bypass contribute to release category group IB. All such sequences are binned to this group. Table 12-7 identifies the importance of CET split fractions to this group. Since assignment to this group is dominated by the bypass nature of the event, only changes in the frequencies of the KPDSs will have a significant impact on the group frequency.

12.2 RELEASE CATEGORY GROUP II (SMALL, EARLY CONTAINMENT FAILURES)

Table 12-8 lists those individual sequences whose frequency is greater than $1x10^{-10}$ per reactor year and that contribute to release category group II. As indicated in Table 12-1, less than 1% of the core damage frequency analyzed in Level 2 contributes to this release category group. Thus, it is not surprising that only a few sequences exceed the arbitrary cutoff of $1.0x10^{-10}$ per reactor year. As can be seen in Table 12-9, only NIFW contributes to this group.

The importance evaluation of the split fractions contributing to release category group II is shown in Table 12-10. Split fraction I2N appears in all of the release category group II frequency. Since liner melt-through is assumed to result in large, early containment failures, it makes no contribution to this release category group.

---

[4] It should be noted that liner melt-through is assumed to result in large, early containment failures. This assumption may not be appropriate for all such events, especially the contribution from melt-through at the sump.

12.3 RELEASE CATEGORY GROUP III (LATE CONTAINMENT FAILURES)

Table 12-11 list those individual sequences whose frequency is greater than $1x10^{-10}$ per reactor year and that contribute to release category group III. As indicated in Table 12-12, sequences associated with KPDS NIFW contribute approximately 88% of the frequency of this group, with KPDS OIAU contributing the remainder. It should be noted that sequences in which containment venting was successful and there was no concurrent containment bypass were also binned to this group.

As shown in Figure 10-3, there is a 50% chance that, for KPDS NIFW, the containment failure will occur within approximately 7 hours. However, this KPDS is dominated by station blockout. Thus, recovery of AC power after vessel breach and yet-to-be-defined accident management strategies may be useful in lowering the frequency of release category group III.

Table 12-13 summarizes the importance evaluation of the split fractions contributing to release category group III. As would be expected, based on the sequences dominating the release category group III frequency, split fraction I3N (containment failure for KPDS NIFW) appears in approximately 88% of the group frequency. As noted in Table 12-1, the frequency associated with large, late containment failures is approximately twice that of small, late failures.

12.4 RELEASE CATEGORY GROUP IV (LONG-TERM, CONTAINMENT RELEASE)

Because no credit is taken for long-term recovery actions, there are no sequences currently assigned to this group. As noted in Table 12-1, sequences involving vent were assigned to release category group III.

12.5 RELEASE CATEGORY GROUP V (VESSEL BREACH PREVENTED)

As shown in Tables 12-14 and 12-15, only KPDSs PIFW and OIAU contribute to the frequency of release category group V. This is to be expected since only these two KPDSs have a split fraction value for Top Event VB (see Section 10.1) that is less than 1.0.

Table 12-1. Summary of Release Category Frequency and General Grouping								
Release Category	Release Category Frequency	General Grouping						
		IA Large Early CF	IB Cont Bypass	II Small Early CF	III Large Late CF	III Small Late CF	IV Cont Intact	V No Vessel Breach
RDGS	7.40E-07							7.40E-07
RIS	4.61E-07							4.61E-07
RDCS	3.96E-07							3.96E-07
NLDGSB	3.45E-07				3.45E-07			
NLEGSB	2.13E-07	2.13E-07						
NLDCSB	1.48E-07					1.48E-07		
NLEGUB	1.45E-07	1.45E-07						
NLDGUB	1.21E-07				1.21E-07			
NLVSY	1.16E-07		1.16E-07					
NHEGSB	9.76E-08	9.76E-08						
WLVS	8.63E-08					8.63E-08		
NHDGSB	7.37E-08				7.37E-08			
NHEGUBY	6.80E-08		6.80E-08					
NLVUY	4.30E-08		4.30E-08					
NHEGUB	4.06E-08	4.06E-08						
NHDCSB	3.16E-08					3.16E-08		
WLVU	1.46E-08					1.46E-08		
NHDGUB	1.29E-08				1.29E-08			
WLEGUB	4.97E-09	4.97E-09						
NLDGSBY	1.95E-09		1.95E-09					
NLECUB	1.69E-09			1.69E-09				
NLEGSBY	7.98E-10		7.98E-10					
NLDCSBY	7.86E-10		7.86E-10					
NLDGUBY	6.24E-10		6.24E-10					
WLEGSB	4.87E-10	4.87E-10						
NHECUB	3.26E-10			3.26E-10				
NLDCUBY	2.51E-10		2.51E-10					
WLDGSB	1.47E-10				1.47E-10			
Total	3.17E-06	5.02E-07	2.32E-07	2.02E-09	5.52E-07	2.80E-07	0.00E+00	1.60E-06
Fraction	1.00	0.1585	0.0732	0.0006	0.1745	0.0885	0.0000	0.5047

Table 12-2. Individual Sequences with Frequencies Greater Than 1 x 10^{-10} per Reactor-Year Contributing to Release Category Group IA				
Index	**Initiator**	**Freq**	**Failed Split Fraction***	**End State****
6	NIFW	1.60-07	/VBN*I2N*L2N*HBF*BEF	NLEGSB
3	MKCU	1.24-07	/VB3*I1M*L1M*S1F*HBF*BEF	NLEGUB
18	NIFW	5.10-08	/VBN*ESN*LM2*HBF*BEF	NHEGSB
21	NIFW	4.64-08	/VBN*ESN*I2N*L2N*HBF*BEF	NHEGSB
5	MKCU	3.44-08	/VB3*ESM*I1M*L1M*S1F*HBF*BEF	NHEGUB
4	NIFW	3.17-08	/VBN*LM1*HBF*BEF	NLEGSB
10	NIFW	1.78-08	/VBN*ET1*I2N*L2N*HBF*BEF	NLEGSB
13	NIFW	9.64-09	/VBN*S12*I2M*L2M*HBF*BEF	NLEGUB
1	MKCU	8.38-09	/VB3*I1M*S1F*I2F*L2D*HBF*BEF	NLEGUB
8	OIAU	4.97-09	/VB1*ESP*S13*I2Q*L2Q*HBF*BEF	WLEGUB
8	NIFW	3.53-09	/BVN*ET1*LM1*HBF*BEF	NLEGSB
24	NIFW	2.80-09	/VBN*ESN*S12*I2M*L2M*HBF*BEF	NHEGUB
4	MKCU	2.59-09	/VB3*ESM*I1M*S1F*I2F*L2D*HBF*BEF	NHEGUB
14	NIFW	2.14-09	/VBN*S12*ET1*I2X*L2X*HBF*BEF	NLEGUB
2	MKCU	9.31-10	/VB3*I1M*S1F*ET1*I2F*L2D*HBF*BEF	NLEGUB
23	NIFW	8.55-10	/VBN*ESN*S12*LM2*HBF*BEF	NHEGUB
12	NIFW	5.30-10	/VBN*S12*LM1*HBF*BEF	NLEGUB
7	OIAU	4.67-10	/VB1*ESP*LM3*HBF*BEF	WLEGSB
20	NIFW	1.43-10	/VBN*ESN*I2N*LM2*HBF*BEF	NHEGSB

* See Table 7-1 for definition of CET top events; Table 10-2 for split fraction values.
** See Figure 11-1 for end state definition.

Note: Exponential notation is indicated in abbreviated form; i.e., 1.7033-07 = 1.7033×10^{-07}.

Table 12-3. KPDS Contribution to Large, Release Category Group 1A - Large, Early Containment Failures		
KPDS	Frequency Assigned to Group	Fraction of Group Frequency
NIFW	3.26E-07	65.03%
MKCU	1.70E-07	33.88%
OIAU	5.46E-09	1.09%
MJAU	0.00E+00	0.00%
PIFW	0.00E+00	0.00%
NJHW	0.00E+00	0.00%
OJAU	0.00E+00	0.00%
Total	5.02E-07	100.00%

Table 12-4. CET Split Fraction Importance to Release Category 1A							
No.	Split Fraction	Importance	Achievement	Reduction	Derivative	S.F. Value	Frequency
1.	BEF	1.00E+00	1.00E+00	0.00E+00	0.00E+00	1.00E+00	5.02E-07
2.	HBF	1.00E+00	1.00E+00	0.00E+00	0.00E+00	1.00E+00	5.02E-07
3.	VBN	6.50E-01	1.00E+00	0.00E+00	0.00E+00	1.00E+00	3.26E-07
4.	I2N	4.47E-01	2.42E+00	6.02E-01	9.13E-07	2.19E-01	2.24E-07
5.	L2N	4.46E-01	1.00E+00	5.82E-01	2.12E-07	9.90E-01	2.24E-07
6.	S1F	3.39E-01	1.00E+00	0.00E+00	0.00E+00	1.00E+00	1.70E-07
7.	I1M	3.39E-01	1.00E+00	0.00E+00	0.00E+00	1.00E+00	1.70E-07
8.	VB3	3.39E-01	1.00E+00	0.00E+00	0.00E+00	1.00E+00	1.70E-07
9.	L1M	3.15E-01	1.00E+00	1.00E+00	2.22E-12	8.30E-01	1.58E-07
10.	ES	2.02E-01	1.32E+00	9.16E-01	2.04E-07	2.07E-01	1.01E-07
11.	LM2	1.04E-01	1.24E+00	8.96E-01	1.71E-07	3.05E-01	5.20E-08
12.	ES	7.37E-02	1.00E+00	1.00E+00	-2.32E-01	2.18E-01	3.70E-08
13.	LM1	7.12E-02	2.22E+00	9.29E-01	6.49E-07	5.50E-02	3.57E-08
14.	ET	4.85E-02	1.02E+00	9.98E-01	1.01E-08	1.00E-01	2.43E-08
15.	S1	3.18E-02	1.60E+00	9.84E-01	3.08E-07	2.55E-02	1.60E-08
16.	L2	2.48E-02	1.00E+00	0.00E+00	0.00E+00	1.00E+00	1.24E-08
17.	I2	2.48E-02	1.02E+00	9.78E+01	2.21E-08	5.00E-01	1.24E-08
18.	L2	2.37E-02	1.00E+00	0.00E+00	0.00E+00	1.00E+00	1.19E-08
19.	I2	2.37E-02	1.00E+00	0.00E+00	0.00E+00	1.00E+00	1.19E-08
20.	ES	1.09E-02	1.00E-00	0.00E+00	0.00E+00	1.00E+00	5.46E-09
21.	VB	1.09E-02	1.05E+00	9.89E-01	2.94E-08	1.86E-01	5.46E-09
22.	L2	9.91E-03	1.00E+00	0.00E+00	0.00E+00	1.00E+00	4.97E-09
23.	S1	9.91E-03	1.10E+00	9.90E-01	5.27E-08	9.34E-02	4.97E-09
24.	I2	9.91E-03	1.01E+00	9.90E-01	9.95E-09	5.00E-01	4.97E-09
25.	L2	4.27E-03	1.00E+00	0.00E+00	0.00E+00	1.00E+00	2.14E-09
26.	L2	4.27E-03	1.00E+00	0.00E+00	0.00E+00	1.00E+00	2.14E-09
27.	LM	9.72E-04	1.19E-04	9.99E-02	9.65E-08	5.05E-03	4.87E-10
28.	ET	0.00E+00	0.00E+00	1.00E+00	0.00E+00	0.00E+00	0.00E+00
29.	I1	0.00E+00	0.00E+00	1.00E+00	0.00E+00	0.00E+00	0.00E+00
30.	I2	0.00E+00	0.00E+00	1.00E+00	0.00E+00	0.00E+00	0.00E+00

Table 12-4. CET Split Fraction Importance to Release Category Group IA (Cont\d)

Definitions:

1. Importance is the fraction of the group frequency with that split fraction failed.
2. Achievement = (Group Frequency with Split Fraction Set to 0.0)/(Group Frequency).
3. Reduction = (Group Frequency with Split Fraction Set to 1.0)/(Group Frequency).
4. Derivative = [δ(Group Frequency)][δ(Split Fraction)].
5. Split fraction value is from master frequency file.
6. Frequency is the total frequency of sequences assigned to the group with this split fraction failed.

Table 12-5. Individual Sequences with Frequencies Greater Than 1 x 10^{-10} per Reactor-Year Contributing to Release Category Group IB

Index	Initiator	Frequency	Failed Split Fraction*	End State**
1	OJAU	1.16-07	/VBO*ESP	NLVSY
1	MJAU	5.26-08	/VV4*ESP*I1B*L1B*S1F*HBF*BEF	NHEGUBY
4	OJAU	3.72-08	/VBO*ESP*S34	MLVUY
1	NJHW	1.54-08	/VB2*ESP*I1B*L1B*S1F*HBF*BEF	NHEGUBY
8	OJAU	5.85-09	/VBO*ESP*S14*S3F	NLVUY
3	OJAU	1.95-09	/VBO*ESP*DV2*I3J*L3J*HBF*BEF	NLDGSBY
7	OJAU	7.98-10	/VBO*ESP*LM3*HBF*BEF	NLEGSBY
2	OJAU	7.86-10	/VBO*ESP*DV2*I3J*HBF*BEF	NLDCSBY
6	OJAU	6.24-10	/VBO*ESP*S34*DV2*I3J*HBF*BEF	NLDGUBY
5	OJAU	2.51-10	/VBO*ESP*S34*DV2*I3J*HBF*BEF	NLDCUBY

*See Table 7-1 for definition of CET top events; see Table 10-2 for split fraction values.
**See Figure 11-1 for end state definition.

Note: Exponential notation is indicated in abbreviated form; i.e., 9.6505-08 = 9.6505 x 10^{-08}.

Table 12-6. KPDS Contribution to Release Category Group 1B - Bypasses		
KPDS	Frequency Assigned to Group	Fraction of Group Frequency
OJAU	1.64E-07	70.67%
MJAU	5.26E-08	22.69%
NJHW	1.54E-08	6.64%
NIFW	0.00E+00	0.00%
PIFW	0.00E+00	0.00%
OIAU	0.00E+00	0.00%
MKCU	0.00E+00	0.00%
Total	2.32E-07	100.00%

Table 12-7. CET Split Fraction Importance to Release Category 1B							
No.	Split Fraction	Importance	Achievement	Reduction	Derivative	S.F. Value	Frequency
1.	ESP	1.00E+00	1.00E+00	0.00E+00	0.00E+00	1.00E+00	2.32E-07
2.	VBO	7.07E-01	1.00E+00	0.00E+00	0.00E+00	1.00E+00	1.64E-07
3.	BEF	3.12E-01	1.00E+00	0.00E+00	0.00E+00	1.00E+00	7.24E-08
4.	HBF	3.12E-01	1.00E+00	0.00E+00	0.00E+00	1.00E+00	7.24E-08
5.	I1B	2.93E-01	1.00E+00	0.00E+00	0.00E+00	1.00E+00	6.80E-08
6.	L1B	2.93E-01	1.00E+00	0.00E+00	0.00E+00	1.00E+00	6.80E-08
7.	S1F	2.93E-01	1.00E+00	0.00E+00	0.00E+00	1.00E+00	6.80E-08
8.	VB4	2.27E-01	1.00E+00	0.00E+00	0.00E+00	1.00E+00	5.26E-08
9.	S34	1.64E-01	1.00E+00	9.99E-01	9.11E-12	2.42E-01	3.81E-08
10.	VB2	6.64E-02	1.00E+00	0.00E+00	0.00E+00	1.00E-00	1.54E-08
11.	S3F	2.52E-02	1.00E+00	0.00E+00	0.00E+00	1.00E+00	5.85E-09
12.	S14	2.52E-02	9.80E-01	1.00E+00	-4.58E-00	3.67E-02	5.85E-09
13.	I3J	1.56E-02	1.00E+00	0.00E+00	0.00E+00	1.00E+00	3.62E-09
14.	DV2	1.56E-02	9.75E-01	1.00E+00	-5.99E-00	2.30E-02	3.62E-09
15.	L3J	1.11E-02	1.00E+00	1.00E+00	4.99E-14	7.13E-01	2.58E-09
16.	LM3	3.44E-03	9.75E+01	1.00E+00	-5.87E+0	5.05E-03	7.98E-10
17.	I1J	0.00E+00	0.00E+00	1.00E+00	0.00E+00	0.00E+01	0.00E+00
18.	ETS	0.00E+00	0.00E+00	1.00E+00	0.00E+00	0.00E+00	0.00E+00
19.	I2J	0.00E+00	0.00E+00	1.00E+00	0.00E+00	0.00E+00	0.00E+00

Definitions:

1. Importance is the fraction of the group frequency with that split fraction failed.

2. Achievement = (Group Frequency with Split Fraction Set to 0.0)/(Group Frequency).

3. Reduction = (Group Frequency with Split Fraction Set to 1.0)/(Group Frequency).

4. Derivative = [δ(Group Frequency)][δ(Split Fraction)].

5. Split fraction value is from aster frequency file.

6. Frequency is the total frequency of sequences assigned to the group with this split fraction failed.

Table 12-8. Individual Sequences with Frequencies Greater Than 1E-10 per Reactor-Year Contributing to Release Category Group II				
Index	**Initiator**	**Frequency**	**Failed Split Fraction***	**End State****
5	NIFW	1.53E-09	/VBN*I2N*S3F*HBF*BEF	NLECUB
19	NIFW	3.26E-10	/VBN*ESN*I2N*S3F*HBF*BEF	NHECUB
9	NIFW	1.69E-10	/VBN*ET1*I2N*S3F*HBF*BEF	NLECUB

* See Table 7-1 for definition of CET top events; Table 10-2 for split fraction values.
** See Figure 11-1 for end state definition.

Table 12-9. KPDS Contribution to Release Category Group II - Small, Early Containment Failures		
KPDS	Frequency Assigned to Group	Fraction of Group Frequency
NIFW	2.02E-09	100.00%
MJAU	0.00E+00	0.00%
OJAU	0.00E+00	0.00%
PIFW	0.00E+00	0.00%
NJHW	0.00E+00	0.00%
MKCU	0.00E+00	0.00%
OIAU	0.00E+00	0.00%
Total	2.02E-09	100.00%

Table 12-10. CET Split Fraction Importance to Release Category II							
No.	Split Fraction	Importance	Achievement	Reduction	Derivative	S.F. Value	Frequency
1.	S3F	1.00E+00	1.00E+00	0.00E+00	0.00E+00	1.00E+00	2.02E-09
2.	HBF	1.00E+00	1.00E+00	0.00E+00	0.00E+00	1.00E+00	2.02E-09
3.	I2N	1.00E+00	4.57E+00	0.00E+00	9.23E-09	2.19E-01	2.02E-09
4.	BEF	1.00E+00	1.00E+00	0.00E+00	0.00E+00	1.00E+00	2.02E-09
5.	VBN	1.00E+00	1.00E+00	0.00E+00	0.00E+00	1.00E+00	2.02E-09
6.	ESN	1.61E-01	7.78E-01	1.05E+00	-5.66E-1	2.07E-01	3.26E-10
7.	ET1	8.39E-02	9.99E-01	1.00E+00	-6.68E-1	1.00E+00	1.69E-10
8.	I1I	0.00E+00	0.00E+00	1.00E+00	0.00E+00	0.00E+00	0.00E+00
9.	LM1	0.00E+00	1.61E-01	1.05E+00	-1.79E-0	5.52E-02	0.00E+00
10.	ETS	0.00E+00	0.00E+00	1.00E+00	0.00E+00	0.00E+00	0.00E+00
11.	L2N	0.00E+00	0.00E+00	1.00E+02	-2.02E-0	9.90E-01	0.00E+00
12.	S12	0.00E+00	0.00E+00	1.03E+00	-2.07E-0	2.55E-02	0.00E+00
13.	LM2	0.00E+00	8.39E-01	1.07E+00	-4.69E-1	3.05E-01	0.00E+00

Table 12-10. CET Split Fraction Importance to Release Category Group II

Definitions:

1. Importance is the fraction of the group frequency with that split fraction failed.
2. Achievement = (Group Frequency with Split Fraction Set to 0.0)/(Group Frequency).
3. Reduction = (Group Frequency with Split Fraction Set to 1.0)/(Group Frequency).
4. Derivative = [δ(Group Frequency)][δ(Split Fraction)].
5. Split fraction value is from master frequency file.
6. Frequency is the total frequency of sequences assigned to the group with this split fraction failed.

Table 12-11. Individual Sequences with Frequencies Greater Than 1E-10 per Reactor-Year Contributing to Release Category Group III				
Index	**Initiator**	**Frequency**	**Failed Split Fraction***	**End State****
2	NIFW	3.45E-07	/VBN*DV3*I3N*L3N*HBF*BEF	NLDGSB
1	NIFW	1.48E-07	/VBN*DV3*I3N*HBF*BEF	NLDCSB
3	OIAU	8.63E-08	/VB1*ESP	WLVS
16	NIFW	7.37E-08	/VBN*ESN*DV3*I3N*L3N*HBF *BEF	NHDGSB
7	NIFW	6.04E-08	/VBN*ET1*S3F*DV3*I3N*L3R *HBF*BEF	NLDGUB
3	NIFW	5.14E-08	/VBN*S32*DV3*I3N*L3R*HBF *BEF	NLDGUB
15	NIFW	3.16E-08	/VBN*ESN*DV3*I3N*L3E*HBF *BEF	NHDCSB
17	NIFW	1.10E-09	/VBN*ESN*S32*DV3*I3N*L3R *HBF*BEF	NHDGUB
5	OIAU	9.63E-09	/VB1*ESP*S33	WLVU
11	NIFW	9.11E-09	/VBN*S12*S3F*DV3*I3N*L3R *HBF*BEF	NLDGUB
7	OIAU	4.94E-09	/VB1*ESP*S13*S3F	WLVU
22	NIFW	1.95E-09	/VBN*ESN*S12*S3F*DV3*I3N *L3R*HBF*BEF	NHDGUB
4	OIAU	1.47E-10	/VB1*ESP*DV4*I3O*L3O*HBF *BEF	WLDGSB

* See Table 7-1 for definition of CET top events; Table 10-2 for split fraction values.

** See Figure 11-1 for end state definitions.

Table 12-12. KPDS Contribution to Release Category Group III - Small, Early Containment Failures		
KPDS	Frequency Assigned to Group	Fraction of Group Frequency
NIFW	7.32E-07	87.87%
OIAU	1.01E-07	12.13%
MJAU	0.00E+00	0.00%
OJAU	0.00E+00	0.00%
PIFW	0.00E+00	0.00%
NJHW	0.00E+00	0.00%
MKCU	0.00E+00	0.00%
Total	8.33E-07	100.00%

Table 12-13. CET Split Fraction Importance to Release Category III							
No.	Split Fraction	Importance	Achievement	Reduction	Derivative	S.F. Value	Frequency
1.	BEF	8.79E-01	1.00E+00	0.00E+00	0.00E+00	1.00E+00	7.32E-07
2.	HBF	8.79E-01	1.00E+00	0.00E+00	0.00E+00	1.00E+00	7.32E-07
3.	I3N	8.79E-01	1.00E+00	0.00E+00	0.00E+00	1.00E+00	7.32E-07
4.	DV3	8.79E-01	1.00E+00	0.00E+00	0.00E+00	1.00E+00	7.32E-07
5.	VBN	8.79E-01	1.00E+00	0.00E+00	0.00E+00	1.00E+00	7.32E-07
6.	L3N	5.02E-01	1.00E+00	1.00E+00	-1.24E-01	7.00E-01	4.18E-07
7.	L3R	1.61E-01	1.00E+00	0.00E+00	0.00E+00	1.00E+00	1.34E-07
8.	ESN	1.42E-01	8.06E-01	1.05E+00	-2.04E-0	2.07E-01	1.18E-07
9.	ESP	1.21E-01	1.00E+00	0.00E+00	0.00E+00	1.00E+00	1.01E-07
10.	VB1	1.21E-01	1.53E+00	8.79E-01	5.44E-07	1.85E-01	1.01E-07
11.	S3F	9.18E-02	1.00E+00	0.00E+00	0.00E+00	1.00E+00	7.64E-08
12.	S32	7.50E-02	9.99E-01	1.00E+00	-2.09E-1	9.46E-02	6.24E-08
13.	ET1	7.26E-02	9.89E-01	1.00E+00	-1.01E-0	1.00E-01	6.04E-08
14.	S12	1.33E-02	6.42E-01	1.01E+00	-3.06E-0	2.55E-02	1.11E-08
15.	S33	1.16E-02	9.99E-01	1.00E+00	-1.63E-1	1.00E-01	9.63E-09
16.	S13	5.93E-03	9.42E-01	1.01E+00	-5.30E-0	9.34E-02	4.94E-09
17.	I3O	1.76E-04	1.00E+00	0.00E+00	0.00E+00	1.00E+00	1.47E-10
18.	DV4	1.76E-04	9.82E-01	1.00E+00	-1.46E-0	1.70E-03	1.47E-10
19.	L3O	1.76E-04	1.00E+00	0.00E+00	0.00E+00	1.00E+00	1.47E-10
20.	I2Q	0.00E+00	9.94E-01	1.01E+00	-9.88E-0	5.00E-01	0.00E+00
21.	LM2	0.00E+00	8.58E-01	1.06E+00	-1.70E-0	3.05E-01	0.00E+00
22.	I2M	0.00E+00	9.87E-01	1.01E+00	-2.21E-0	5.00E-01	0.00E+00
23.	I2N	0.00E+00	1.34E-01	1.24E+00	-9.23E-0	2.19E-01	0.00E+00
24.	LM1	0.00E+00	2.63E-01	1.04E+00	-6.49E-0	5.55E-02	0.00E+00
25.	I1I	0.00E+00	0.00E+00	1.00E+00	0.00E+00	0.00E+00	0.00E+00
26.	LM3	0.00E+00	8.79E-01	1.00E+00	-1.01E-0	5.05E-03	0.00E+00
27.	I2O	0.00E+00	0.00E+00	1.00E+00	0.00E+00	0.00E+00	0.00E+00
28.	ETS	0.00E+00	0.00E+00	1.00E+00	0.00E+00	0.00E+00	0.00E+00

Table 12-13. CET Split Fraction Importance to Release Category Group III (Cont\d)

Definitions:

1. Importance is the fraction of the group frequency with that split fraction failed.
2. Achievement = (Group Frequency with Split Fraction Set to 0.0)/(Group Frequency).
3. Reduction = (Group Frequency with Split Fraction Set to 1.0)/(Group Frequency).
4. Derivative = [δ(Group Frequency)][δ(Split Fraction)].
5. Split fraction value is from master frequency file.
6. Frequency is the total frequency of sequences assigned to the group with this split fraction failed.

Table 12-14. Individual Sequences with Frequencies Greater Than 1E-10 per Reactor-Year Contributing to Release Category Group V				
Index	**Initiator**	**Frequency**	**Failed Split Fraction***	**End State****
2	PIFW	7.40E-07	/I3Y*L3Y	RDGS
1	OIAU	4.61E-07	/	RIS
1	PIFW	3.90E-07	/I3Y	RDCS
2	OIAU	6.08E-09	/I3Z	RDCS

* See Table 7-1 for definition of CET top events; Table 10-2 for split fraction values.

** See Figure 11-1 for end state definitions.

Table 12-15. KPDS Contribution to Release Category Group V - No Vessel Breach		
KPDS	Frequency Assigned to Group	Fraction of Group Frequency
PIFW	1.13E-06	70.73%
OIAU	4.68E-07	29.27%
NIFW	0.00E+00	0.00%
MJAU	0.00E+00	0.00%
NJHW	0.00E+00	0.00%
MKCU	0.00E+00	0.00%
OJAU	0.00E+00	0.00%
Total	1.60E-06	100.00%

13. INSIGHTS AND POTENTIAL PLANT IMPROVEMENTS

The Level 2 analysis brought into light some plant features which are important to the ability of the plant to mitigate severe accidents. Those features will be discussed below.

1. Drywell Floor Concrete Curb

The 1 ft wide, 6" inches high concrete curb was the main contributor in reducing the probability of a liner melt through. The containment of molten corium for a longer period of time may help in buying time for recovery actions. The curb has therefore a positive contribution to accident mitigation.

2. Sandbed Thinning

The sandbed region thickness has been slightly reduced due to the corrosion problem but the impact on the structural integrity was minimal (8 psi below head flange leakage pressure). The failure criterion for the liner was based on 1% plastic strain which is a very strict criterion. A best estimate criterion of 3% would have been more realistic, which would have improved the leak before break probability.

3. Torus Structural Capacity

The structural analysis performed under this project showed that the backfit that was done to the Oyster Creek torus in the early 80's resulted in improving its pressure capacity by 25% to a best estimate limit of 153 psig.

4. Release Characteristics

a. The earliest release will take place two (2) hours after the accident (Fig. 11-2 through 11-6) which is within the allowed evacuation time (KRC4: NIFWB2).

b. The worst release (KRC5, Fig. 11-5) is caused by the bypass scenario (scram discharge volume failure to isolate, MJAU). This is because any water dumped into the vessel will come out (or portion of it) to the reactor building and will not be available for in-containment mitigation. Even here one has approximately ten (10) hours to respond.

   If one would argue that all other release categories will end up with the same release characteristics, with respect to CSI distribution as KRC5 because of ultimate revaporization of fission products, then it is clear that such a process might take place much later than the ten (10) hours seen for KRC5 (Figure 11-5). This is because of the availability of water supply to the vessel and out the breach into the containment (fire water) which would help in delaying the revaporization process. It is therefore safe to assume that there is a minimum of ten (10) hours (for any scenario) available before any release of CsI, greater than 0.11 of Table 11-6 would take place.

5. Containment Cooling

In all the scenarios analyzed (except the bypass scenario MJAU) a common behavior was seen which is failure of containment heat removal on NPSH due to high torus temperature. Therefore, even if power is restored, operators will be reluctant to operate those pumps beyond their NPSH temperature limit. But in all such scenarios drywell pressure starts to increase which ultimately fails the containment. This pressure increase would improve the NPSH limits, therefore a possibility might exist to operate containment spray in torus cooling mode to bring water temperature below the normal NPSH limit, then to switch to drywell spray mode to bring pressure down and save the containment. This possibility may be investigated during the accident management guideline development process.

14. SUMMARY AND CONCLUSIONS

Relative to published BWR Mark I PRA studies, there appears to be specific vulnerabilities associated with the response of the Oyster Creek plant to severe accidents. Specifically,

1. The Oyster Creek core damage frequency (determined in Level 1) is low and is lower than that reported for Peach Bottom in NUREG-1150.

2. A significant fraction of the core damage reported in Level 1 can be arrested in-vessel, thereby preventing vessel breach and subsequent challenges to the Oyster Creek containment.

3. The conditional probability of early containment failures for Oyster Creek is significantly less than that for Peach Bottom (as reported in NUREG-1150) despite the fact that (1) bypass events were addressed in Oyster Creek and binned with large, early failures, and (2) a rigorous treatment of drywell liner thinning was factored into the Oyster Creek containment capacity analysis. Offsetting these considerations, somewhat, is the nominal credit given for the drywell curb that protects the liner from debris attack in many scenarios.

4. The current Level 2 results for Oyster Creek show no conditional probability of an intact containment. This is due primarily to the fact that the recovery of electrical power was not considered once core damage was in progress; thus, there was no recovery of containment heat removal or drywell sprays.

5. The apparent correlation between vessel breach and containment failure results from the fact that the frequency of core damage is dominated by events involving loss of DC power and station blackout. Thus, there is little capability for mitigating either in-vessel or ex-vessel severe accident phenomena.

Because of the relatively low frequencies associated with the various containment failure modes, no specific hardware or procedural changes are being recommended at the current time. However, during the accident management phase of the IPE process, the results and insights obtained in this Level 2 analysis will again be reviewed with the intent of identifying hardware and/or procedural changes that could improve the risk posture of the Oyster Creek plant.

CONTAINMENT OVERPRESSURE CAPACITY FOR THE OYSTER CREEK NUCLEAR POWER PLANT

October 1991

Prepared for:

GPU NUCLEAR CORPORATION
One Upper Pond Road
Parsippany, New Jersey 07054

EQE Project Number: 52096.01

APPROVAL COVER SHEET

TITLE: Containment Overpressure Capacity for the Oyster Creek Nuclear Power Plant

REPORT NUMBER: 52096.01-R-001

CLIENT: GPU Nuclear Corporation

PROJECT NO.: 52096.01

REVISION RECORD				
REV. NO.	DATE	PREPARED	REVIEWED	APPROVED
0	10/15/91	Hassan Hadidi-T.	[signature]	[signature]

TABLE OF REVISIONS

Rev. No.	Revision Description	Revision Date
	Draft	5/31/91
0	Incorporate GPU Comments	10/15/91

CONTENTS

TABLES

FIGURES

1. INTRODUCTION

A probabilistic risk assessment of the Oyster Creek Nuclear Power Station is being conducted by GPU Nuclear Corporation in conjunction with PLG, Inc. to evaluate the probability of radioactive release from the site. In this study, systems models, event trees, and fault trees are used to determine the risk. EQE Engineering is under contract to GPU Nuclear Corporation to establish the capacity of the containment structure for elevated temperature and pressure loadings resulting from an accident involving core damage. The probability of failure as a function of internal pressure has been developed for critical failure modes of the containment. The variability in the probability of failure is also included. In addition, estimated leak areas are also given. This information can be incorporated in the plant containment system models to determine the probability of radioactive release from the site.

The Oyster Creek containment structure consists of a GE boiling water reactor (BWR) Mark I containment, which includes a steel drywell and a toroidal suppression chamber. The drywell has the shape of an inverted "light bulb," i.e., a spherical shell intersected by a right circular cylinder. A 2:1 semiellipsoidal head shell is joined to the top of the cylinder by a bolted flange connection. The drywell sphere has an inside radius of 35 ft. and a minimum measured shell thickness of 0.6815" at elevation 51'-10" while the cylindrical shell has a radius of 16.5 ft. and a minimum measured thickness of 0.6122" at elevation 87'-5" (Reference 19). The minimum thickness in the sandbed region is 0.8028 inches (Reference 19). The suppression chamber torus is fabricated of 20 mitered cylindrical shell segments joined together to form the "circular" torus, which has a major radius of 50.5 feet about the axis of the drywell. At each mitered joint, the shell is stiffened by a ring girder. Each torus segment has an inside diameter of 30 ft. and a shell thickness of 0.385". The lower half of each torus segment is reinforced by 1.25 in thick straps which are welded to the torus shell.

On the exterior, the drywell is enclosed in concrete of varying thickness from the base elevation up to the elevation of the top head. From there, the concrete continues vertically to the level of the top of the spent fuel pool.

Several potential failure modes were investigated for the containment by estimating the median pressure capacities. The controlling failure modes were identified by ranking them according to their estimated median pressure capacities. For the critical failure modes, the variabilities in the pressure capacities were estimated, which then allows for the probability of failure to be described as function of pressure. In addition, failure modes were evaluated for high temperature conditions.

2. PROBABILISTIC DESCRIPTION OF CAPACITY

In order to fit into the PRA context, a probabilistic description of the pressure capacity of the containment structure is required. Also, since the pressure capacity is treated as a random variable, it is possible for more than one failure mode to significantly contribute to the risk. Therefore, several failure modes must be evaluated. This section discusses how the capacities are described in a probabilistic form.

It should be noted that in the current investigation, stresses are not categorized as primary membrane, primary bending, etc., which are then compared with different allowables depending on the load condition as is required in a code or design calculation. Rather, failure is based on expected ultimate strengths and elongations using median material properties and associated variabilities.

2.1 DEVELOPMENT OF FAILURE PROBABILITIES

The pressure capacities are evaluated using limit state analyses for the various failure modes considered. The capacities are dependent on several factors, including the material properties, modeling assumptions, and the postulated failure criteria. A major source of uncertainty in the failure criteria is the expected strain resulting in failure. All welds are full penetration and the probability of failure at membrane strains below yield is considered to be quite low. On the other hand, biaxial strains and gage length effects as well as strain concentrations and bending significantly reduces the expected membrane strain at failure when compared to elongation data developed from standard specimen ultimate tests. Since test data from vessel test are extremely limited, considerable variability is introduced not only in the failure criteria, but in analytical modeling and other assumptions. Since many of the base parameters are random and the methods used to evaluate the capacities are subject to some uncertainty, the pressure capacity for any failure mode is also considered to be a random variable. It is assumed that the pressure capacities have a lognormal

distribution. This assumption is made because a lognormal distribution has been shown to be a valid description of the variability in material strengths. In addition, for a random variable that can be expressed as the product and quotient of several random variables, the distribution of the dependent variable tends to be lognormal regardless of the distributions of the independent base variables.

With the pressure capacity assumed to be a lognormal random variable and denoting it as P, the probability of failure occurring at a pressure less than a specific value p is expressed as:

$$P_f = \text{Prob}(P \leq p) = \Phi\left[\frac{\ln(p/\hat{P})}{\beta_C}\right] \qquad (2\text{-}1)$$

Where

P_f = probability that failure occurs at a pressure $P \leq p$

P = random pressure capacity

β_C = logarithmic standard deviation of P

$\hat{P}$ = median pressure capacity

$\Phi(\cdot)$ = cumulative distribution function for a standard normal random variable

In Equation (2-1), the pressure capacity for a given failure mode is probabilistically described by the following expression.

$$P = \hat{P} \cdot M \cdot S \qquad (2\text{-}2)$$

in which $\hat{P}$ is the median pressure capacity, M is lognormally distributed random variable having a unit median and a logarithmic standard deviation β_M representing the uncertainty in modeling, and S is also a lognormally distributed random variable with a unit median value and a logarithmic standard deviation β_S representing the uncertainty in the material properties. The overall uncertainty in the median capacity is

obtained by taking the square root of the sum of the squares of β_M and β_S.

The median pressure capacity represents the internal pressure level for which there is a 50% probability of failure (leakage) for a given failure mode. The median values are evaluated from limit state analyses for the different failure modes. The uncertainties, β_M and β_S, are associated with variability due to a lack of knowledge related to differences between the analytical model and the real structure. Modeling uncertainties are associated with the assumptions used to develop analytical models and their ability to properly represent the failure condition. The strength uncertainties are associated with variabilities related to the material resistance. Examples of the sources of such uncertainties include: variability in concrete strength, steel yield strength, stress-strain relationships, and the influence of elevated temperatures on material strength. The evaluation of the median capacities and the associated variabilities for the postulated failure modes is discussed in Section 3.

2.2 VARIABILITY IN MATERIAL PROPERTIES

The drywell is fabricated from ASME SA-212 Grade B steel. Based on Chicago Bridge and Iron test results (Reference 1) median yield and ultimate stresses of 50.7 and 78.9 ksi, respectively, were obtained at room temperature. The variation of the estimated median yield strength as a function of temperature is shown in Table 2-1. Similarly, the temperature variation of the modulus of elasticity of the steel is shown in Table 2-2.

Based on the test results mentioned above, the logarithmic standard deviation of the yield strength is estimated to be $\beta = 0.07$.

In addition to the variability in yield stress, variability exists in the post-yield stress-strain relationship. Since some degree of inelastic deformation is expected for most modes of containment shell failure, this variability must also be accounted for.

2.3 MODELING VARIABILITY

Uncertainties will exist in the estimated pressure capacities due to differences between the analytical idealization of the structure and the real conditions. There are numerous possible sources of modeling uncertainties. Examples of the sources of modeling uncertainties include: assumptions used to develop the internal force distributions, failure criteria, and the use of empirical formulae. Moreover, since they are dependent on the particular failure mode under consideration, they must be evaluated on a case-by-case basis. Bounding analytical assumptions such as different boundary conditions can often be used to establish an estimate of the modeling variability. However, in many instances, the evaluation of these uncertainties would require very detailed analysis and/or extensive data which may not be available. As a result, it was necessary to use subjective evaluation and engineering judgment to estimate these uncertainties. The evaluation of the modeling uncertainties associated with the estimated pressure capacities is included in the discussion of the specific failure modes in the next section.

Table 2-1

MEDIAN YIELD STRESS FOR SA-212 GRADE B STEEL

Temp (°F)	Median Yield Stress (ksi)
70	50.7
100	50.7
200	46.1
300	45.1
400	43.6
500	41.1
600	37.5
700	36.5
800	34.0

Table 2-2

TEMPERATURE VARIATION OF THE MODULUS OF ELASTICITY

Temp (°F)	E (ksi)
70	29,500
100	29,500
200	28,800
300	28,300
400	27,700
500	27,300
600	26,700
700	25,500
800	24,200

3. ANALYSIS OF CONTAINMENT CAPACITY

The capacity of the Oyster Creek containment is estimated based on incipient leakage as the failure criterion. In this section, the potential failure modes of the containment shell are investigated. The loads considered include temperature, pressure, and dead load. The effects of temperature are limited to its influence on the material strength. The median pressure capacities and the associated variabilities are estimated for the controlling failure modes. Failures of both the drywell and the suppression chamber (torus) are considered. The failure modes examined include:

1. Membrane failures of the drywell shell (sphere, cylinder, head shell)
2. Failure of the drywell head flange seal
3. Failure of the vent line from the drywell to the suppression chamber
4. Failure of the suppression chamber shell
5. Failure at penetrations.

All of the failure modes evaluated here were considered to be quasi-static. In other words, the pressure rise times were assumed to be of sufficient duration that the dynamic response characteristics of the containment shell could be neglected, and the temperatures in the material were assumed to have reached steady-state. The results presented here are based on metal temperatures.

The median values and logarithmic standards deviations of the failure pressures for the controlling failure modes at temperatures of 300, 400, 500, 600 and 700°F are summarized in Tables 3-1 through 3-5. Also, given in these tables are the 95% confidence nonexceedance values for each failure mode. The effects of increased temperatures at 800°F and greater are discussed in Section 4. The following subsections discuss the evaluation of failure pressures. The example evaluations of the median capacities discussed in this section were developed assuming a

temperature of 300°F, which is slightly greater than the design accident temperature of 281°F.

3.1 DRYWELL SHELL FAILURE

Several potential failure modes were investigated for the drywell shell for the overpressure load condition. These included the major sections of the drywell: the sphere, the sphere/cylinder knuckle, the cylinder, and the head shell, which are shown in Figure 3-1. The limit pressures were estimated using methods based on limit analysis as outlined in References 2 and 3 as well as by simple shell theory. The typical median failure criteria for the drywell is represented by a membrane strain limit of 1%. In addition, the effects of temperature on the strength of the drywell steel plate are included.

3.1.1 Sphere

The median failure pressure of the spherical portion of the drywell shell was estimated using simple shell theory in which it was modeled as a sphere subjected to an internal pressure. The expansion of the sphere is limited by the 3 inch gap between the drywell and the biological shield wall. When contact occurs, the membrane strain in the sphere is 0.0071, which is greater than yield, yet well below the strain hardening range. Therefore, when the sphere contacts the shield wall, the steel shell will be essentially at the yield stress, although the strain will be in the plastic range. The pressure at which contact occurs can then be estimated from the equation

$$P_y = \frac{2\,\bar{\sigma}_y t}{R} \qquad (3\text{-}1)$$

Using a shell thickness of 0.6815 inch, a radius of 420 inch and the median yield stress at 300°F of 45.1 ksi, the median internal pressure required to cause the sphere to contact the shield wall is estimated to be 155 psi. However, at this strain level, the material is judged to

have a low probability of failure, since the SA 212 Grade B carbon steel is expected to be capable of sustaining larger membrane strains.

While uniaxial tensile tests (Reference 6) indicate ultimate strains for SA-212 Grade B steel on the order of 30%, a median failure criterion of 1% membrane strain was used for the drywell shell. This reduction in the maximum strain capacity was conservatively taken to account for biaxial strain effects, gage length effects, strain concentrations, and bending effects. All of these factors tend to reduce the expected material ductility when compared to the uniaxial test data.

Since the sphere contacts the shield wall at a membrane strain of 0.0071, the internal pressure must also deform the reinforced concrete shield wall in order to develop the additional membrane strain in the steel shell to reach the failure criterion. At that point, the containment structure can be considered to be a reinforced concrete pressure vessel with a pre-stressed liner. To achieve a membrane strain of 1% in the drywell shell, an additional strain of 0.0029 must be developed. A review of the shield wall shows that the inside surface of the shield wall maintains a spherical surface compatible with the drywell, but the outer surface does not remain spherical because the wall thickness changes. At the thinnest section, the shield wall is 55 inches thick.

To estimate the capacity of the drywell/shield wall system, the shield wall was idealized as a thick-walled spherical shell with a thickness of 55 inches and an inside radius of 420 inches. At the critical section, the shield wall is reinforced with #11 bars spaced at 6 inches in both the hoop and meridional directions at the inside face. The reinforcing of the outside face is twice the reinforcing at the inside face. The median yield stress of the reinforcing bars is taken to be 48 ksi at room temperature. Since an additional strain of 0.0029 must be developed at the inside face of the shell to reach the failure criterion of 1% strain for the drywell, the reinforcing bars at both the inside and outside faces of the shield wall are expected to yield. A temperature gradient through the shield wall was assumed to vary

linearly. The stress in the drywell shell at 1% membrane strain was taken to be equal to the 6% above the yield stress to account for strain hardening. Neglecting any concrete tensile stress contribution, the median pressure capacity of the sphere was estimated to be 353 psi.

To estimate the modeling uncertainties, first consider the variability in the force distribution of the reinforcing in the shield wall. It is judged that a 1.65 ß variation can be represented by the bars at the outer face having a stress of 1/3 of the yield stress, while the inside face bars and the drywell shell are at yield. Using this force distribution, at room temperature, the pressure for equilibrium is 291 psi (vs. 376 psi when outer fall bars are taken to be at yield stress). Therefore, the variability associated with the internal force distribution is estimated as

$$ß = - \ln(291/376)/1.65 = 0.16$$

Also, as part of the modeling uncertainty, an additional variability of 0.10 is included to account for the potential of a lower capacity due to strain concentrations. The overall modeling uncertainty becomes

$$ß_M = (0.16^2 + 0.10^2)^{1/2} = 0.19$$

The uncertainties associated with the material properties include contributions from the yield stress. The variabilities in the yield stress of the drywell shell and the reinforcing are 0.08 and 0.13, respectively, with the variability due to temperature effects on the yield stress taken to be 0.05. Therefore, the uncertainty in the median capacity due to material properties is estimated as

$$ß_S = (0.08^2 + 0.13^2 + 0.05^2)^{1/2} = 0.16$$

The overall uncertainty in the median capacity is taken as the square root of the sum of the squares of $ß_M$ and $ß_S$, which gives

$$ß_C = (0.19^2 + 0.16^2)^{1/2} = 0.25$$

3.1.2 Sphere/Cylinder Knuckle

For the sphere/cylinder knuckle, the median pressure capacity was estimated using an analytic expression for the limit pressure of the intersection of spherical and cylindrical shells (Reference 3). The limit state for the knuckle involves the development of circumferential plastic hinges and the formation of a plastic collapse mechanism such that the knuckle bows outward. It is assumed that, when the limit mechanism forms, the membrane strains in the shell have reached their limiting values. This method has been used to estimate the capacities for other Mark I containment structures (References 2 and 3) and has given good correlation with finite element analyses. The median pressure capacity was estimated from

$$P = (1.2)(4)P_S\hat{\sigma}_y\frac{T}{D} \qquad (3\text{-}2)$$

Where the factor 1.2 represents the difference between the measured experimental capacities and the empirically predicted pressure capacities. The parameter, P_S, is determined from the expression

$$\sqrt{\frac{T}{D}\left\{\left[1+\left(\frac{t}{T}\right)^2\right](1-P_S)\right\}} = P_S\frac{d}{D}\sqrt{1-\left(\frac{d}{D}\right)^2} - \frac{d}{D}\frac{t}{T}\sqrt{2\frac{t}{d}\left(1-2\frac{d}{D}\frac{T}{t}P_S\right)} \qquad (3\text{-}3)$$

where

t = cylinder wall thickness
T = sphere wall thickness
d = cylinder diameter
D = sphere diameter

Because the drywell has a thickened knuckle ring at the junction of the cylinder and the sphere, the thickness of the knuckle ring, 2.5625 inch, was used for both t and T in the above equation to determine the value of P_S. Using the above, the median pressure capacity for the knuckle

was estimated to be 180 psig for a shell temperature of 300°F. Failure is expected to initiate in the thickened portion of the knuckle or in the heat affected zone in either the cylinder or sphere. The crack propagation direction is unknown but can be either into the cylinder or sphere or circumferential around the knuckle.

The modeling uncertainty arises from the equation used to predict the failure pressure. It is estimated based on the results of comparisons of experimental data with the theoretically predicted values as reported in Reference 3. From a very limited amount of data, the ratio of the experimental to theoretical pressure had a coefficient of variation of 0.19. Assuming a lognormal distribution, the coefficient of variation then corresponds to a logarithmic standard deviation of 0.19 for modeling uncertainly. The logarithmic standard deviation of the material strength is estimated to be 0.09, which includes the variability of the yield stress of the drywell steel and the influence of temperature. Thus, the overall uncertainty, β_c, becomes 0.21.

3.1.3 Cylinder

The median pressure capacity of the cylindrical section of the drywell was estimated using the limit expression for a stiffened cylindrical shell as described in Reference 2. The failure mechanism involves an outward bulging of the shell with plastic hinges forming at the shell boundaries where discontinuities in the shell stiffness occur. The plastic limit mechanism was assumed to form when the membrane strain reaches a value of 1%. The median pressure capacity was estimated from

$$P = \hat{\sigma}_y \frac{t}{r} \left(\frac{1}{1 - 4\epsilon_0 \frac{r^2}{s_1^2}} \right) \left(\frac{2}{\sqrt{3}} + \frac{12Zr}{ts_1^2} \right) \qquad (3\text{-}4)$$

where

t = shell thickness
r = cylinder radius

ϵ_0 = pre-mechanism membrane strain
s_1 = spacing between stiffeners, clear length of the shell
Z = plastic section modulus per unit length of the shell, $t^2/4$

The gap between the cylinder and the shield wall is 3 inches. Since the radius of the cylinder is 198 inches, the hoop strain in the shell when it makes contact with the shield wall is 0.0152 or 1.52%. Because the median strain in the shell was assumed to be 1% when the failure mechanism forms, interference with the concrete shield wall is not expected prior to the development of the assumed failure mechanism.

To calculate the median failure pressure, the cylinder thickness of 0.6122 inches was used. A value of 245.7 inches was used for the length s_1. For shell temperature of 300°F, the median pressure capacity was estimated to be 175 psig.

The modeling uncertainties enter from the use of the above empirical equation to estimate the failure pressure. Based on comparisons with finite element analyses, the logarithmic standard deviation of the equation was estimated to be 0.11 in Reference 2. An additional uncertainty of 0.14 was also included to account for the effects of the boundary conditions of the shell, since the shell is not actually stiffened and the length of the cylinder was taken as the length between changes in plate thickness. Therefore, the overall modeling uncertainty was estimated as a logarithmic standard deviation of 0.17. The uncertainty of the material was estimated as β_s=0.08, which includes the contributions of the variability in the yield stress and the shell thickness. The resulting overall combined uncertainty then becomes 0.19.

3.1.4 Sphere Sand-Bed Region

An inspection of the steel shell (November 1986) prior to restart from the 11R outage in the sand-bed region revealed that some degradation of the shell had taken place during the years since completion of

construction. Based on the ultrasonic (UT) inspection results, (Reference 19) the lowest average measured thickness value for the sand-bed region is 0.8028 inch compared to the as-designed thickness of 1.154 inch. A measured variation in thickness of ± 0.0085 inches was found for this location. It is our understanding the sand is to be removed. Hence, the analysis of the shell at the sand-bed region was performed without accounting for the beneficial effects of the sand. Failure was conservatively considered to occur at 1% strain level due to the combined membrane and bending stresses. For a shell temperature of 300°F, median pressure capacity was estimated to be 134 psig.

The uncertainty of the material strength was estimated as $\beta_S = 0.09$, which includes the contributions of the variability in the material yield stress, shell thickness, and the influence of temperature. The modeling uncertainty was estimated to be 0.20. The resulting overall combined uncertainty becomes 0.22.

3.1.5 Head Shell

The drywell head consists of a 2:1 semi-ellipsoidal shell with a 1-1/2 inch thickness in the cylindrical part of the shell and 1-3/16 inch thick ellipsoidal part. The potential failure modes examined included asymmetrical buckling and plastic collapse in the knuckle region of the shell as well as hoop failure of the cylinder. References 2 and 3 presented empirical equations to predict the limit pressures for these failure modes for semi-ellipsoidal shells. These empirical equations were developed from the results of finite element analyses of semi-ellipsoidal shells. For the buckling mode, failure was defined as the point at which bifurcation occurs on the pressure-displacement curve. Plastic collapse was conservatively defined as the point at which the crown displacement is twice its yield value.

For the asymmetric, elastic-plastic buckling, the critical pressure is estimated from:

$$P_{cr} = 10.4\sigma_y \left(\frac{t}{2r}\right)^{1.25} \qquad (3\text{-}5)$$

where

σ_y = is the yield stress

t = is the head thickness

r = is the radius of the attached cylinder

ϵ_y = is the yield point strain

For the plastic collapse mode, the limit pressure is estimated from

$$P_o = \frac{\sigma_y t(1 + 50\epsilon_y)}{r} \qquad (3\text{-}6)$$

The ranges of parameters investigated were

$200 < r/t < 750$

$30ksi < \sigma_y < 60ksi$

and the strain hardening slope, S, = 0, 5, and 10 percent.

The above analysis results are sensitive to the analytical modeling assumptions. For instance, for strain hardening steel heads, buckling is predicted for semi-ellipsoidal heads only when deformation theory is used. No buckling is analytically predicted using flow theory (Reference 6). Equations 3-5 and 3-6 are also conservative by about 10 percent based on analysis results. Results of tests for steel head buckling pressure capacities are very limited. Reference 7 shows a ratio of experiment to theory pressures of 1.59 to 1.97. Thus, while the above equations are considered an adequate basis for design, they appear to be excessively conservative for use in establishing median-centered buckling capacity. For use in this investigation, the analytically predicted (Equations 3-5 and 3-6) buckling pressures were increased by a factor of 1.78 to determine the expected median

capacities. In all cases, the P_o plastic collapse capacity controls for steel heads.

The median pressure capacities estimated using these expressions resulted in values that were significantly higher than the cylinder. At 300°F, the median hoop failure capacity of the cylinder portion of the head (1½ inch thickness) is expected to be in excess of 360 psig. Plastic collapse was found to have a median pressure capacity of 560 psig for a shell temperature of 300°F with a HCLPF pressure capacity above 390 psig. Thus, the failure of the drywell head was judged not to be a controlling failure mode.

3.2 DRYWELL HEAD FLANGE CONNECTION

Another significant failure mode of the drywell is the potential for leakage through the bolted head flange connection, which has a pressure unseating seal. That is, the leak mechanism is developed by the opening of a gap between the flanges since the internal pressure tends to pull apart the flanges. The flanges are held by 96 bolts, each with a diameter of 2-1/2 inches. Details of the flanges are shown in Figure 3-2. The bolts are fabricated from ASME SA-193 Grade B7 steel. The seal is provided by double rectangular cross section seal rings made of a silicone rubber compound. Several factors influence the pressure capacity of this connection, including: the condition and behavior of the seals, the amount of pre-load in the flange bolts, the amount of flange rotation due to the shell deformation induced by the internal pressure, and the stiffness of the flange bolts.

The flange bolts are pre-loaded by a bolt installation torque of from 1400 to 1800 ft-lb such that the median expected tensile force is about 45.3k. To overcome the net flange compression of the bolt pre-load and the dead weight of the head shell, a median internal pressure of about 36 psig is required. Increasing the pressure beyond 36 psig would then lead to the opening of a gap between the flanges. However, a slight separation of the flanges does not necessarily infer leakage due to the presence of the seal rings. At lift off pressure, the bolt tensile

stress is still well below yield as is the shell and flanges. Both seal rings must be bypassed for leakage to occur. After flange separation, rotation of both the upper and lower flanges occurs due to the 3 inch offset of the bolts from the plane of the drywell and head cylinders. (c.f. Figure 3-2). Rotational stiffness of both upper and lower flanges were developed by treating both flanges as composite section rings formed by two horizontal rings together with the vertical sections of the cylinders located between the horizontal plates. These rings were then assumed to be loaded by the distributed twisting moment created by the bolt tensile load times the bolt eccentricity. Using the bolt dimensions and the results of the flange ring analyses described above, a stiffness relation between the incremental bolt force and the flange gap at the outer seal ring was developed. It was found that the contributions to the flange gap due to bolt stretch and flange rotation were of the same order of magnitude with approximately twice as much contribution from rotation. From this stiffness relation, a relationship between the flange gap and the incremental pressure was developed for the temperature range of interest.

For a given flange gap, the potential for leakage depends on the ability of the seal rings to maintain a seal. This depends on the amount of rebound of the seal material as a gap is opened as well as the initial compression of the seal rings. The resiliency of the elastomer is measured in terms of its compression set, which is defined as the fraction of the initial compression that is retained as permanent deformation. After being in service, there will be some permanent set in the seal ring due to exposure to the operating temperature. In addition, there will also be some compression set due to the increased temperature in the accident condition. In order to estimate the behavior of the elastomer under extreme conditions, a brief literature review was conducted. Data on various elastomers from tests conducted by Sandia Laboratories (Reference 8), researchers in the U.K. (Referenced 9 and 10), and a seal manufacturer were reviewed. It was found that the silicone rubber could not be relied upon to hold a seal for temperatures much greater than 500 degrees Fahrenheit in a steam

environment. At these temperatures, the material becomes severely degraded. However, there is little data on the compression set of silicone rubber seal rings subjected to relatively short duration, high temperature transients or for long term exposures to moderate temperatures. Based upon test data for fluorocarbon and ethylene propylene elastomers, the long term compression set of a seal ring after exposure to the operating temperature in the range of 200°F could be quite high depending on the length of exposure.

The median compression set was estimated in two parts. The first part represented the expected compression set from the exposure to the normal operating conditions. Thus, it depends on the operating temperature and the service life of the seal. The maximum exposure period is one refueling cycle since the rings are replaced at that interval. The second part of the compression set is associated with the additional set caused by the accident temperatures. As in Reference 10, it is assumed that these two effects are additive.

$$C_S = C_{S_{\text{Normal Oper.}}} + C_{S_{\text{Accident}}}$$

At the start of the accident, (assuming 6000 hours after start-up, corresponding to approximately mid fuel cycle) the accident set is negligible, such that

$$C_S = 0.4$$

and

$$\delta_{ref} = 0.1875(1 - 0.40) = 0.1125 \text{ inches}$$

Assuming the metal temperature is again 300°F, an additional pressure of about 106 psig is required to overcome the seal rebound, or

$$p = 106 + 36 = 142 \text{ psig}$$

Head flange leak pressures for both the instantaneous and 70 hour accident conditions are plotted in Figure 3-4 for the mid-fuel cycle condition.

Due to the lack of information on the long term compression set of silicone rubber seal rings, the compression set due to the operating conditions was estimated from data on ethylene propylene (EP) rubber. From Reference 9, for an EP rubber o-ring exposed to a temperature of 100°C (212°F) for about 6000 hours, a compression set of approximately 60% would result. Based on seal life versus temperature data for various compounds from Parker Seals in Reference 11, it would be expected that the silicone rubber would have a somewhat lesser compression set than that for the EP rubber. However, for a replacement interval corresponding to a refueling cycle, the length of exposure can be longer than 6000 hours. Due to the lack of data, it is very difficult to quantify the variations in the compression set caused by these factors. Therefore, as a best estimate, the compression set of the seal rings was taken to be 40% due to 6000 hours exposure at the operating temperature of 200-212°F. At 212°F and 70 hours, a median residual set of about 5% is expected. Using these limited data, an estimate of the long term residual set as a function of time after start-up at normal operating temperature in the range of 200-212°F was developed for the silicone rubber seal rings as shown in Figure 3-3. The additional compression set due to the accident temperature conditions is estimated from data obtained from Parker Seals for silicone rubber o-rings from the standard ASTM compression set test. For an exposure of 70 hours at a temperature of 302°F, the median compression set for various silicone rubber compounds is about 12%. Therefore, the total compression set for estimating the median 70 hour pressure capacity at an accident temperature of 300°F is taken as the sum

$$C_s = 0.40 + 0.12 = 0.52$$

When the head shell flanges are bolted together, the seal rings are compressed a total of 3/16 inches. Noting that the median total

compression set is 52%, the median net rebound of the seal ring is estimated as:

$$\hat{\delta}_{reb} = 0.1875\ (1 - C_s)$$

$$= 0.1875\ (1 - 0.52) = 0.090 \text{ inches}$$

The median failure pressure at incipient leakage corresponds to the opening of a flange gap of 0.090 inches such that the rebound of the seal ring is overcome. To do this, an additional pressure of 85 psi is required beyond the 36 psi necessary to overcome the flange median clamping force due to the bolt pre-load and the dead weight of the head shell. Therefore, the estimated median 70 hour pressure capacity for the head flange at a temperature of 300°F becomes:

$$P = 85 + 36 = 121 \text{ psi}$$

Again, the bolt stress at this pressure is still below yield. Thus, if the pressure is reduced, the leak area will reduce (although there will likely be some degradation of the seal due to the high velocity gas leakage).

Because this failure mode does not depend on the material strengths (at least up to yield of the bolts), but rather on deformations, the uncertainties are all attributed to modeling. There are three main contributors to the overall uncertainty in the median capacity: the variability in the seal rebound, the variability in the flange bolt pre-load, and the variability in the flange gap stiffness relation. Overall, the variability in the seal rebound is expected to be the dominant contributor due to the uncertainties associated with the estimated median compression set. To estimate the modeling uncertainty associated with the compression set, the instantaneous leak pressure for 0% compression set is considered to be a +3ß upper value corresponding to mid fuel cycle life (approximately 6000 hours) Therefore, the logarithmic standard deviation corresponding to the uncertainty in the seal rebound at various times in the fuel cycle becomes:

$$\beta_{time} = \frac{1}{3} \ln \frac{215}{142} = 0.14$$

where 215 psig corresponds to the leak pressure at the beginning of the fuel cycle (no long term residual set) and 142 psig corresponds to the 6000 hour normal operating temperature residual set (40%) instantaneous leak pressure.

In addition to the variability in the long term residual set related to the time the accident occurs in the fuel cycle, variability exists in the long term residual set due to the uncertainty in the type of silicone rubber compound used and the sparsity of data as shown in Figure 3-3. After the initiation of an accident, temperatures of the seal rings can be expected to increase above the normal operating temperature. The residual set of the seal rings corresponding to the accident conditions is also a function of time, temperature and rubber compound. Figure 3-4 shows typical silicone rubber 'o'-ring 70 hour residual set data for various compounds for a temperature range of 100 to 225°C (212 to 437°F).

In addition to the uncertainty associated with the seal ring behavior, variability in the leak pressure is introduced from the initial bolt torque, preload induced in the bolt from a given torque, Young's moduli of the bolt and drywell materials, and uncertainty in the analytical models used to calculate the flange rotations after flange separation. The overall expected variation in leak pressure for both instantaneous leak pressure and leak pressure 70 hours into the accident are shown in Figure 3-5 for an accident occurring at approximately midway through a refueling cycle. The variability in leak pressure is temperature dependent, particularly after the effects of the accident temperature are considered. In addition, the variability associated with the time the accident occurs during the fuel cycle must be included.

Although a thermal analysis of the bolted flange was outside the scope of this investigation, it is expected that a temperature difference is likely to exist between the bolts and the shell particularly in the

early stages of the accident transient. Any temperature difference will induce thermal stresses in the bolts which will increase the clamping force and hence leak pressure. A 100°F temperature difference results in an increase of about 70 psig in leak pressure.

To estimate the median leak areas, the median flange gap for a given pressure is first estimated using the flange gap stiffness relation. It is assumed that, once leakage starts, the pressure can be sustained in order that the bolts can further elongate. The median leak areas are estimated as the product of some fraction of the circumference of the flange and the open gap through which the gas can escape.

The seal rings are rectangular section rings recessed into rectangular grooves around the circumference of the bottom flange. The upper surface is recessed 1/8 inch below the top surface of the bottom flange. Once leakage occurs, considerable erosion of the rubber is expected, and the leak gap is expected to be controlled by the metal to metal separation. The median flange leak area, $inch^2/\Delta p$, where Δp is the pressure increase in psig above the leak pressure, is shown in Figure 3-6 for the temperature range from 200 to 700°F. The lognormal standard deviation on leak area is expected to be about 0.76 over the same temperature range. The above leak area is expected to be applicable for pressures below about 240 psig at 200°F to 195 psig at 700°F. Above these pressures, yield of the bolts with subsequent large increases in leak area is expected. At temperatures above 700°F, creep of the bolts is expected such that the leak area is a function of time at pressure as discussed in the following section.

3.3 VENT LINE FROM THE DRYWELL TO THE SUPPRESSION CHAMBER

Ten vent lines run from the lower part of the drywell sphere to the suppression chamber. At the intersection with the drywell, the pipe has an inside diameter of 96.125 inches and thickness of 0.4375 inches. Around the penetration, the drywell has an increased thickness of 2.029 inches. Due to the potential for expansion of the drywell and the torus, the vent line is fitted with two expansion bellows. The critical

failure modes include a membrane failure of the penetration at the junction with the drywell shell due to internal pressure and membrane failure of the bellows due to pressure.

Equations (3-2) and (3-3) were used to estimate the median capacity for a membrane failure at the intersection of the drywell and the vent line, since it is the junction of a cylindrical and spherical shell. For a shell temperature of 300°F, the median pressure capacity was estimated to be 192 psig. This is a conservative estimate of the capacity, since the expression used to estimate the limit pressure does not include the beneficial effects of the additional stiffeners around the penetration. As with the drywell sphere/cylinder knuckle, the modeling uncertainty enters from the limit equation used to predict the failure pressure. A logarithmic standard deviation of 0.19 was estimated for modeling. Also, for the uncertainty in the material strength, logarithmic standard deviation of 0.09 was estimated.

To investigate the magnitude of the stresses in the expansion bellows, estimates of the membrane stress were developed using elastic analysis methods from Reference 14. For an internal pressure P, the membrane stress in the bellows is estimated from

$$S_m = \frac{P}{N_p t} h + \left[\frac{a\bar{R}}{\frac{\pi}{2} - 1 \quad a + h} \right] \qquad (3\text{-}8)$$

where N_p is the number of Plies in the bellows (conservatively assumed to be 1) and t, a, h, and R are characteristic dimensions of the bellows, as shown in Figure 3-7.

The bellows are made of ASME SA-240 Grade 304 Stainless Steel material. Bellows were assumed to fail at 1% strain level. At 300°F, based on a median stress value of 39.3 ksi at failure, median pressure capacity was estimated to be 156 psig. The modeling and strength variabilities were estimated to be 0.17 and 0.12, respectively, which results in an overall uncertainty of 0.21.

3.4 SUPPRESSION CHAMBER SHELL (TORUS)

The suppression chamber consists of 20 cylindrical shells that are mitered and joined together to form the "circular" torus. A plan view of the torus is shown in Figure 3-8. At each of the mitered joints, the torus is stiffened by ring girders as shown in Figure 3-9. Each cylindrical shell has an inside diameter of 30 ft. and a thickness of 0.385 inch. Noting that the ring girders have greater stiffness than the shell for radial expansion, the failure mode of the torus corresponded to an inter-ring expansion of the shell in which the shell "barrels" out from the ring girders as the internal pressure is increased. To estimate the failure pressure, each section of the torus was idealized as a stiffened cylindrical shell. The median failure pressure was estimated using Equation (3-4). As for the cylindrical portion of the drywell, the failure mechanism is assumed to form when the membrane strain reaches a value of 1%. For use in Equation (3-4), the length of the cylinder was taken to be the centerline length of the mitered section, 16 ft. The lower half of the torus is reinforced by welding 1.25 inch thick SA-516 Grade 70 straps which are typically 16 inches wide and are typically spaced at 13 inches. The effect of these straps was included by "smearing" the 1.25 inch thickness of the straps over the entire lower half of the torus shell which results in an equivalent shell thickness of 0.594 inch for the lower half of the torus. As a result of including the effect of the straps, the calculated pressure capacity given by Equation (3-4) increases by 25% in comparison with the case when the straps are neglected. At a shell temperature of 300°F, the median failure pressure was estimated to be 153 psig.

The sources of modeling variability include the equation used to predict the failure pressure, the modeling of the contribution of the straps, and the effect of idealizing the mitered cylinder as an ideal cylinder. To represent these variabilities, the overall logarithmic standard deviation was estimated to be 0.18. For the material strength, the logarithmic standard deviation was estimated to be 0.12, which includes

the variability in the yield stress and the uncertainty due to the temperature effects on the material properties. The overall combined uncertainty is estimated as 0.22.

3.5 MAJOR PENETRATIONS

Several major penetrations were also evaluated for pressure capacity. Among these are the personnel lock (Penetration X-1) and the X-52 and X-64 manholes. The personnel lock consists of an 8'-4" ID cylindrical sleeve with two pressure seating rectangular doors and bulkheads. The assembly is fabricated from SA 212 Grade B plate with silicone rubber seal rings for both doors. The center line of the hatch is located 9'-9" below the equator of the sphere. Potential modes of failure investigated included buckling of the inner portion of the cylindrical sleeve, hoop failure of the external portion of the sleeve, weld failure of the bulkhead welds, failure of the sleeve bolts, and bending of the inner and outer bulkheads and doors. Pipe penetrations are not expected to control.

The lowest capacity failure mode was found to be bending of the outer door bulkhead with median failure pressure of about 109 psig over the 200 to 700°F temperature range. However, for the inner cavity between the doors to become pressurized, leakage of the inner door must occur. Due to the much stiffer inner bulkhead, bending failure of the bulkhead is not expected at pressures below about 300 psig, although some leakage past the seal may be expected at temperatures above about 700°F. Other failure modes including bending of the stiffened door, weld failure, or tensile failure of the SA 320-L7 sleeve bolts were found to have significantly greater pressure capacities.

Both the X-64 and X-52 manhole covers are flat plates attached to the shell by studs. The X-64 cover is a 32 inch O.D. 1-1/4 inch thick plate attached by twenty four 5/8 inch diameter 304 SS studs on a 29-1/2 inch diameter bolt circle. A 1/8 inch flat silicone rubber gasket is used, and the edge of the plate is seal welded to the shell after installation. The X-52 plate is 1-1/2 inch thick locally relieved

around the outer periphery to form indenting rings for the elastomeric seal rings. It is restrained by twenty four 1 inch diameter SA 193-B7 studs located on a 29-1/2 inch diameter bolt circle. Both these penetrations were found to have high capacities.

3.6 CAPACITIES OF CRITICAL FAILURE MODES AT OTHER TEMPERATURES

Tables 3-1 to 3-5 give the median capacities and associated variabilities for the controlling failure modes at metal temperatures of 300°F to 700°F. The elevated temperatures reduce the yield stress of the drywell steel and, thus, the median capacities reduce with increasing temperature. However, for the head flange, leakage is controlled by the flange separation and the rebound of the seal rings. For temperatures less than 500°, the leak pressure is mainly influenced by the amount of rebound of the seal ring. The seal ring compression set was estimated using data from References 8-11 as well as test data obtained from the Parker Seal Group. At temperatures of 500° and greater, the seal ring is assumed to be completely degraded. Leakage at the head flange then is assumed to occur when the flange separates. As a result, at temperatures of 500°, 600°, and 700°, the median leak pressure for the head flange corresponds to the pressure required to overcome the clamping force due to the pre-load in the bolts. At temperatures of 700° and less, no bolt stress relaxation is expected. Therefore, the head flange median leak pressure remains at 36 psig for 500° to 700°. The effects of bolt stress creep at higher temperatures is discussed in the following section.

3.7 CORRELATION OF FAILURE MODES

For the purpose of estimating the correlation between structural failure modes, the uncertainty is often subdivided into two independent components.

1. Uncertainty in strength

2. Uncertainty in modeling

These uncertainties may be represented by two independent random factors with logarithmic standard deviations β_M and β_S, respectively. The combined coefficient of variation is then given by:

$$\beta = \sqrt{\beta^2_M + \beta^2_S}$$

The advantage of splitting the uncertainty into these two components is that for a given pair of failure modes the uncertainty factor for one of the components may be correlated for both modes, while the other is independent. A review of the Oyster Creek failure modes and the expected degree of correlation between these modes indicates this breakdown into two independent components is not required. This results from the judgement that in each case for modes where the uncertainty in strength was found to be correlated, the uncertainty in modeling was also found to be correlated. Perfect correlation is assumed whenever the degree of correlation is estimated to be more than one-half.

For the failure modes listed in Table 3-1 (and for higher temperatures), the head flange is considered to be independent (both in strength and modeling) of the remaining modes. The remaining failure modes in Table 3-1 are considered to be dependent since they are based on the same material properties and very similar analytical methods.

Table 3-1

CAPACITIES OF THE CONTROLLING FAILURE MODES AT 300°F
(MID FUEL CYCLE)

Failure Mode*	$\hat{P}$ (psig)	ß	95% Conf. (psig)
Head Flange (Instantaneous)	142	0.11	119
Head Flange (70 Hours)	121	0.18	90
Shell Sand Bed Region (Sand Removed)	134	0.22	93
Torus	153	0.22	106
Ventline Bellows	156	0.21	110
Cylinder	175	0.19	128
Cylinder/Sphere Knuckle	180	0.21	127
Ventline	192	0.21	136
Sphere	353	0.25	234

* For all failure modes except head flange, large, uncontrolled leak areas result

Table 3-2

CAPACITIES OF THE CONTROLLING FAILURE MODES AT 400°F
(MID FUEL CYCLE)

Failure Mode*	$\hat{P}$ (psig)	ß	95% Conf. (psig)
Head Flange (Instantaneous)	140	0.11	117
Head Flange (70 Hours)	78	0.56	31
Shell Sand Bed Region (Sand Removed)	130	0.22	90
Ventline Bellows	143	0.21	101
Torus	148	0.22	103
Cylinder	170	0.19	124
Cylinder/Sphere Knuckle	174	0.21	123
Ventline	186	0.21	132
Sphere	345	0.25	228

* For all failure modes except head flange, large, uncontrolled leak areas result

Table 3-3

CAPACITIES OF THE CONTROLLING FAILURE MODES AT 500°F
(MID FUEL CYCLE)

Failure Mode*	$\hat{P}$ (psig)	ß	95% Conf. (psig)
Head Flange (Instantaneous)	138	0.11	115
Head Flange (70 Hours)	36	0.09	31
Shell Sand Bed Region (Sand Removed)	122	0.22	85
Ventline Bellows	130	0.21	92
Torus	140	0.22	97
Cylinder	160	0.19	117
Cylinder/Sphere Knuckle	164	0.21	116
Ventline	175	0.21	124
Sphere	332	0.25	220

* For all failure modes except head flange, large, uncontrolled leak areas result

Table 3-4

CAPACITIES OF THE CONTROLLING FAILURE MODES AT 600°F
(MID FUEL CYCLE)

Failure Mode*	$\hat{P}$ (psig)	ß	95% Conf. (psig)
Head Flange (Instantaneous)	136	0.11	114
Head Flange (70 Hours)	36	0.09	31
Shell Sand Bed Region (Sand Removed)	112	0.22	78
Ventline Bellows	117	0.21	83
Torus	128	0.22	89
Cylinder	146	0.19	107
Cylinder/Sphere Knuckle	149	0.21	105
Ventline	160	0.21	113
Sphere	314	0.27	201

* For all failure modes except head flange, large, uncontrolled leak areas result

Table 3-5

CAPACITIES OF THE CONTROLLING FAILURE MODES AT 700°F
(MID FUEL CYCLE)

Failure Mode*	$\hat{P}$ (psig)	β	95% Conf. (psig)
Head Flange (Instantaneous)	128	0.09	110
Head Flange (70 Hours)	36	0.09	31
Shell Sand Bed Region (Sand Removed)	109	0.22	76
Ventline Bellows	114	0.21	81
Torus	124	0.22	86
Cylinder	143	0.19	105
Cylinder/Sphere Knuckle	145	0.21	103
Ventline	156	0.21	110
Sphere	301	0.26	196

* For all failure modes except head flange, large, uncontrolled leak areas result

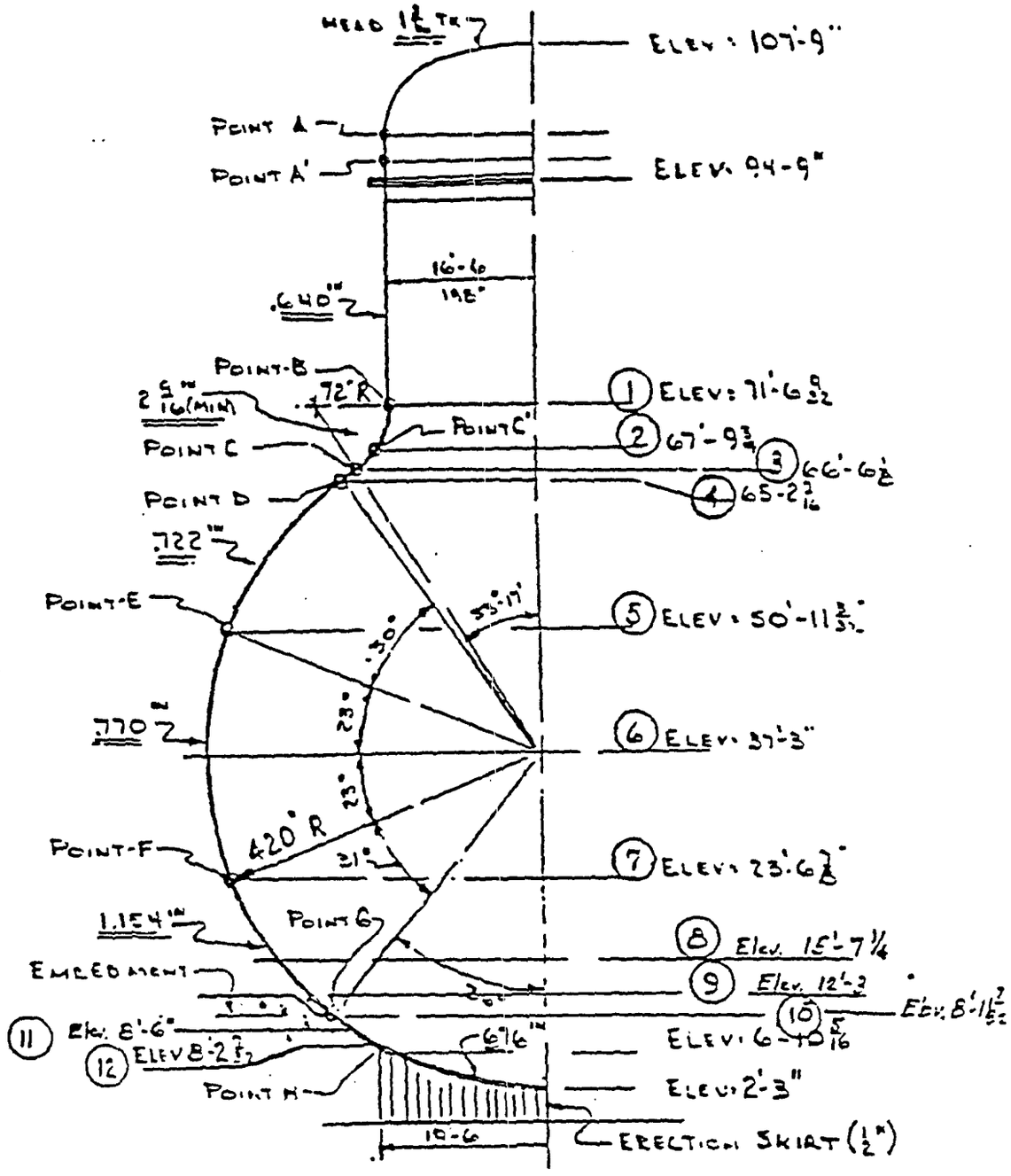

Figure 3-1: Oyster Creek Drywell

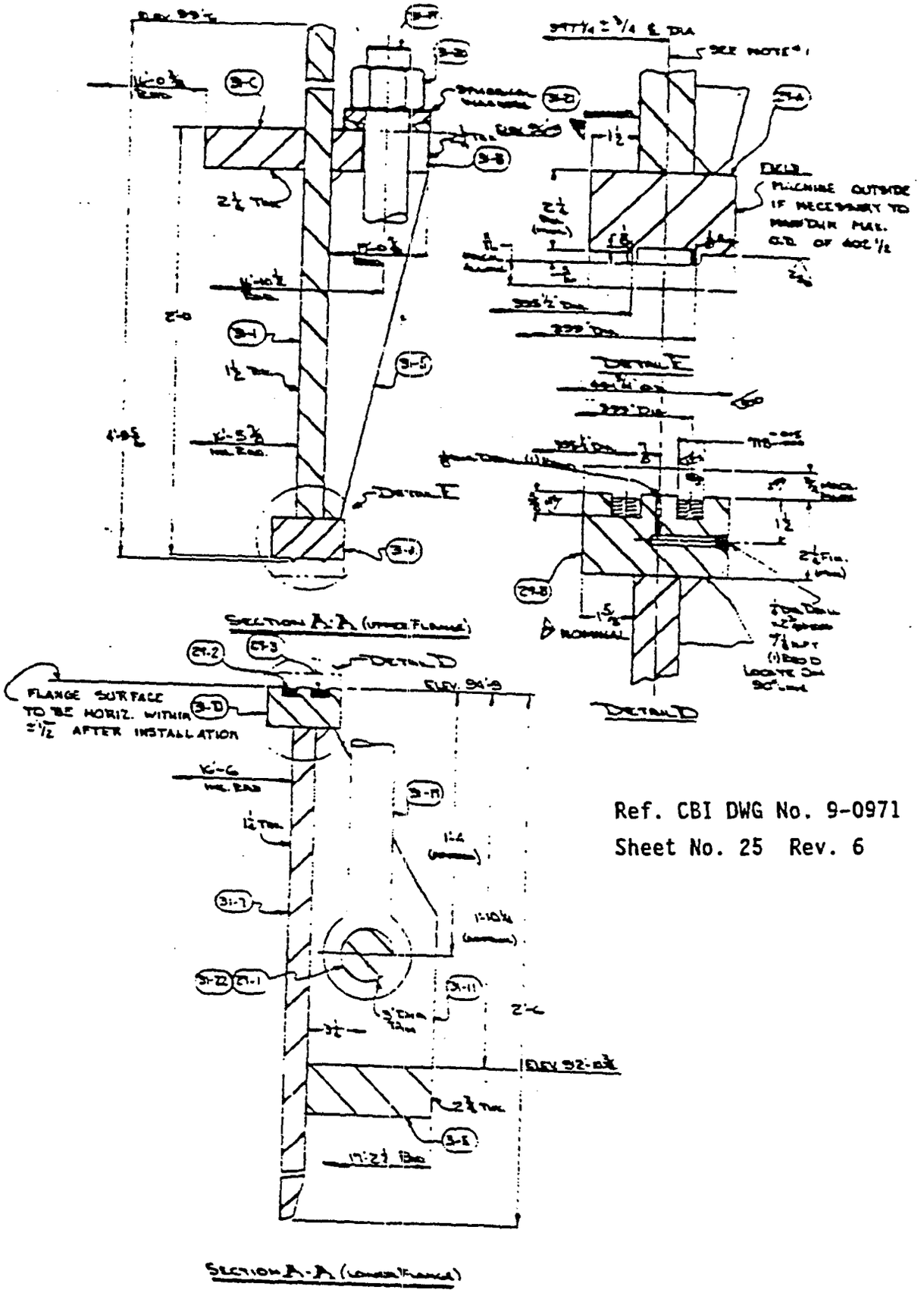

Ref. CBI DWG No. 9-0971
Sheet No. 25 Rev. 6

Figure 3-2: Drywell Head Flange Details

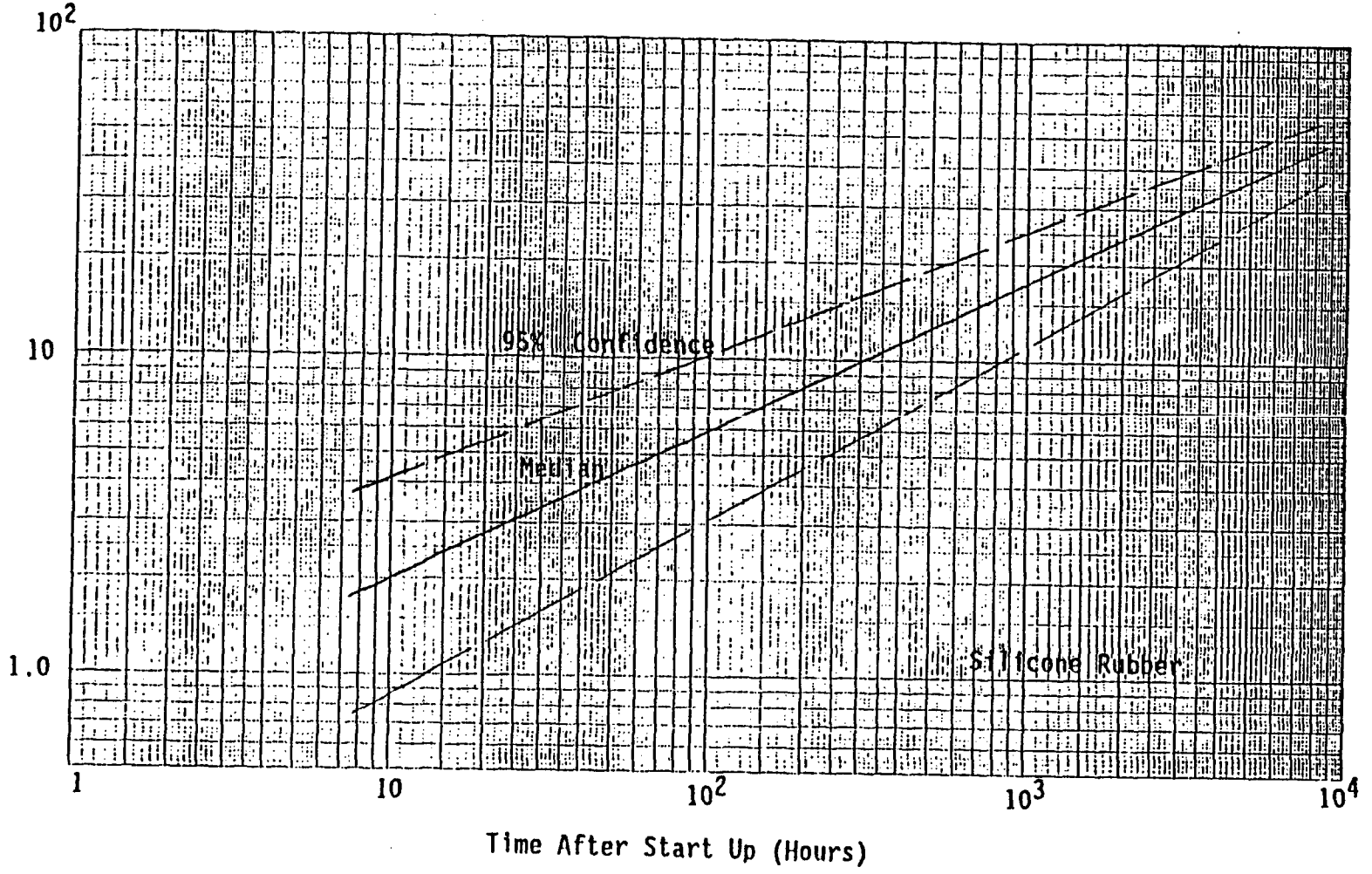

Figure 3-3: Residual Set at 200-212 °F Operating Temperature

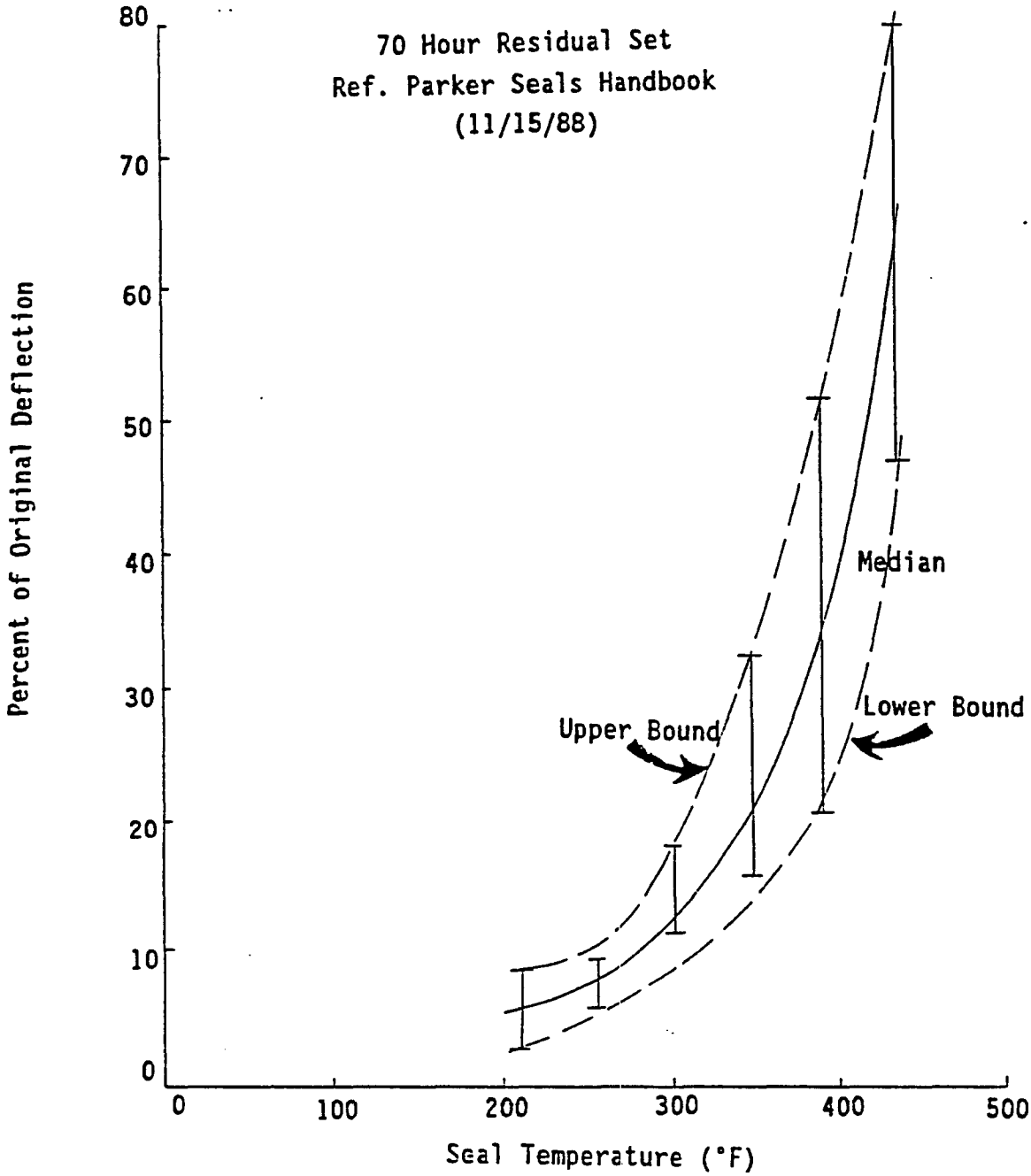

Figure 3-4: Silicone Rubber Residual Set

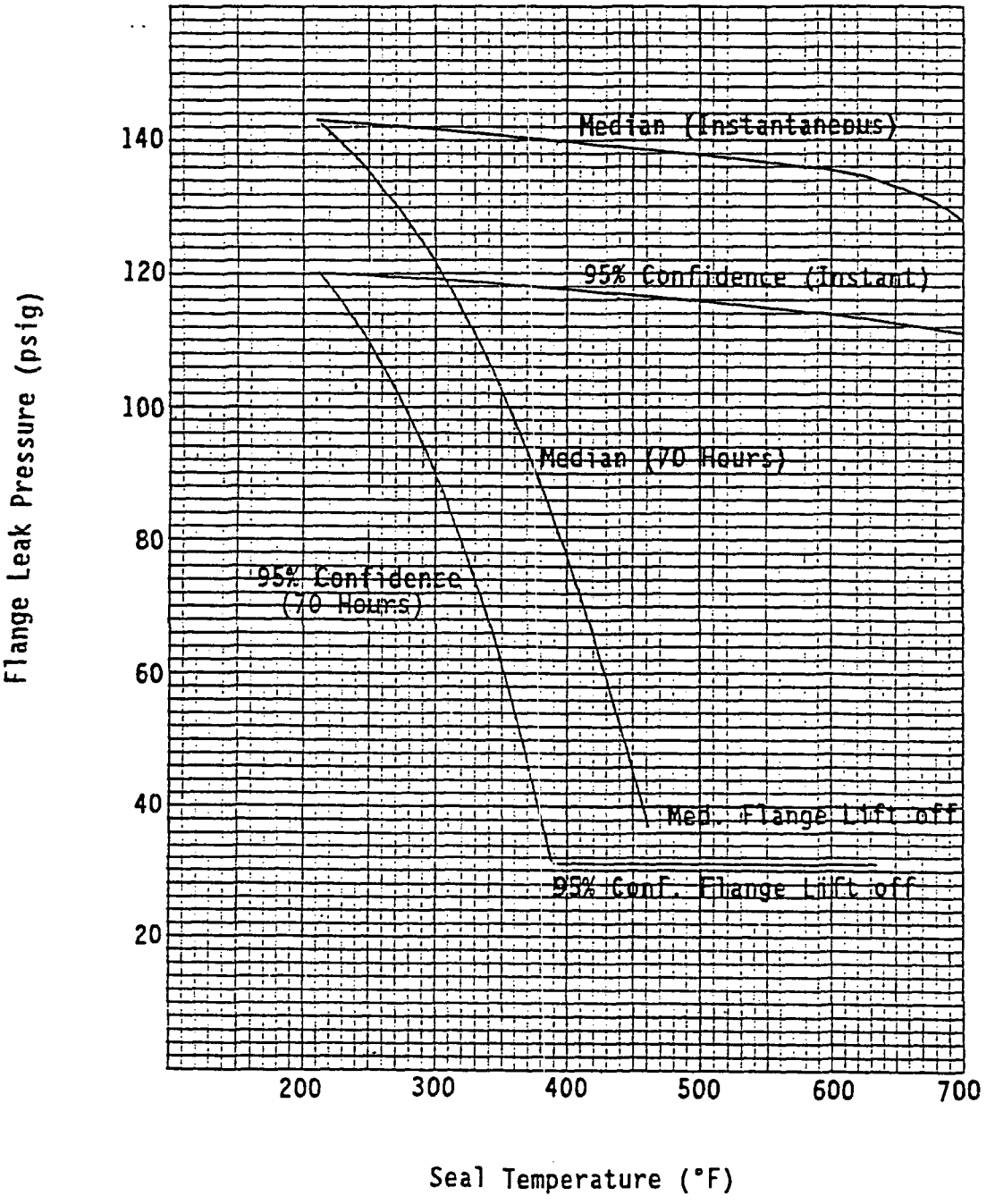

Figure 3-5: Head Flange Leak Pressure (Mid-Fuel Cycle)

2232nb/oyst-3

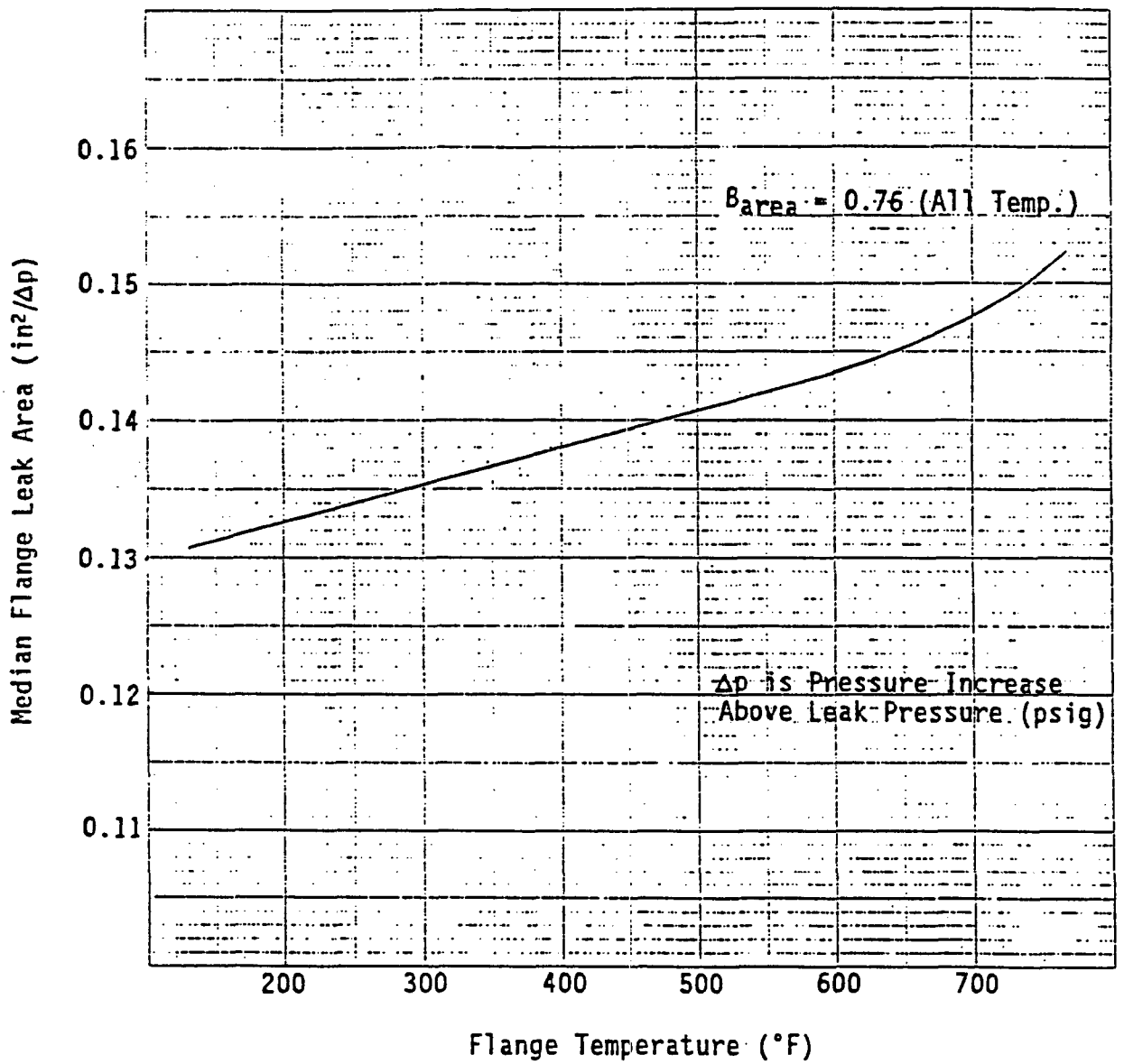

Figure 3-6: Head Flange Leak Area

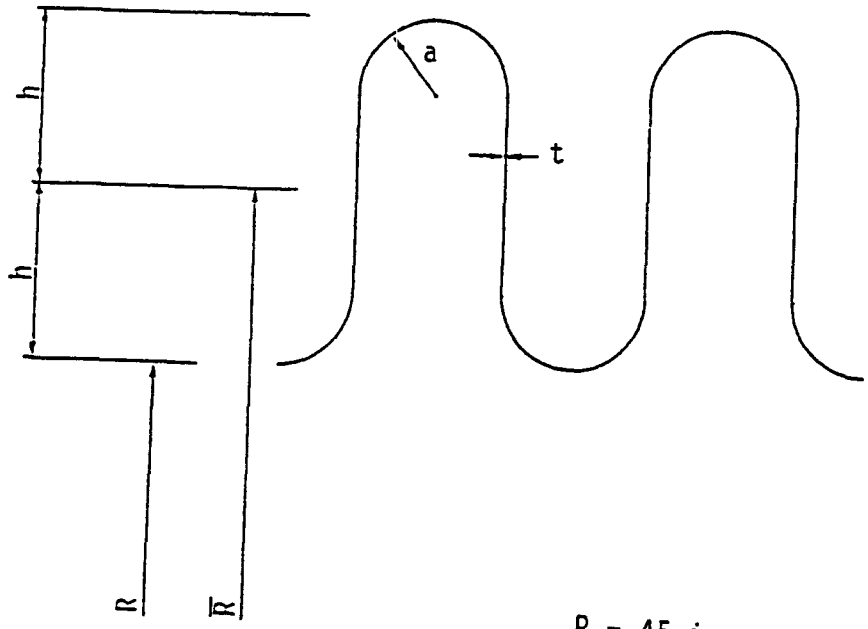

R = 45 in.

$\bar{R}$ = 46 in.

h = 1.0 in.

t = 0.075 in.

a = 0.50 in.

Figure 3-7: Characteristic Dimensions of the Vent Line Bellows

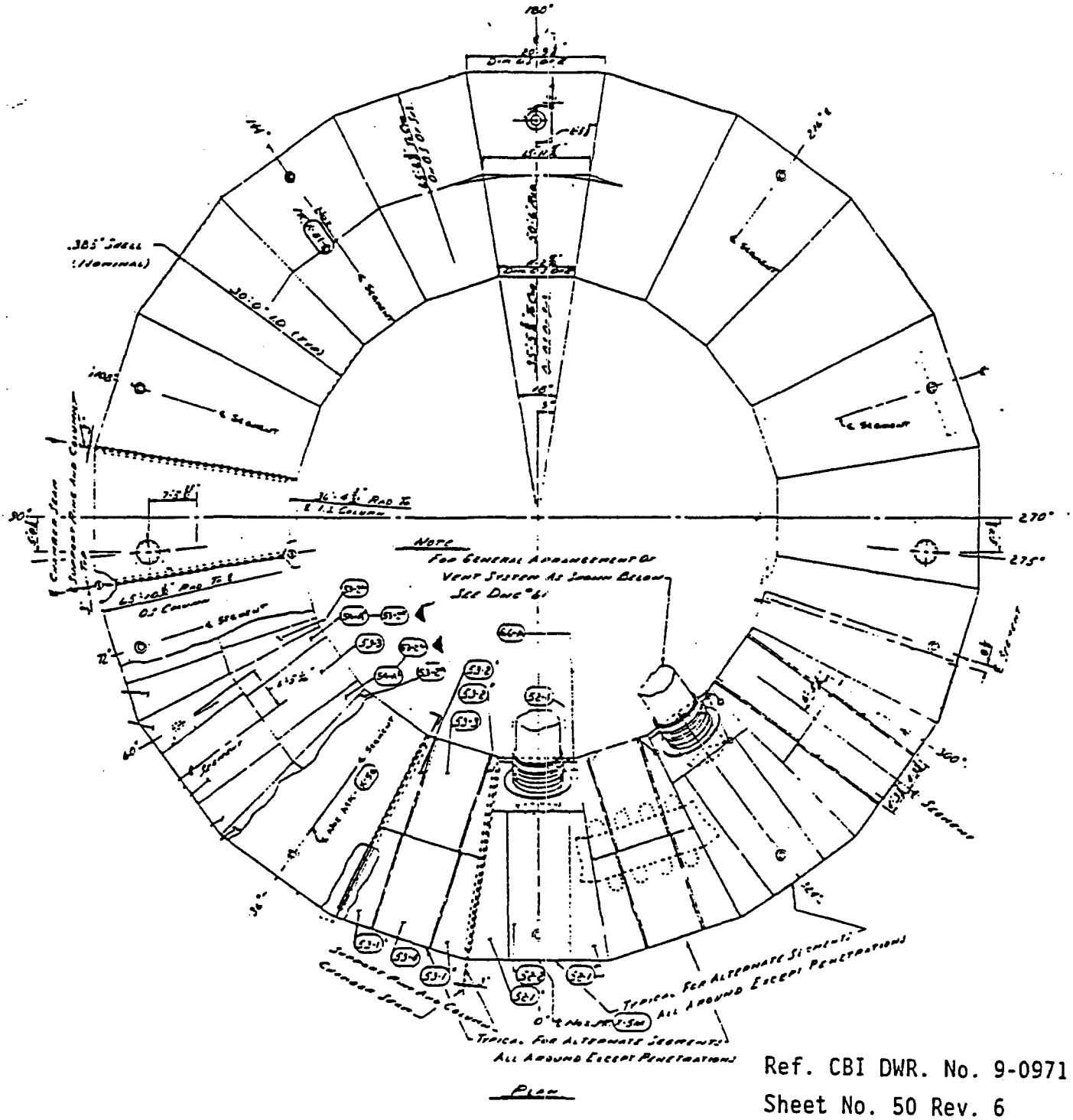

Ref. CBI DWR. No. 9-0971
Sheet No. 50 Rev. 6

Figure 3-8: Plan View of the Torus

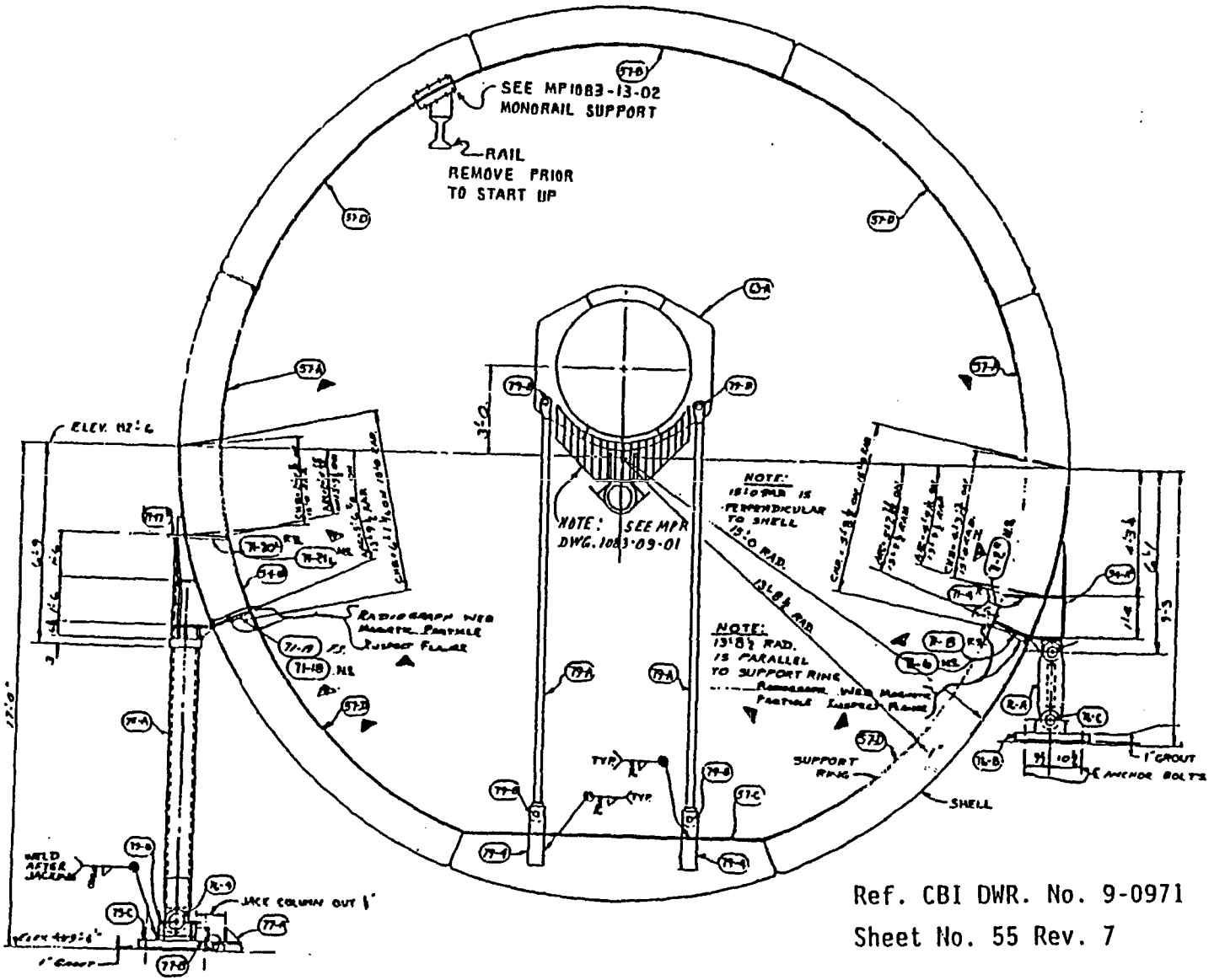

Ref. CBI DWR. No. 9-0971
Sheet No. 55 Rev. 7

Figure 3-9: Cross Section of the Torus

4. CONTAINMENT CAPACITY AT HIGH TEMPERATURES

In this section, the capacity of the containment structure is evaluated for high temperature conditions. The median capacities and associated variabilities discussed in Section 3 were developed for an accident temperature of 300°F. Median pressure capacities were also presented for temperatures up to 700°. Accident temperatures in excess of 300°F, while unlikely, are possible for various accident scenarios. Therefore, the effects of very high temperatures were investigated for the controlling failure modes. All results presented herein are based on metal temperatures. No heat transfer or thermal analyses, either steady-state or transient, were conducted in the current investigation. Some conservatism is thereby introduced if the gas temperature inside the containment is assumed equal to the metal temperature.

Temperatures of 800°F and greater are considered in this section. Since the head flange was found to be the critical location for the low temperature conditions, the evaluation for high temperatures focuses on that part of the containment structure. With the high temperatures, there is the potential for creep and bolt relaxation which significantly affect the leak pressure capacity as well as the leak areas. Since creep effects become significant at these temperatures, time now enters into the description of the containment capacity and the leak areas.

The potential failure modes of the containment structure reviewed in this section include leakage at the head flange due to bolt elongation and the time dependent stress rupture of the flange bolts and the drywell shell. Leak areas may be calculated based on the bolt creep deformations presented here.

Some other potential modes of failure at high temperatures were considered but were found to not control. Among these is the interference of several pipes near the top of the drywell with the concrete shield wall penetrations. At high temperatures, the annular clearance between the pipe and the penetration may be closed due to the vertical thermal expansion of the drywell. However, preliminary

calculation indicates the pipes will crush prior to fracture of the pipe or drywell. Thus, although some reduction in flow can result, it does not appear that breach of the drywell pressure boundary will occur at the temperatures being considered here.

4.1 DRYWELL HEAD FLANGE

As discussed in Section 3, leakage through the head flange is dependent on the rebound of the seal-rings, the force-deformation relation of the flange bolts, and the effective pre-load in the bolts. Elevated temperatures affect all of these factors. For temperatures less than 500°F. the silicone rubber seal rings have some rebound, but it is temperature dependent. However, for temperatures of 500°F and greater, the seal rings become severely degraded and are assumed to be ineffective with no rebound (100% compression set). The force-deflection relation between the flange gap and the bolt force is temperature dependent since the modulus of elasticity of steel is temperature dependent. In addition, as the temperature is increased, the yield stress of the flange bolt steel is reduced. This increases the potential for yielding to occur in the bolts. Once yielding develops in the bolts, large increases in the flange gap are induced by small increments of pressure. At elevated temperatures, the effective pre-load in the bolts can be reduced due to relaxation. The effects of relaxation are most significant at very high temperatures. For each of these factors, the elevated temperatures tend to reduce the pressure for incipient leakage as well as increase the leak areas.

Table 4-1 shows the median incipient leak pressures for the head flange for temperatures ranging from 200° to 1200°F. The median leak pressures for 300° to 700° were presented in Section 3 and are repeated here for comparison. For temperatures less than 500°, the median leak pressure is mainly influenced by the rebound of the seal rings. The compression set increases with increasing temperature which results in decreasing leak pressures. The uncertainties in the median leak pressures are also mainly influenced by the variability in the rebound of the seal rings. At temperatures of 500° and greater, the seals are assumed to be

completely degraded and leakage occurs at the pressure that causes a gap to open between the flanges. As a result, for temperatures greater than 500° the median leak pressure is controlled by the effective flange compression due to the pre-load in the bolts. The amount of stress relaxation of the bolt pre-load due to temperature is based on data from Reference 16. For the relaxation effects, it is assumed that the metal temperatures have reached a steady state. Between temperatures of 500° and 1000°, the median incipient leak pressure remains constant at 36 psi. This is because the initial bolt stress is relatively low and, at these temperatures, there is essentially no relaxation in the bolt stress, leaving the effective pre-load unchanged. The variabilities in the leak pressures in this temperature range are also reduced because there is no contribution from the seal rebound. For temperatures greater than 1000°, significant bolt stress relaxation is expected to occur. As the temperature increases, the relaxed stress decreases, which then reduces the effective flange compression and reduces the leak pressure. For example, based on data from Reference 16, at 1000°F, the relaxed stress in the flange bolt was estimated to be about 9 ksi, which is a slight reduction from the initial pre-load stress of 9.2 ksi. As a result, the effective flange clamping force is reduced and the leak pressure at 1000° is reduced slightly to 35 psi. In addition, with the effects of bolt stress relaxation included, the variability in the median leak pressures increases. At 1200°, it is judged that the relaxation is such that there is essentially no residual stress in the bolts. Therefore, only the dead weight of the head shell provides the flange compression and the median leak pressure then is only about 1 psi.

The influence of temperature on the seals, the force-deformation relation of the bolts, and the pre-load impact the instantaneous flange gap and leak area. However, due to the high temperatures, creep in the bolts can become substantial. Since creep is a time dependent process, the bolts continue to stretch over time. At a given pressure and temperature, the total flange gap is made up of two parts, an instantaneous gap and the additional time dependent gap due to creep, which can be expressed as

$$\Delta Gap_{total} = \Delta instant + \Delta creep \quad (4\text{-}1)$$

From Equation (4-1), the leak area can be separated into two parts: an instantaneous leak area and a leak area due to bolt creep. The instantaneous leak area is analogous to the leak areas evaluated for the low temperature case in Section 3. The median instantaneous leak areas are estimated from

$$\hat{A}_{L_{instant}} = L_{eff} \quad \hat{\Delta}instant \quad (4\text{-}2)$$

where L_{eff} is the effective length of the leak of the head flange at the outer seal ring. Since we are considering temperatures much higher than 500°F, the term representing the seal ring rebound does not appear in the above equation.

The median leak area associated with the bolt creep is estimated from

$$\hat{A}_{L_{creep}} = L_{eff} \ \hat{\Delta}creep \quad (4\text{-}3)$$

The elongation of the flange bolts due to creep is discussed in a subsequent subsection.

4.1.1 Bolt Stress-Rupture Life

At temperatures in excess of about 800°F, there is the possibility of creep and stress-rupture failure in the materials which were used for the Oyster Creek containment structure. Neither the drywell shell or the refueling head flange bolts were designed for temperatures in this range so that high temperature steels or other high temperature alloys were not used. Since the head bolt and shell material are not typically used in high temperature design applications test properties are extremely limited at high temperatures.

The refueling head bolts are SA-320-L7 which is an AISI 4140 steel, quenched and tempered at 1100°. Minimum ASME code properties at room temperature are 105,000 psi yield and 125,000 psi ultimate. At high temperatures, bolt fracture can occur with time at stresses well below the corresponding short term tensile strength. Particularly, in the

threaded portion of the bolts, stress-rupture may be influenced by the notch sensitivity of the material.

Limited stress-rupture test data on unnotched AISI 4140 steel at 1000° and 1200° (References 17 and 18) and at 850° and 950° (Reference 16) exists. In order to account for the time-dependent stress relationship at other temperatures and stresses, the approach used in the current investigation was to utilize the available experimental data for unnotched specimens to develop a Larson-Miller stress-rupture master curve and then reduce this curve by the same reduction factor for notched specimen data as exists for SA-193 Grade B14.

The variability associated with the stress rupture life of the bolts results primarily from two sources. The first is the inherent variability in the time to failure of an unnotched specimen at known stress and temperature (analogous to the variability in strength, β_S, at low temperatures). The second source is again the modeling variability resulting from the use of a Larson-Miller master curve to predict the rupture of the bolts at other times and temperatures for which test data are not available as well as the estimation of the notch sensitivity. Boyer (Reference 17) lists the coefficient of variation as ranging from 14.3% to 16.6% at 1022° and somewhat greater values for a series of tests at 1112°. For this investigation, an average β_S for time to rupture of 0.16 was used. Boyer (Reference 17) further shows a range of values from comparison of Larson-Miller prediction with tests. From these data, and providing some allowance for notch sensitivity, a lognormal standard deviation for modeling, β_M, of 0.44 was estimated which results in a total variability, β, of 0.47 associated with the time to rupture for the bolts.

4.1.2 Bolt Creep

A similar approach was utilized to develop the bolt creep strains and corresponding bolt creep elongation at elevated temperatures except that no reduction for notch sensitivity was used. Only a very short segment of the bolt is threaded while the remainder of the bolt length is a uniform diameter (2-1/2 inch). From the limited creep test data

available for AISI 4140 steel (References 17 and 18), Larson-Miller master curves were developed for 1, 2, 5, and 10% creep. From these master curves, a plot of median time to discrete values of creep strain at containment internal pressures from 36 to 200 psig was developed shown in Figure 4-2 for temperatures ranging from 800° to 1200°F. Also shown in Figure 4-2 are the median cut-offs in the creep curves above which stress-rupture or high temperature yield in the bolts must be considered. Although these cut-offs are not exact deterministic values due to the overlap in creep, stress-rupture, and yield strength variabilities, care must be exercised in calculating creep elongations in these regions.

From Figure 4-2, times to other creep strains may be obtained by interpolation or extrapolation. Knowing the effective bolt length (approximately 40 inches), the contribution of the creep to the total gap in Equation (4-1), and hence, the leak area as a function of time may be found as the product of the bolt creep elongation and the effective length of the leak, L_{eff}. As shown in Equation (4-1), these creep leak areas are added to the instantaneous leak areas.

Even less information on expected variabilities associated with creep is available compared with the variability for stress rupture. It is therefore conservatively estimated that the total ß associated with creep of about 0.47 to be used.

4.2 DRYWELL SHELL

At high temperatures, the potential failure modes of the drywell shell involve time dependent stress rupture. The creep effects can be large enough such that failure of the shell may occur at moderate or low pressures in combination with the high temperatures when sustained over a period of time. The combinations of temperature, pressure, and time for failure were estimated using a Larson-Miller stress rupture diagram for SA 212 Grade B steel, which was developed from representative carbon steel data presented in Reference 15.

To evaluate the stress rupture conditions, the membrane hoop stresses were used. These were evaluated for the sphere and the cylinder of the drywell as follows:

Sphere:

$$\sigma = \frac{PR_S}{2t_S}$$

Cylinder:

$$\sigma = \frac{PR_C}{t_C}$$

in which R_S is the radius of the sphere (420 inches), t_S is the sphere thickness (0.722 inches), R_C is the radius of the cylinder (198 inches), and t is the thickness of the cylinder (0.640 inches). The cylinder was found to control.

At a given pressure, the shell stress can be found. Using the Larson-Miller diagram, the median times to failure for various temperatures could be estimated. This was done for 100° temperature intervals between 800°F and 1200°F for containment internal pressures ranging from 50 to 180 psig. Figure 4-3 shows these results for the median shell rupture times. Interpolation may be used to estimate the rupture life at temperatures other than the intervals shown on the figure.

As discussed for the stress rupture of the flange bolts, the variability in the stress rupture life comes from two sources. The first is the inherent uncertainty in the estimated time to failure at a given stress and temperature. This is analogous to the strength variability and, as with the flange bolts, a ß value of 0.16 was used. The second source of variability is the modeling uncertainty associated with the use of the Larson-Miller master curve to predict the rupture of the drywell shell material for various combinations of time, temperature and stress.

Again, as used in the evaluation of the flange bolts, a logarithmic standard deviation for modeling, β_M, of 0.44 was estimated. Therefore, a total logarithmic standard deviation of 0.47 is associated with the median times to rupture for the drywell shell.

Table 4-1

LEAK PRESSURES AND TEMPERATURES OF THE HEAD FLANGE - MID FUEL CYCLE, 70 HOUR

Temperature (°F)	Median Leak Pressure (psig)	β	95% Confidence (psig)
200	142	0.10	120
300	121	0.18	90
400	78	0.56	31
500	36	0.09	31
600	36	0.09	31
700	36	0.09	31
800	36	0.09	31
900	36	0.09	31
1000	35	0.64	18
1100	20	0.84	9
1200	1		1

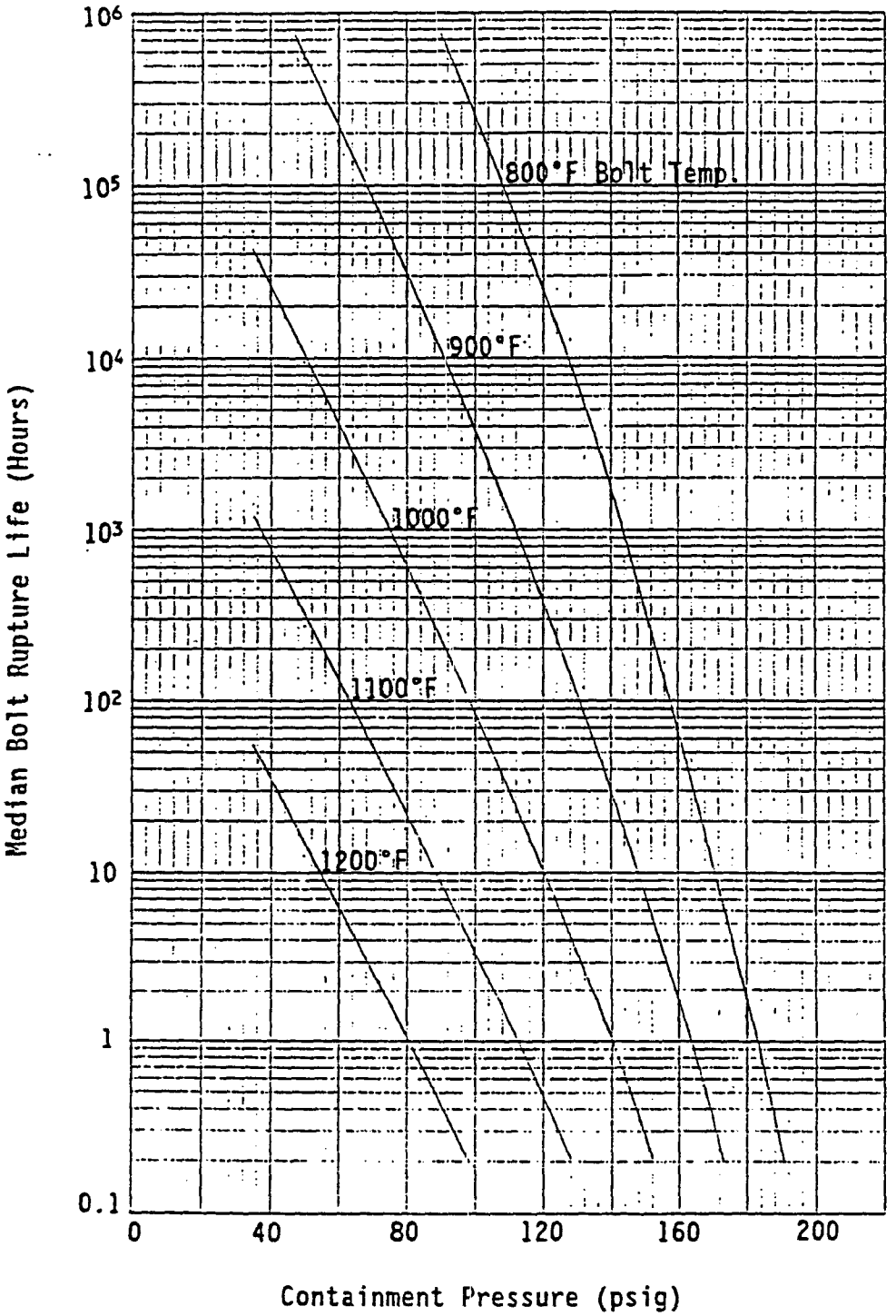

Figure 4-1: Median Bolt Rupture Life

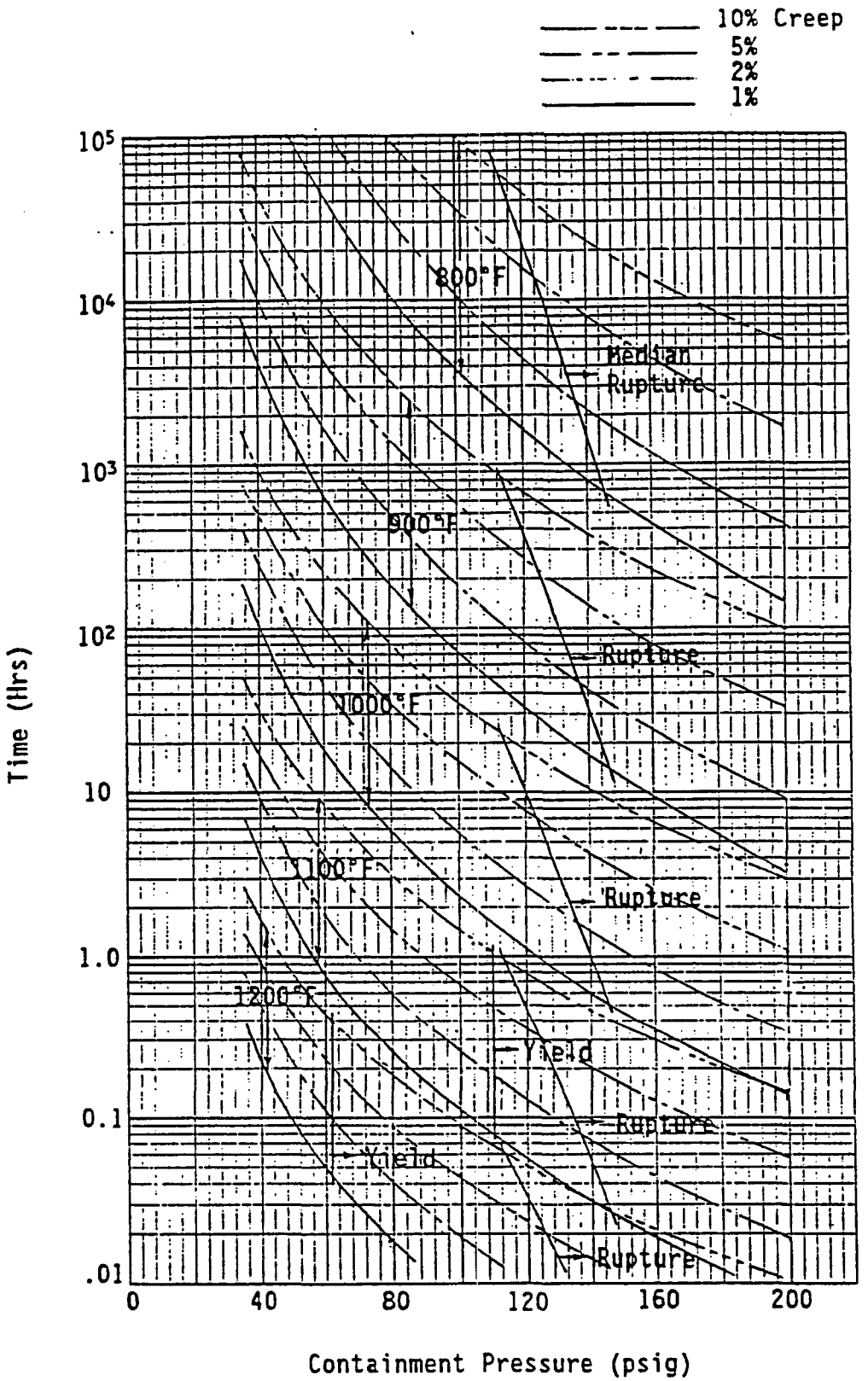

Figure 4-2: Median Bolt Creep

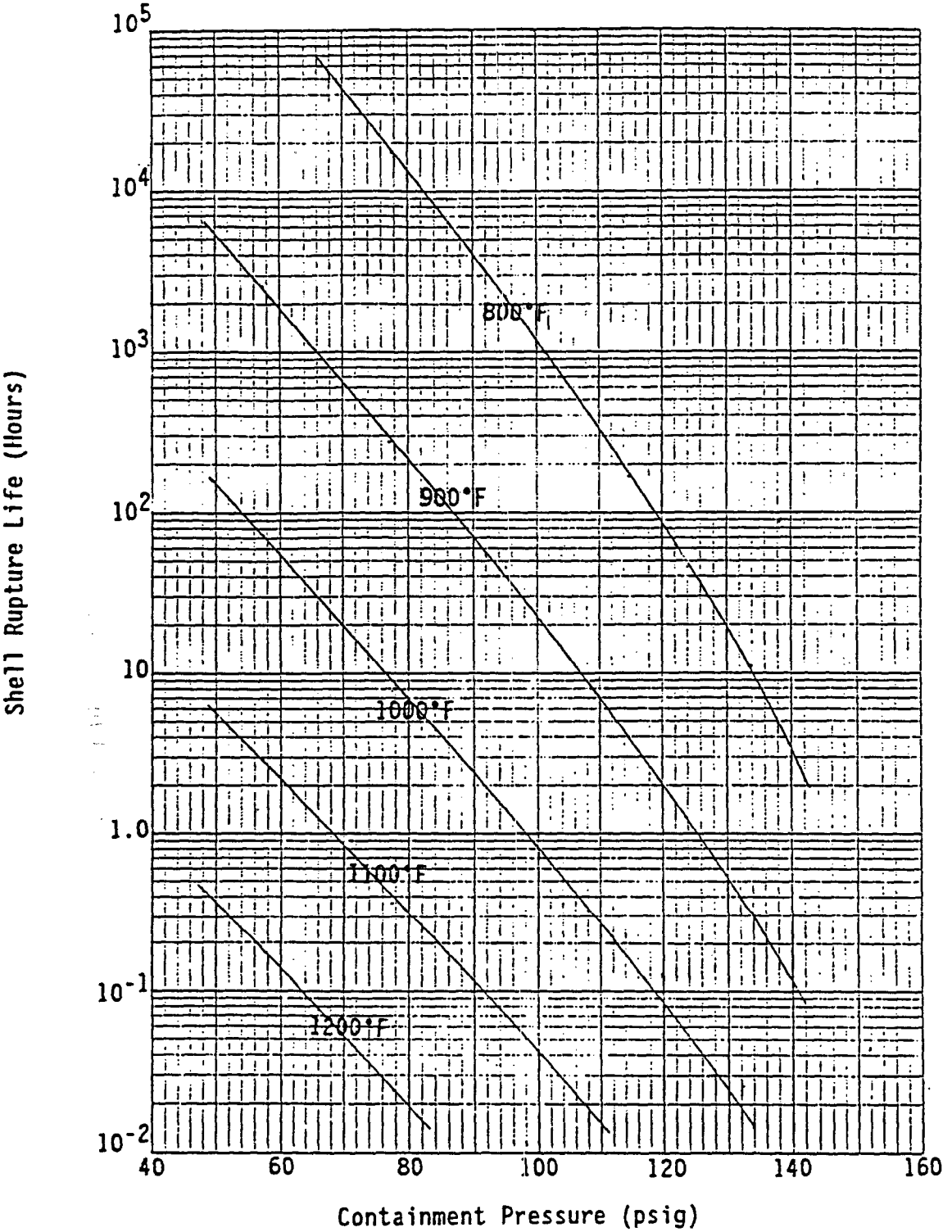

Figure 4-3: Median Drywell Shell Rupture Life

5. SUMMARY

The overpressure capacity of the containment structure at the Oyster Creek Nuclear Power Plant has been discussed in the report. The capacities are reported as probabilistic quantities in terms of median failure pressures and their associated variabilities. In this investigation, failure was interpreted as leakage from the containment. Although several potential failure modes were investigated, the median capacities of only the controlling failure modes were reported. These controlling failure modes were investigated for containment metal temperatures ranging from 300° to 1200°F. The potential failure modes examined included:

1. Membrane failures of the drywell shell
2. Failure of the drywell head flange seal
3. Failure of the vent line from the drywell to the suppression chamber (torus)
4. Failure of the suppression chamber shell
5. Failure at penetrations

In all cases, the failure modes were considered to be the result of a quasi-static pressure loading. The pressure rise times were assumed to be sufficiently long such that the dynamic transient response of the containment structure could be neglected. Also, the material temperatures were assumed to have reached a steady state, particularly after some period of time at accident temperatures.

The failure mode having the lowest median pressure capacity was found to be leakage at the bolted head flange connection of the drywell. At low temperatures, the median leak pressure was found to be governed by the rebound of the seal rings in the flange. At very high temperatures, the median leak pressure was primarily influenced by the amount of the bolt pre-load stress relaxation caused by the elevated temperatures. Median

leak areas and the associated variabilities for the head flange were reported for a range of pressures and temperatures.

Following the head flange failure at 300°F, the other controlling failure modes include: the sand bed region of the sphere (sand removed), torus, ventline bellows, cylinder/sphere knuckle, cylinder, ventline and the remaining spherical portion of the drywell.

Due to the very high temperatures considered, the effects of time dependent creep and stress rupture were investigated for the head flange bolts and the drywell shell. For temperatures greater than 800°, the median rupture life of the flange bolts was estimated. The required time to reach 1%, 2%, 5%, and 10% creep was also estimated for the bolts. This then leads to an additional time dependent leak area due to bolt creep in the high temperature regime.

6. REFERENCES

1. Rothrock, E.W. (CBI) to K.H. Kregg (Burns & Roe) Personal Communication.

2. Greimann, L.G. et. al., "Reliability Analysis of Steel Containment Strength," NUREG/CR-2442, June, 1982.

3. Greimann, L., Fanous, F., and Bluhm, D., "Final Report, Containment Analysis Techniques, A State-of-the-Art Summary," NUREG/CR-3653, March, 1984.

4. "Technical Report 10.1, Containment Structural Capability of Light Water Nuclear Power Plants," IDCOR Program Report, Technology for Energy Corporation, July, 1983.

5. Clauss, D.B., "Failure Mechanisms of LWR Steel Containment Buildings Subject to Severe Accident Loadings," Proceedings of the Third Workshop on Containment Integrity, NUREG/CP-0056, August, 1986.

6. Galletly, G.D. and R.W. Aylward, "Plastic Collapse and Controlling Failure Pressures of Thin 2:1 Ellipsoidal Shells Subjected to Internal Pressure," Trans. of the ASME, Journal of Pressure Vessel Technology, Vol. 101, February 1979, pp. 64-71.

7. Galletly, G.D., "Elastic and Elastic-Plastic Buckling of Internally Pressurized 2:1 Ellipsoidal Shells," Trans. of the ASME, Journal of Pressure Vessel Technology, Vol. 100, November 1988, pp. 335-343.

8. Brinson, D.A. and Graves, G.H., "Evaluation of Seals for Mechanical Penetrations of Containment Buildings," NUREG/CR-5096, August, 1988.

9. Blakeston, M.L., Tomblin, K.A., and Ward, J., "The Testing of Elastomers for Channel Seal Plugs in a Steam Generating Heavy Water Nuclear Reactor," Proceedings of the Eighth International Conference on Fluid Sealing, 1978.

10. Chivers, T.C., George, A.F., and Hunt, R.P., "High Integrity Static Elastomer "O" Ring Seals and Their Performance Through Thermal Transients," Proceedings of the Ninth International Conference on Fluid Sealing, 1981.

11. "Parker O-Ring Handbook," Prepared by Parker Seal Group, 1982.

12. Shigley, J.E., Machine Design, McGraw-Hill, 1956.

13. Galambos, T.V. and Ravindra, M.K., "Properties of Steel for Use in LRFD," Journal of the Structural Division, ASCE, Vol. 104, No. ST9, September, 1978.

14. Anderson, W.F., "Analysis of Stresses in Bellows Part I-Design Criteria and Test Results," NAA-SR-4527, Atomics International, Canoga Park, California, 1964.

15. "Technical Report 17.5, Draft Final Report of IDCOR-85, An Investigation of High Temperature Accident Conditions for Mark-I Containment Vessels," IDCOR Program Report, Technology for Energy Corporation, August, 1986.

16. Metals Handbook, Volume 1, Properties and Selection of Metals, 8th Edition, American Society for Metals, 1961.

17. Boyer, H.E., Atlas of Creep and Stress-Rupture Curves, ASM International, 1988.

18. Aerospace Structural Metals Handbook, Volume I, Ferrous Alloys, ASD-TDR-63-741, March, 1961.

19. Moore, J., GPU Nuclear Claculation No. C-1302-187-5300-017, 7/2/91.

20. Hadidi-Tamjed, H. and Wesley D., EQE Calculation No. 52096.01-C-001, 10/10/91.

APPENDIX B. VOLUME FOR DEBRIS TRAPPING IN VENT PIPE

This appendix documents the calculation of the debris volume that could become trapped in a vent pipe adjacent to the pedestal door. Because of the tortuous path for debris entrained in the blowdown gas flow in a high pressure vessel melt-through scenario, only a small fraction of the ejected debris is expected to be in a particle size range that could be entrained into the vent pipes. The purpose of the calculation is to estimate the volume and depth of debris that could become trapped in the vent pipe, so that it can be compared to the volume of debris that is expected to be discharged at vessel breach, and to the depth of debris that could cause melt-through of the vent pipe. A melt-through of the vent pipe would result in a suppression pool bypass at vessel breach.

The geometry of the vent pipe is shown in Figure B-1. The volume that can fill with debris is made up of two elements:

1. The volume in the angle segment of the right circular cylinder, V_C.
2. The volume in the spherical end cap, V_S.

The equation for the angle segment of the right circular cylinder is given in Reference A-1 as

$$V_C = \frac{hr^3}{b} (\sin \alpha - \tfrac{1}{3}\sin^3 \alpha - \alpha \cos \alpha)$$

and

$$\alpha = \arccos (1 - b/r)$$

Evaluating this equation for b = r in Figure A-1 yields $V_C = 77.6$ ft^3.

The total volume in the spherical end cap is given by

$$V_{s,\,max} = \frac{\pi c}{6} (3r^2 + c^2) = 21.8 \text{ ft}^3$$

For the condition at b = r, the volume in the spherical end cap is approximately one half of $V_{s,\,max}$ or 10.9 ft^3. This is about 14% of the volume in the cylindrical portion. Therefore, the major volume is contributed by the cylindrical portion, and the total volume is approximated as

$$V_{total} = 1.14 \times V_C$$

Figure B-2 shows the debris volume (V_{total}) that can accumulate in the vent pipe as a function of the debris depth d. The debris depth at the elevation of the bottom of the vent pipe ring header is approximately 2.3 feet as scaled from the drywell drawings. At this depth, the debris volume is approximately 47 ft^3.

REFERENCES

B-1. Rektorys, K. (editor), *Survey of Applicable Mathematics*, M.I.T. Press, 1969.

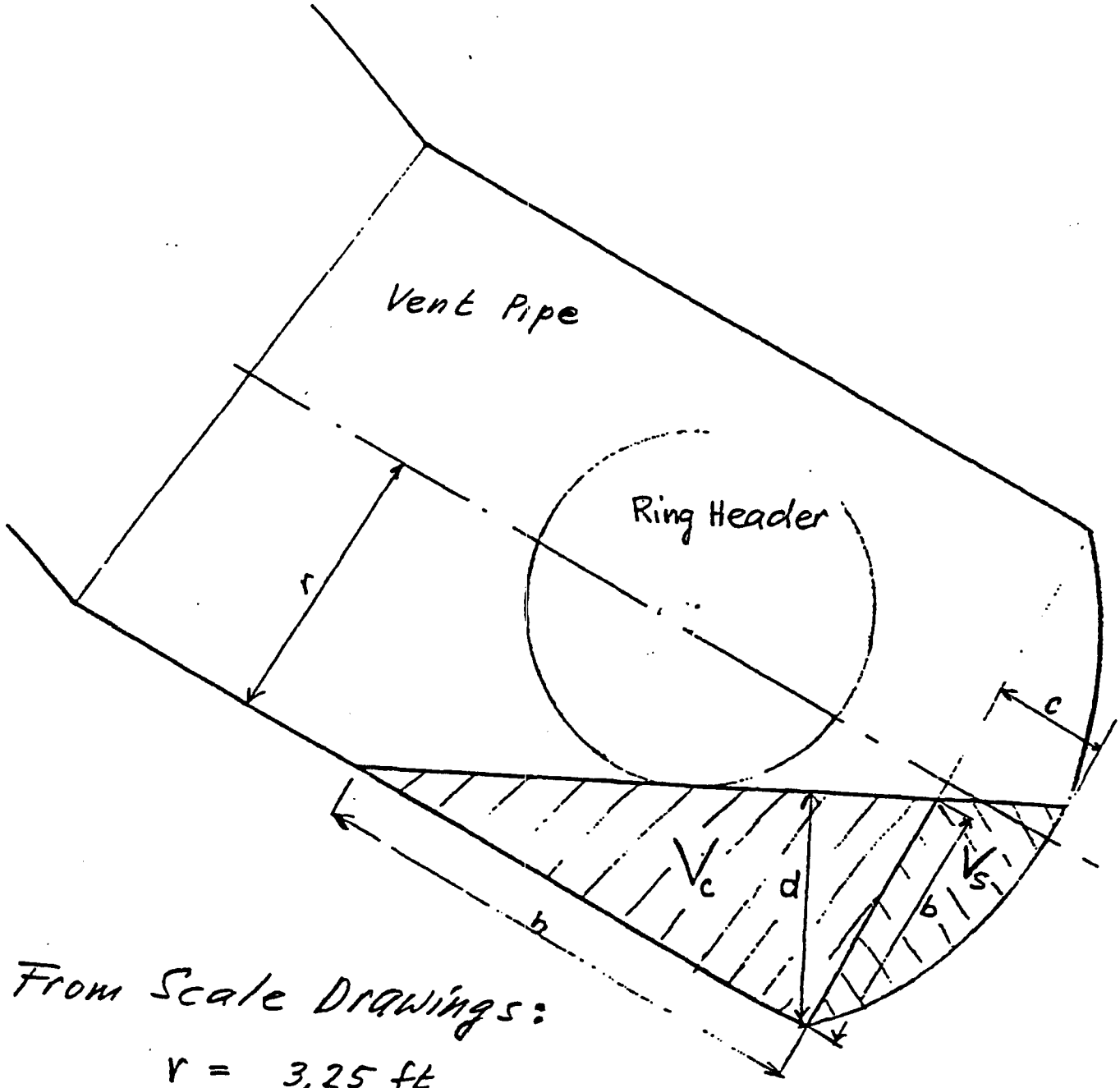

From Scale Drawings:

r = 3.25 ft
h = 8.45 ft
d = 2.30 ft
b = 2.50 ft
c = 1.25 ft

Figure B-1. Geometry for Debris Trapping in Vent Pipe

DEBRIS TRAPPING IN VENT PIPE
DEBRIS VOLUME (CUBIC FEET)
50
40
30
20
10
0
0
0.4
0.8
1.2
1.6
2
2.4
DEPTH OF DEBRIS (FEET)

APPENDIX C. PROCEDURE TO DETERMINE KEY RELEASE CATEGORIES

This appendix describes the steps taken to quantify the containment event tree (CET) and to determine the key release categories and their frequencies.

The CET is a logic structure with branching points. At each branching point, a split fraction must be entered that describes the probability of taking the downward path (the failure path) at that point. These split fractions are therefore also called the failure fractions, and they are developed in Section 10. The split fraction rules listed in Table 10-1 determine which split fraction value is used at which branching point in the CET, and Table 10-2 lists the numerical values of all the split fractions used.

The source term event tree (STET), shown in Figure 11-1, is used to define the release categories and to decide how to assign them to the CET end states. The STET is translated into the CET end state binning rules shown in Tables 11-1 and 11-2. With these rules, one release category is assigned to each CET end state. The CET quantification keeps track of the sequences and their frequency going to each end state. The STET is not used directly in the quantification process; it is only an aid to define the release categories and to develop the rules for assigning release categories to the CET end states. The CET quantification for all KPDS produces a table of release category frequency ordered by decreasing frequency, which is shown in the first two columns of Table 11-3.

In the next step, each release category in Table 11-3 is compared to the release categories with a higher frequency to determine if it can be binned with an enveloping release category or key release category (KRC). Binning to a KRC is permitted if the KRC has a higher frequency and constitutes a more severe source term. A more severe release category is, for example, one with an unscrubbed release (Letter U) compared to a scrubbed release (Letter S). The right-hand column in Table 11-3 shows how the release categories in the first column were assigned to the KRCs, and Table 11-4 identifies the KRCs.

The last step is to determine the source term for each KRC. The accident sequence to be modeled in MAAP to calculate the source term is defined by identifying, first, the Level 2 initiating event, which is the KPDS, that contributes most to the frequency of the KRC. The CET quantification produces frequency-ranked lists of sequences contributing to each release category and to each KRC. In all cases, the dominant sequence for a KRC was chosen to represent the KRC in the source term calculation. This sequence can be identified by inspecting the sequence lists for each KRC or by examining the sequence lists for the release groups in Tables 12-2, 12-4, 12-6, 12-8, and 12-9 to find the highest frequency contributor to a release category. The translation of this sequence into a definition of the MAAP sequence for the source term calculation was described in Section 11.3.3.

APPENDIX D: INDEPENDENT REVIEW

D.1 Introduction

Generic Letter 88-20, "Individual Plant Examination" requested each licensee to "... formally include an independent in-house review to ensure the accuracy of the documentation package and to validate both the IPE process and results". This review is in addition to and separate from the request to have "... utility engineers who are familiar with the details of design, controls, procedures and system configurations, involved in the analysis as well as the technical review". This Appendix provides an overview of the process used for the "independent in-house" review, the participants in the review and delineates review comments and their disposition.

D.2 Review Method

In early 1992 an Independent In House Review Group (IIHRG) was formed to review the first draft and early results of the Level 2 PRA. This multi-disciplinary and multi-organizational group consisted of management level personnel and senior level engineers who had not been significantly involved in the development of the Level 2 PRA. (See list of individuals involved in Table D-1). This provided the necessary degree of independence. These individuals were selected on the basis of their integrated understanding of Oyster Creek plant design, operation and maintenance. A prior knowledge of PRA techniques was not a prerequisite although some members had prior exposure to PRA approaches.

In parallel with this effort, a consultant from EPRI who was independent of the study also undertook a separate review. This individual, Dr. Ed Fuller, while unfamiliar with the many Oyster Creek specifics, is an expert in Level 2 PRA modeling techniques through extensive experience in the field.

The comments received from both independent reviews are contained in section D.5 along with the disposition of each.

D.3.1 IIHRG

The purpose of the IIHRG review was to assure that the Level 2 PRA was reasonably accurate and that it reflects the design and operation of Oyster Creek. The IIHRG review was largely a collegial process wherein in-house personnel made presentations on the content of the study, talking through various portions of the model. IIHRG members reviewed these portions before hand and offered comments orally in a group setting. Some comments elicited further comments from other members of the IIHRG and significant amounts of discussion resulted. The recorded comments and their disposition are contained in Section D.3.3.

D.3.2 List of IIHRG Members

1. N. Chrissotomos - Operations Manager
2. S. Greco - Supervisor, Reactor Plant Engineering
3. G. Cropper - Operations Training Manager
4. P. Cervenka - Senior Engineer, Operations Engineering
5. R. Milos - Senior Safety Review Engineer

6. S. Tuminelli - Manager, Engineering Mechanics

D.3.3 IIHRG Comments

1. Independent In-House Review Group (IIHRG):

Q1: The report should more clearly state why Oyster Creek is being compared to Peach Bottom even though it has no isolation condensers.

A1: The basis for the comparison is primarily the containment design which is Mark I for both plants. Peach Bottom analysis is also well documented in NUREG-1150. Other features, such as isolation condensers, which may affect the Level 1 PRA results, are of secondary importance to the Level 2 analysis. See Section 1.5.

Q2: Is there a significant amount of water on the drywell floor for high pressure cases involving safety valve lift? This should be clear in the report.

A2: No. Containment spray is not available in these scenarios. Any condensed steam which might be present in the initial phases will quickly evaporate as the drywell heats up especially after vessel breach when molten fuel falls into the drywell. Note Section 5.2, Presence of Water on Drywell Floor.

Q3: Is any credit taken for water inventory in RBEDT? This could possibly be pumped (about 4000 gallons) to drywell floor to possibly help to reduce source term.

A3: No credit was taken. There is no easy way to pump this water into the drywell. The only available path is a 'hose' connection under gravity flow used when needed during outage work and is normally isolated.

Q4: The criteria for selecting the KPDSs should be clearly and prominently stated.

A4: The selection criteria were based on NRC guidelines as stated in Section 8.1. The representative sequence for each KPDS was chosen on the basis of its frequency contribution to that KPDS and/or its severity. In some cases, scenarios with low CDF contribution were chosen because they resulted in more severe consequences.

Q5: Is the Oyster Creek containment median pressure capacity different from other plants in the head flange leakage mode? Discuss the limiting nature of sand bed region vs. other containment failure modes.

A5: The median leakage pressure at the head flange is no different from other Mark I plants (142 psig). The sand bed region pressure capacity with design thickness assumed at the 95% percentile level (i.e. 95% of the liner at that region has a thickness higher than design value) was 153 psig. Under these circumstances, the probability of a leak through the

drywell head flange before a break through the sand bed region would be appreciable because head flange limit is 11 psi below sand bed which is generally typical of other plants. When the sand bed region pressure capacity was redone using measured up-to-date thickness data assuming that the average of such data represented a median value for the whole region, the pressure capacity was lowered to 134 psig. This resulted in a decrease in the leak before break probability (i.e. the likelihood that head lift is the dominant failure mode). In fact, the analysis here assumes, for conservatism with respect to the time to containment failure, that the leak before break probability is zero although the sand bed region pressure capacity is only 8 psi below the head flange median pressure. Another conservatism is the fact that the measured thickness data were only for the thinnest accessible areas of the sand bed region and yet were used with an average representing the median thickness of the whole region. This approach assures a conservative estimate of the time to containment breach.

Q6: Have you taken credit for all possible human actions? Are post-vessel breach recoveries modeled in this analysis? Address in report.

A6: Credit for human responses were taken only for operator actions that are based on existing procedures. No credit was taken for post vessel breach recoveries. While post-core damage containment venting is modeled, no credit was taken for recovery of electrical power following core damage. This represents a conservatism in the analysis. See Section 1.5.

Q7: If containment failure is an inevitable consequence of vessel breach as this analysis indicates, the validity of the EOP philosophy to always save the containment may need to be revisited and possibly revised. Discuss this issue in the report.

A7: The EOP philosophy of saving the containment was always followed in the scenarios analyzed. The containment failures analyzed in this study are due to postulated losses of the containment cooling function and not because of the EOP philosophy. Since recoveries of containment cooling post vessel breach were not modeled it is fully expected that the analysis would show that the containment would eventually fail.

Q8: The concrete curb in the drywell is an important feature of the Oyster Creek design. A fuller description is needed in the report, and its effects on the results should be discussed.

A8: Section 1.5 has been updated to reflect a fuller description of the concrete curb and its effects.

Q9. The containment structural analysis was based on a 1% strain limit which is quite conservative, a 3% limit is more in line with a best estimate value. Also, the clamping force exerted by the drywell head bolts on the flange is believed to be excessive

because the temperature difference between the drywell and the head bolt region is less than the assumed values of 50-100°F based on plant data.

The combination of both effects would lower the leakage threshold of the head flange seal and improves the leak before break probability.

A9. The above issues were discussed with EQE and it was stated that the best estimate may be a 3% strain limit but the NRC is more comfortable with a 1% limit. Plant thermocouples inside the drywell in the head flange region (E1. 89' to 95') show a temperature range of 168°F - 243°F (at power) while the measurements taken outside the head region (inside the concrete-drywell head gap) show a range of 160°F - 180°F (taken from May 89' til September 90') near the bolts. This shows a temperature difference of 10 - 80°F depending on the season. The analysis, however, assumes a temperature difference of 50 - 100°F during accident condition which may be conservative.

D.4.1 Independent Consultant Review

A separate independent review was conducted by Dr. Ed Fuller of EPRI. This was a comprehensive review of the MAAP modeling techniques and the report draft. His review comments and their disposition are documented in Section D.4.2 below.

D.4.2 Independent Consultant Comments

Q1. On P. 1-4 in the first paragraph of Section 1.5 there is a typo. It should read "molten corium attack" and not "molten corrosion attack".

A1. Corrected.

Q2. On P. 3-5 there seem to be errors and/or mis-entries in the table. For example, the words "Linear 12,700" in the Peach Bottom column do not line up with a descriptor. There is also a large discrepancy between the two values for wetwell minimum water volume. Finally, the value for Peach Bottom's containment design pressure is missing.

A2. Corrected.

Q3. In section 4.2.1 on page 4-1 there is a discussion about the choice of the no-blockage option. You should be aware that the EPRI Guidance Document prepared by GKA recommends that the local blockage option be used, and only use the no-blockage option for sensitivity studies. Your justification is that you obtain conservative values for containment pressurization. Perhaps so, but you should realize that it is a non-conservative treatment of fission product release. With the no-blockage option you tend to predict more cesium and iodine deposition in the suppression pool, and hence less revaporization later in the accident.

A3. The choice of the no blockage option for Oyster Creek is believed to result in a conservative approach for hydrogen generation and fission product release consistent with EPRI Guidance document cited. The EPRI document states that "In one or two accident sequences in which high fission product retention would be expected (e.g. station blackouts without induced primary system failures or depressurization by operator action), calculations should be repeated with the blockage option on ...". The scenario in question for Oyster Creek is the high pressure station blackout (NIFW). In this scenario the relief valves (piped to the torus) are assumed closed and the safeties (piped to the drywell) are the only pressure relief source available in the vessel. Therefore, with no blockage a high hydrogen and fission product releases are expected which will be directed to the drywell through the safeties and no fission product scrubbing or deposition in the suppression pool will take place simply because nothing will go to the torus. Other boilers have SRVs piped to the suppression pool and in either mode (relief or safety) gases will go to the suppression pool where fission product scrubbing will take place.

The other scenarios have low pressure vessel failure except MKCU KPDs (ATWS Scenarios). The source term release category dominated by ATWS is KRC3 (NLEGUB) and the ATWS sequence that dominated this category was the one with stuck open relief valve and stuck open vacuum breaker (see section 11.3.4) and therefore, transformed to a low pressure sequence during core heatup. Therefore, the no blockage option for Oyster Creek represented the most conservative hydrogen generation and fission product release and is consistent with the basis for EPRI recommendation.

Q4. On P. 4-2, the last sentence of section 4.2.2 is not clear.

A4. The sentence refers to the use of the mechanistic freeze model (IFREEZ = 1) and the no blockage (FCRBLK = -1) options.

Q5. At the bottom of P. 4-2 there is a discussion of ATWS power. It should be noted that the modified Chexal-Layman correlation in MAAP is based on RETRAN calculations, in which a one-dimensional space-time kinetics model was invoked. RELAP5, on the other hand, only used point kinetics and thus is less accurate for predicting the response to an ATWS. I, therefore, strongly recommend using the modified Chexal-Layman correlation option in MAAP, which has been favorably compared against TRAC-G. The latter code also has a spacetime kinetics model.

A5. The Chexal-Layman option was used first but the results seen were not believable especially when feedwater was turned on to maintain level at TAF as the sequence requires. The power used to jump to 65% rated when cold water was turned on (i.e. when subcooled water was involved) which did not make sense. The RELAP5 ATWS analysis, although based on point kinetics, does account for spacial effects through the region reactivity table used in a multi-nodal core. The implication of any differences in power generation because of kinetics models are believed to be of little concern at the power level in question (less than 20%) and its impact on source term or core damage is believed to be negligible.

Q6. **As discussed in Section 4.3.5, your reactor building model is overly conservative. Unless multiple failure locations result, thus giving rise to a "chimney effect", reactor building DFs of five (5) or more can be expected. Please refer to EPRI NP-6586-L, which documents the results of a comprehensive study of this issue.**

A6. *The choice of not having a reactor building model was based on the assumption that the probability of a leak before break is zero, i.e. a catastrophic failure in the containment will take place thus pressurizing the reactor building by a 0.25 psi very quickly resulting in failure of blow-out panels rendering the reactor building ineffective, also see A. 12 below.*

Q7. **I have two comments on P. 5-2. First, regarding oxidation during blowdown, this is not a large effect since it takes place over a very short time. Second, with respect to enhancement of fission product release by oxidation of fine particles, it should be noted that the volatile fission products (cesium, iodine, and the noble gases) would already have been released and the lower-volatility fission products would not be experiencing high-enough temperatures to be vaporized. Thus, the phenomenon alluded to is not very likely to occur.**

A7. *We agree with your comments and above section has been updated accordingly.*

Q8. **On page 6-1 reference is made to Appendix A. Please note that the Appendix does not have the details referred to in the text, and is about a totally different topic.**

A8. *The correct Appendix A has been attached.*

Q9. **On page 7-6, there is a discussion about debris causing melt through of a vent pipe. If this were to happen, could debris enter the suppression pool? If this could indeed happen, what would be the consequences?**

A9. *The debris in question are assumed to be fine particles and if this were to happen, they would enter the suppression pool vapor space resulting, as assumed, a suppression pool bypass.*

One would postulate that these particles would ultimately settle in the pool water. The heat load of such particles on the torus is negligible due to the shear size and amount of water in the pool.

Q10. **On P. 9-2, there is a discussion about fire water injection to prevent vessel failure. What is the relative likelihood that the fire water would not be injected, and what would be the consequences?**

A10. *This issue is discussed more fully in Section 10.1 on the quantification of top event VB, Vessel Breach Prevented. Firewater is available in 100% of the PIFW plant damage states as determined by the Level 1 model. Other plant damage states either are assumed to*

have no potential for in-vessel recovery or, in the case of PDS OIAU, a fraction are determined to be recoverable. (See p 10-3 and Table on p 10-4.)

Q11. Concerning the discussion on the bottom of P. 10-4, it should be noted that late revaporization of cesium iodine and cesium hydroxide has the potential of greatly affecting the source term. Temperatures in the drywell could get so high that all of the cesium and iodine not already scrubbed by the suppression pool water could be revaporized off surfaces in the RCS and the drywell and flow directly to the reactor building and possibly to the environment.

A11. The analyses show that vessel breach result in containment failure and fission product release start during the first 10 hours (See Table 11-5). Scenarios that result in core damage but no vessel breach and hence no containment failure (PIFW, see discussion in 10.1) are low pressure scenario where water injection is assumed to be available and hence fission product scrubbing is in effect. Therefore, late revaporization (after 24 hours) will not be of concern because of either the containment has already failed or water injection is available, also see A.13 below.

Q12. On P. 10-15, in the discussion of BE, a statement is made that the reactor building must remain structurally intact and that the SGTS must continue to operate in order to have fission product removal from the atmosphere. This is not true! Fission product removal can occur--the actual removal rate is a function of the residence time of the aerosols in the building. EPRI NP-6586-L shows the, for reactor buildings similar to Oyster Creek's (Categories A and B), DFs of 5-10 can be expected if failures occur only at the blowout panels. On the other hand, if failures also simultaneously occur in to the turbine building, a chimney effect could result that would not allow for significant deposition. Thermal hydraulic and geometric effects are thus very important.

A12. EPRI NP-6586-L refers to analyses for type A plants (BWR-2, Table 4-2, Vol. 1) including station blackouts, main steam line V-sequence and RHR discharge line V-sequences. The sequence of interest to Oyster Creek analysis is the station blackout but the containment failure used in above document was 0.01 ft^2 (Table 4-3, Volume 1) resulting in 0.86 hours until the blow-out panels failed (see Section 5, Volume 2). In Oyster Creek analysis the drywell failure area ssumed was 1 ft^2 which would result in a much faster pressurization rate for the Reactor Building and would make above result non-conservative, because the decontamination takes place during the 0.86 hours of residence time before the blow-out panels fail.

Q13. In the discussion of the NIFW sequence in Section 11.3.3, there appears to be an inconsistence. On page 11-8 it is stated that the containment fails at 4.9 hours. On the other hand, Table 9-1 shows a time of 7.7 hours. Of greater importance than resolving the inconsistency is the fact that the MAAP calculation was terminated after only ten (10) hours. As can be seen in Table 11-6, more than half of the CsI inventory is still in the vessel. It would be expected that all of this material would be revaporized eventually, probably before twenty four (24) hours. Given your

conservative assumption of no reactor building effectiveness, your release fraction would not be 0.08, but would instead be 0.60. Incidentally, the NRC and its contractors are well-aware of the revaporization phenomenon. I, therefore, strongly recommend that this case be rerun, for a time limit of at least thirty six (36) hours following vessel breach. The new source terms should be reported instead of the ones you now report. This comment applies to all of the MAAP runs used to represent the key release categories. Incidentally, the case representing KRC 4 would then probably result in a CsI release fraction of 0.89. Now we can begin to see the importance of being able to take some credit for the reactor building effectiveness.

A13. *The 7.7 hours on Table 9-1 refer to the base case of NIFW while the 4.9 hours on page 11-8 refer to the perturbed case (NIFWW) where one safety valve sticks open after 1.9 hours into the accident. In the base case no safety valves were assumed to stick open.*

The NIFWBI is the high pressure station blackout with a stuck open safety valve (this sequence was found to be the major contributor, see 11.3.3, 11.3.5) but with containment failure at containment mean failure pressure of 137 psia (same as NIFWW but with containment failure). It is assumed here that fire water is available and will continue to dump water into the drywell even after containment failure (the piping into the containment might break, but water will still fall inside the drywell). This water will cover the drywell floor where the corium is and will scrub fission products produced. The liner will leak through the failure area to the sandbed region into the concrete then to the torus room or other places but the continuous supply of water through the fire system will assure fission product retention by the water. This process will also assure the continuous reduction of the concentration of fission products in the water and hence retards and possibly prevents the revaporization process.

The NIFWB2 (KRC4) is the same as NIFWBI except that the containment fails at vessel breach. The MJAU sequence (KRC5), on the other hand, is a bypass sequence where portion of the fire water dumped into the vessel will leak out bypassing the containment and will not be available for scrubbing. That is believed to be the reason for the high CsI release fraction. As far as OJAUV is concerned, although this is partly a bypass sequence (RWCU pressure reducing station failure, see 9.2.3), but the bypass portion gets terminated at vessel breach and the scenario becomes a TW sequence. The above explanation for the NIFWBI will also apply.